



University  
of Glasgow

Fields, Laura Ashley (2013) *Local cAMP signalling and phosphodiesterase activity in an in vitro model of cardiac hypertrophy*. PhD thesis.

<http://theses.gla.ac.uk/4755/>

Copyright and moral rights for this thesis are retained by the author

A copy can be downloaded for personal non-commercial research or study, without prior permission or charge

This thesis cannot be reproduced or quoted extensively from without first obtaining permission in writing from the Author

The content must not be changed in any way or sold commercially in any format or medium without the formal permission of the Author

When referring to this work, full bibliographic details including the author, title, awarding institution and date of the thesis must be given

**Local cAMP signalling and  
phosphodiesterase activity in an *in vitro*  
model of cardiac hypertrophy.**

**Laura Ashley Fields  
BSc (Hons), MRes**

Submitted in fulfilment of the requirements for the  
Degree of Doctor of Philosophy.

Institute of Neuroscience and Psychology  
College of Medical, Veterinary and Life Sciences  
University of Glasgow

# Abstract

---

Cardiac hypertrophy often develops to compensate for hemodynamic overload and therefore, in its early stages, hypertrophy is considered to be an adaptive response. Nonetheless, prolonged exposure to a hypertrophic stimulus is associated with heart failure.

In the heart, the compartmentalisation of the cAMP/ PKA signalling pathway plays a critical role to achieve the specificity of response and maintains regular cardiac function. Alterations in this signalling pathway have been linked to the pathophysiology of cardiac hypertrophy. Phosphodiesterases (PDEs) provide the only means of hydrolysing cAMP and therefore are essential components in the spatial and temporal control of the cAMP response. By restricting the diffusion of cAMP, PDEs prevent unspecific activation of PKA and phosphorylation of downstream targets. PDEs are therefore able to regulate the kinetics of cAMP signalling dynamics.

In this study, an *in vitro* model of chronic catecholamine-induced cardiac hypertrophy of adult rat ventricular myocytes (ARVM) was utilised. This model allowed the investigation of the function of PDEs in regulating compartmentalised cAMP signals in cardiac hypertrophy. Using FRET-based cAMP sensor Epac1\_camps fused to the unique dimerisation/docking domain sequences that anchors PKA-RI and PKA-RII subunits to AKAPs, this study demonstrated that, similar to neonatal rat ventricular myocytes (NRVM), adult myocytes also display restricted cAMP diffusion. These cAMP microdomains are regulated by different families of PDEs. In particular, PDE2, PDE3 and PDE4 appear to control the pool of cAMP generated in the PKA-RI compartment, whereas only PDE2 and PDE4 were found to modulate cAMP in the PKA-RII compartment in ARVM.

In the *in vitro* cardiac hypertrophy model, a reduction in cAMP generation was detected upon  $\beta$ -adrenergic stimulation and altered PDE activity was visualised using FRET-based imaging. This investigation showed that PDE2 activity is significantly increased in the PKA-RII compartment of hypertrophic cardiac myocytes, while an overall reduction in PDE3 activity was detected. Immunofluorescence experiments revealed altered PDE4 localisation in hypertrophic myocytes.

Advances in cyclic nucleotide signalling research, in particular of the activity and regulation of PDEs, have shown that an interaction between the cAMP and cGMP signalling pathways exists. Integration between these two pathways is mediated by the modulation of cAMP-degrading PDEs by cGMP. Allosteric binding of cGMP to the GAF domains of PDE2 enhances its activity, whereas cGMP reduces the activity of PDE3 by acting as a competitive inhibitor. PDE2 and PDE3 therefore may act as a connection between these two signalling cascades and it is possible to predict the existence of distinct signalling units *in vivo* in which cGMP, by acting on PDE2 or PDE3, can selectively modulate cAMP levels.

Intracellular cGMP generated by stimulation of the particulate GC (pGC) by atrial natriuretic peptide (ANP) or stimulation of the soluble GC (sGC) by the NO donor SNAP is compartmentalised into discrete microdomains. Stimulation of the pGC had no effect on cAMP signalling in the PKA-RII compartment. Activation of sGC generated a pool of cGMP which lead to a reduction in cAMP response in the PKA-RII compartment upon  $\beta$ -AR stimulation. Both GCs generated cGMP in the PKA-RI compartment which lead to an increase in cAMP response. Further investigation revealed that cGMP is able to modulate cAMP signalling in the PKA-RI compartment by PDE3 and by PDE2 in the PKA-RII compartment.

It was hypothesised that the observed differences in cAMP signalling and PDE contribution in hypertrophic myocytes in the PKA-RI and PKA-RII subcellular compartments may be due to variations in the pools of cGMP. Employing genetically encoded FRET-based biosensors for cGMP targeted to PKA-RI and PKA-RII compartments, basal levels of cGMP were found to be significantly increased in both compartments of hypertrophic myocytes which could explain the altered PDE2 and PDE3 activity in hypertrophic ARVM.

Finally, this study shows that PDE2 activity is necessary to achieve full development of the catecholamine-induced hypertrophic response. Pharmacological inhibition of PDE2 with Bay 60-7550 prevents NE-induced cardiomyocyte hypertrophy. Overexpression of PDE2A2 was found to induce hypertrophic growth, even in the absence of increased adrenergic drive, thus indicating that PDE2 activity promotes development of cardiomyocytes hypertrophy. PDE2 localisation is vital for its regulation of hypertrophic growth. Displacement of endogenously active PDE2 from its specific intracellular localisation, using a catalytically inactive PDE2A2, was sufficient to counteract

catecholamine-induced hypertrophic growth As PDE2 is a dual specific PDE, it was important to establish whether the anti-hypertrophic effects of PDE2 inhibition were mediated by activation of the cGMP/ PKG or cAMP/ PKA signalling pathways. The data presented here, show that the effects of pharmacological inhibition of PDE2 is PKA dependent.

Together, these findings confirm the involvement of PDE2 in the progression of hypertrophy in cardiomyocytes and indentify PDE2, specifically coupled to the PKA-RII compartment, as a possible novel target for the development of therapeutic treatment for hypertrophy.

# Declaration

---

I hereby declare that the work presented in this thesis has been carried out by me unless otherwise cited or acknowledged. The work is entirely of my own composition and has not been submitted, in whole or in part, for any other degree at the University of Glasgow or any other institution.

Laura Ashley Fields

June 2013

# Table of Contents

---

<b>Abstract</b> .....	<b>2</b>
<b>Declaration</b> .....	<b>5</b>
<b>Table of Contents</b> .....	<b>6</b>
<b>List of Tables</b> .....	<b>12</b>
<b>List of Figures</b> .....	<b>13</b>
<b>Acknowledgements</b> .....	<b>17</b>
<b>Abbreviations</b> .....	<b>18</b>
<b>1 Introduction</b> .....	<b>21</b>
1.1 Signal transduction by cyclic nucleotides (concept of second messenger). .....	21
1.2 cAMP signalling pathway .....	22
1.3 cAMP synthesis: Adenylyl Cyclases .....	23
1.4 Cyclic nucleotide degradation: phosphodiesterases .....	26
1.4.1 The catalytic domain .....	28
1.4.2 The Regulatory domain.....	29
1.5 Effectors of cyclic nucleotides .....	32
1.5.1 PKA.....	32
1.5.2 Epac.....	34
1.5.3 CNG .....	36
1.6 cAMP signalling in the heart.....	37
1.7 Compartmentalisation of cAMP/ PKA signalling in cardiomyocytes. ....	42
1.7.1 Compartmentalisation of PKA by A-kinase anchoring proteins.....	44
1.7.2 GPCR and AC compartmentalisation .....	51
1.7.3 Compartmentalisation of cAMP .....	52
1.7.4 Compartmentalisation of cAMP by PDEs .....	54
1.8 cAMP hydrolysing PDE families expressed in the heart .....	56

1.8.1	PDE2 .....	56
1.8.2	PDE3 .....	61
1.8.3	PDE4 .....	63
1.9	Real-time detection of cAMP .....	65
1.9.1	CNG based sensors .....	65
1.9.2	FRET .....	66
1.9.3	FRET-based cAMP indicators .....	66
1.9.4	Epac-based sensors.....	68
1.10	Cardiac Hypertrophy.....	69
1.10.1	Signalling pathways regulating cardiomyocyte hypertrophy .....	71
1.10.1.1	cGMP/ PKG.....	73
1.10.1.2	Calcineurin/ NFAT .....	75
1.10.1.3	G-protein coupled receptors.....	76
1.10.1.4	cAMP/ PKA signalling in cardiac hypertrophy .....	77
<b>2</b>	<b>Thesis Aims .....</b>	<b>83</b>
<b>3</b>	<b>Materials and Methods .....</b>	<b>84</b>
3.1	Materials .....	84
3.2	Cellular Biology .....	84
3.2.1	Primary Isolation Optimisation .....	84
3.2.1.1	Collagenase .....	85
3.2.2	Adult Rat Ventricular Myocytes (ARVM) .....	85
3.2.2.1	Isolation of ARVM .....	85
3.2.2.2	Troubleshooting .....	87
3.2.2.3	Preparation of Laminin-coated coverslips .....	88
3.2.3	<i>In-vitro</i> hypertrophy protocol.....	88
3.2.4	Infection of ARVM with adenovirus vectors carrying FRET-based sensors	89
3.2.5	CHO culture and transfection.....	89
3.2.6	Media, Buffers and compounds for Cellular Biology .....	90

3.3	Molecular Biology .....	91
3.3.1	Agar plates .....	91
3.3.2	Transformation of Chemically Competent Cells .....	91
3.3.3	DNA extraction and purification.....	92
3.3.4	Storage of plasmid DNA.....	93
3.3.5	Quantification of nucleic acids.....	93
3.3.6	DNA Sequencing .....	94
3.3.7	Restriction enzymes and Ligation.....	94
3.3.8	Agarose Gel Electrophoresis.....	94
3.3.9	PCR and DNA purification .....	95
3.3.10	Generation of FRET-based constructs .....	95
3.3.11	Generation of Ad5 recombinant vectors .....	95
3.3.11.1	Adenovirus production in AD-293 Cells.....	96
3.3.11.2	Harvest virus from AD293 cells .....	97
3.3.11.3	Amplification of Virus.....	97
3.3.11.4	Medium for AD293 cells .....	97
3.3.11.5	Adenovirus purification .....	98
3.3.11.6	Titration by end-point dilution.....	98
3.4	Protein Analysis .....	100
3.4.1	Preparation of lysates and protein quantification.....	100
3.4.2	SDS-PAGE.....	101
3.4.3	Western immunoblotting.....	101
3.4.4	Buffers and compounds for SDS-PAGE and Western immunoblotting .....	104
3.4.5	Immunoprecipitation (IP) assay .....	105
3.5	Cell based experiments.....	106
3.5.1	Manual measurements of cell size .....	106
3.5.2	Real-time xCELLigence measurements.....	106
3.5.3	Phosphodiesterase Activity Assay .....	107

3.5.3.1	Protein Sample Preparation .....	107
3.5.3.2	Assay procedure.....	108
3.5.3.3	Determination of Phosphodiesterase Activity .....	108
3.5.3.4	Buffers and compounds for PDE assay .....	109
3.6	Quantitative Real-Time PCR.....	110
3.6.1	RNA extraction .....	111
3.6.2	Reverse Transcription .....	112
3.6.3	TaqMan real-time PCR .....	113
3.7	Microscopy .....	115
3.7.1	Immunostaining and Confocal Imaging.....	115
3.7.2	FRET based imaging.....	116
3.7.2.1	Imaging set up.....	116
3.7.2.2	FRET experimental procedure and data analysis .....	118
3.7.2.3	Buffers and compounds for FRET .....	120
3.8	Statistical analysis .....	120
<b>4</b>	<b>Intracellular cAMP signalling dynamics in adult cardiac myocytes. ....</b>	<b>121</b>
4.1	Introduction .....	121
4.2	Results .....	123
4.2.1	Expression of a cAMP FRET-based sensor and its localisation to the PKA-RI and PKA-RII compartments .....	123
4.2.2	Characterisation and properties of RI_epac and RII_epac in adult myocytes.....	127
4.2.3	Phosphodiesterase-mediated regulation of cAMP in subcellular compartments in cardiac myocytes. ....	132
4.3	Conclusions .....	139
<b>5</b>	<b>cAMP signalling dynamics in an <i>in vitro</i> model of cardiac hypertrophy. ....</b>	<b>141</b>
5.1	Introduction .....	141
5.2	Results .....	144

5.2.1	Norepinephrine induced hypertrophy in an adult myocyte <i>in vitro</i> model of cardiac hypertrophy. ....	144
5.2.2	Expression and localisation of cAMP FRET-based sensors to the PKA-RI and PKA-RII compartments in hypertrophic myocytes .....	150
5.2.3	Comparison of compartmentalised cAMP signalling in control and hypertrophic adult cardiomyocytes. ....	160
5.2.4	Contribution of individual PDEs to the control of the cAMP response to catecholamines in the PKA-RI and type II compartments in hypertrophic myocytes. ....	166
5.2.5	Changes in individual PDE families expression as assessed by protein and mRNA level in hypertrophic ARVM .....	175
5.2.6	Alteration in phosphodiesterase localisation in hypertrophic myocytes.....	180
5.3	Conclusions .....	183
<b>6</b>	<b>The interplay between cAMP and cGMP and its impact on cardiac hypertrophy.. .....</b>	<b>186</b>
6.1	Introduction .....	186
6.2	Results .....	189
6.2.1	cGMP-mediated modulation of cAMP levels in the PKA-RI and PKA-RII subcellular compartments.....	189
6.2.1.1	The effect of cGMP on the local ISO-induced cAMP response in the presence of selective inhibitors. ....	191
6.2.2	cGMP-mediated local modulation of cAMP levels in the PKA-RI and PKA-RII compartments in hypertrophic myocytes. ....	194
6.2.3	Investigation of cGMP levels at the PKA-type I and PKA-type II locations using targeted cGMP FRET based sensors. ....	195
6.2.4	$\beta_3$ -adrenergic receptor signalling in the PKA-RI and PKA-RII compartments of hypertrophic cardiomyocytes .....	199
6.3	Conclusion.....	202
<b>7</b>	<b>Role of Phosphodiesterase type 2 in the development of cardiac hypertrophy. 206</b>	
7.1	Introduction .....	206
7.2	Results .....	208

7.2.1	<i>In vitro</i> inhibition of PDE2 with Bay 60-7550 prevents NE induced cardiomyocyte hypertrophy .....	208
7.2.2	PDE2 overexpression in ARVM induces hypertrophy .....	210
7.2.3	Exploring the effect that overexpressing the catalytically inactive PDE2A2 has on cAMP signalling dynamic in adult cardiomyocytes .....	212
7.2.4	Is the anti- hypertrophic effect of PDE2 inhibition dependent of cAMP/PKA or cGMP/PKG downstream signalling? .....	216
7.3	Conclusion.....	224
<b>8</b>	<b>Conclusion and Future Perspectives.....</b>	<b>226</b>
<b>9</b>	<b>List of References .....</b>	<b>233</b>

## List of Tables

---

Table 1-1. Tissue distribution of ACs. Adapted from (Sadana and Dessauer, 2009). .....	25
Table 1-2. The families of phosphodiesterases, detailing specificity for either cAMP or cGMP. Adapted from (Mehats et al. 2002). .....	27
Table 1-3. A kinase anchoring proteins (AKAPs) distribution and properties. Adapted from (Pidoux and Tasken 2010). .....	45
Table 3-1. List of primary antibodies and dilutions used for each type of application.....	102
Table 3-2. List of secondary antibodies and dilutions used for each type of application..	103
Table 3-3. Oligonucleotide sequence of primers and probes used for RT-PCR.....	114

# List of Figures

---

Figure 1-1. The cyclisation of ATP to form cAMP. ....	23
Figure 1-2. Schematic representation of adenylyl cyclase. Adapted from (Willoughby and Cooper 2007).....	24
Figure 1-3. Schematic representation of phosphodiesterase structure. Adapted from (Mehats et al. 2002).....	28
Figure 1-4. Schematic representation of the structures of the mammalian phosphodiesterase (PDE) families. Adapted from (Conti and Beavo 2007).....	31
Figure 1-5. Regulatory subunits of PKA. ....	33
Figure 1-6. The multi domain structure of Epac. ....	36
Figure 1-7. Activation of $\beta$ -adrenergic receptors triggers the PKA-mediated phosphorylation of several targets involved in the excitation-contraction coupling (ECC) process.....	39
Figure 1-8. Schematic representation of cGMP-induced conformational changes of PDE2 resulting in activation. Adapted from (Francis et al. 2011). ....	58
Figure 1-9. Schematic representation of PKA-GFP based sensor. ....	67
Figure 1-10. Signalling pathways involved in cardiac hypertrophy and the progression to heart failure. ....	72
Figure 3-1. The Langendorff perfusion system used to perform isolations.....	86
Figure 3-2. Image of an adult rat ventricular myocyte (ARVM) isolation before counting and seeding the cells, showing both healthy (rod shaped) myocytes and dead (round) myocytes. ....	87
Figure 4-1. Schematic representation of RI_epac and RI_epac FRET-based cAMP sensors. ....	124
Figure 4-2. Localisation of RI_epac and RII_epac FRET sensors in ARVM. ....	125
Figure 4-3. Summary of colocalisation statistics. ....	126
Figure 4-4. An example of a FRET experiment in cardiomyocytes transduced with the targeted cAMP sensors. RI_epac and RII_epac.....	128
Figure 4-5. Summary of the basal $I_{CFP}/I_{YFP}$ ratio values detected in the ARVM transduced with RI_epac or RII_epac. ....	129
Figure 4-6. Summary of FRET measurements of cAMP levels in ARVM expressing RI_epac or RII_epac. ....	130

Figure 4-7. Summary of speed of FRET change ( $\Delta\text{FRET}/\Delta t$ ) after each stimuli. ....	131
Figure 4-8. The contribution of phosphodiesterases (PDEs) in ARVM transduced with RI_epac or RII_epac. ....	133
Figure 4-9. Summary of FRET change upon the selective inhibition of PDE2.....	134
Figure 4-10. Summary of FRET change upon the selective inhibition of PDE3.....	135
Figure 4-11. Summary of FRET change upon the selective inhibition of PDE4.....	137
Figure 4-12. Summary of experiments recording effect of selective PDE inhibition on ISO stimulation.....	138
Figure 5-1. Norepinephrine treatment induces hypertrophic growth in ARVM.....	147
Figure 5-2. Comparison of growth in control and NE treated ARVM. ....	148
Figure 5-3. Reactivation of the fetal gene program in NE treated ARVM. ....	149
Figure 5-4. Localisation of RI_epac and RII_epac FRET sensors in hypertrophic ARVM. ....	151
Figure 5-5. Summary of sensor localisation analysis. ....	153
Figure 5-6. . Representative example of a FRET experiment in hypertrophic cardiomyocytes transduced with the targeted cAMP sensors.....	154
Figure 5-7. Summary of the analysis of basal $I_{\text{CFP}}/I_{\text{YFP}}$ ratio value in control and hypertrophic ARVM expressing RI_epac or RII_epac.....	155
Figure 5-8. Summary of FRET measurements of cAMP signals in hypertrophic ARVM expressing RI_epac or RII_epac. ....	157
Figure 5-9. Summary of rate of FRET change ( $\Delta\text{FRET}/\Delta t$ ) after each stimuli. ....	159
Figure 5-10. Summary of FRET measurements of cAMP signals in control and hypertrophic ARVM expressing RI_epac or RII_epac upon addition of isoproterenol. ...	161
Figure 5-11. Summary of FRET measurements of cAMP production in control and hypertrophic ARVM expressing RI_epac or RII_epac upon addition of isoproterenol and IBMX. ....	162
Figure 5-12. Summary of FRET measurements of cAMP production in control and hypertrophic ARVM expressing RI_epac or RII_epac upon addition of isoproterenol, IBMX and forskolin. ....	163
Figure 5-13. The contribution of phosphodiesterases (PDEs) in control and hypertrophic ARVM transduced with RI_epac or RII_epac.....	165
Figure 5-14. Summary of basal cAMP levels in ARVM in the presence or absence of PDE2 inhibitor Bay 60-7550 (Bay) in the control and hypertrophic myocytes (NE).....	166
Figure 5-15. Summary of FRET change upon the selective inhibition of PDE2 in control and hypertrophic (NE treated) ARVM.....	168

Figure 5-16. Summary of basal cAMP levels in ARVM in the presence or absence of PDE3 inhibitor cilostamide (Cilo) in the control and hypertrophic (NE treated) ARVM.	169
Figure 5-17. Summary of FRET change upon the selective inhibition of PDE3 in control and hypertrophic (NE treated) ARVM.	170
Figure 5-18. Summary of basal cAMP levels in ARVM in the presence or absence of PDE4 inhibitor rolipram (Rol) in the control and hypertrophic (NE treated) ARVM.	171
Figure 5-19. Summary of FRET change upon the selective inhibition of PDE4 in control and hypertrophic (NE treated) ARVM.	172
Figure 5-20. cAMP hydrolysing activities of different PDE families in control and hypertrophic ARVM.	174
Figure 5-21. PDE2 mRNA and protein levels in control and hypertrophic ARVM.	176
Figure 5-22. PDE3A mRNA and protein levels in control and hypertrophic ARVM.	177
Figure 5-23. PDE4B mRNA and protein levels in control and hypertrophic ARVM.	178
Figure 5-24. PDE4D mRNA and protein levels in control and hypertrophic ARVM.	179
Figure 5-25. Localisation of PDE families in control and hypertrophic ARVM.	182
Figure 6-1. Summary of the effect of cGMP on the cAMP response to isoproterenol in PKA-RI and PKA-RII subcellular compartments.	190
Figure 6-2. Summary of the effect of cGMP on the cAMP response to ISO in PKA-RI and PKA-RII subcellular compartments after selective PDE inhibition.	193
Figure 6-3. Summary of the effect of cGMP on the cAMP response to ISO in PKA-RI and PKA-RII subcellular compartments in hypertrophic ARVM.	195
Figure 6-4. Schematic representation of the FRET-based cGMP sensors used in this study.	196
Figure 6-5. Summary of the basal ICFP/ IYFP ration values detected with the targeted cGMP sensors RI-Cygmt-2.1 and RII-Cygn-2.1.	197
Figure 6-6. Comparison of cGMP intracellular levels between control and hypertrophic ARVMs.	198
Figure 6-7. Summary of the investigation of $\beta_3$ -AR signalling in PKA-RI and PKA-RII compartments in control and hypertrophic ARVM.	201
Figure 7-1. Inhibition of PDE2 prevents hypertrophy induced by norepinephrine treatment in ARVM.	209
Figure 7-2. Overexpression of PDE2A2 causes hypertrophic growth in isolated ARVM.	211
Figure 7-3. Summary of FRET change in ARVM overexpressing PDE2A2dn.	213
Figure 7-4. . Summary of FRET change in hypertrophic ARVM overexpressing PDE2A2dn.	215

Figure 7-5. The anti-hypertrophic effects of PDE2 inhibition is PKG independent.....219

Figure 7-6. The anti-hypertrophic effects of PDE2 inhibition are PKA-dependent. ....220

Figure 7-7. cAMP increase due to forskolin, rolipram or cilostamide, but not Bay 60-7550 stimulation has pro-hypertrophic effects.....222

Figure 7-8. Inhibition of PDE3 or PDE4 did not affect NE-induced cardiomyocytes hypertrophic growth. ....223

# Acknowledgements

---

Firstly, I would like to thank my supervisor Prof Manuela Zacco for her advice, continued support and guidance during my PhD as well as for careful review of this thesis

I am grateful to all the past and present members of the Zacco lab, for their helpful discussions, encouragement, ideas and support over the past few years. In particular, I would like to thank Anna, Annetta, Alessandra, Frank and Craig. I have gained many valuable skills and techniques thanks to these people.

I would also like to thank John Craig who was very supportive in the final year of my PhD and assisted with the primary ARVM culture and adenovirus preparation when I was too busy to continue doing this alone.

Thanks to Fiona and Marie-Anne I now know everything there is to know about the latest celeb gossip or the ice hockey. You both were a pleasure to share an office with and I wish you both every success for the future. I was also like to recognise Ian for creating an enjoyable atmosphere in our office and at nights out...even after his retirement. I would especially like to thank him for reviewing this thesis.

During the final year of my PhD, I joined the Baillie lab. I would like to thank everyone for being so friendly and keeping me sane over these final few months with cake and banter until late in the evening. In particular I'd like to thank Krishna, Miranda, Jon and Ashleigh.

Lastly, I would like to thank my family and friends for their continued love and support. I would like to mention my fiancé David, my parents and Sister Nicole, who have all helped me overcome the difficult times and encouraged me at every step. I couldn't have done this without you.

## Abbreviations

$\beta$ -AR =  $\beta$ -adrenergic receptor

aa = amino acid

AC = adenylyl cyclases

AKAP = A Kinase anchoring proteins

ANOVA = analysis of variance

ANP= atrial natriuretic peptide

ATP = adenosine triphosphate

ARVM = adult rat ventricular myocytes

BNP= brain natriuretic peptide

bp = base pairs

CaM = calmodulin

cAMP = 3', 5' cyclic adenosine monophosphate

cGMP = 3', 5' cyclic guanosine monophosphate

CCD = charged-coupled device

CFP = cyan fluorescent protein

cGMP = 3', 5' cyclic guanosine monophosphate

CBD = cyclic nucleotide binding domains

CNB= Cyclic nucleotide-binding domains

CNG = Cyclic nucleotide-Gated Channels

CRE = cAMP response element

CREB = CRE binding protein

D/D = docking domain

DAG = diacylglycerol

DCM = dilated cardiomyopathy

DEP = Dishevelled, Egl-10, and Pleckstrin

ECC = excitation-contraction coupling

E.coli = Escherichia coli

EHNA = erythro-9-2-hydroxy-3-nonyl adenine

EPAC = exchange proteins directly activated by cAMP

FRET = fluorescence resonance energy transfer

GAP = GTPase-activating protein

GDP = guanosine diphosphate

GAF = cGMP-regulated cyclic nucleotide phosphodiesterase, certain adenylyl cyclases,  
and *E.coli* transcription factor Fh1A

GEFs = guanine nucleotide exchange factors

GFP = green fluorescent protein

GPCR = G protein-coupled receptors

GTP = guanosine triphosphate

HF = heart failure

IBMX = 3-isobutyl-1-methylxantine

IP3 = inositol-triphosphate

ISO = isoproterenol

MAP2 = microtubule associate protein 2

mRFP = monomeric red fluorescent protein

NA = numerical aperture

NE = norepinephrine

NFAT= nuclear factor of activated T-cells

NRVM = neonatal rat ventricular myocytes

OD = optical density

PDE = phosphodiesterase

PGE1 = prostaglandin E1

PIP3 = Phosphatidylinositol-trisphosphate

PKA = cAMP-dependent protein kinase

PKG = cGMP-dependent protein kinase

PKI = Protein Kinase Inhibitor

PP1 = proteins phosphatase 1

PP2A = protein phosphatase 2A

PPi = inorganic pyrophosphate

RA = Ras-association domain

REM = regulatory domain named Ras exchange motif

RT-PCR = Reverse transcription polymerase chain reaction

RyR = ryanodine receptor

sAC = soluble adenylyl cyclase

SEM = standard error of measurement or mean 18

SERCA = sarcoplasmic reticulum Ca<sup>2+</sup>-ATPase

TAC = thoracic aortic constriction

tmACs = trans-membrane adenylyl cyclases family

TnC = troponin C

TnI = troponin I

UCR= upstream conserved region

YFP = yellow fluorescent protein

# 1 Introduction

---

## 1.1 Signal transduction by cyclic nucleotides (concept of second messenger).

Signal transduction is the process by which information, provided externally to the cell in the form of hormones, ions, and other signalling molecules, is converted into intracellular information that regulates the internal function of the cell. This external stimulus acts as the “first messenger”, whereas an intermediate molecule, which transmits the signal from receptor to target inside the cell, is the “second messenger”. Many second messenger molecules are small and therefore diffuse rapidly through the cytoplasm, enabling signals to move quickly throughout the cell. By binding and activating protein kinases, channels or other proteins, second messengers mediate specific intracellular responses. The most studied second messengers are cyclic nucleotides, such as 3', 5' cyclic adenosine monophosphate (cAMP) and 3', 5' cyclic guanosine monophosphate; calcium ( $\text{Ca}^{2+}$ ) and phosphatidylinositol derivatives, such as phosphatidylinositol-trisphosphate (PIP3), diacylglycerol (DAG) and inositol-triphosphate (IP3), controlling the release of intracellular  $\text{Ca}^{2+}$  stores.

cAMP was first discovered by Dr. Earl W. Sutherland while studying phosphorylase, the enzyme responsible for the conversion of glycogen to glucose. The activity of this enzyme was increased by hormones, such as glucagon and norepinephrine (Sutherland and Cori 1951). While purifying phosphorylase from dog liver extracts, Sutherland found another enzyme which catalyses the inactivation of phosphorylase. Later this inactivating enzyme was confirmed as a phosphatase (Wosilait and Sutherland 1956). Further studies lead to the discovery that the activation/ inactivation of the phosphorylase were a result of an enzyme-catalysed phosphorylation-dephosphorylation reaction that required ATP and  $\text{Mg}^{2+}$ . The way in which AMP promoted phosphorylase activation was eventually elucidated

when Krebs and Fisher discovered phosphorylase kinase, an enzyme that phosphorylates phosphorylase (Krebs and Fischer 1956).

Sutherland and colleagues continued studying the effect of hormones on glycogen breakdown. Fractionation of the cells revealed this process was mediated by a heat stable factor which could activate phosphorylase (Berthet et al. 1957). This factor was identified as an adenine ribonucleotide that could be produced from ATP by the particulate fraction from different tissues, including liver, heart, skeletal muscle and brain (Rall and Sutherland 1958). The structure of this compound was reported by Lipkin et al. as adenosine 3'-5'-monophosphate (cyclic AMP or cAMP) (Lipkin 1959). By the early 1960s, cAMP, the synthetic activity (adenylyl cyclase) and the degrading activity (phosphodiesterase (PDE)) had been described. Moreover, the hormone receptors and adenylyl cyclase activity were found to be confined to membranes (Rall and Sutherland 1958; Sutherland and Rall 1958; Beavo and Brunton 2002).

Sutherland was awarded the 1971 Nobel Prize for “his discovery concerning the mechanism of the action of the hormones”, which would prove to be the first of five Nobel Prizes recognising research on this molecule. cAMP is now recognised as a universal regulator of cellular function.

## 1.2 cAMP signalling pathway

Cyclic adenosine monophosphate (cAMP) is a ubiquitous second messenger responsible for a huge number of cellular processes, including memory formation, cardiac frequency and strength of contraction, differentiation and gene transcription, cell growth and tumour genesis.

The generation of cAMP begins when an extracellular first messenger (neurotransmitter, hormone, chemokine, lipid mediator, or drug) binds to a G protein-coupled receptor (GPCR) on the plasma membrane. GPCRs are coupled to a stimulatory G protein (Gs) and ligand binding produces and exchange of GDP for GTP on the Gs protein resulting in the dissociation of the alpha subunit (G $\alpha$ s). As shown in Figure 1-1, the release of the G $\alpha$ s

subunit stimulates adenylyl cyclase (AC) to catalyse the cyclisation of ATP to generate cAMP and pyrophosphate (PPi).

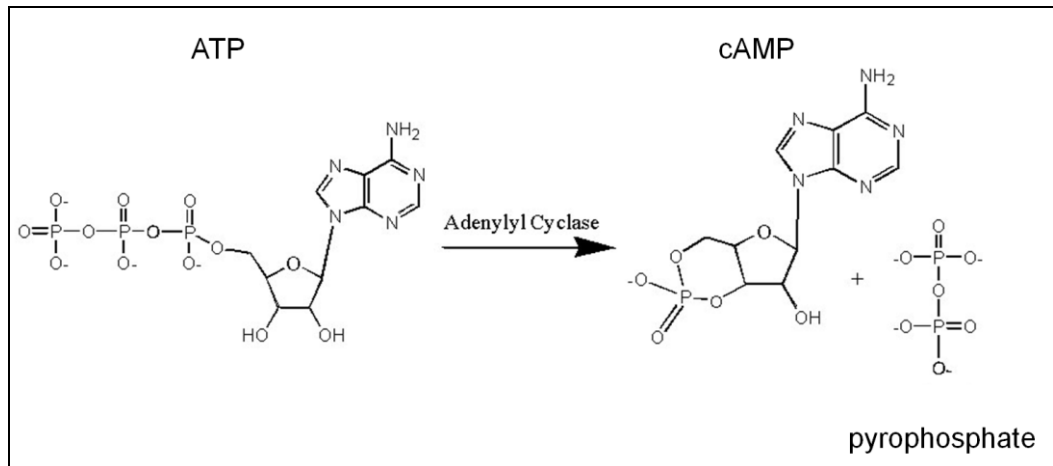


**Figure 1-1. The cyclisation of ATP to form cAMP.**

The intracellular level of cAMP depends on the balance between synthesis and degradation, thereby results from the activities of adenylyl cyclases (AC), the only enzymes that can generate cAMP, and phosphodiesterases (PDEs), the only enzymes capable of degrading cAMP into 5-AMP.

cAMP exerts its effects by the activation of a limited number of effectors. These are the cAMP-dependent protein kinase (PKA), the exchange proteins directly activated by cAMP (Epac1 and Epac2) and the cAMP-gated ion channels (CNG).

### 1.3 cAMP synthesis: Adenylyl Cyclases

Adenylyl cyclases (ACs) are ATP-pyrophosphate lyases that synthesise ATP to cAMP and pyrophosphate. To date there are 10 known AC isoforms that are differentially expressed in various cell types – nine membrane-bound isoforms (AC1-AC9) and one soluble form (sAC). Membrane-bound AC isoforms are large proteins of approximate 120–140 kDa that share a common secondary structure comprising of an intracellular N-terminus, that retains the regulatory properties of ACs, two repeats of a module composed of six transmembrane

spans (Tm1 and Tm2) separated by two large cytoplasmic domains (C1 and C2) (Figure 1-2). The overall similarity of the different adenylyl cyclases is ~ 60% and C1 and C2 contain a region of approximately 255- 330 amino acids that are highly conserved (C1a and C2a). On the contrary, the N- and C-terminal of C1 and C2 domains (C1b and C2b) are the most variable portions of the enzyme for all the AC isoforms (Sunahara et al. 1996). C1a and C2a dimerisation constitutes, in fact, the ATP-binding site. Within these motifs two aspartic acid residues coordinate two  $Mg^{2+}$  metal ions necessary for catalytic activity. These mediate the attachment of the ATP, promoting the cyclisation of the cAMP and the release of PPi (Cooper 2003).

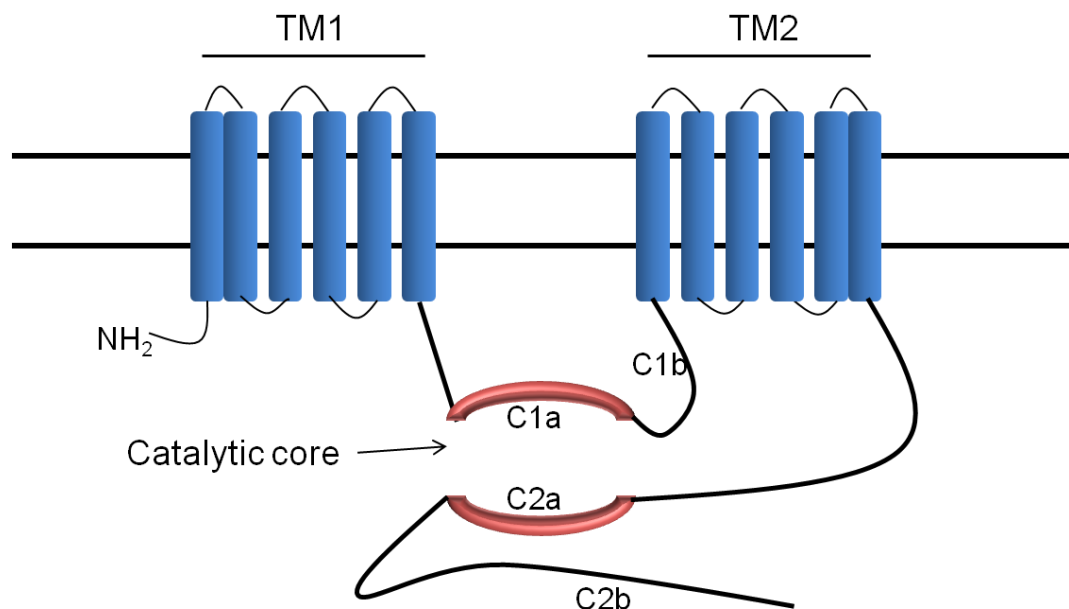


**Figure 1-2. Schematic representation of adenylyl cyclase. Adapted from (Willoughby and Cooper 2007).**

Although AC isoforms share a highly conserved secondary structure, these enzymes differ in tissue distribution (as shown in Table 1-1), as well as specific regulation. AC5 and AC6 are major isoforms in the heart, with AC5 being expressed in adult tissue and AC6 in fetal and adult cardiac tissue, AC1 and AC8 are mainly expressed in the brain, whereas AC2, AC4, AC7 and AC9 are widely expressed in multiple tissues (Defer et al. 2000).

**Table 1-1. Tissue distribution of ACs. Adapted from (Sadana and Dessauer, 2009).**

<b>AC Isoform</b>	<b>Tissue expression</b>
AC1	Brain, adrenal medulla
AC2	Brain, lung, skeletal muscle, heart
AC3	Olfactory epithelium, pancreas, brain, heart, lung, testis, BAT
AC4	Widespread
AC5	Heart, striatum, kidney, liver, lung, testis, adrenal, BAT
AC6	Heart, kidney, liver, lung, brain, testis, skeletal muscle, adrenal, BAT
AC7	Widespread
AC8	Brain, lung, pancreas, testis, adrenal
AC9	Widespread
sAC	Testis and detected in all tissues

All ACs, with the exception of sAC, are stimulated by the GTP-bound  $\alpha$  subunit of  $G_s$  ( $G_{sa}$ ), which are released from inactive heterotrimeric G-protein complexes after the agonist binds to the receptor. AC can also integrate signals from intracellular calcium, from other G-protein subunits, such as  $G_{\beta\gamma}$  and the inhibitory  $G_i$  and  $G_o$ , and from protein kinase C (PKC).

PKC can also regulate the activity of AC5 (Kawabe et al. 1994) and AC6 (group III) (Cheung et al. 2005). PKA-mediated phosphorylation inhibits the activity of AC5 and AC6 (Beazely and Watts 2006).

The key to regulation of AC is the interface between the C1 and C2 domains which forms a single ATP-binding site. Forskolin, a potent AC activator, stimulates AC1-AC8 and promotes the interaction between the two cytosolic domains (C1 and C2), resulting in formation of an active catalytic site (Zhang et al. 1997). Both forskolin and  $G_{sa}$  increase the affinity between the C1 and C2 domains by  $\sim 10$ -fold (Sunahara et al. 1997). Further studies suggest that  $G_{sa}$  and forskolin may induce a  $7^\circ$  rotation of the two domains that brings key catalytic elements from the two domains close to each other.

## **1.4 Cyclic nucleotide degradation: phosphodiesterases**

Phosphodiesterase (PDE) are a superfamily of phosphohydrolases that selectively catalyse the hydrolysis of the 3', 5' cyclic phosphate bonds of 3', 5'- adenosine monophosphate (cAMP) or 3', 5'- guanosine monophosphate (cGMP) to produce the corresponding 5'-nucleotide, 5'-AMP and 5'-GMP.

To date, 21 genes encoding PDEs have been identified in mammals. These genes transcribe multiple protein products by alternative splicing and/or the use of alternative promoters and it is estimated that this results in more than 100 different mRNA products, most of which can be translated into different proteins (Bender and Beavo 2006). The table below (Table 1-2) shows the 21 genes which have been categorised into 11 distinct families of PDEs (PDE1 – PDE11) based on their amino acid sequence, substrate selectivity, regulatory and pharmacological properties, and kinetics (Beavo 1995; Bender and Beavo 2006). Of the 11 PDE families, 3 selectively hydrolyse cAMP (PDEs 4, 7, and 8), 3 families are selective for cGMP (PDEs 5, 6, and 9), and 5 families hydrolyse both cyclic nucleotide with varying efficiency (PDE 1, 2, 3, 10, and 11) (Conti and Beavo 2007). PDEs 1, 2, 3, and 4 are expressed in many tissues, whereas others are more restricted. In most cells, PDE3 and PDE4 provide the major portion of cAMP-hydrolysing activity (Francis et al. 2011).

**Table 1-2. The families of phosphodiesterases, detailing specificity for either cAMP or cGMP. Adapted from (Mehats et al. 2002).**

PDE Family	Name	cAMP $K_m$ ( $\mu\text{m}$ )	cGMP $K_m$ ( $\mu\text{m}$ )
PDE1	Ca <sup>2+</sup> -CaM-stimulated	1–30	3
PDE2	cGMP-stimulated	30–100	10–30
PDE3	cGMP-inhibited	0.1–0.5	0.1–0.5
PDE4	cAMP-specific	0.5–4	>50
PDE5	cGMP-specific	>40	1.5
PDE6	Photoreceptor	2000	60
PDE7	cAMP-high affinity	0.2	>1000
PDE8	cAMP-high affinity	0.7	>100
PDE9	cGMP-high affinity	>100	0.07
PDE10	Dual substrate	0.5	3
PDE11	Dual substrate	1	0.5

The 11 families of mammalian PDEs all share a common structure (Figure 1-3), with a conserved catalytic domain (with 18%-46% sequence identity (Zhang et al. 2004)) of approximately 270 amino acids at the C-terminus, and regulatory domain, placed between the amino terminus and the catalytic domain.

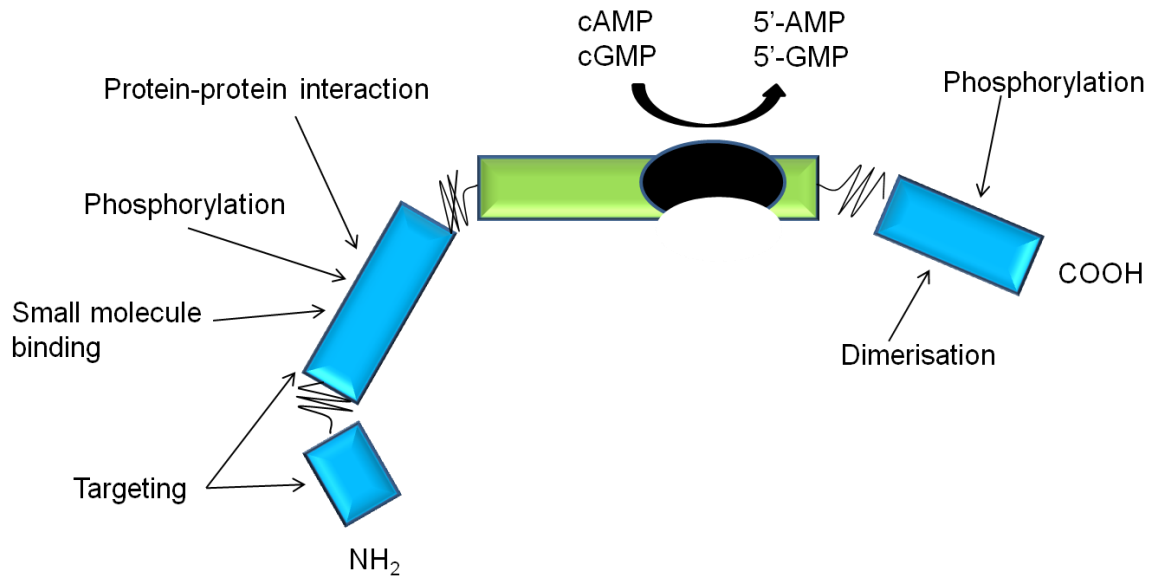


**Figure 1-3. Schematic representation of phosphodiesterase structure. Adapted from (Mehats et al. 2002).**

### 1.4.1 The catalytic domain

The functional structure of the catalytic domain, which constitutes the core of the PDE, is highly conserved in all PDEs, where the sequence of any catalytic domain family express between 25 to 51% amino acid sequence identity with any other (Francis et al. 2011). The x-ray crystallographic structure of the catalytic domain of nine families of PDEs has been resolved. The catalytic domains adopt a compact  $\alpha$ -helical structure, consisting of 15-17  $\alpha$ -helices, which can be divided into three sub-domains. These domains define a deep binding-pocket where the substrates (cAMP or cGMP) or inhibitors attach (Francis et al. 2011). Below this binding-pocket are two divalent metal binding sites ( $Zn^{+}$  and  $Mg^{2+}$ ). The metal binding site that binds zinc has two histidine and two aspartic acid residues that are absolutely conserved among all PDEs and are responsible for interaction with the cyclic nucleotide purine. Structural studies have revealed that the cyclic nucleotide specificity of the catalytic site depends largely on one particular invariant glutamine. This glutamine functions as the key specificity determinant by a “glutamine switch” mechanism, and stabilises the binding of the purine ring in the binding pocket through hydrogen bonds that form with either cAMP or cGMP or both, depending on the orientation of the glutamine

(Zhang et al. 2004). In one orientation the hydrogen bond (H-bond) network supports guanine binding leading to cGMP selectivity and in the other orientation the network supports adenine binding resulting in selectivity toward cAMP. In dual-specific PDEs a key histidine residue may enable the invariant glutamine to toggle between cAMP and cGMP (Zhang et al. 2004).

## 1.4.2 The Regulatory domain

Unlike the catalytic domain, the N-terminus regulatory domain is highly variable between PDEs, resulting in the unique characteristics of each PDE family. Of the several domains mapped to the N terminus, three types are present in multiple PDE families. These include domains for ligand binding, oligomerisation, kinase recognition/ phosphorylation, and regions that auto-inhibit the catalytic domain. Docking domains are also present at the N-terminus.

Numerous types of protein domains provide regulatory control over the catalytic domains. PDE2, PDE5, PDE6, PDE10 and PDE11 include at their N-terminal regulatory region two tandem protein domains named GAF (GAF-A and GAF-B). The acronym GAF is derived from cGMP-activated PDEs, **a**denylyl cyclase, and **F**h1A, enzymes where they were first documented (see Figure 1-4). GAF domains are known to function as regulatory elements that bind nucleotides or other small molecules. Studies investigating the crystal structure of the region of PDE2 containing its tandem GAF domains, have indicated that GAF-A is likely involved in dimerisation, whereas GAF-B is involved in cGMP binding (Martinez et al. 2002). In PDE5 and PDE6, cGMP binds to the GAF-A domain. PDE1 contains a Ca<sup>2+</sup>/calmodulin (CaM)-binding site. Binding of Ca<sup>2+</sup>/calmodulin to PDE1 induces a 10-fold increase in the enzyme V<sub>max</sub> without affecting affinity for the substrate (Conti and Beavo 2007). PDE4 has upstream conserved regions (UCRs), UCR1 and UCR2. UCR2 corresponds to an auto-inhibitory domain that negatively regulates PDE catalytic activity, while phosphorylation sites have been identified in the UCR1 region (Sette and Conti 1996; Houslay and Adams 2003).

PDE8 has a response regulator receiver (REC) domain and a per-arn-t-sim (PAS) domain. Like GAF domains, PAS domains are involved in ligand binding and protein-protein

interactions, and they share some structural similarities (Wang et al. 2008). PDE3, PDE7 and PDE9 have no available data on their oligomerisation state, although some indicate that they too exist as dimers (Huai et al. 2004; Scapin et al. 2004).

The other conserved types of regulatory domain at the N-terminus are phosphorylation sites. PDE1 isoforms A, B and C can be phosphorylated by PKA or CaM-kinase II (CaMKII), at the N-terminus. These phosphorylations decrease the binding and calmodulin induced activation *in vitro* (Florio et al. 1994). It has been reported that PDE2A can be phosphorylated by tyrosine kinase (Bentley et al. 2001). PDE3 has an amino-terminal transmembrane domain that contains six hydrophobic helices and numerous PKA and PKB phosphorylation sites; PKB-mediated phosphorylation of PDE3B increases the catalytic activity of the enzyme (Kitamura et al. 1999; Zmuda-Trzebiatowska et al. 2006). At the N-terminus of UCR1 of all long forms of PDE4, there is a highly conserved motif (RRESF), that can be phosphorylated by PKA and thus leading to increased catalytic activity of the enzyme (Sette and Conti 1996). cGMP binding to the GAF domain of PDE5, increases the accessibility of the Ser 92/102 residue and promotes PKG-mediated phosphorylation. This phosphorylation then activates the catalytic domain and decreases the  $K_m$  for the substrate (Bessay et al. 2007).

Some PDEs possess also auto inhibitory domains, PDE6 for example has an inhibitory subunit ( $P\gamma$ ) whose affinity for the enzyme is enhanced by the binding of cGMP to the GAF domains (Cote 2004). PDE7 and PDE9 have no identified specific protein domains. Phosphorylation or prenylation sites have been described at the C-terminal domains of some PDEs; however, nothing is yet known about the function of these C-terminal regions of PDEs (Conti and Beavo 2007).

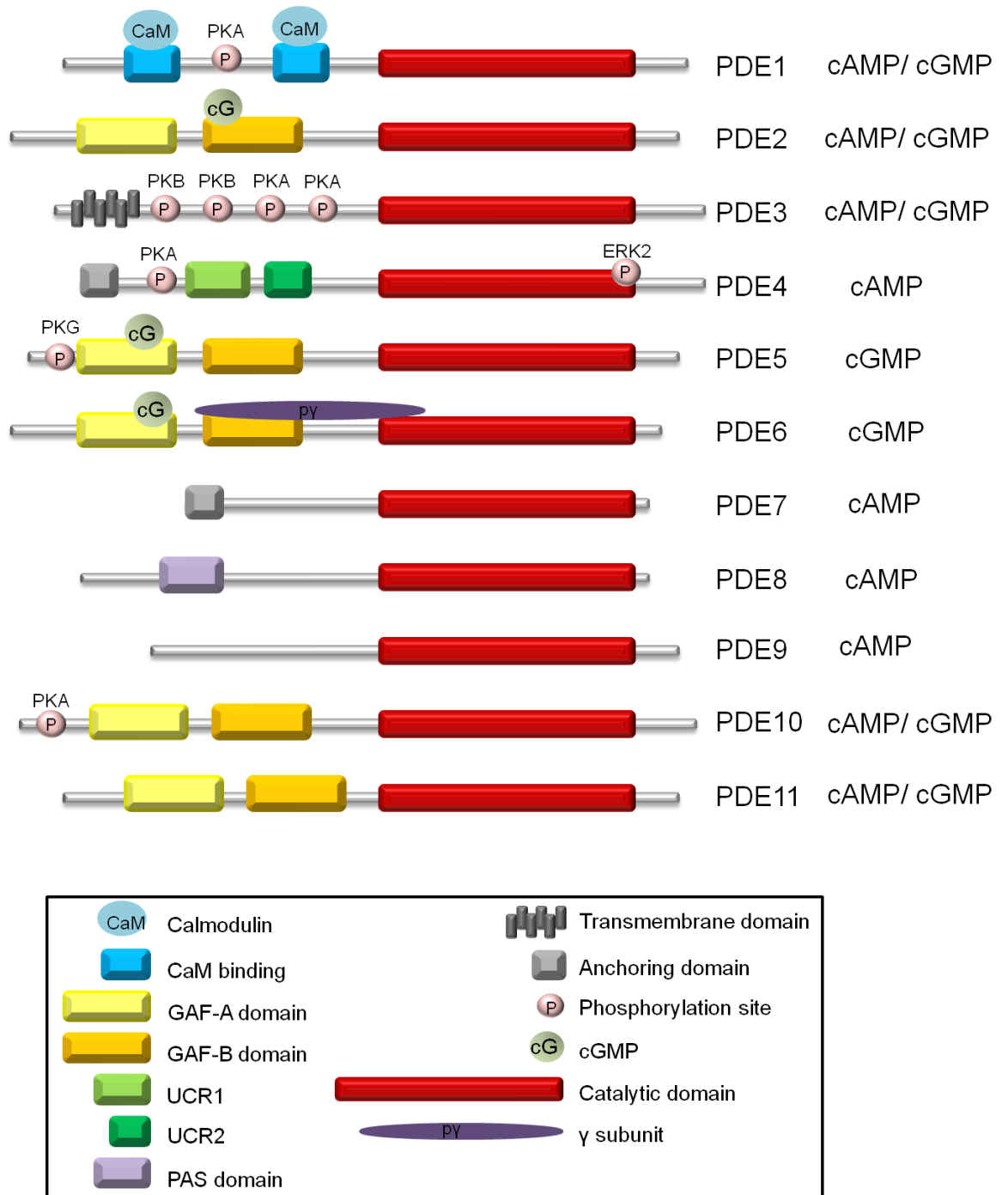


Figure 1-4. Schematic representation of the structures of the mammalian phosphodiesterase (PDE) families. Adapted from (Conti and Beavo 2007).

## 1.5 Effectors of cyclic nucleotides

### 1.5.1 PKA

Protein kinase A (PKA) was the first effector of cAMP to be identified. It was originally isolated in the laboratory of Ed Krebs in 1968, and is considered to be the principal cellular receptor for cAMP (Walsh et al. 1968). Under basal conditions, PKA is a heterotetramer composed of two catalytic (C) subunits non-covalently bound to a regulatory (R) subunit dimer. cAMP binds cooperatively to two sites, termed A and B, on each R subunit, however in PKAs inactive form, only the B site is available for binding. When site B is occupied by cAMP, the binding of cAMP to the A site is enhanced. Binding of four cAMP molecules, two to each R subunit, leads to a conformational change and dissociation into an R subunit dimer with four cAMP molecules bound and two C monomers. Active catalytic subunits are then free to phosphorylate Serine and Threonine residues in target proteins (Krebs and Beavo 1979; Taylor et al. 1990; Smith et al. 1999; Taylor et al. 1999; Kopperud et al. 2002; Tasken and Aandahl 2004).

The C subunit isoforms (C $\alpha$ , C $\beta$  and C $\gamma$ ) have indistinguishable kinetic and biochemical properties (Buechler and Taylor 1990; Taylor et al. 1990). In contrast, the two classes of R subunits (type I: isoforms RI $\alpha$ , RI $\beta$ , and type II: isoforms RII $\alpha$ , RII $\beta$ ) show different functional and biochemical properties. PKA holoenzymes are classified as either type I or type II, depending on the subtype of regulatory subunit present. PKA type-I is more readily dissociated by cAMP than PKA type-II (showing a  $K_{act}$  of 50-100 nM and 200-400 nM, respectively) (Dostmann et al. 1990; Cummings et al. 1996). R isoforms are differentially expressed in tissues and their subcellular distribution also appears to be distinct. PKA-RII is predominately associated with cellular structures and organelles as it has the ability to bind to A kinase anchoring proteins (AKAPs) (Wong & Scott 2004). Traditionally, PKA-RI was thought to be mainly cytosolic (Corbin and Keely 1977). However, it has been shown that PKA-RI also binds to AKAPs, although with a lower affinity than PKA-RII (Colledge and Scott 1999). Dual specific AKAPs have been described (Huang et al. 1997) as well as RI-selective AKAPs (Angelo and Rubin 1998).

Intracellular localisation of PKA is mediated by the N-terminal dimerisation/ docking (D/D) domain of the R-subunits. The Figure below (Figure 1-5) illustrates the regulatory

subunits of PKA with a D/D domain, followed by a PKA inhibitor site and two tandem cAMP binding domains (CBDs) (Heller et al. 2004). Structural studies have indicated that the RII subunits dimerise at the NH<sub>2</sub> terminus in an anti-parallel fashion forming a four-helix bundle motif which is necessary for both AKAP binding and dimerisation (Newlon et al. 1999; Newlon et al. 2001). The first 23 amino acids in the D/D domain sequence of the RII subunit are reported to be involved in AKAP binding. Deletion of the 1-5 sequence in PKA-RII abolishes the AKAP binding without interfering with the dimer formation (Hausdorff et al. 1990; Hausken et al. 1994). Anchoring of PKA occurs through an amphipathic helical motif of 14–18 amino acid residues present in the AKAP and a hydrophobic groove formed on top of the NH<sub>2</sub> terminal helices at the D/D domain (Newlon et al. 1999). The PKA-RI D/D domain contains a similar helix bundle formation; however the dimerisation motif of RI is shifted further from the NH<sub>2</sub> terminus and involves amino acids 12 to 61. It is thought that the NH<sub>2</sub> terminus in RI is helical and folds back onto the four-helix bundle and has a Y-like shape as opposed to the X-like shape of the RII motif, and thus may contribute to differences in AKAP binding specificity. (Banky et al. 1998; Banky et al. 2000).

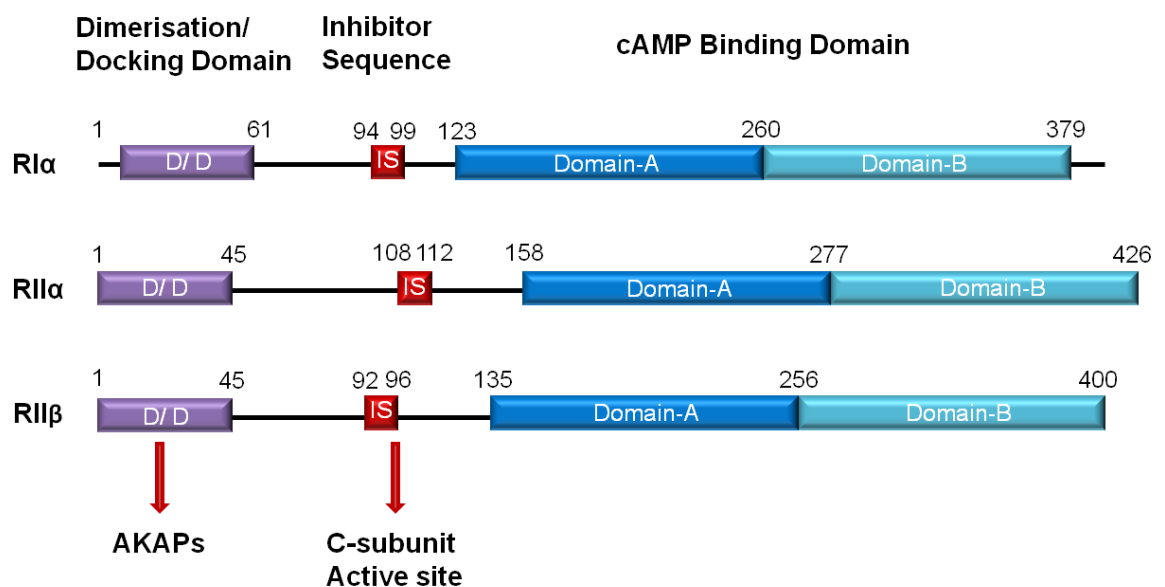


Figure 1-5. Regulatory subunits of protein kinase A (PKA).

**Subunits present a dimerisation/docking domain (D/D) (responsible for binding to A-Kinase Anchoring Proteins (AKAPs)), an inhibitory site (IS) and two cAMP binding domains (Domain A and Domain B). Adapted from (Taylor et al. 2008).**

## 1.5.2 Epac

The exchange proteins activated by cAMP (Epacs) were first discovered in 1998, when de Rooij and colleagues showed that the small GTPase Rap1 could be activated by cAMP independently of PKA. They discovered a new protein containing a cAMP-binding site and similar to that of GEFs (guanine-nucleotide-exchange factor) for Ras and Rap1 (de Rooij et al. 1998).

The small G protein Rap, which is part of the larger Ras family, switches between the inactive guanosine diphosphate (GDP), bound state and the active guanosine triphosphate (GTP) bound state. cAMP-dependent activation of Epac promotes the exchange of GDP for GTP, hence switching on the Rap GTPases. Epac represents a crucial intracellular effector for cAMP and is responsible for many of its effects from cardiac contraction through regulation of some calcium channels in cardiomyocytes and permeability of vascular epithelium to insulin secretion in pancreatic beta cells (Bos 2003; Ruiz-Hurtado et al. 2013). In cardiac myocytes, Epac signalling increases Cx43 (connexin43) recruitment at cell–cell contact and enhances adherens junctions formation which is a prerequisite for gap junction (GJ) assembly which mediates electrical excitation (Somekawa et al. 2005).

Following  $\beta$ -AR ( $\beta$ -adrenergic receptor) stimulation, a Epac/Rap/PLC $\epsilon$ /PKC $\epsilon$ /CaMKII (Ca<sup>2+</sup>/calmodulin-dependent protein kinase II) signalling pathway regulates SR (sarcoplasmic reticulum) Ca<sup>2+</sup> release in mouse cardiac myocytes (Oestreich et al. 2007).

In rat ventricular myocytes, acute stimulation with Epac-specific cAMP analogue 8-pCPT-2'-O-Me-cAMP induces a decrease in the [Ca<sup>2+</sup>]<sub>i</sub> transient amplitude and this is correlated with an increase in cardiac myocyte contraction via PLC-, PKC- and CaMKII-dependent phosphorylation of sarcomeric proteins such as cardiac myosin-binding protein C (MBP-C) and troponin (Pereira et al. 2007; Cazorla et al. 2009).

Two variants of Epac have been identified, Epac1 and Epac2 (see Figure 1-6), which are present in most tissues with varying levels of expression. Epac1 and Epac2, are encoded by two distinct genes, RAPGEF3 and RAPGEF4 (de Rooij et al. 1998; Kawasaki et al. 1998)

and contain an N-terminal regulatory domain that has one (Epac1) or two (Epac2) cyclic nucleotide-binding domain (CNB) domains and a DEP (Dishevelled, Egl-10, and Pleckstrin) region, known to be involved in membrane localisation (de Rooij et al. 2000). The relevance of the additional CNB domain in Epac2 is unknown. This domain does bind cAMP, but with lower affinity than the other CNB domain. Moreover, its deletion does not affect auto-inhibition or the binding of cAMP to the other CNB domain (de Rooij et al. 2000).

The C-terminal catalytic region activates Rap1. This region is comprised of the enzymatic GEF domain, CDC25-homology domain (HD) and the Ras exchange motif (REM), which is required for stability of the GEF domain. An additional Ras-association domain (RA) lies between REM and CDC25-HD domains (de Rooij et al. 1998; de Rooij et al. 2000). The regulatory region at the N-terminal domain of Epac is an auto-inhibitory domain that blocks GEF activity. In the inactive conformation, Epac is folded and the regulatory domain inhibits the Rap association to the catalytic site preventing Rap binding to the CDC25-HD. Binding of cAMP to Epac induces a conformational changes, unfolding the protein and releasing the auto-inhibitory effect of the regulatory region, exposing the catalytic domain resulting in Rap activation (Rehmann et al. 2006).

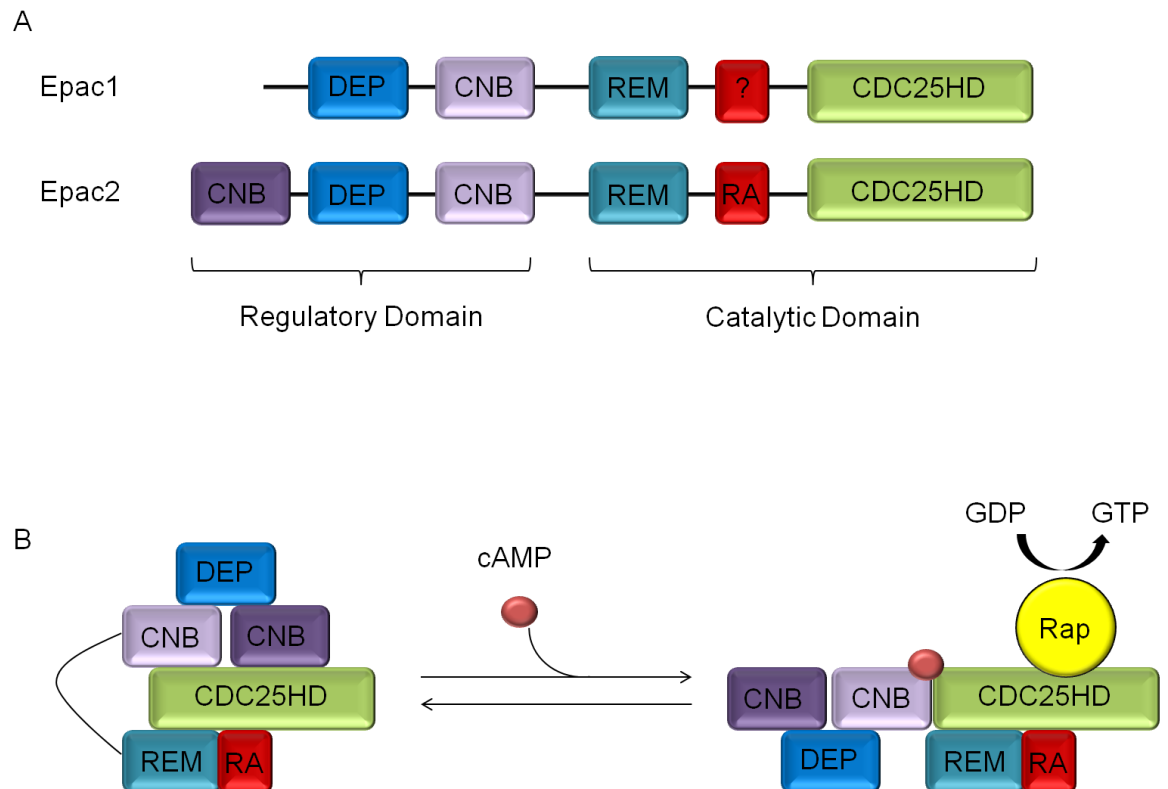


**Figure 1-6. The multi domain structure of Epac.**

**(A) Domain structure of Epac1 and Epac2, signifying the regulatory region with the cyclic nucleotide-binding domain(s) (CNB) and the catalytic region with the CDC25-homology domain (CDC25HD) responsible for the guanine-nucleotide-exchange activity. The Desheveled-Egl-10-Pleckstrin (DEP) domain is involved in membrane localisation, the Ras exchange motif (REM) stabilises the catalytic helix of CDC25HD and the Ras-association (RA) domain is a protein-interaction motif. (B) Schematic activation of Epac2 by cAMP results in a conformational change and enables the interaction with Rap and, consequently, the conversion of RapGDP to RapGTP. Adapted from (Bos 2006).**

### 1.5.3 CNG

Cyclic nucleotide-gated channels (CNG) are ion channels, belonging to the superfamily of voltage-gated ion channels, which are activated by cAMP or cGMP binding. Cyclic nucleotides regulate the opening of these channels by binding directly to a conserved cyclic nucleotide-binding (CNB) domain on the channel (Yu et al. 2005). Binding induces a conformational change that serves to open the channel pore. CNG channels are cation channels, and allow the flow of  $\text{Na}^+$ ,  $\text{K}^+$  and  $\text{Ca}^{2+}$  ions across membranes, thus converting

cyclic nucleotide signals into changes in membrane potential and intracellular calcium levels.

CNG channels were first identified in cone photoreceptors (Haynes and Yau 1985) in olfactory sensory neurons (OSNs) (Nakamura and Gold 1987) and in the pineal gland (Dryer and Henderson 1991). CNG channels are also present at high levels in the sinoatrial node and conduction system of the heart, where they are involved in the control of cardiac automaticity (Baruscotti et al. 2010).

## 1.6 cAMP signalling in the heart

cAMP/ PKA signalling mediates the sympathetic control of excitation-contraction coupling (ECC) in cardiomyocytes. ECC is the process in which electrical excitation of the cardiomyocytes is coupled to contraction and relaxation of the heart (Bers 2008).

Calcium ( $\text{Ca}^{2+}$ ) is a key mediator of the ECC process. During the cardiac action potential (AP) and membrane depolarisation,  $\text{Ca}^{2+}$  entry through L-type  $\text{Ca}^{2+}$  channels (L-TCC) triggers the  $\text{Ca}^{2+}$ -induced  $\text{Ca}^{2+}$  release (CICR) from the sarcoplasmic reticulum (SR), a specialised intracellular  $\text{Ca}^{2+}$  store. Increasing  $I_{\text{Ca}}$  via L-TCC leads to a local increase in  $\text{Ca}^{2+}$  in a region where the SR is in close proximity to the sarcolemma and where ryanodine receptors (RyR) are localised. The local rise in  $\text{Ca}^{2+}$  concentration triggers the release of large concentrations of stored  $\text{Ca}^{2+}$  from the SR into the cytosol via RyR.

$\text{Ca}^{2+}$  influx and release lead to an increase of the intracellular  $\text{Ca}^{2+}$  concentration, allowing  $\text{Ca}^{2+}$  to bind to the myofilament protein troponin C (TnC), resulting in cardiac contraction (Bers 2008). In order for the bound  $\text{Ca}^{2+}$  to dissociate from TnC and the cardiac muscle to relax (lusitropy) the cytosolic concentration of  $\text{Ca}^{2+}$  must decline. This is mainly achieved by the SR Ca ATPase (SERCA), which pumps  $\text{Ca}^{2+}$  back into SR, and the sarcolemmal  $\text{Na}^+/\text{Ca}^{2+}$  exchange (NCX), which removes  $\text{Ca}^{2+}$  from the myocyte (Bers and Guo 2005).

Regulation of cAMP/ PKA signalling is crucial for the appropriate catecholamine-mediated modulation of cardiac contractility (Bers 2008). As shown in Figure 1-7,  $\beta$ -ARs stimulation activates ACs to generate cAMP; cAMP in turn activates PKA. PKA then phosphorylates several proteins involved in the ECC process such as L-

TCC, RyR, troponin I (TnI), myosin binding protein C (MBP-C) and phospholamban (PLB).

PKA mediates the phosphorylation of L-TCCs and RyRs, increasing the open probability of the channels and thus increasing  $\text{Ca}^{2+}$  influx into the cell. PKA phosphorylation of these targets increases the amount of  $\text{Ca}^{2+}$  released from the SR, and as a result, a larger amount of  $\text{Ca}^{2+}$  ions are available for sarcomere contraction at systole (Bers and Guo 2005).

The lusitropic effect occurs upon PKA phosphorylation of TnI, PLB and MBP-C.

Phosphorylation of TnI reduces the sensitivity of the sarcomeric myofilaments to  $\text{Ca}^{2+}$  and encourages the rapid dissociation of  $\text{Ca}^{2+}$  from the myofilaments (Zhang et al. 1995). Both TnI and MCB-P play an imperative role in modulating the crossbridge cycling in heart muscle (Winegrad 1999). PLB exhibits an inhibitory effect on the transport of  $\text{Ca}^{2+}$  by the SERCA pump. When PLB is closely associated with SERCA, the rate of  $\text{Ca}^{2+}$  transport is reduced. PKA phosphorylation of PLB dissociates it from SERCA, blocking the inhibitory effect of PLB (Verboomen et al. 1992), resulting in a more efficient  $\text{Ca}^{2+}$  re-uptake in the SR and results in relaxation.

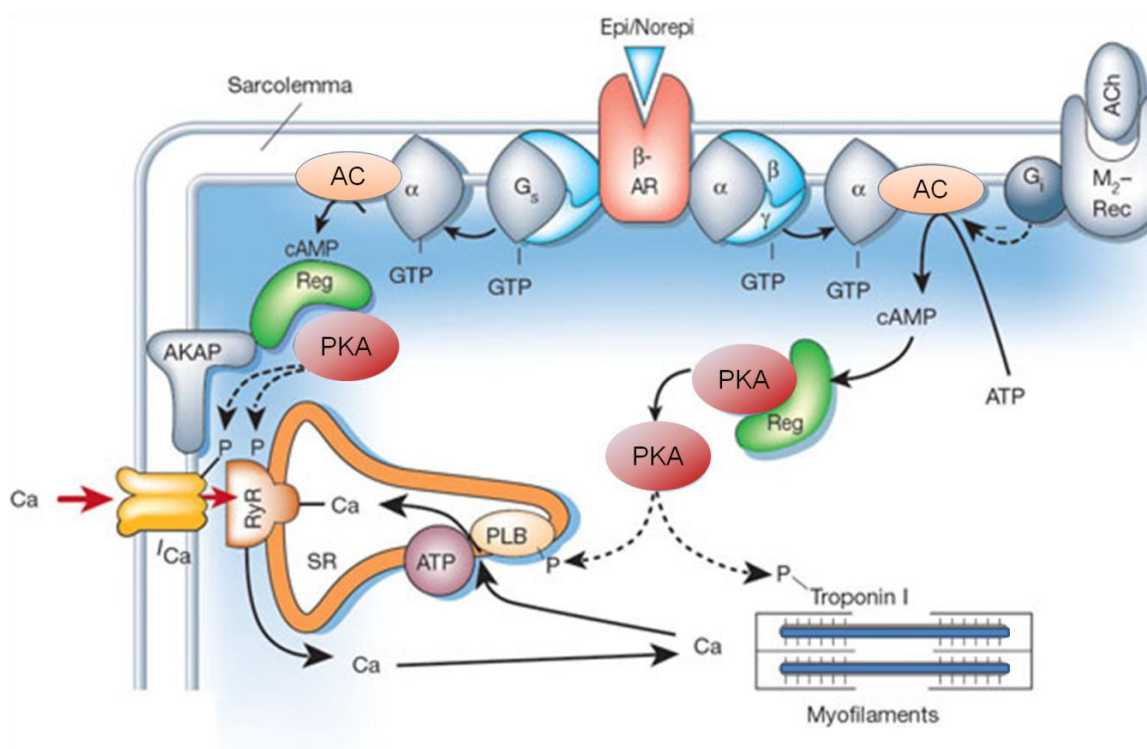


**Figure 1-7. Activation of  $\beta$ -adrenergic receptors triggers the PKA-mediated phosphorylation of several targets involved in the excitation-contraction coupling (ECC) process.** (AC, adenylyl cyclase; ACh, acetylcholine; AKAP, A kinase anchoring protein;  $\beta$ -AR,  $\beta$ -adrenergic receptor; M<sub>2</sub>-Rec, M<sub>2</sub>-muscarinic receptor; PLB, phospholamban; Reg, PKA regulatory subunit; SR, sarcoplasmic reticulum). Adapted from (Bers 2002).

It has also been demonstrated that cAMP-activated PKA controls the frequency of contraction by phosphorylation of ryanodine receptors and other Ca<sup>2+</sup>-cycling proteins in the sino-atrial node (SAN), leading to altered calcium cycles and increased diastolic currents through Na<sup>+</sup>/Ca<sup>2+</sup> exchangers (Lakatta et al. 2010).

Pacemaker activity in the heart originates in the SAN. Myocytes in the SAN produce spontaneous action potentials; these propagate, through specialised conduction systems, first to the atria and then to the ventricles, and thus drive cardiac rhythmic contraction. It has been shown that spontaneous diastolic depolarisation of SAN cells initiate action potentials to set the rhythm of the heart. This mechanism of spontaneous depolarisation has traditionally been attributed to a "voltage clock" mechanism, mediated by voltage-sensitive membrane currents, such as the hyperpolarisation-activated pacemaker current (I<sub>f</sub>) regulated by cyclic adenosine monophosphate (cAMP) (Brown et al. 1979). This current is also referred to as a "funny" current because, unlike the majority of voltage-sensitive

currents, it is activated by hyperpolarisation rather than depolarisation. The funny channel becomes activated at the end of the action potential (at voltages from -40/-50 mV to -100/-110 mV), which corresponds to the range in which diastolic depolarisation occurs. The funny channel then depolarises the membrane to a level at which L-type  $\text{Ca}^{2+}$  channels open to initiate the upstroke in the SA node action potential.  $I_f$  is a mixed  $\text{Na}^+$ - $\text{K}^+$  inward current activated by hyperpolarisation and modulated by the autonomic nervous system (DiFrancesco 1985; DiFrancesco et al. 1986).

The f-channels are encoded by the hyperpolarisation-activated, cyclic nucleotide-gated (HCN) channel gene family. These are intermembrane proteins that serve as non-selective ligand-gated cation channels in the plasma membranes of heart cells. Of the four known HCN subunits, HCN4 is the most highly expressed in the mammalian SAN (Ishii et al. 1999; Liu et al. 2007). cAMP exerts its modulatory effects on the  $I_f$  current by directly binding to HCN channels (DiFrancesco and Tortora 1991). This is more likely to occur when channels are in the open state and binding of cAMP to the channel stabilises this open configuration. This mechanism results in a shift of the  $I_f$  activation curve to more positive voltages, accelerates activation and slows deactivation kinetics. Point mutations of HCN4 are associated with baseline sinus bradycardia, though the maximum heart rate achieved during exercise is normal (Nof et al. 2007). This implies that  $I_f$  is not the only mechanism of SAN automaticity, especially during sympathetic activation.

Recently, spontaneous  $\text{Ca}^{2+}$  release from the sarcoplasmic reticulum (SR) has been suggested to modulate sinus rhythm (Vinogradova et al. 2005). When the SR is full, the probability of spontaneous  $\text{Ca}^{2+}$  release increases. Because the SR  $\text{Ca}^{2+}$  content is controlled in part by the membrane voltage, it is important to recognise that the activation of the  $\text{Ca}^{2+}$  clock and the membrane ionic clock are interdependent. Lakatta et al. proposed that the  $\text{Ca}^{2+}$  clock is manifested by spontaneous, but precisely timed, rhythmic, local  $\text{Ca}^{2+}$  releases from sarcoplasmic reticulum (SR) that appear shortly before firing of the next AP (Bogdanov et al. 2001; Vinogradova et al. 2002; Vinogradova et al. 2006). The elevated  $\text{Ca}_i$  activates NCX inward current causing diastolic depolarisation, which co-ordinately regulates the sinus rate along with the voltage clock. PKA-dependent phosphorylation of proteins that regulate cell  $\text{Ca}^{2+}$  balance and spontaneous SR  $\text{Ca}^{2+}$  cycling, ie, PLB and L-TCC, controls the phase and size of SR  $\text{Ca}^{2+}$  release, NCX current and thus is crucial for pacemaker function (Vinogradova et al. 2006).

Therefore cAMP regulation of ECC results in an increase in contractile force and frequency of the heart in response to acute catecholamine exposure. However, prolonged catecholamine stimulation of the cAMP pathway results in detrimental effects such as cardiac remodelling, cardiac hypertrophy and the development of heart failure which is accompanied by a marked down-regulation of  $\beta_1$ -AR expression and thus a significant desensitisation of the heart to inotropic  $\beta$ -adrenergic stimulation (Fowler et al. 1986; Engelhardt et al. 1999; Lohse et al. 2003; Barry et al. 2008).

Both  $\beta_1$ - and  $\beta_2$ -ARs are expressed in cardiac myocytes and mediate an increase in contractility via  $G_s$ -dependent coupling to adenylyl cyclase to generate cAMP (Xiao and Lakatta 1993). However,  $\beta_2$ -ARs can also couple to signalling pathways independent of cAMP or  $G_s$  and, in particular, to a pertussis toxin (PTX)–sensitive pathway mediated by  $G_i$ . Overexpression of  $\beta_2$ -AR in transgenic mice resulted in a limited contractile response due to  $G_i$  signalling (see 1.10.1.3), which inhibits adenylyl cyclase (Milano et al. 1994). Only when  $G_i$  proteins were inactivated by PTX treatment did these animals with overexpressed  $\beta_2$ -ARs fully stimulate contractility (Xiao and Lakatta 1993). In addition to this, activation of  $G_i$  has the potential to couple  $\beta_2$ -ARs to other important signalling pathways, such as the MAP kinases (Daaka et al. 1997).

It has been reported that selective stimulation or transgenic overexpression of  $\beta_2$ -AR coupled to cAMP, does not lead to hypertrophy, cardiomyocyte apoptosis and heart failure (Milano et al. 1994; Communal et al. 1999). Communal and colleagues measured apoptosis using flow cytometry and terminal deoxynucleotidyl transferase (TdT)–mediated nick end-labelling (TUNEL) staining in isolated adult rat ventricular myocytes (ARVM) and found that  $\beta$ -AR–stimulated apoptosis was abolished by the  $\beta_1$ -AR–selective antagonist but was potentiated by the  $\beta_2$ -AR–selective antagonist. The effect of  $\beta_2$ -AR was found to be mediated by  $G_i$  and the authors suggest that  $\beta_2$ -AR stimulation may even be protective (Communal et al. 1999). A number of other studies have confirmed protective and anti-apoptotic effect of  $\beta_2$ -AR stimulation via  $G_i$  (Ahmet et al. 2004; Ahmet et al. 2005). Chesley et al. demonstrate that  $\beta_2$ -ARs activate a PI3K–dependent, pertussis toxin–sensitive signalling pathway in neonatal rat cardiac myocytes that is required for protection from apoptosis-inducing stimuli (Chesley et al. 2000).

cAMP signalling via Epac seems to be one of the key factors downstream of chronic catecholamine stimulation of  $\beta_1$ -ARs, which mediates the development of cardiac

hypertrophy via the activation of the pro-hypertrophic gene transcription and via the activation of CaMKII (see 1.10.1) (Metrich et al. 2008; Breckler et al. 2011). Metrich and co-workers demonstrated that Epac1 expression is increased in the hearts of thoracic aortic constriction (TAC) treated rats. ARVM isolated from these animals displayed exaggerated cellular growth in response to Epac activation. This response involved the small GTPase Ras, the phosphatase calcineurin, and  $\text{Ca}^{2+}$ /calmodulin-dependent protein kinase II rather than its classic effector, Rap1 (1.5.2) (Metrich et al. 2008). Although these effects were shown to be PKA-independent, PKA does play a major role in a number of hypertrophy models associated with chronic catecholamine stimulation and activation of the cAMP pathway (discussed in detail in 1.10.1.4).

In cardiac myocytes, a variety of proteins other than those involved in the ECC process, are also affected by cAMP and PKA phosphorylation. These proteins include metabolic enzymes and transcription factors (Muller et al. 2001; Sheridan et al. 2002). Moreover,  $\beta$ -ARs are not the only receptors that signal via cAMP and activation of PKA; many other GPCRs whose activation leads to cAMP production are expressed in cardiomyocytes. The result is that an overabundance of chemical signals will propagate responses in the heart, some of which will lead to the generation of cAMP and activation of PKA. This raises the question of how myocytes can translate the multiple signals generated in response to individual extracellular stimuli appropriately, so to achieve the required functional outcome, while avoiding off-target phosphorylation and unwanted effects.

## **1.7 Compartmentalisation of cAMP/ PKA signalling in cardiomyocytes.**

The cAMP/ PKA pathway mediates a large number of extracellular signals and is responsible for a large variety of physiological effects. cAMP is a small and hydrophilic molecule and has been defined as a ‘long range’ second messenger (Kasai and Petersen 1994) as it has the potential to quickly diffuse within the intracellular environment. Thus property of cAMP, however, raises the question of how a second messenger that can rapidly fill the entire cell can avoid non-selective activation of all the PKA subsets present in the cell and maintain fidelity of response. As cells can respond specifically to different

extracellular stimuli that signal via cAMP, therefore there must be some mechanism to maintain specificity of cAMP/ PKA signalling and prevent phosphorylation of unsuitable targets upon GPCR stimulation. A number of studies conducted over recent years have proposed that accuracy of signalling in this pathway is due to compartmentalisation of cAMP and of the other molecular components involved in signal propagation (Kasai and Petersen 1994; Fischmeister et al. 2006; Lissandron and Zaccolo 2006; Vandecasteele et al. 2006; Zaccolo et al. 2006; Zaccolo 2009). This concept is based on the idea that cAMP is generated in different and distinct compartments, thus making the cyclic nucleotide available for activation of only a limited subset of PKA enzymes, with the subsequent phosphorylation of only a defined number of substrates.

The first evidence in support of the hypothesis of compartmentalisation of cAMP signalling came from experiments performed more than 30 years ago by Brunton and co-workers in isolated perfused hearts (Brunton et al. 1979) and in primary ventricular myocytes (Buxton and Brunton 1983). They observed that isoproterenol (ISO), a specific agonist of  $\beta$ -adrenergic receptors, and prostaglandin E1 (PGE1) elevated intracellular cAMP to comparable levels, yet the two stimuli caused the activation of different pools of PKA in cardiomyocytes. PGE1 activated PKA present in the soluble fraction of the cells, whereas ISO activated subsets of PKA in both the soluble and particulate fractions (Brunton et al. 1979; Buxton and Brunton 1983). Further investigation demonstrated that ISO caused phosphorylation of phosphorylase kinase (Keely 1977), TnI (Brunton et al. 1979) and several other PKA phosphorylation targets, whereas no changes in these substrates was observed upon PGE1 stimulation (Hayes et al. 1979). Based on these observations, it was postulated that not only PKA is targeted to specific locations within the myocyte, but also that different pools of cAMP must coexist within the cell.

More recently, Jurevicius and colleagues combined whole-cell patch-clamp recordings and a double capillary for extracellular microperfusion to study subcellular compartmentation upon  $\beta$ -AR stimulation of the L-TCC currents. The authors inserted the two capillaries at two positions, separated by a 5 $\mu$ m thin wall, in a sealed frog ventricular myocyte. They reported that a local application of a saturating concentration of ISO (1  $\mu$ M) caused local activation of  $I_{Ca}$  (non-maximal increase was detected), whereas local application of 30 $\mu$ M forskolin (a non-selective AC activator) caused maximal activation of  $I_{Ca}$  throughout the cell (Jurevicius and Fischmeister 1996). Dose response curves indicated that ISO induced a 40-fold, higher cAMP concentration close to the  $Ca^{2+}$  channels, in the part of the cell

exposed to the stimuli, than it did in the rest of the cell, whereas forskolin only induced a 4-fold increase. cAMP compartmentalisation was disrupted upon addition of 3-isobutylmethylxanthine (IBMX), a non-selective PDE inhibitor. Jurevicius and Fischmeister concluded that  $\beta$ -ARs are functionally coupled to nearby  $\text{Ca}^{2+}$  channels via local elevations of cAMP and that PDE activity may be responsible for limiting the rise of cAMP.

### **1.7.1 Compartmentalisation of PKA by A-kinase anchoring proteins**

It has been established that the specificity of cAMP signal transduction is achieved, in part, by spatial control of its main effector PKA. If PKA is in close proximity of its targets there is a greater chance of phosphorylation of the intended protein. The identification of A-kinase anchoring proteins (AKAPs) has confirmed that the spatial control of PKA is an important factor in the compartmentalisation of the cAMP signalling pathway. AKAPs are a large family of structurally unrelated proteins that have in common the ability to bind to PKA and thereby tether it to a specific location within the cell (Wong and Scott 2004).

Table 1-3 details AKAPs which have been identified thus far and the tissue and subcellular localisation of each.

Microtubule-associated protein-2 (MAP2) was the first AKAP to be characterised as it co-purifies with PKA-RII isolated from brain extracts (Lohmann et al. 1984). Since then, the AKAP family has grown to over 50 members that are classified by their ability to co-purify with PKA catalytic activity from tissues. Although structurally diverse, all AKAPs share several common features including PKA-anchoring, unique localisations and the ability to form complexes with other signalling molecules.

**Table 1-3. A kinase anchoring proteins (AKAPs) distribution and properties. Adapted from (Pidoux and Tasken 2010).**

<b>AKAP (gene nomenclature committee name)</b>	<b>Tissue</b>	<b>Subcellular localisation</b>	<b>Properties</b>
<b>S-AKAP84/ DAKAP1/ AKAP121/ AKAP149 (AKAP1)</b>	Testis, thyroid, heart, lung, liver, skeletal muscle, and kidney	Outer mitochondrial membrane/endoplasmic reticulum/nuclear envelope/sperm midpiece	Dual-specific AKAP. Binds lamin B and PP1
<b>AKAP-KL (AKAP2)</b>	Kidney, lung, thymus, and cerebellum	Actin cytoskeleton/apical membrane of epithelial cells	Multiple splice variants
<b>AKAP110 (AKAP3)</b>	Testis	Axoneme	Binds G $\alpha_{13}$
<b>AKAP82/ FSC1 (AKAP4)</b>	Testis	Fibrous sheath of sperm tail	Dual-specific AKAP
<b>AKAP75/79/150 (AKAP5)</b>	Bovine/human/rat orthologs	Plasma membrane/post-synaptic density	Binds PKC, calcineurin (PP2B), $\beta$ -AR, SAP97, and PSD-95
<b>mAKAP (AKAP6)</b>	Heart (mAKAP $\beta$ , shorter), skeletal muscle and brain (mAKAP $\alpha$ , longer)	Nuclear membrane	Binds PDE4D3, Epac, MEKK/MEK5/E RK5 and PDK1 (only mAKAP $\alpha$ )
<b>AKAP15/18 <math>\alpha</math> <math>\beta</math> <math>\gamma</math> <math>\delta</math> (AKAP7)</b>	Brain, skeletal muscle, pancreas, and heart	Basolateral ( $\alpha$ ) and apical ( $\beta$ ) plasma membrane, cytoplasm ( $\gamma$ ), secretory vesicles ( $\delta$ )	
<b>AKAP95 (AKAP8)</b>	Heart, liver, skeletal muscle, kidney, and pancreas	Nuclear matrix	Binds Eg7/condensin Zinc-finger motif. Binds PDE7A
<b>AKAP450/AKAP350/ Yotiao/CG-NAP/Hyperion (AKAP9)</b>	Brain, pancreas, kidney, heart, skeletal muscle, thymus, spleen, placenta, lung, and liver	Post-synaptic density/neuromuscular junction/centrosomes/ Golgi	Binds PDE4D3, PP1, PP2A, PKN, and PKC $\epsilon$
<b>D-AKAP2 (AKAP10)</b>	Liver, lung, spleen, and brain		Dual-specific AKAP
<b>AKAP220/hAKAP220 (AKAP11)</b>	Testis and brain	Vesicles/peroxisomes/centrosome	Binds PP1. Dual-specific AKAP
<b>Gravin (AKAP12)</b>	Endothelium	Actin cytoskeleton/cytoplasm	Binds PKC and $\beta$ -AR Xgravin-like (Xgl) is

			also a putative AKAP
<b>AKAP-Lbc/Ht31/Rt31 (AKAP13)</b>	Ubiquitous	Cytoplasm	Ht31 RII-binding site used in peptides to disrupt PKA anchoring. Rho-GEF that couples $G\alpha_{12}$ to Rho
<b>MAP2B</b>	Ubiquitous	Microtubules	Binds tubulin. Modulation of L-type $Ca^{2+}$ channels
<b>Ezrin/AKAP78</b>	Secretory epithelia	Actin cytoskeleton	Dual-specific AKAP
<b>T-AKAP80</b>	Testis	Fibrous sheath of sperm tail	
<b>AKAP80/MAP2D</b>	Ovarian granulosa cells		FSH-regulated protein, identified as MAP2D
<b>SSeCKS (Src-suppressed C kinase substrate)</b>	Testis and elongating spermatids	Actin remodelling	Gravin-like
<b>Pericentrin</b>	Ubiquitous	Centrosome	Binds dynein and $\gamma$ -tubulin
<b>WAVE-1/Scar</b>	Brain	Actin cytoskeleton	Binds Abl and Wrp
<b>Myosin VIIA</b>	Ubiquitous	Cytoskeleton	Binds RI
<b>PAP7</b>	Steroid-producing cells (adrenal gland and gonads)	Mitochondria	Binds RI
<b>Neurobeachin</b>	Brain	Golgi apparatus	
<b>AKAP28</b>	Primary airway cells	Ciliary axonemes	
<b>Myeloid translocation gene (MTG) 8 and 16b</b>	Lymphocytes	Golgi apparatus	Binds PDE7A
<b>AKAP140</b>	Granulosa cells and meiotic oocytes		
<b>AKAP85</b>	Lymphocytes	Golgi apparatus	
<b>BIG2 (Brefeldin A-inhibited guanine nucleotide-exchange protein 2)</b>		Cytosol and Golgi apparatus	Binds $RI\alpha/RI\beta$ and $RII\alpha/RII\beta$ through three separate PKA-binding domains
<b>Rab32</b>		Mitochondria	Binds RI
<b>Synemin</b>	Heart	ntercalated discs, sarcolemma, IFs, and Z-lines	PKA–RII-binding AKAP Is increased significantly in failing

			hearts
<b>Myospryn</b>	Muscle-specific	The costamere of striated muscle	Harbors three bona fide PKA-anchoring domains that bind to RII $\alpha$
<b>Alpha4 integrins</b>		Plasma membrane	Binds PKA type I
<b>Sphingosine kinase type 1-interacting protein (SKIP)</b>	Heart	Ventricular tissue	Shows a partly similar sequence to AKAP11
<b>MyRIP (myosin Va–Rab27a-interacting protein)</b>		Perinuclear region	Homolog to zebrafish Ze-AKAP2 PKA–RII-binding AKAP
<b>SFRS17A (splicing factor, arginine–serine-rich 17A)</b>		Nucleus and sliceosome	Dual specific AKAP

Anchoring of PKA to AKAPs is achieved by binding the N-terminal D/D domain of the R subunit of PKA to an amphipathic helix of 14–18 residues within the AKAP (Carr et al. 1991). This binding motif of AKAPs is arranged to form five turns of an amphipathic helix which exposes a hydrophobic face on one side and charged residues along the other side, thereby allowing extensive hydrophobic interactions between the two proteins (Newlon et al. 1999; Newlon et al. 2001). To date, the majority of AKAPs identified bind to the PKA-RII regulatory domain of PKA (Wong and Scott 2004), although several RI-specific AKAPs have now been discovered (Angelo and Rubin 1998). One example of AKAPs which anchors PKA-RI exclusively is sphingosine kinase interacting protein (SKIP), which has been found to be expressed in mitochondria in the heart (Means et al. 2011). The structural differences were investigated and it was discovered that anchoring of PKA-RII to AKAPs occurs when the hydrophobic side of the  $\alpha$ -helix in the AKAP lies across the four helix bundle formed by the PKA-RII D/D (Newlon et al., 2001). Whereas, the extreme N-terminus of RI subunit is believed to be helical. This additional helix folds back on the four helix bundle causing a steric hindrance for high affinity anchoring to AKAPs (Banky et al. 2000). Dual-affinity AKAPs have also been identified. These include for example D-AKAP1 and D-AKAP2, which can anchor both of the PKA R subunits (Huang et al. 1997; Wang et al. 2001). Dual-affinity AKAPs contain an additional binding motif, RISR (RI specific region) at the N-terminus of the conserved helix, which enhances the affinity of

AKAPs for PKA-RI by providing an additional site of contact for the AKAP-RI interaction (Jarnaess et al. 2008).

The importance of AKAP tethering of PKA was emphasised in studies utilising disrupter peptides to impair the PKA-AKAP interaction. The Human thyroid PKA anchoring protein (Ht31) was the first PKA-AKAP disruptor peptide generated (Carr et al. 1992). Fink and colleagues have shown that in cardiac myocytes anchoring of PKA by AKAPs is crucial for appropriate response to  $\beta$ -adrenergic stimulation. The authors used the Ht31 peptide which binds the PKA regulatory subunit type II (RII) with high affinity. This peptide competes with endogenous AKAPs for PKA-RII binding. As a result, cardiomyocytes exhibited an increased rate and amplitude of cell shortening and relaxation upon ISO stimulation and PKA-dependent phosphorylation of TnI and MBP-C on ISO stimulation was significantly reduced in Ht31-expressing cells due to a delocalisation of PKA-RII (Fink et al. 2001). A number of other peptides have now been developed to specifically disrupt interactions between PKA-RI-AKAPs or PKA-RII-AKAPs. These disruptor peptides, such as SuperAKAP-IS (Gold et al. 2006) and the RI-anchoring disruptor (RIAD) (Carlson et al. 2006) have further elucidated the individual contribution of anchored PKA-RII or PKA-RI in mediating different cellular responses (Di Benedetto et al. 2008; Roder et al. 2009).

In cardiac tissue several AKAPs have been identified. These include AKAP18 $\alpha$ , AKAP18 $\delta$ , AKAP79, AKAP250, Yotiao, muscle AKAP (mAKAP), AKAP-Lbc, AKAP220, D-AKAP1 and -2, AKAP95, MAP2, Brefeldin A-inhibited guanine nucleotide-exchange protein 2, ezrin, sphingosine kinase type 1-interacting protein (SKIP), gravin, synemin, myospryn, troponin T, and the phosphoinositide 3-kinase p110 $\gamma$  (Diviani et al. 2011).

AKAP18 $\alpha$  (also called AKAP15) is a membrane associated anchoring protein that directs PKA to the L-TCC through a direct interaction between the C-terminal region and the cytoplasmic domain of the channel. Therefore  $\beta$ -AR stimulation generates a pool of cAMP which activates PKA held in close proximity of the L-TCC. Thus rapid and efficient phosphorylation of the channel is achieved, leading to an increase in its open probability (Fraser et al. 1998; Gray et al. 1998).

The L-TCC also forms a complex with AKAP79/150 (AKAP79, human form; and AKAP150, murine form). Recent investigations in adult mice cardiomyocytes has revealed that AKAP79/150 forms a macromolecular signalling complex containing the  $\beta$ -AR, adenylyl cyclase 5 and 6, PKA, calcineurin, caveolin-3, and a subset of L-TCC specifically phosphorylated in response to sympathetic stimulation (Nichols et al. 2010). Nichols and co-workers showed that in a knockout model of AKAP150 that PKA-mediated phosphorylation of RyRs receptors and PLB was also inhibited. It was proposed that generation of cAMP microdomains by AKAP150 recruitment of AC5 and AC6, encourages PKA mediated regulation of L-TCC, PLB and RyRs located in caveolin-3-associated T-tubule/SR junctions (Nichols et al. 2010).

AKAP18 $\delta$ , another variant of the AKAP18 gene, regulates the activity of the sarcoplasmic reticulum  $\text{Ca}^{2+}$ -ATPase (SERCA2) and mediates cardiac relaxation upon  $\beta$ -adrenergic stimulation. AKAP18 $\delta$  achieves this activity by favouring the PKA-mediated phosphorylation of PLB, thus promoting cardiomyocytes relaxation via SERCA2-mediated  $\text{Ca}^{2+}$  reuptake into the SR. Disruption of the AKAP18 $\delta$ -PLB complex in cardiomyocytes with Ht31 or AKAP18 $\delta$  knock-down, was shown to impair  $\beta$ -AR-induced  $\text{Ca}^{2+}$  reuptake from the cytosol and inhibits lusitropic effects (Lygren et al. 2007).

Another AKAP present in cardiac tissue is mAKAP. mAKAP is an example of an AKAP which, apart from its primary function of anchoring and targeting PKA, also acts to multi-scaffold proteins, linking upstream activators with their downstream targets and allowing for specificity of transduction as well as for integration and linear relay of multiple signalling pathways (Bauman et al., 2006). mAKAP is reported to form a complex with RyR2 channel, PKA, FKBP12.6 (a protein that binds and modulates the RyR2 by stabilising a closed conformation of the channel), protein phosphatase PP1 and PP2A, and PDE4D3 (Marx et al. 2000; Dodge et al. 2001; Carlisle Michel et al. 2004). PKA phosphorylation events are controlled by a negative feedback loop within this signalling complex. Under normal basal conditions, PKA is inactive at this complex. However  $\beta$ -AR stimulation increases cAMP levels causing the release of the catalytic subunit of mAKAP-anchored PKA and consequent phosphorylation of Ser54 on PDE4D3. This results in a 2- to 3-fold increase of PDE4D3 catalytic activity (Sette and Conti 1996) leading to a reduction in local cAMP concentration in the vicinity of the RyR where mAKAP anchors PDE4D3. Marx and colleagues have proposed that mAKAP binding results in PKA-mediated phosphorylation of Ser2809 on RyR2, thereby decreasing the binding affinity for

FKBP12.6 and resulting in an increased open probability of the  $\text{Ca}^{2+}$ -release channel (Marx et al. 2000). Excessive PKA-mediated phosphorylation of RyR2 leads to a “leaky”  $\text{Ca}^{2+}$  channel in heart failure patients and results in cardiac dysfunction and arrhythmias (Lehnart et al. 2005). The proposed model is that PDE4D3 anchored to mAKAP would ensure the generation of a local negative feedback loop at the RyR2, preventing hyperphosphorylation of the channel (Lehnart et al. 2005). The authors found that in the failing heart, the complex between PDE4D2 and RyR2 is reduced. Using mice models containing a mutant where RyR2 could not be PKA phosphorylated, they showed a suppression of cardiac arrhythmias and dysfunction while PDE4D<sup>-/-</sup> mice present a progressive cardiomyopathy, and exercise-induced arrhythmias despite normal global cAMP signalling (Lehnart et al. 2005).

mAKAP has also been shown to organise another macromolecular complex composed of PKA, PDE4D3, Epac1 and extracellular signal-regulated kinase 5 (ERK5) and by anchoring Epac1 and ERK5 via their direct interaction with PDE4D3, mAKAP creates a second negative feedback loop (Dodge-Kafka et al. 2005). mAKAP-associated ERK5 kinase module suppresses PDE4D3 activity thus producing a local increase in cAMP, which sequentially activates Epac1. Epac1 can activate the small GTPase Rap1, which in turn inhibits the MAP/ERK kinase-kinase thus releasing the inhibition of PDE4D3 by ERK5 (Dodge-Kafka et al. 2005).

Yatiao (AKAP9) is another AKAP which has been suggested to be an important regulator of cardiac function. Marx and colleagues showed that Yatiao forms a complex with protein phosphatase 1 (PP1), the RII and the C-subunit of PKA and to the  $\text{I}_{\text{KS}}$  channel subunit hKCNQ1 (human  $\alpha$  subunit of the slowly activating cardiac  $\text{K}^+$  channel) (Marx et al. 2002). The KCNQ1 channel mediates repolarisation of the cardiomyocytes plasma membrane and is vital for the regulation of the cardiac action potential (AP) duration. Mutations have been identified in the KCNQ1-binding region of Yatiao (S1570L) (Chen et al. 2007) and in the Yatiao-binding region of KCNQ1 (G589D) (Fodstad et al. 2004) in patients with long QT syndrome (LQTS). In 2009, PDE4D3 was also discovered to be an important component of this complex (Terrenoire et al. 2009). PDE4D3 contributes to finely tune local cAMP levels regulation of the  $\text{I}_{\text{KS}}$  channel activity resulting in another negative feedback loop whereby  $\beta$ -AR stimulation leads to active PKA which phosphorylates PDE4D3 increasing its activity and terminating the local cAMP signal (Terrenoire et al. 2009).

## 1.7.2 GPCR and AC compartmentalisation

The signalling components upstream of PKA signalling have also been reported to be compartmentalised. cAMP is generated in response to hormone or neurotransmitter binding to a specific G-protein coupled receptor (GPCR) leading to a release of a Gs protein which activates an adenylyl cyclase (AC) to convert ATP to cAMP. If AC and GPCR were able to move freely within the plasma membrane, then there would be a non-specific activation of all PKA subsets and therefore superseding the advantages of having PKA tethered in close proximity of its targets. GPCRs, including  $\beta$ -adrenergic receptors and serotonin receptors, have been shown to localise in two related membrane microdomains, lipid rafts and caveolae (Patel et al. 2008). Lipid rafts are regions in the lipid bilayer of the plasma membrane rich in cholesterol and other lipids and caveolae are a subset of lipid-rafts forming invaginations of the plasma membrane and enriched in the protein caveolin (Patel et al. 2008). Calaghan and co-workers have demonstrated that, in adult rat ventricular myocytes, caveolae can modulate excitation-contraction coupling and  $\beta_2$ -AR signalling by regulating the efficiency of  $\text{Ca}^{2+}$ -induced  $\text{Ca}^{2+}$  release from the sarcoplasmic reticulum (Calaghan and White 2006). The same authors have recently published data showing caveolae play a direct role in the compartmentalisation of cAMP by restricting  $\beta_2$ -AR cAMP signals to the sarcolemmal compartment in adult myocytes (Calaghan et al. 2008). They showed, using FRET based biosensors for cAMP, that disruption of caveolae resulted in  $\beta_2$ -AR cAMP signals in the PKA-RII compartment and promoted selective PKA-mediated phosphorylation of PLB (Macdougall et al. 2012). Nikolaev and colleagues have also shown, using FRET imaging, that  $\beta_2$ -ARs are localised in T-tubules in adult rat myocytes, whereas  $\beta_1$ -ARs are more evenly spread throughout the plasma membrane (Nikolaev et al. 2010). The authors provided evidence that, in a rat model of chronic heart failure (CHF),  $\beta_2$ -ARs are redistributed from the T-tubules to the cell crest making the  $\beta_2$ -AR cAMP signal more propagating (Nikolaev et al. 2010). Redistribution of the receptor may result on a loss of  $\beta_2$ -AR signalling which normally has cardioprotective properties and may acquire the characteristics of the  $\beta_1$ -AR response, thus contributing to the heart failure phenotype.

Additionally, diverse ACs isoforms have been shown to localise in different locations on the plasma membrane. The  $\text{Ca}^{2+}$ -sensitive isoforms of ACs (AC1, AC3, AC5, AC6, AC8) but not the  $\text{Ca}^{2+}$ -insensitive isoforms (AC2, AC4, AC7) have been detected in lipid-rafts

membrane structures (Willoughby and Cooper 2007). Interestingly, as discussed above, adenylyl cyclases have also been found to form complexes with AKAPs (Dessauer 2009). AC5 has been shown to associate with the AKAP79 complex in the heart as well as brain extracts. AC5 cyclase activity is inhibited by PKA phosphorylation, thus AKAP79 binding creates a PKA-dependent negative feedback regulation of cAMP synthesis (Bauman et al. 2006). In cardiac myocytes, AC5 also forms a complex with mAKAPs and in brain tissue, AC1, AC2, AC3 and AC9 are associated with Yotiao (Dessauer 2009).

### 1.7.3 Compartmentalisation of cAMP

3', 5'-cyclic adenosine monophosphate (cAMP) is a hydrophilic molecule, with a diffusion constant in the range of 270–780  $\mu\text{m}^2/\text{s}$  (Kasai and Petersen, 1994). As mentioned above, if cAMP were free to diffuse in the cell, ligand binding to any GPCRs would generate a global rise in cAMP levels and subsequent activation of all PKA subsets, whatever their subcellular localisation, resulting in phosphorylation of all PKA targets within the cell. This would abolish any specificity in the response to cAMP elevation. Recent evidence suggests that the cAMP signal is itself compartmentalised to restrict diffusion and to prevent the unsuitable activation of effectors. Rich and colleagues used an adenovirus encoding the  $\alpha$  subunit of the rat olfactory CNG channel (CNG2, CNC $\alpha$ 3) with mutations C460W and E583M, to monitor cAMP levels near the surface membrane in both human embryonic kidney (HEK) cell populations and single cells. Total cAMP accumulation in cell populations by measuring the conversion of [3H]ATP into [3H]cAMP. They reported that prostaglandin E1 (PGE1) stimulation of human embryonic kidney cells caused a transient increase in cAMP concentration near the membrane while the total cellular cAMP rose to a steady level. Pre-treatment with phosphodiesterase (PDE) inhibitors blocked the decline in cAMP levels near the membrane (Rich et al. 2001a). DiPilato and co-workers utilised FRET based fluorescent indicators to report intracellular cAMP dynamics through its effectors Epac1 in HEK cells. They generated a cAMP FRET-based sensor targeted to the plasma membrane by inserting a sequence to the C terminus of the cytosolic sensor. This study revealed a faster cAMP response at the membrane than in the cytoplasm and mitochondria upon  $\beta$ -AR stimulation (DiPilato et al. 2004). Mongillo et al. used a similar method to study cAMP signalling dynamics in neonatal rat ventricular

myocytes (NRVM) and the compartmentalisation of PDEs. The authors reported compartmentalised cAMP signalling in this cell type using fluorescent FRET based indicators fused to the regulatory and catalytic subunits of PKA. Real-time FRET imaging and selective PDE inhibitors revealed that PDE4, rather than PDE3, appears to be responsible for modulating the amplitude and duration of the cAMP response to  $\beta$ -agonists. Immunocytochemistry established that these PDE families are localised to distinct compartments in cardiomyocytes (Mongillo et al. 2004).

Several hypotheses have been put forward to explain the mechanism of the spatial restriction of cAMP. One such mechanism suggests that cAMP is restricted by a physical barrier, formed by elements of the endoplasmic reticulum underneath the plasma membrane, limiting cAMP diffusion inside the cytosol (Rich et al. 2000). The authors use adenovirus expressed cyclic nucleotide-gated channels as sensors for cAMP in HEK cells. They find that upon forskolin stimulation the endogenous adenylyl cyclase in C6-2B glioma cells produced high concentrations of cAMP near the channels, yet the global cAMP concentration remained low. The authors suggest a 3-D barrier to cAMP diffusion in addition to a 2-D colocalisation of membrane proteins (Rich et al. 2000). Another hypothesis proposed is “PKA mediated buffering” suggesting that cAMP binding to the R subunit of PKA reduces the diffusion rate (Saucerman et al. 2006). Saucerman et al. employed the A-kinase activity reporter 2 (AKAR2), a real-time indicator of PKA-mediated phosphorylation, to study cAMP/ PKA signalling in rat neonatal cardiomyocytes. This sensor revealed that PGE1 stimulated higher PKA activity in the cytosol than at the sarcolemma, whereas ISO caused similar increases in emission levels for both cytosolic and membrane-tagged PKA sensors but triggered faster sarcolemmal responses than cytosolic. The authors propose that PKA signalling may generate both “spatially heterogeneous and asynchronous phosphorylation signals”. In this study, localised UV photolysis of “caged” cAMP triggered gradients of PKA-mediated phosphorylation, enhanced by phosphodiesterase activity and PKA-mediated buffering of cAMP (Saucerman et al. 2006).

There are different hypothesis on how spatial propagation of cAMP is regulated but the majority of the available data point to an important role played by PDEs which are thought to limit diffusion of cAMP within the cell.

### 1.7.4 Compartmentalisation of cAMP by PDEs

The first indication that PDE activity may control cAMP compartmentalisation came from the study performed by Jurevicius and co-workers, as previously mentioned (see 1.7). Briefly, the authors investigated  $\text{Ca}^{2+}$  transients in two physically isolated portion of an isolated frog ventricular myocyte (Jurevicius and Fischmeister 1996) using whole cell patch clamp recordings and found that isoproterenol stimulation resulted in activation of  $I_{\text{Ca}}$  localised at the site of stimulus application, whereas non-selective ACs activator forskolin results in activation of  $I_{\text{Ca}}$  both at local and distant sites. Interestingly, they found that after the addition of 3-isobutyl-1-methylxanthine (IBMX), a non-selective PDE inhibitor, cAMP compartmentation was greatly reduced (Jurevicius and Fischmeister 1996), suggesting PDEs play a major role in ‘shaping’ and maintaining the subcellular cAMP gradients.

Utilising advances in real-time imaging techniques, such as fluorescence resonance energy transfer (FRET)-based imaging, Zaccolo and Pozzan established that, in rat neonatal myocytes (NRVM),  $\beta$ -AR stimulation causes a local increase of cAMP, providing the first direct visualisation of microdomains of cAMP (Zaccolo and Pozzan 2002). Upon addition of IBMX, cAMP was found to be free to diffuse in the cytosol and subsequent loss of specificity of signal (Zaccolo and Pozzan 2002), again indicating that PDEs play a key role in limiting the spatial propagation of the cAMP signal.

Further investigation of cAMP dynamics in cardiomyocytes showed that different PDE isoforms are localised in defined intracellular compartments and confirmed their role in shaping cAMP gradients. Mongillo and colleagues revealed, using real-time imaging in neonatal rat ventricular myocytes (NRVM), that the cAMP generated by  $\beta$  AR stimulation is controlled mainly by PDE4 whereas PDE3, although representing about 30% of the total PDE activity, exerts only a marginal effect (Mongillo et al. 2004). Interestingly, immunostaining experiments showed that PDE3 and PDE4 localise in distinct compartments within cardiac myocytes which may account for the different effect of their inhibition seen upon  $\beta$ -AR activation (Mongillo et al. 2004). More recently, the same author discovered that PDE2 also plays a significant role in the compartmentalised signalling of cAMP in cardiomyocytes (Mongillo et al. 2006). PDE2 was shown to significantly blunt cAMP increase upon  $\beta$ -AR stimulation, although it represents only 1%

of the total PDEs activity in cardiac myocytes and was again shown to have a unique localisation, corresponding to cell to cell junctions and sarcomeric Z-lines in NRVM (Mongillo et al. 2006).

In the same year, Terrin et al. published further evidence confirming the importance of the intracellular localisation of individual PDE isoforms using a dominant negative approach (Terrin et al. 2006). This technique exploits a catalytically inactive PDE isoform that, when overexpressed in a cell, will displace the endogenous PDE enzyme by removing it from any intracellular site where it may be anchored, thus exerting a dominant-negative effect locally and effectively abolishing the enzymatic activity at that specific site (Baillie et al. 2003). Displacement of endogenous PDE4D isoforms was shown to be sufficient to disrupt the cAMP gradients between the bulk cytosol and plasma membrane upon PGE1 stimulation in HEK293 cells (Terrin et al. 2006). The same paper also proposed the idea that rather than creating a physical barrier, PDEs act as “sinks” draining cAMP from discrete locations and thus keeping the concentration of cAMP low to protect effectors from inappropriate phosphorylation, thus ensuring the specificity of the signal. Multiple PDE families are expressed in the same cell and each may include multiple genes and several splice variants, therefore, the number of isoforms expressed within a cell may be substantial all with unique functional roles due to their intracellular localisation and regulatory mechanisms. The activity of different PDEs that are uniquely regulated and localised within the cell thus results in multiple and simultaneous domains with varying cAMP concentrations irrespective of their distance from the AC that generated the cAMP (Terrin et al. 2006).

## 1.8 cAMP hydrolysing PDE families expressed in the heart

In the heart several PDE families have been identified, including PDE1, PDE2, PDE3, PDE4, and PDE8 (Lugnier 2006). In recent years, advances in molecular biology techniques, such as dominant-negative, knock-down or knock-out models and the use of selective PDE inhibitors has allowed for a better understanding of how each individual PDE enzyme contributes to the compartmentalisation of cAMP signalling pathways in cardiomyocytes.

### 1.8.1 PDE2

PDE2 is a dual-specific enzyme with the ability to hydrolyse both cAMP and cGMP (Martins et al. 1982). PDE2, originally referred to as cGMP-stimulated PDE (cGS-PDE), was first recognised by Beavo and colleagues in 1971 (Beavo et al. 1971). They reported that cGMP increased the rate of cAMP hydrolysis when added to both soluble and particulate PDE preparations in a number of different tissues from an adult rat, including liver, brain, kidney, heart, and thymus (Beavo et al. 1971). Further investigation led to the discovery that PDE2 degrades both cAMP and cGMP, with  $K_m$  values of 30  $\mu\text{mol/L}$  for cAMP and 10  $\mu\text{mol/L}$  for cGMP, and displays positive co-operativity for both cyclic nucleotides (Erneux et al. 1981; Martins et al. 1982). Martins et al. also reported that in the presence of low levels of cGMP, the rate of PDE2 hydrolysis of cAMP is increased by almost 6-fold (Martins et al. 1982).

The crystal structure of the PDE2A was determined by Martinez and colleagues, who revealed the regulatory region of PDE2 contains two tandem GAF domains (GAF-A and GAF-B) (Martinez et al. 2002). The results of this study indicated that the first GAF domain (residues 215-366, GAF-A) is followed by a “connecting helix” (residues 367-398), a short linker (residues 399-402), and the second GAF domain (residues 403-555, GAF B). GAF-A is involved in dimerisation, whereas GAF-B domain binds cGMP with high affinity and selectivity (Martinez et al. 2002; Martinez et al. 2005).

More recently, Pandit et al. analysed the X-ray crystal structure of human PDE2A. PDE2A is a protein of 941 amino acids, organised in four domains: N terminus (1–214), GAF-A (215–372), GAF-B (393–541), and catalytic (579–941) which functions as a homodimer (Pandit et al. 2009). They produced a construct PDE2 (residues 215-900), which crystallised, while still maintaining the essential characteristics of the full-length protein. PDE2A (215–900) shows a linear extended organisation of the GAF-A, GAF-B and catalytic domains, which were connected by long  $\alpha$ -helices. Comparison of this construct with that of the full length PDE2 structure, suggests that cGMP binding induces a conformational change in GAF-B and the adjoining linker that connects it to the catalytic domain (Figure 1-8). They described that the catalytic domain of PDE2A presents an “open” and a “closed” conformation, which is determined by the orientation of the H-loop (residues 702-723). In the “closed” conformation the H-loop is folded into the active site thereby completely occluding the substrate-binding site. For the catalytic site to adopt the “open” conformation the H-loop has to swing out, allowing the substrate to get access to the binding pocket (Pandit et al. 2009). Pandit and colleagues report that that cGMP binding to GAF-B domain of PDE2 causes a conformational change at the linker region of the catalytic domain, freeing the H-loops from the dimer interface, where it adopts the “open” structure to allow substrate access (Pandit et al. 2009).

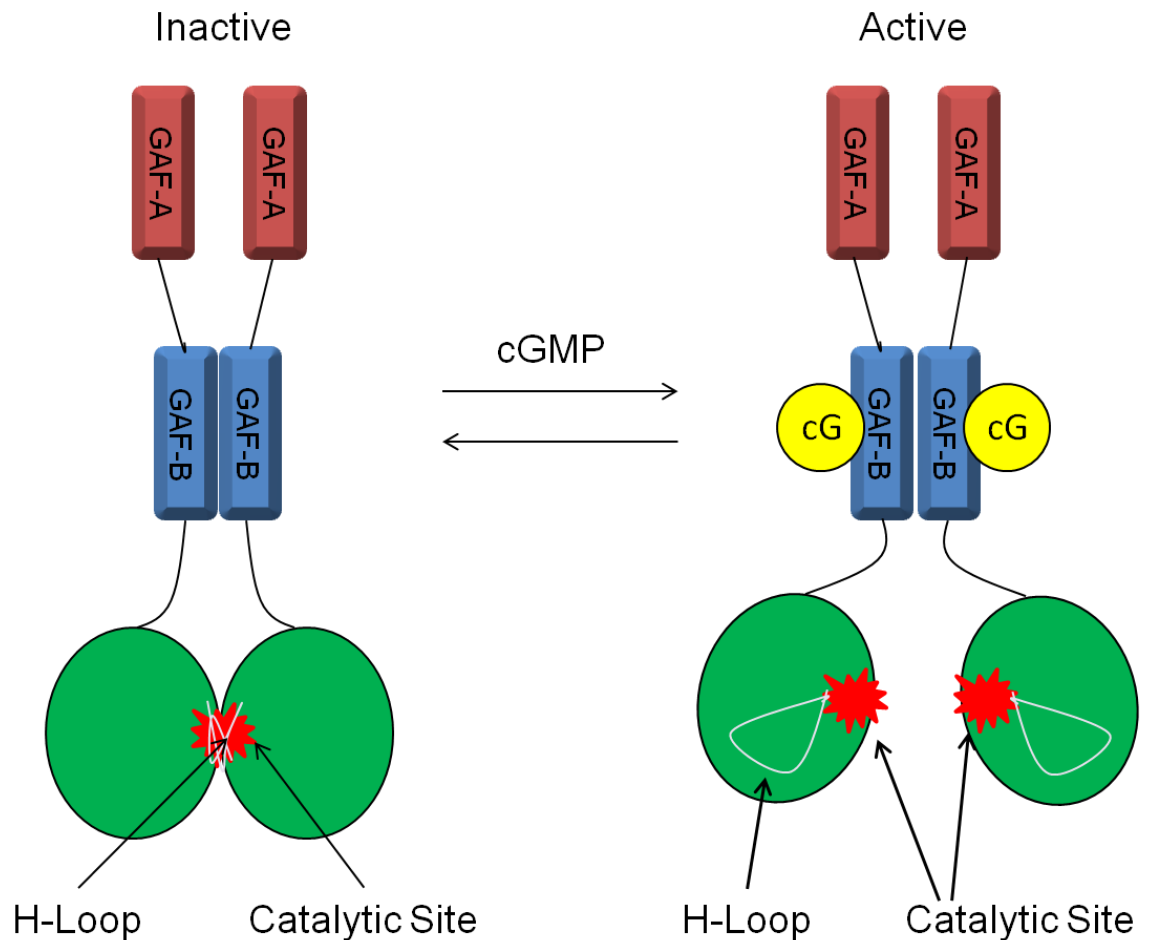


**Figure 1-8. Schematic representation of cGMP-induced conformational changes of PDE2 resulting in activation. Adapted from (Francis et al. 2011).**

PDE2, as with other PDEs, is confined in discrete regions or cell types within tissues. PDE2 has been found to localise at the Golgi (Geoffroy et al. 1999) the nuclear envelope (Lugnier et al. 1999), sarcoplasmic reticulum (Lugnier and Komasa 1993), Z-bands of neonatal rat ventricular cardiomyocytes (Mongillo et al. 2006) and at lipid rafts of brain cells (Noyama and Maekawa 2003). The specific localisation of PDE2 is responsible for the compartmentalised regulation of determined cellular functions depending on cyclic nucleotide levels. In endothelial cells, under basal conditions, PDE2A is present in veins and capillaries in cardiac and renal tissue, but not in larger vessels, i.e. arterial endothelial cells (Sadhu et al. 1999).

PDE2 is encoded by a single gene (PDE2A), and currently three variants of this enzyme have been identified (PDE2A1, PDE2A2 and PDE2A3), which are all identical, except for

the N-terminal-region (17 - 24 amino acids). (Sonnenburg et al. 1991; Rosman et al. 1997). This unique N-terminal sequence is thought to be responsible for the differences in intracellular localisation. PDE2A1 lacks the amino-terminal targeting sequence and is, therefore, mainly soluble (Bender and Beavo 2006). There are no known differences in kinetic behaviour between the PDE2A variants. All PDE2 isoforms have been identified in cardiac tissue, including both atrial and ventricular myocytes of a number of different species (Miller and Yan 2010)

A unique function of PDE2 is its ability to mediate “cross-talk” between the cAMP and cGMP signalling pathways, as PDE2 hydrolysis of cAMP and cGMP is enhanced by binding of cGMP to its GAF-B domain. This is best exemplified by the atrial natriuretic peptide (ANP)-mediated control of blood pressure, where in adrenal glomerulosa cells, stimulation of cGMP by ANP activated PDE2 and resulted in a reduction of cAMP levels within the cell (MacFarland et al. 1991). When administered acutely, ANP elicits potent and short-lasting systemic hypotension in a wide variety of mammalian and non-mammalian species (Brenner et al. 1990) due to cGMP synthesis and subsequent activation of PDE2. In platelets, high levels of nitric oxide (NO) stimulate the production of cGMP, which activates PDE2 and reduces intracellular cAMP concentrations (Dickinson et al. 1997). Numerous studies have indicated that PDE2 mediated “cross-talk” between the two cyclic nucleotide pathways is crucial for normal heart function (Mery et al. 1995; Rivet-Bastide et al. 1997; Vandecasteele et al. 2001; Fischmeister et al. 2005; Mongillo et al. 2006; Stangherlin et al. 2011).

In myocytes, PDE2 has been exposed as being a major regulator of cyclic nucleotide signalling and to modulate the ECC process. For example, at the L-TCC, PDE2 was found to mediate the cGMP-induced inhibition of the  $I_{Ca}$  in both human atrial myocytes (Rivet-Bastide et al. 1997) and frog ventricular myocytes (Mery et al. 1995). In adult rat cardiac fibroblasts, NO attenuates cAMP accumulation via sGC–cGMP-PDE2 stimulation (Gustafsson and Brunton 2002). Similarly, in pacemaker cells, the effect of NO on heart rate is mediated by inhibition of L-type  $Ca^{2+}$  current via a signalling pathway involving the synthesis of cGMP and stimulation of PDE2 (Han et al. 1995).

In addition, cGMP activation of PDE2 was shown to regulate the cAMP response to  $\beta$ -AR stimulation in rat neonatal ventricular myocytes (Mongillo et al. 2006). Using a FRET-

based imaging approach, Mongillo and colleagues demonstrated that activation of soluble guanylyl cyclase (sGC) by sodium nitroprusside (SNP) leads to activation of PDE2 and a 50% reduction in the amplitude of the cAMP response to norepinephrine (NE). Although PDE2 could not block the rise in cAMP levels after the addition of adenylyl cyclase activator forskolin, PDE2 effectively blocks the increase in cAMP concentration induced by stimulation of the  $\beta_1$  and  $\beta_2$ -adrenergic receptors (Mongillo et al. 2006). The authors found that the mechanism by which NE treatment activates PDE2 to hydrolyse cAMP involves activation of  $\beta_3$ -ARs and a subsequent activation of endothelial nitric oxide synthase (eNOS), which generates NO and in turn cGMP via activation of sGC (Mongillo et al. 2006) Recently Stangherlin et al. published experiments performed in NRVMs using targeted FRET-based sensors that allow monitoring of cAMP or cGMP in defined subcellular compartments (Stangherlin et al. 2011). These FRET-based sensors for cAMP were targeted to either RI- or RII-selective AKAPs. This paper indicated that cGMP can regulate localised cAMP responses in cardiac myocytes. The authors reported that PDE2 activity appears to be mainly coupled to the PKA-RII compartment, whereas PDE3 activity is coupled to the PKA-RI compartment. Stimulation of sGC increases the cAMP response to isoproterenol selectively in the PKA-RI compartment via inhibition of PDE3, whereas the cAMP response is reduced in PKA-RII compartment via cGMP-mediated activation of PDE2 (Stangherlin et al. 2011). Activation of pGC by atrial natriuretic peptide (ANP) showed an effect selectively in the PKA-RII compartment, where the rise in cGMP reduced cAMP via activation of PDE2 upon catecholamine stimulation. The cAMP response in the PKA-RI compartment was unaffected. These data demonstrate that cGMP signals are also compartmentalised and the effects of cGMP in regulating cAMP signalling are related to the source of cGMP.

PDE2 family members are also referred to as cGMP-stimulated PDEs as cGMP binding to the N-terminal GAF domains of the enzyme stimulates its catalytic activity markedly. Most functional data published on the PDE2 family was gathered using the PDE2 inhibitor, erythro-9-(2-hydroxy-3-nonyl) adenine (EHNA). However, this compound may generate artefacts as it is known to inhibit adenosine deaminase therefore increasing extracellular adenosine levels which may increase intracellular cAMP upon binding to Gs coupled receptors (Miller and Yan 2010). Recently new, more selective inhibitors have been developed, these include 9-(6-phenyl-2-oxohex-3-yl)-2-(3, 4-dimethoxybenzyl)-purin-6one (PDP), and BAY60-7550 and have been successfully used in a number of functional

studies (Diebold et al. 2009; Stangherlin et al. 2011). PDE2 is selectively inhibited by Bay60-7550 with a  $K_i$  value of  $\sim 3.8$  nM (Masood et al. 2009).

## 1.8.2 PDE3

The PDE3 family contains two variants, PDE3A and PDE3B. PDE3 isoforms bind both cAMP and cGMP with a similar affinity (cAMP ( $K_m \sim 80$  nmol/L) and cGMP ( $K_m \sim 20$  nmol/L), which act as mutually competitive substrates. Due to the higher catalytic rate for cAMP, PDE3 is inhibited by cGMP (Degerman et al. 1997). PDE3 is selectively inhibited by a number of nonglycosidic cardiotonic agents (e.g., cilostamide, amrinone and milrinone) (Osadchii 2007). PDE3 is selectively inhibited by cilostamide with a  $K_i$  value of  $\sim 11.5$   $\mu$ M (Yamamoto et al. 1983).

Cardiac myocytes express 3 isoforms of PDE3A, PDE3A1, PDE3A2 and PDE3A3 which all share an identical sequence except for differences in the lengths of the N-terminal region, which is involved in intracellular localisation and contains phosphorylation sites. PDE3A1 contains 2 intracellular localising domains, NHR1 and NHR2. NHR1 consists of hydrophobic loops that insert into intracellular membranes, whereas NHR2 appears to localise the enzyme through protein–protein interactions and sites for PKA and PKB phosphorylation. PDE3A2 has a similar structure to PDE3A1, but lacks the NHR1 and the PKB phosphorylation site. PDE3A3 is primarily cytosolic and lacks the NHR1, NHR2, domains and the 3 phosphorylation sites (Hambleton et al. 2005).

PDE3A is downregulated in heart failure and this leads to the induction of the pro-apoptotic transcriptional repressor ICER (Inducible Cyclic AMP Early Repressor) (Smith et al. 1997). Elevated ICER represses anti-apoptotic proteins such as Bcl-2 and the PDE3A gene, thus creating a positive feedback loop (Ding et al. 2005).

Recently, Patrucco and co-workers established that PDE3B accounts for  $\sim 30\%$  of the total PDE3 cAMP-hydrolysing activity in mouse hearts (Patrucco et al. 2004). PDE3B is associated with phosphoinositide 3-kinase  $\gamma$  (PI3K $\gamma$ ) and Epac1 in a macromolecular complex at the level of the sarcolemmal membrane which is critical for controlling local cAMP homeostasis and may play an important role in regulating cardiac function (Patrucco et al. 2004). Perino et al. showed that p110 $\gamma$ -anchored PKA activates PDE3B thus enhancing cAMP degradation and phosphorylating p110 $\gamma$  to inhibit PIP3 production.

However these results are controversial, as loss of PI3K $\gamma$  selectively abolishes PDE4, but not PDE3 activity in subcellular compartments containing the SR Ca<sup>2+</sup>-ATPase and not RyR2 or L-TCCs (Kerfant et al. 2007). Furthermore, a number of different authors were not able to detect PDE3B expression in mouse cardiac myocytes (Kerfant et al. 2007; Osadchii 2007).

Inhibition of PDE3 activity in cardiomyocytes isolated from a number of different species was shown to increase Ca<sup>2+</sup>-current at the L-TCC and thus enhance the rate and magnitude of developed contraction and relaxation (Vandecasteele et al. 2001). These inotropic effects lead to the development and clinical use of PDE3 inhibitors for the acute treatment of congestive heart failure (CHF). By inhibiting cAMP hydrolysis in cardiac muscle, PDE3 inhibitors should overcome the reduction in intracellular cAMP content thereby increasing myocardial contractility. However, despite short-term inotropic effects, adverse effects such as increased mortality due to arrhythmias and sudden death were commonly found in several clinical trials using PDE3 inhibitors, such as milrinone, in heart failure patients (Movsesian and Alharethi 2002; Movsesian and Kukreja 2011). The concept of compartmentalised cAMP signalling has been invoked to explain these unexpected long term deleterious effects. It has been suggested that long-term use of PDE3 inhibitors results in an increase in the phosphorylation of a large number of PKA substrates, with both beneficial and adverse effects on the heart. As cAMP signalling is compartmentalised, the idea of selectively increasing cAMP concentration in certain subcellular compartments rather than increasing the total cellular cAMP, might prove to be more effective (Movsesian 2002).

Again PDE3 allows for cAMP and cGMP interplay as cGMP binding to PDE3 results in an inhibition of the enzyme and increased levels of cAMP. At a concentration of <50 nM, cGMP inhibits PDE3; at concentrations between 200 and 500 nM, cGMP activates PDE2 (Zaccolo and Movsesian 2007). As already discussed, Mery and colleagues identified that low concentrations of cGMP increased the L-type Ca<sup>2+</sup> current via PDE3 inhibition, whereas a higher concentration of cGMP strongly reduced L-TCC current via activation of PDE2 in frog ventricular myocytes (Mery et al. 1995). More recently, it has been reported that, in adult rat cardiac myocytes isolated from failing hearts, treatment with natriuretic peptide C (CNP) resulted in enhanced  $\beta$ 1-AR mediated contractile response via PDE3 inhibition (Qvigstad et al. 2010).

### 1.8.3 PDE4

In contrast to PDE2 and PDE3, PDE4 is cGMP-independent. In human ventricular tissue, the  $K_m$  values of PDE4 for cAMP were shown to be about 25-fold lower as compared to  $K_m$  values for cGMP, indicating high specificity for cAMP hydrolysis (Reeves et al. 1987). In murine ventricular myocytes, the PDE4 family is the major regulator of the cAMP increase generated in response  $\beta$ -AR stimulation, (Mongillo et al. 2004; Xiang et al. 2005) and in regulating PKA-mediated phosphorylation of vitally important components of the ECC process, including L-TCC, RyR2, and PLB (Lehnart et al. 2005; Kerfant et al. 2007; De Arcangelis et al. 2008). PDE4 activity is selectively inhibited by rolipram and Ro 20-1724 with  $K_i$  values of 2- 3  $\mu$ M (Osadchii 2007).

The PDE4 family consists of four genes (PDE4A, PDE4B, PDE4C and PDE4D) encoding 18 different enzyme isoforms. 90% of the total PDE4 cAMP-hydrolysing activity in rat cardiomyocytes is provided by PDE4D and PDE4B, while only 10% of the activity is formed by PDE4A and PDE4C (Mongillo et al. 2004; Rochais et al. 2006). PDE4B and PDE4D have unique intracellular localisations due to their distinctive N-terminal domains and thus can regulate specific intracellular responses. In neonatal rat cardiac myocytes PDE4B is localised to the sarcomeric M-line, whereas PDE4D is localised to the Z-line of sarcomere (Mongillo et al. 2004). In mouse ventricular myocytes, IP experiments revealed that both PDE4B and PDE4D are anchored at the L-TCC in adult rat ventricular myocytes (ARVM) (Leroy et al. 2011). PDE4B seems to regulate L-type  $Ca^{2+}$ -current during  $\beta$ -AR stimulation but PDE4D does not appear to have any effect (Leroy et al. 2011). Patch-clamp experiments were performed in AMVMs isolated from mice deficient in the corresponding genes (Pde4b<sup>-/-</sup>, and Pde4d<sup>-/-</sup> mice).  $I_{CaL}$  potentiation by ISO remained unchanged for Pde4d<sup>-/-</sup>, while treatment with rolipram strongly enhanced the effect of ISO on  $I_{CaL}$ , suggesting that this isoforms does not modulate the  $\beta$ -AR stimulation of  $I_{CaL}$ . In contrast,  $\beta$ -AR stimulation was significantly enhanced in ventricular myocytes isolated from Pde4b<sup>-/-</sup> mice compared with that from WT mice (Leroy et al. 2011).

Among the PDE4D family, PDE4D3, PDE4D5, PDE4D8, and PDE4D9 have been detected as active proteins in the heart (Fischmeister et al. 2006) and the PDE4D3 isoform has been reported to be an essential component of the ryanodine receptor (RyR) macromolecular complex (Lehnart et al. 2005). PDE4D3 was found to be part of at least two macromolecular complexes organised by Yotiao and mAKAP (See 1.7.1). In the Yotiao complex, PDE4D3 is recruited at the KCNQ1/KCNE1 potassium channel together

with PKA and PP1. PDE4D3 regulates the PKA-mediated phosphorylation of the KCNQ1 subunit, which is involved in controlling the I<sub>K</sub>S current and the action potential (AP) duration (Terrenoire et al. 2009). In the mAKAP complex at the SR, PDE4D3 joins with RyR2 channel, PKA, FKBP12.6, PP1 and PP2A to tightly regulate Ca<sup>2+</sup> cycling (Marx et al. 2000)

Additionally, it has been shown that PDE4D5 can be dynamically engaged by  $\beta$ -arrestin in close proximity of  $\beta_2$ -ARs. Upon agonist activation,  $\beta_2$ -AR couples to G<sub>s</sub> to generate cAMP, which activates the AKAP79-anchored PKA (Lynch et al. 2005). PKA mediated phosphorylation of  $\beta_2$ -AR triggers a shift in receptor coupling for G<sub>s</sub> to G<sub>i</sub> (Baillie et al. 2003). Recruiting PDE4D5 to the plasma membrane specifically decreases the sub-plasma membrane cAMP concentration inhibiting the subsequent PKA-mediated phosphorylation of the  $\beta_2$ -AR and rapidly terminates the PKA signalling.(Baillie et al. 2003).

PDE4D8 and PDE4D9 have also been shown to interact with  $\beta$ -ARs via  $\beta$ -arrestin. PDE4D8 forms a complex with  $\beta_1$ -AR and dissociates upon agonist binding to the receptor (Richter et al. 2008). Recently, De Arcangelis and colleagues established that  $\beta_2$ -AR stimulation induces PDE4D9 dissociation from the receptor and encourages PDE4D8 recruitment (De Arcangelis et al. 2010).

Richter and colleagues recently published evidence that antagonist occupancy of the  $\beta_1$ -AR receptor in HEK cells, activates a previously unreported signal at the cell membrane by promoting the release of a PDE4, resulting in a local increase in cAMP levels and activation of PKA in the proximity of the receptor (Richter et al. 2013). The authors reported that treatment with various  $\beta_1$ -AR antagonists, including alprenolol (ALP), CGP-20712A (CGP), metoprolol (MET), propranolol (PRO) and carvedilol (CAR), induced  $\beta_1$ -AR/PDE4 complex dissociation. Treatment of  $\beta_1$ -AR-Hek293 cells with PRO, ALP and CAR triggered a significant increase in global cellular cAMP as measured by radioimmunoassay (RIA). This rise in cAMP occurs without stimulation of cAMP synthesis by adenylyl cyclase (Richter et al. 2013).

## 1.9 Real-time detection of cAMP

The greatest advancement in the study of temporal and spatial regulation of cAMP signal transduction came from the development of real time detection approaches to measure cAMP in intact living cells. Currently there are two methods for measuring cAMP in intact living cells: biosensors based on cyclic nucleotide gated (CNG) ion channels or biosensors based on Fluorescence Resonance Energy Transfer (FRET). These methods have been produced as classical approaches, such as radioimmuno assays (RIA) or other antibody-based detection methods; provide information about cAMP dynamics that is averaged over the whole cell population whereas information at the single cell level may be more physiologically relevant.

### 1.9.1 CNG based sensors

One method for studying cAMP signalling dynamics in intact living cells exploits the over-expression of an olfactory CNG channel (Rich et al. 2000; Rich et al. 2001a). CNGs are directly opened by cyclic nucleotides (1.5.3) and their activation can be measured by electrophysiological recordings of  $\text{Ca}^{2+}$  activated chloride currents or  $\text{Ca}^{2+}$  imaging with a  $\text{Ca}^{2+}$ -indicator (e.g. Fura-2). Wild-type CNG channels show several limitations. They exhibit a lower affinity for cAMP than for cGMP (Rich et al. 2001a; Rich et al. 2001b), they can be directly opened by nitric oxide (Broillet 2000) and they are negatively regulated by  $\text{Ca}^{2+}$ -calmodulin binding via a feedback loop mechanism (Liu et al. 1994). To overcome these issues, a mutated and deleted version of the CNG channel,  $\Delta 61-90/\text{C460W}/\text{E583M}$ , was generated (Rich et al. 2001a). This new sensor is almost insensitive to cGMP and sensitive to low cAMP concentrations. In addition, the regulation of the channel by  $\text{Ca}^{2+}$ -calmodulin has been removed by deletion of residues 61–90. However there are still some problems with this detection method, for example, it can only monitor cAMP dynamics at the plasma membrane and the increased calcium influx can modulate the activity of ACs and calcium sensitive PDEs. As a consequence, the cAMP concentration that is detected by the sensor may not be physiological.

## 1.9.2 FRET

Fluorescence resonance energy transfer (FRET), also called Förster resonance energy transfer, was first described in 1940 by Theodor Förster (Förster 1948). Although the technique itself is not new, it has found novel biological applications with the development of recent fluorescent dyes and also new optical methods with higher spatial resolution. FRET is a physicochemical phenomenon that occurs between a donor fluorescent molecule in the excited state and an acceptor fluorescent molecule in the ground state. The energy transfer between donor and acceptor does not involve emission of photons therefore it is defined as energy of resonance. With FRET, the intensity of the donor's fluorescence emission decreases and in parallel, there is an increase in the acceptor's emission intensity. In order for FRET to occur, the donor-acceptor distance must be between 1 and 10 nm, the two fluorophores must be appropriately oriented in space, and there must be a substantial overlap (at least 30%) between the donor's emission spectrum and the acceptor's excitation spectrum (Clegg 1996). FRET efficiency decreases with the sixth power of the distance between donor and acceptor, and therefore a minimal perturbation of the spatial relationship between the two fluorophores can drastically alter the efficiency of energy transfer. These factors make FRET a sensitive technique for investigating a variety of biological phenomena that produce changes in molecular proximity.

## 1.9.3 FRET-based cAMP indicators

A new generation of FRET-based indicators provides a means of visualising localised cAMP fluctuations in intact living cell with high spatial resolution. There are two major components of cAMP FRET-based indicators: there must be a sensor which consists of two protein domains or a protein domain undergoing a conformational change upon cAMP binding; and a donor and acceptor fluorophore pair which are fused to the sensor.

The first FRET-based sensor that allowed the real-time imaging of cAMP in living cells was FICRhR (Adams et al. 1991). The authors produced a sensor based on PKA, where the regulatory (R) and catalytic (C) subunits of PKA were labelled with rhodamine and fluoresceine, respectively. In the absence of cAMP, R and C subunits are associated to

form a tetramer (R<sub>2</sub>C<sub>2</sub>) and the two dyes are close enough for FRET to occur. When cAMP binds to the R subunits, the C subunits dissociate and FRET is impaired (Adams et al. 1991). However this probe for cAMP has some technical limitations and has therefore not found wide application. These include: the requirement to microinject a large amount of protein complex ( $\mu\text{M}$ ) (procedure not applicable to all cells type the labelled subunits generate aggregates; the labelled subunits interact non-specifically with cellular structures (Goaillard et al. 2001).

To overcome these limitations, a new group of genetically encoded cAMP-biosensors were developed which could be introduced into cells by transfection. Zaccolo and colleagues generated a sensor, R-CFP/C-YFP, where the regulatory (RII $\beta$ ) and the catalytic subunit (C $\alpha$ ) of PKA are fused to the cyan and the yellow mutants of GFP, respectively (see Figure 1-9) (Zaccolo et al. 2000). The sensor has been shown to have high sensitivity for cAMP with  $\text{EC}_{50} = 0.3 \mu\text{M}$  and can therefore be used as a measurement for intracellular cAMP (Mongillo et al. 2004). Furthermore, the RII $\beta$  subunit of the probe binds via its D/D domain to endogenous AKAPs present in the cell, allowing detection of cAMP fluctuations in specific compartments. Transfection of cells with the R-CFP/C-YFP has made it possible to visualise microdomains of cAMP in various cell types, including NRVM, to clarify the role different PDE families play in shaping intracellular cAMP gradients (Zaccolo et al. 2000; Mongillo et al. 2004).

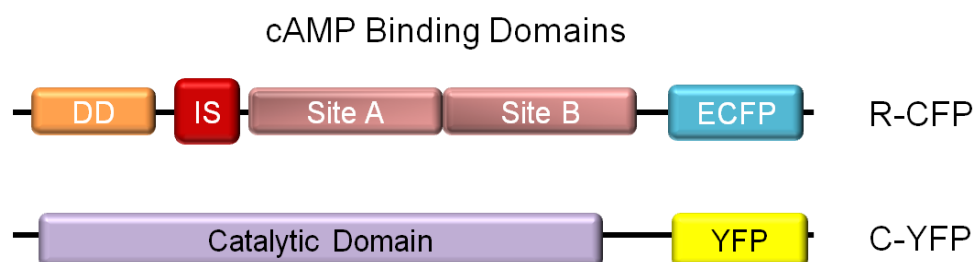


**Figure 1-9. Schematic representation of PKA-GFP based sensor.**

There are, however, still some limitations with using this type of sensor, for example, since the C and R subunits are expressed from two distinct plasmids, it is difficult to predict if equal concentrations of C and R are present in transfected cells. Taylor et al. also showed

that the cAMP-dependent dissociation of R and C subunits occurs through a cooperative mechanism and therefore the kinetics reported by the sensors may be slower than the actual kinetics of cAMP (Taylor et al. 2005). The C subunit of the sensor is also catalytically active and can therefore phosphorylate downstream targets of the cAMP/ PKA pathway resulting in an alteration of cAMP dynamics.

### 1.9.4 Epac-based sensors

A new generation of uni-molecular indicators based on Epac proteins have been developed that do not have the same issues which have been reported with PKA sensors. Epac undergoes a structural change upon cAMP binding and this mechanism has been used to develop FRET-based indicators by fusing the Epac1 protein to cyan and yellow GFP variants (Nikolaev et al. 2004). When CFP is excited at 440 nm, FRET will occur and result in YFP emission at 545 nm at the expenses of CFP emission at 480 nm. However, when cAMP levels rise, cAMP binds to Epac1 resulting in a conformational change in the structure of the FRET probe. The two fluorophores move further apart and there is a reduction in FRET, where CFP excitation at 440 nm results in reduced emission of YFP at 545 nm and an increase of CFP emission at 480 nm.

In the same year, two other groups used the full length Epac1 protein sandwiched between cyan fluorescent protein (CFP) and the yellow fluorescent protein (YFP), forming the ICUE sensor (DiPilato et al. 2004), and the CFP-Epac-YFP sensor (Ponsioen et al. 2004). This sensor was localised to the nuclear envelope and to perinuclear compartments, so to obtain a cytosolic indicator, the DEP domain (amino acids 1–148) was detected. Moreover, in order to render the indicator catalytically dead, other mutations were introduced (T781A, F782A) leading to the generation of CFP-Epac ( $\delta$ DEP-CD)-YFP, also called H30 (Ponsioen et al. 2004; Terrin et al. 2006).

More recently our lab generated targeted cAMP sensors based on the soluble Epac1 camps sensor (Nikolaev et al. 2004). RI\_epac and RII\_epac were generated by fusing the N-terminus of Epac1-camps to the dimerisation and docking domain sequences of the PKA regulatory subunit RI $\alpha$  and RII $\beta$  respectively (Di Benedetto et al. 2008). As PKA-RI and PKA-II display different subcellular localisation, these sensors would localise to different

compartments by AKAP binding (see 1.7.1) once expressed in intact cells. When expressed in cardiac myocytes, these probes demonstrate a different distribution pattern, with RI\_epac showing a tight striated pattern overlaying with both the Z and the M sarcomeric lines whereas RII\_epac shows a very strong localisation that corresponds to the M line and a much weaker localisation overlaying the Z line. The two targeted reporters show equal sensitivity to cAMP (Di Benedetto et al. 2008). A study using RI\_epac and RII\_epac to detect cAMP dynamics in intact cardiac myocytes revealed that stimulation of different GPCR leads to the activation of specific PKA isoforms and, in turn, to specific phosphorylation of downstream targets. The authors of this study also demonstrated that the pool of cAMP generated in either the PKA-RI or PKA-II compartment, is regulated by a unique subsets of cAMP degrading phosphodiesterases (PDEs).

## 1.10 Cardiac Hypertrophy

Cardiovascular disease (CVD) is one of the leading causes of disease-related mortality worldwide, accounting for 17.3 million deaths per annum (WHO estimated in 2008 <http://www.who.int/mediacentre/factsheets/fs317/en/>). In many forms of CVD, hypertrophic growth of the heart occurs in an attempt to manage the increased hemodynamic demand caused by an excessive cardiac workload. This process, known as hypertrophy, is classified as “pathological” hypertrophy. Hypertrophic growth which occurs in healthy individuals following exercise or pregnancy is characterised as “physiological” hypertrophy and is not linked to cardiac damage. Although the augmented heart size during the early stages of pathological hypertrophy is considered an adaptive response required to sustain cardiac output after increased biomechanical stress; prolonged pathological hypertrophy is associated with a significant increase in the risk for sudden death or progression to heart failure, independent of the underlying cause of hypertrophy (Levy et al. 1990; Vakili et al. 2001). During pathological hypertrophy, the heart remodels and becomes less elliptical and more spherical (Douglas et al. 1989). With the development of ventricular dilation comes a progressive decline in cardiac output despite continuous activation of the hypertrophic program to adjust the pressure overload. The late-phase “remodelling” process that leads to failure is associated with functional perturbations of cellular  $\text{Ca}^{2+}$  homeostasis (Bers 2002) and ionic currents (Hill 2003),

predisposing the heart to ventricular dysfunction and malignant arrhythmia. In addition to this, morphological changes include increased rates of apoptosis (Haunstetter and Izumo 2000), fibrosis, and chamber dilation. Currently there is no cure for heart failure, and long term survival of heart failure patients remains poor, with one third dying within one year of diagnosis (McMurray and Pfeffer 2005).

Hypertrophic growth develops in two ways, either *concentric hypertrophy*, caused by chronic pressure overload in which increase in myocyte length is less than increase in myocyte width, leading to reduced left ventricular volume and increased wall thickness. Or *eccentric hypertrophy*, which occurs due to volume overload in which the increase in myocyte length is greater than the increase in myocyte width, leading to dilatation and thinning of the heart wall (Beltrami et al. 2001).

Cardiac hypertrophy is defined as an increase in the size, but not in the number, of individual cardiac myocytes. In addition to this, cardiomyocytes develop enhanced protein content and a higher organisation of the sarcomere (Chien et al. 1991; Sugden and Clerk 1998). These processes are due to activation of the immediately early genes (c-jun, c-fos, c-myc) and the fetal genes [atrial natriuretic peptide (ANP),  $\beta$ -myosin heavy chain ( $\beta$ -MHC) and skeletal alpha actin (SKA)], which are considered to be common markers of cardiac hypertrophy (Chien et al. 1991; Komuro and Yazaki 1993). These so-called fetal genes are normally only expressed in the developing heart and are repressed in the adult myocardium, however hypertrophic growth results in a reactivation of these genes in adult hearts. Activation of the fetal gene program allows co-ordinated synthesis of the proteins needed to bring about increased cardiac myocyte size and adjustment to the increased cardiac workload (Barry et al. 2008).

A growing number of intracellular signalling pathways have been characterised as important transducers of the hypertrophic response (Molkentin and Dorn 2001). Some of these pathways are required for successful adaptation to the increased overload to the heart whereas others have been classed as maladaptive, as they result in contractile dysfunctions leading ultimately to heart failure (Levy et al. 1990; Vakili et al. 2001; Selvetella et al. 2004).

### **1.10.1 Signalling pathways regulating cardiomyocyte hypertrophy**

A growing number of intracellular signalling pathways have been characterised as important transducers of the hypertrophic response (as shown in Figure 1-10). These include specific G-protein isoforms, calcineurin and nuclear factor of activated T-cells (NFAT), protein kinase G (PKG), Phosphoinositide 3-kinase (PI3K) and Mitogen-Activated Protein Kinase (MAPK), to name but a few (Frey and Olson 2003; Barry et al. 2008). These molecules operate in an orchestrated manner to generate interdependent pathways and complex cross-talking signalling networks and therefore the mechanisms involved in cardiac hypertrophy are still not fully understood. However the more recent development of genetically modified mouse models has greatly advanced our understanding of the complexities that surround the cardiac growth response, and have contributed to a greater understanding on the role of individual signalling molecules involved in cardiac hypertrophy.

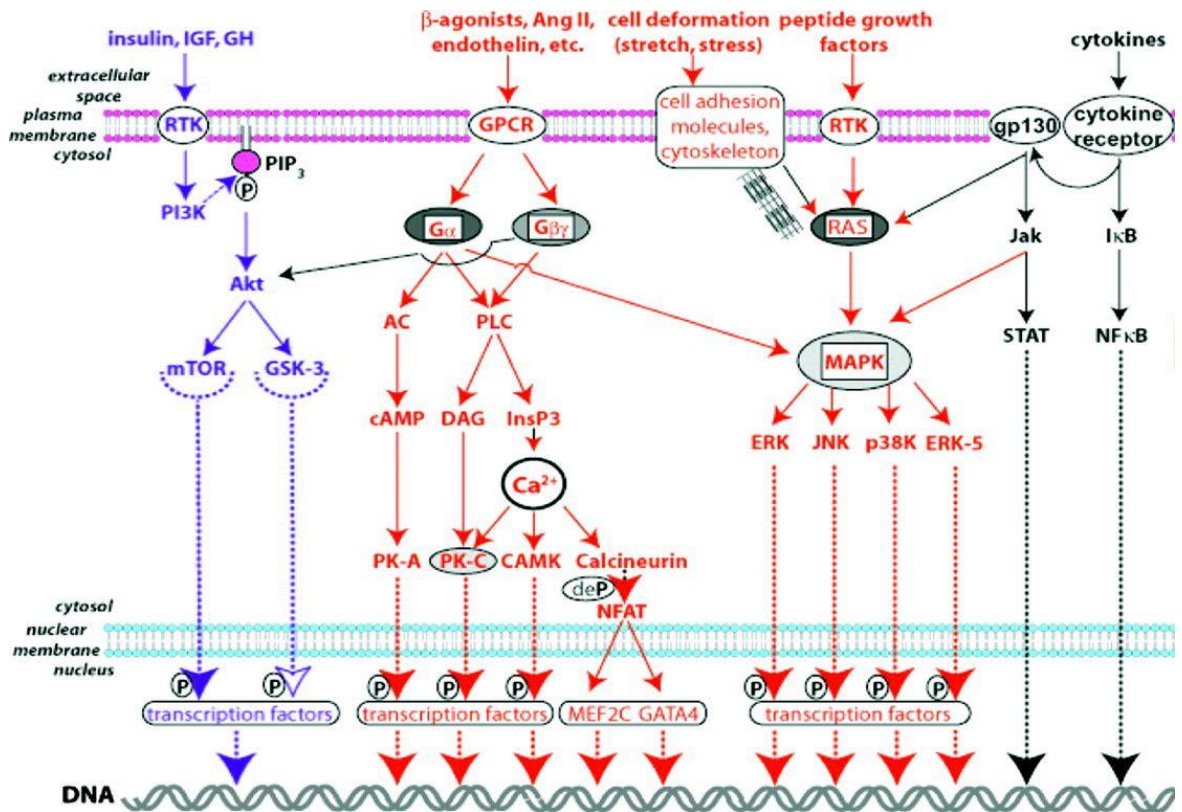


Figure 1-10. Signalling pathways involved in cardiac hypertrophy and the progression to heart failure.

Proliferative signalling pathways that mediate cardiac hypertrophy. The PI3K/PIP<sub>3</sub>/Akt pathway is activated when insulin, insulin growth factor (IGF), and growth hormone (GH) bind to receptor tyrosine kinases (RTK). Phosphorylation of phosphatidylinositol tris phosphate (PIP<sub>3</sub>) by phosphoinositide 3'-OH kinases (PI3K) activates Akt, a protein kinase that phosphorylates mammalian target of rapamycin (mTOR) and inhibits glycogen synthetase kinase 3 (GSK-3). Neurohumoral mediator binding to G-protein-coupled receptors (GPCR) activates adenylyl cyclase (AC) to form cAMP, which stimulates PKA. G $\alpha_q$  and G $\beta\gamma$  activate phospholipase C (PLC) to form diacylglycerol (DAG) and inositol tris phosphate (InsP<sub>3</sub>). DAG stimulates protein kinase C (PKC). Calcium released by InsP<sub>3</sub> activates PK C and calcium/calmodulin kinase (CAMK). Calcium also activates calcineurin, a protein phosphatase that dephosphorylates nuclear factor of activated T cell (NFAT) which activates transcription factors MEF2C and GATA4. Peptide growth factor binding to RTKs and cytoskeletal signalling pathways activate Ras which stimulates mitogen-activated protein kinase (MAPK) pathways; the latter include extracellular receptor-mediated kinases (ERK), c-Jun kinase (JNK), and p38 kinase (p38K). Activated cytokine receptors release an inhibitory effect of I $\kappa$ B on nuclear factor- $\kappa$ B (NF $\kappa$ B) and activate gp130-mediated signalling pathways that stimulate janus kinase (Jak) to activate signal transducer and activator of transcription (STAT) and MAP kinases. Pathways in red mediate mainly maladaptive hypertrophy; those in blue, mainly adaptive hypertrophy. Cytokine-activated pathways (black) can activate both adaptive and maladaptive growth. Adapted from (Katz 2008).

### 1.10.1.1 cGMP/ PKG

One well-described signalling pathway involved in the regulation of hypertrophic responses is the 3', 5-cyclic guanosine monophosphate (cGMP)/ protein kinase G (PKG) signalling pathway. Generation of cGMP by NO activation of soluble guanylyl cyclases (sGC) was shown to reduce the hypertrophic response to norepinephrine (NE) (Calderone et al. 1998) or angiotensin II (Ang II) stimulation (Ritchie et al. 1998). Atrial and brain natriuretic peptides (ANP and BNP) which, by activating the membrane-bound particulate guanylyl cyclases (sGC) stimulate the production of cGMP, have also been found to exert anti-hypertrophic effects *in vitro* (Calderone et al. 1998; Rosenkranz et al. 2003). ANP and BNP are found at high levels during embryonic development and in early neonates but are absent in healthy adults (Gardner 2003), however in the hypertrophic heart the expression levels of ANP and BNP are found to be significantly increased (Silberbach and Roberts 2001; Tremblay et al. 2002; Molkentin 2003). In fact, expression of the genes encoding ANP and BNP is one of the most reliable markers for activation of the hypertrophic program in clinical states and experimental models associated with hypertrophy. Some recent studies have reported that natriuretic peptides exert a regulatory influence over cardiac hypertrophy. Neonatal rat ventricular myocytes (NRVM) stimulated with an ANP receptor antagonist lead to increased protein syntheses and cell size as well as reactivation of the fetal gene program. Zaprinast, a cGMP analogue and an inhibitor for a cGMP-specific phosphodiesterase, suppressed the basal and PE-stimulated protein syntheses (Horio et al. 2000). Thus, ANP may play a role as an autocrine factor in the regulation of cardiac myocyte growth. Another study reported that in NRVM and cardiac fibroblasts, treatment with ANP or the NO donor S-nitroso-N-acetyl-D, L- penicillamine (SNAP) attenuated the effects of NE-induced hypertrophy. The authors suggest that this effect was most likely by a cGMP-mediated inhibition of NE-stimulated  $Ca^{2+}$  influx (Calderone et al. 1998).

Recent studies using targeted gene deletion in mice have been particularly informative with regard to the role of the NPs in modulating cardiac hypertrophy. Deletion of the *Npr1* gene encoding the natriuretic peptide receptor A (NPR-A) in mice resulted in moderate elevations in blood pressure, with a disproportionate increase in cardiac weight (i.e. hypertrophic growth) and interstitial fibrosis (Lopez et al. 1995; Oliver et al. 1997). Knowles and colleagues used transverse aortic constriction (TAC) to induce pressure overload in the *Npr1* *-/-* mice, which resulted in a 15-fold increase in atrial natriuretic

peptide (ANP) expression, a 55% increase in left ventricular weight/body weight (LV/BW), dilatation of the LV, and significant decline in cardiac function (Knowles et al. 2001). In TAC treated wild-type mice, the authors described only a three-fold increase in ANP expression, an 11% increase in LV/BW, a 0.2 mm decrease in LV end diastolic dimension, and no change in fractional shortening (Knowles et al. 2001). These results suggest that the NPR-A system has direct anti-hypertrophic actions in the heart. Failure of the natriuretic peptide system, at the ligand, receptor or post-receptor level, could account for the progression in cardiac dysfunction that accompanies longstanding hypertrophy and heart failure.

The role of cGMP/ PKG effect in cardiac hypertrophy has been described in various knockout mice lacking elements of this signalling pathway. Holtwick and colleagues showed that mice with a cardiomyocyte specific deletion of constitutively active guanylyl cyclase-A (GC-A), which is normally activated by natriuretic peptides to produce cGMP, exhibited mild cardiac hypertrophy and an increase in mRNA expression of fetal genes ANP,  $\alpha$ -skeletal actin and  $\beta$ -myosin heavy chain. Pressure overload induced by transverse aortic constriction (TAC) in this mouse model lead to an exaggerated hypertrophic response as well as enhanced cardiac fibrosis and marked cardiac dysfunction (Holtwick et al. 2003). In the same year, Zahabi et al engineered transgenic mice that overexpressed a catalytic fragment of the GC-A domain of the atrial natriuretic peptide receptor in a cardiomyocyte-specific manner. They found increased GC-A attenuated the effects of both ISO treatment and abdominal aortic constriction on cardiac wall thickness, cardiomyocyte size and prevented the onset of the fetal gene expression program (Zahabi et al. 2003). Mice lacking eNOS and/or nNOS also develop cardiac hypertrophy, dysfunction and increased premature mortality (Barouch et al. 2003; Li et al. 2004; Flaherty et al. 2007). Conventional PKG-I knockout mice die young and perhaps too early to develop any cardiac hypertrophy (Pfeifer et al. 1998). Wollert and colleagues showed that *in vitro* adenoviral overexpression of PKG-I $\beta$  in neonatal rat cardiac myocytes enhanced the anti-hypertrophic effect of NO in phenylephrine-stimulated cardiac myocytes (Fiedler et al. 2002; Wollert et al. 2002). However, the significance of the PKG pathway in modulating cardiac hypertrophy has been recently questioned. Lukowski and colleagues showed that, when compared to wild type mice, the degree of cardiac hypertrophy induced either by isoproterenol (ISO) infusion or by TAC was not changed in total PKG knock-out mice or in mice lacking PKG specifically in cardiomyocytes, indicating that the development of

cardiac hypertrophy is not amplified by the absence of endogenous PKG (Lukowski et al. 2010).

It has been reported that enhancement of the cGMP/ PKG pathway by inhibiting PDE mediated hydrolysis of cGMP reduces cardiac hypertrophy (Takimoto et al. 2005; Miller et al. 2009). Takimoto and colleagues showed that pharmacological inhibition of PDE5 with Sildenafil reverses hypertrophy, suppresses remodelling and improves cardiac function in mouse hearts subjected to thoracic aortic constriction (TAC). In addition, the authors suggested that the anti-hypertrophic effects of Sildenafil are mediated by the cGMP/PKG signalling pathway (Takimoto et al. 2005). Miller et al. published data which indicated that PDE1 inhibition with IC86340 is able to attenuate the hypertrophic response induced by chronic isoproterenol infusion *in vivo* (Miller et al. 2009). The authors also showed that expression levels of the dual-specific PDE1 are significantly up-regulated in various *in vivo* and *in vitro* models of hypertrophy. Results obtained with selective PKG or PKA inhibitors, indicated that PDE1 seems to regulate cardiac hypertrophy via modulation of cGMP/PKG signalling pathways (Miller et al. 2009). The role of PDE5 in regulating cardiac hypertrophy was also questioned by Lukowski and co-workers, as endogenous PDE5 could not be detected in cardiomyocytes from either wild type mice or mice lacking cardiac-specific PKG (Lukowski et al. 2010). Further studies are required to fully understand the role of cGMP/ PKG in cardiac hypertrophy.

### 1.10.1.2 Calcineurin/ NFAT

One of the most studied maladaptive pathways is the calcineurin pathway. Calcineurin is a calcium/calmodulin-regulated, serine/ threonine phosphatase that dephosphorylates members of the NFAT transcription factor family, causing their nuclear translocation and the activation of immune response genes such as interleukin-2 (Crabtree 1999). The physiological role of calcineurin was initially elucidated in T-cells where an increase in cytoplasmic calcium concentrations promoted the association of calmodulin with calcineurin and consequent activation of the enzyme (Olson and Williams 2000).

Molkentin et al. have demonstrated the role of calcineurin in cardiac hypertrophy, generating transgenic mice that overexpressed activated forms of calcineurin or NFAT3 in the heart (Molkentin et al. 1998). These mice were shown to develop cardiac hypertrophy

and heart failure before two months of age. Pharmacological inhibition of calcineurin activity with the immunosuppressant drugs cyclosporin A (CsA) and FK 506, which inhibits calcineurin's ability to activate NFAT transcription factors, blocked the hypertrophic response of isolated cardiomyocytes to Ang II and PE. Furthermore, CsA treatment by subcutaneous injection prevented cardiac hypertrophy and associated pathology in calcineurin transgenic mice. (Molkentin et al. 1998). These results suggest the involvement of calcineurin in a 'maladaptive' type of hypertrophy as transition toward heart failure was accelerated. However, the role of calcineurin in the progression of cardiac hypertrophy is still controversial mainly due to conflicting results of *in vivo* experiments using the calcineurin inhibitors cyclosporine A (CsA) and FK506 to treat various rodent models of hypertrophy. However, interpretation of *in vivo* results is difficult as the doses of CsA required to inhibit calcineurin activity in the heart are about 10-fold higher than those required for immunosuppression and are associated with significant systemic toxicity. As well as this, calcineurin is not cardio-specific, therefore inhibition of its activity by CsA or FK506 may modify the cardiac effects via systemic influences (Frey and Olson 2003). The discovery of several endogenous calcineurin inhibitors, such as AKAP79, Cabin/Cain, and DSCR/MCIP has allowed for alternative methods of investigation. Overexpression of the calcineurin-binding domain of AKAP79 (see 1.7.1) in neonatal rat cardiomyocytes prevents PE-induced hypertrophy (Taigen et al. 2000). AKAP79 interacts with calcineurin as well as protein kinases A and C (see 1.5.1), creating yet another point of integration between hypertrophic signalling pathways.

### 1.10.1.3 G-protein coupled receptors

Another clear example of maladaptive mechanism is the signalling pathway associated to activation of the G-protein-coupled-receptor (GPCR). GPCR are crucial in normal cardiovascular function and in mediating the "fight or flight" response to endogenous catecholamines such as adrenaline, noradrenaline and angiotensin. The most important myocardial GPCRs include adrenergic (comprised of several subtypes of  $\alpha$ - and  $\beta$ -adrenergic receptors) and muscarinic receptors, which are coupled to three principal classes of heterotrimeric GTP-binding proteins,  $G_s$ ,  $G_q/G_{11}$ , and  $G_i$ . G proteins consist of the subunits  $G_\alpha$  and  $G_{\beta\gamma}$ , which upon receptor activation dissociate and independently activate intracellular signalling pathways.  $G_q$  is the target of Ang II, ET-1, and  $\alpha$ -

adrenergic stimulation that have been demonstrated to determine hypertrophic responses in cardiomyocytes (Sadoshima et al. 1993; Nicol et al. 2000; Maruyama et al. 2002).

Several studies have highlighted the involvement of  $G_q$  signalling in the development of hypertrophy and transition to heart failure. Sakata et al showed that transgenic mice overexpressing  $G_q$  develop a pronounced hypertrophy that rapidly progresses to heart failure in response to pressure-overload via aortic banding (Sakata et al. 1998), suggesting that excessive activation of the  $G_q$  pathway is mainly deleterious. Transgenic mice with inhibited  $G_q$  signalling developed significantly less ventricular hypertrophy than control animals after pressure-overload was induced by aortic stenosis (Akhter et al. 1998). Furthermore, transgenic mice lacking both  $G_q$  and  $G_{11}$  in cardiomyocytes showed no hypertrophy in response to pressure-overload induced by TAC (Wettschureck et al. 2001). The lack of hypertrophic response in both of these studies proves that the  $G_q/G_{11}$ -mediated pathway is essential for cardiac hypertrophy induced by pressure overload.

Milano et al. showed that overexpression of a constitutively active  $\alpha 1B$ -adrenergic receptor in the heart induced cardiac hypertrophy (Milano et al. 1994) while mice lacking this receptor failed to develop hypertrophy in response to chronic infusion of adrenergic agonists but still displayed a hypertrophic response to pressure overload (Vecchione et al. 2002).

#### **1.10.1.4 cAMP/ PKA signalling in cardiac hypertrophy**

Stimulation of  $\beta$ -adrenergic receptors ( $\beta$ -ARs) activates adenylyl cyclase (AC), generating 3', 5' cyclic adenosine monophosphate (cAMP), and results in positive chronotropic, inotropic, and lusitropic effects on the heart (Bers 2008). Catecholamines released from the sympathetic nervous system in response to stress or exercise rapidly increase the cardiac output via this signalling pathway. As previously discussed (1.6), a number of publications have revealed that persistent stimulation by catecholamines leads to hypertrophic growth, ventricular dysfunction and, in the long term, to heart failure. In cardiac myocytes, both  $\beta_1$ - and  $\beta_2$ -ARs have been reported to mediate an increase in contractility via  $G_s$ -dependent coupling to adenylyl cyclase to generate cAMP (Xiao and Lakatta 1993). Chronic catecholamine treatment results in a significant downregulation of

$\beta_1$ -AR expression only, leading to desensitisation of the heart to inotropic  $\beta$ -adrenergic stimulation (Fowler et al. 1986; Engelhardt et al. 1999; Lohse et al. 2003; Barry et al. 2008).

The most abundant adrenergic receptor in the heart is the  $\beta_1$ -AR which is coupled to  $G_s$ . Overexpression of  $\beta_1$ -ARs in hearts of transgenic mice initially increases contractile function to isoproterenol, but eventually results in progressive cardiomyocyte hypertrophy and fibrosis leading to heart failure (Engelhardt et al. 1999). Likewise, transgenic mice overexpressing  $G_s$  also developed cardiac hypertrophy (Gaudin et al. 1995; Iwase et al. 1996). Antos and colleagues demonstrated that transgenic mice overexpressing PKA develop dilated cardiomyopathy associated with cardiomyocyte hypertrophy and fibrosis, suggesting that PKA mediates the adverse effects of chronic  $\beta$ -adrenergic signalling (Antos et al. 2001). It has been suggested that AC may actually have cardioprotective effects. Elevated cardiac adenylyl cyclase activity was shown to result in long-term enhanced function, and in transgenic mouse models that suffer from cardiac failure (due to  $G_q$  overexpression).

To investigate the hypothesis that increased AC6 would be cardioprotective, Roth and colleagues crossbred mice with  $G_q$ -associated cardiomyopathy and those with cardiac-directed expression of AC6 (Roth et al. 2002). Survival was increased by cardiac-directed expression of AC6 and hypertrophic growth was abolished. The overexpression of AC6 was also found to improve contractility (Roth et al. 2002). Goa et al. also reported transgenic mice with cardiac-directed overexpression of AC6 demonstrate improved contractile function (Gao et al. 2002). Gao and colleagues later showed that AC6 overexpression increases calcium cycling in cardiomyocytes and enhances cardiac function by down-regulating phospholamban, a sarcoplasmic reticulum  $Ca^{2+}$ -ATPase inhibitor (Gao et al. 2004). Another study found that AC6, but not AC5, mRNA is decreased in rats with cardiac hypertrophy after myocardial infarction (Espinasse et al. 1999). Overexpression of AC5 was found to restore cyclic AMP signalling and contractile deficits in the  $G_{\alpha q}$ -hypertrophic mice, however cardiac hypertrophy still developed (Tepe and Liggett 1999). Okumura and colleagues demonstrated that decreasing AC5 expression may have a protective role in mice where hypertrophy was induced by aortic banding (Okumura et al. 2003). The authors showed that, on comparison of AC5 knock out (AC5KO) mice and WT littermates, the number of apoptotic myocytes was increased significantly in WT (4-fold)

at both 1 and 3 weeks after TAC, and the number was significantly less in AC5KO (2-fold). More importantly, cardiac apoptosis was induced prior to cardiac dysfunction in WT. The same group also demonstrated that the disruption of AC5 results in more effective desensitisation after chronic catecholamine stress and protects against the development of myocyte apoptosis and deterioration of cardiac function (Okumura et al. 2009). The findings suggest that, at least in adult myocytes, AC5 may lead to cardiac dysfunction and its disruption may have a cardioprotective effect.

$\beta_2$ -adrenergic receptors couple to  $G_i$ , inhibiting AC and thus directly opposing  $G_s$ -dependent signalling. In 1988, Neumann et al. published the first evidence of  $G_i$  up-regulation occurring in patients with heart failure (Neumann et al. 1988). This was later confirmed by Bristow and colleagues who reported that in myocardial tissue from patients with heart failure the  $G_i$  content was increased by ~30%, and basal AC activity was depressed by ~70% (Hershberger et al. 1991).  $G_i$  is upregulated in hypertensive hypertrophy before the development of overt failure (Bohm et al. 1992), indicating that  $G_i$  up-regulation may precede decompensation. Mice genetically engineered to express a conditional  $G_i$ -coupled receptor demonstrated a profound decrease in heart rate upon stimulation resulting in cardiomyopathy and lethal arrhythmias (Redfern et al. 1999).

Heart failure is accompanied by impaired  $\beta$ -AR function through both a decreased number of receptors and functional uncoupling. Inhibition of  $\beta$ -adrenergic receptor kinase ( $\beta$ -ARK or GRK), a kinase believed to mediate these processes, by overexpression of the inhibitory peptide  $\beta$ -ARKct attenuates cardiomyopathy secondary to deficiency of the sarcomeric protein MLP (Rockman et al. 1998). Moreover,  $\beta$ -ARKct overexpression significantly blunts the development of cardiac hypertrophy and delays development of systolic dysfunction in transgenic mice overexpressing the sarcoplasmic reticulum  $Ca^{2+}$ -binding protein, calsequestrin (CSQ). These mice have a severe cardiomyopathy and markedly shortened survival (9 weeks), whereas CSQ/  $\beta$ -ARKct mice exhibited a significant increase in survival age (15 weeks) and displayed less cardiac dilatation (Harding et al. 2001). This data again demonstrates the beneficial effects of  $\beta$ -ARK inhibition of cardiac hypertrophy.

These data suggest that components of the  $\beta$ -adrenergic signalling pathway may have different consequences on cardiac hypertrophy and failure. One explanation for the variation in effect of  $\beta$ -AR stimulation in animal models of cardiac hypertrophy is that in

cardiac myocytes cAMP/PKA signalling is compartmentalised (see 1.7). It is therefore possible that distinct and localised pools of cAMP mediate different downstream functional effects in cardiomyocytes.

Current therapeutic treatment for dilated cardiomyopathy and heart failure are aimed at improving cardiac contractility by raising cAMP production through  $\beta$ -AR antagonists and phosphodiesterase inhibitors. Several PDE3 inhibitors – including, milrinone, amrinone, and enoximone – were developed as therapeutic agents for the treatment of ischaemic and dilated cardiomyopathy. The use of these inhibitors was shown to have short-term beneficial effects on cardiovascular function in treated patients in numerous studies, however long-term use of such drugs resulted in negative side effects such as arrhythmias and increased mortality (Movsesian and Alharethi 2002; Movsesian and Kukreja 2011). These detrimental consequences of long-term use of PDE3 inhibitors may be explained by the fact that non-selective inhibition of PDE3 would lead to a global activation of PKA, by increased intercellular cAMP. This would result in generalised phosphorylation of all substrates of PKA, including those involved in mediating both beneficial and adverse effects. Based on this model, selective modulation of compartmentalised PDEs activity may result in a more effective treatment without the negative side effects. A more detailed description of the spatial organisation of the individual cAMP/PKA signalling sub-compartments and of their specific regulation in cardiac myocytes would be required to develop novel therapeutics able to treat cardiovascular disease. Importantly, a better understanding of the regulation and function of individual PDE isoforms has in cardiomyocytes is essential as very little is known about the role of compartmentalised PDEs in regulating cAMP signalling in heart disease. In fact, few have published data on the role of PDEs in cardiac hypertrophy, and often results are conflicting

Abi-Gerges and colleagues studied the expression of PDEs and their regulation in single hypertrophied cardiomyocytes isolated from Wistar rats exposed to pressure-overload by surgical thoracic aortic banding (TAC). Subsarcolemmal cAMP signals were detected by whole-cell patch-clamp recordings of the associated cyclic nucleotide-gated (CNG) current ( $I_{\text{CNG}}$ ) and PDE activity and protein levels were assessed. They reported a decrease in both PDE3 and PDE4 cAMP-hydrolyzing activity in TAC- animals, together with marked  $\beta$ -adrenergic receptor desensitisation. Furthermore, western blot analysis revealed that PDE3A, PDE4A and PDE4B, but not PDE4D, expression levels were decreased in

hypertrophic myocytes (Abi-Gerges et al. 2009). In 2010, Mokni et al. investigated the activities of various PDE isoforms in Wistar rats where hypertrophy was induced by chronic infusion of angiotensin II (Ang II). It was reported that the cAMP hydrolysing activity of PDE4 is increased, whereas PDE1, PDE2 and PDE3 cAMP-degrading activities are unchanged. Utilising a real-time PCR approach, the same study shows a significant decrease in mRNA levels of PDE4D and no change in PDE2A, PDE3A, PDE3B, PDE4A, PDE4B or PDE4C which is somewhat in contradiction of the PDE activity assay results (Mokni et al. 2010).

These studies show that, during cardiac hypertrophy, alterations in PDE expression and activity may occur. To fully understand compartmentalised cAMP signalling and PDE regulation in cardiac hypertrophy and whether selective modulation of PDEs activity may be exploited as a therapeutic treatment, further investigation is necessary. As previously mentioned (1.10.1.4), PDE inhibitors for several families have been used clinically or are currently being investigated in clinical trials for treatment for a number of different cardiovascular diseases. The PDE3 family have been used for a number of years to treat chronic heart failure, although their long-term use has generally been shown to increase mortality (Packer et al. 1991; Movsesian 2002; Movsesian and Alharethi 2002). More recently, PDE5 specific inhibitors have been used to treat pulmonary hypertension by reducing pulmonary vascular resistance (Galie et al. 2010). Some studies have also suggested that PDE5 inhibitors may be useful as a treatment for models of ischemia–reperfusion, left and right ventricular hypertrophy, and congestive heart failure (Kumar et al. 2009). However there have been some suggestions that PDE5 inhibitors may have limited effects on vascular tone in humans, which indirectly contribute to the cardioprotective effects.

Dual PDE inhibitors inducing synergic potencies with lesser undesirable side effects have been envisioned. Indeed, dual PDE3/4 inhibitors are now designed as therapeutic agents for chronic obstructive pulmonary disease (COPD). By combining both inhibitions, these compounds have additive and synergistic bronchodilatory and anti-inflammatory effects (Banner and Press 2009).

Another approach to obtain efficient therapeutic effect, without the negative side effects, may be to specifically target the altered PDE family and in particular the altered isoform so that all other forms remain unaltered. For this to occur, it would be necessary to

characterise the all PDE isozymes present in the studied model and then identify which PDE isoforms are altered in the diseased state before selectively inhibiting the PDE of interest. The outcome of this type of treatment would be restoration of the altered PDEs and associated cellular function without changing the other non-altered PDEs. Selective pharmacological inhibition of individual PDE isoforms has proved difficult due to the fact that existing inhibitors target the catalytic site and this domain is highly conserved among isoforms, and thus, does not allow for discrimination between isoforms. One alternative approach is to displace the individual PDE isoform from its specific subcellular anchor site. This may be possible with the use of disruptor peptides (Christian et al. 2011; Sin et al. 2011) or overexpression of catalytically inactive PDE isoforms (dominant-negative approach see 7.2.2) (Houslay et al. 2007; Stangherlin et al. 2011), although further investigation is required to better develop these treatment strategies.

## 2 Thesis Aims

---

In the heart, compartmentalised cAMP/PKA signals play a key role in the regulation of excitation contraction coupling (ECC). Recent studies have demonstrated that impairment of cAMP/ PKA compartmentalisation by altered PDE expression/ activity or AKAP binding, can lead to the development of heart disease. One such cardiovascular disease where altered PDE activity and expression levels have been described is cardiac hypertrophy. Understanding the fine control of cAMP and the regulation and function of individual PDE isoforms in normal and hypertrophied hearts, may provide new valuable insight for the development of novel therapeutics for the treatment of cardiac hypertrophy.

Previous data (unpublished) in neonatal rat ventricular myocytes, transfected with Epac1-camps FRET sensor, indicated PDE2 activity is significantly increased in hypertrophic cardiac myocytes and pharmacological inhibition of PDE2 with Bay 60-7550 counteracts NE-induced cardiomyocytes hypertrophy.

Therefore the hypothesis that altered PDE2 activation induces hypertrophy, after excessive catecholamine stimulation, was tested in adult rat ventricular myocytes. Utilising targeted FRET-based biosensors in an *in vitro* model of cardiomyocyte hypertrophy, the role of cAMP phosphodiesterases in the development of cardiac hypertrophy was investigated.

## 3 Materials and Methods

---

### 3.1 Materials

The chemicals used in this study were of analytical grade. All chemicals were supplied by Sigma-Aldrich unless otherwise indicated.

### 3.2 Cellular Biology

All tissue culture was performed in sterile conditions using biological safety class II vertical laminar flow cabinets. Cells were grown in 37°C incubators maintained at 5% CO<sub>2</sub>.

#### 3.2.1 Primary Isolation Optimisation

The goal of a cell isolation procedure is to maximise the yield of functionally viable, dissociated cells; however there are several parameters which may affect this outcome, such as:

1. Type of tissue
2. Species of origin
3. Age of the animal
4. Genetic modification(s) (knockouts, etc.)
5. Dissociation medium

6. Enzyme(s)
7. Impurities in any crude enzyme preparation
8. Concentration(s) of enzyme(s)
9. Incubation times

From the literature it is clear the greatest variation in dissociation protocols is the enzyme used and the dissociation conditions (i.e. concentration of enzyme and incubation times).

### **3.2.1.1 Collagenase**

Collagenases are endopeptidases that digest native collagen, the major fibrous component of animal extracellular connective tissue and are widely used in cell dissociation protocols.

Due to the variation between batches of collagenase, Worthing Biochem offers a sampling service in order to pre-test a particular batch of enzyme. The customer is sent 3 batches of collagenase to test in their experiment and selects the most effective of the group to order in bulk.

## **3.2.2 Adult Rat Ventricular Myocytes (ARVM)**

### **3.2.2.1 Isolation of ARVM**

Primary adult cardiac ventricular myocytes were isolated from the hearts of 200g-250g Wistar rats (Harlan Laboratories) with the following protocol.

Male Wistar rats were stunned by a blow to the head and killed by cervical dislocation. The thoracic cavity was opened and the heart was quickly removed and placed in ice-cold Krebs solution (see 3.2.6 for all medias and buffer used for this protocol). The heart was mounted and tied via the aorta on to the cannula of a Langendorff perfusion system and perfused with Krebs solution at 37°C for approximately 5 minutes until all the blood had been washed out from the coronary vessels. Hearts were then perfused with an enzyme

solution containing 0.66mg/ml collagenase type I (Worthington) and 0.04mg/ml protease type XIV in warm Krebs. Enzyme solution was collected from the heart and re-circulated once the initial solution had passed through the heart. The heart was kept warm by heating the perfusate and using a heated jacket or lamp around the heart.



**Figure 3-1.** The Langendorff perfusion system used to perform isolations.

**A.** Buffer and enzyme are heated in a water bath and driven through the system by a peristaltic pump. The cannula was attached to a glass reservoir which kept the enzyme warm and also acted as a bubble trap. **B.** Image of a rat heart attached to the cannula during retrograde perfusion with enzyme.

The heart was judged as being digested once the tissue felt soft to the touch and the colour had become pale and almost translucent (this took around 9-11 minutes depending on the size of heart). The perfusion was stopped, the heart was removed from the cannula and the ventricles were finely chopped in a Krebs solution containing 0.5% BSA. The tissue was gently triturated with a Pasteur pipette in order to dissociate the myocytes, and the supernatant transferred into a 15ml tube. The process was repeated until all the tissue was dissolved or there were no more living myocytes dissociating.

This whole process was conducted in calcium free solution and therefore the calcium levels must be raised to physiological levels. The  $\text{CaCl}_2$  concentration in the cell solution

was gradually increased over time by adding 0.1 mM CaCl<sub>2</sub> every 20 minutes until a final concentration of 1mM CaCl<sub>2</sub> was obtained. Cells were then allowed to settle by gravity for 20 minutes before removing supernatant and resuspending the pellet in supplemented M199 medium. Cells were counted using a haemocytometer. Only rod shaped quiescent cells were considered viable. Cells were seeded at 50,000 cells per 24mm laminin-coated glass microscope coverslips and incubated at 37°C for at least 2 hours before infection.



**Figure 3-2. Image of an adult rat ventricular myocyte (ARVM) isolation before counting and seeding the cells, showing both healthy (rod shaped) myocytes and dead (round) myocytes.**

### 3.2.2.2 Troubleshooting

There are various possible results for tissue dissociation and being able to correctly recognise what these results are will help to identify the corrective actions to take next time. For example if the dissociation outcome is:

**Low yield and low viability of cells:** This is an over/under digestion, cellular damage. Change to less digestive type enzyme and/or decrease working concentration. (e.g. from trypsin to collagenase/ from Type 2 collagenase to Type 1).

**Low yield but high viability of cells:** Suggests under dissociation.

Increase enzyme concentration and/or incubation time and monitor both yield and viability response. If yield remains poor, evaluate a more digestive type enzyme and/or the addition of secondary enzyme(s).

**High yield but low viability of cells:** Suggests this was a good dissociation but there is cellular damage.

Enzyme is overly digestive and/or at too high a working concentration. Reduce concentration and/or incubation time and monitor yield and viability response.

**High yield and high viability:** The ideal dissociation.

### 3.2.2.3 Preparation of Laminin-coated coverslips

Laminin (mouse purified, Millipore) was prepared to manufacturer's specifications and stored at 4°C. Laminin was diluted to 20 µg/ml in supplemented M199 medium and 24 mm cover glasses (VWR International) were sterilised with an ether ethanol solution (1:1) and set in a 6 well tissue culture (TC) plate to allow them to dry. Each coverslip was coated with 250 µl of laminin and incubated at 37°C for a minimum of 1 hour. Laminin was removed by aspiration before use.

### 3.2.3 *In-vitro* hypertrophy protocol

For hypertrophy induction, ARVM were seeded onto laminin coated coverslips at 50,000 cells per slide and incubated at 37°C for 2 hours to allow living cells to attach to the glass. After this time the medium was aspirated and replaced. 1 µM norepinephrine (NE) in serum free medium was added to the hypertrophic myocytes and an equal amount of DMSO was added to control myocytes before viral infection (which occurs on same day as induction of hypertrophy).

### 3.2.4 Infection of ARVM with adenovirus vectors carrying FRET-based sensors

Isolated ARVM were infected with the desired multiplicity of infection (MOI) using the following equation:

$$\begin{aligned} \text{number of cells} \times \text{desired MOI (1000 in this case)} \\ = \text{total PFU (plaque forming units)} \end{aligned}$$

After seeding the cells onto laminin coated coverslips and incubating for 2 hours as mentioned above, the medium was aspirated to remove dead cells and fresh supplemented M199 containing the calculated amount of virus was added. Cells were incubated at 37 °C overnight (~18 hours) prior to use.

### 3.2.5 CHO culture and transfection

CHO-K1 cells from Hamster Chinese ovary cells were thawed in a water bath at 37°C and added drop wise to 5 ml of pre-warmed medium, centrifuged for 5 minutes at 300 x g, re-suspended in fresh medium and seeded in a 75 cm<sup>2</sup> flask containing 10 ml of the appropriate medium. Cells were fed every 2-3 days by changing medium, and split into new flasks when 80-90% confluent.

#### **CHO freezing**

Cells were trypsinised with trypsin-EDTA 0.05 % (Invitrogen), centrifuged for 5 minutes at 2,700 x g re-suspended in 3 volumes of FBS and 1 volume of freezing solution (3.2.6) added drop wise. Cells were then dispensed into 2 ml cryo vials and transferred to -80°C for 24h. Cells were then stored in liquid nitrogen tank.

### 3.2.6 Media, Buffers and compounds for Cellular Biology

#### Kreb's Solution

NaCl	120 mM
Hepes	20 mM
NaH <sub>2</sub> PO <sub>4</sub>	0.52 mM
KCl	5.4 mM
MgCl <sub>2</sub>	3.5 mM
Taurine	20 mM
Creatine	10 mM
Glucose *	11.10 mM

\* glucose added prior to use.

Adjusted to pH 7.4, filter sterilised and stored at 4°C.

#### Supplemented M199 medium (for ARVM)

MEM199 (Invitrogen)	500 ml
Taurine	5 mM
L-Carnitine	2 mM
Creatine	5 mM
Pen/Strep	100 i.u. ml <sup>-1</sup>

Filter sterilised and stored at 4°C

#### Tyrode Solution

NaCl	134 mM
Glucose	11 mM
KCl	4 mM
MgSO <sub>4</sub>	1.2 mM
NaH <sub>2</sub> PO <sub>4</sub>	1.2 mM
HEPES	10 mM

Adjusted to pH 7.34, filter sterilised and stored at 4°C.

**Supplemented Hams F12 medium (for CHO-K1 cells)**

Ham's F-12 (Invitrogen)	500 ml
Glutamine (Invitrogen)	2 mM
Penicillin	1 U/ ml
Streptomycin	1 µg/ ml
FBS (Invitrogen)	10 %

**Freezing Solution (for CHO-K1 cells)**

DMEM	
Glucose	12 %
DMSO	40 %

## 3.3 Molecular Biology

### 3.3.1 Agar plates

Agar plates were prepared by autoclaving LB agar broth (1 % tryptone, 0.5 % yeast extract, 170 mM NaCl and 1.5% agar), cooling the mixture ~45°C, and then the appropriate antibiotic (ampicillin or kanamycin) for the plasmid antibiotic resistance gene was added, before pouring into 90 mm Petri dishes. Agar plates were stored sealed at 4°C for up to one month.

### 3.3.2 Transformation of Chemically Competent Cells

Chemically competent TOP10 cells (Invitrogen) were stored at -80°C and thawed on ice for 10 minutes immediately prior to use. 2-2.5 ng of plasmid DNA was added per 50 µl aliquot of competent cells on ice, and mixed gently. Tubes were incubated for 15 minutes on ice, heat shocked at 42°C for 30 seconds, and returned to ice for a further 2 minutes. 450 µl of pre-warmed SOC media (Invitrogen) was aseptically added to the cells, and tubes

were incubated at 37°C for 1 hour in a shaking incubator. 20-200 µl of the transformation mix was spread onto pre-warmed agar plates containing the appropriate antibiotic. Plates were incubated upside down at 37°C overnight. Colony growth indicated successful transformation of cells.

### 3.3.3 DNA extraction and purification

Single putative positive colonies were picked from agar plates using a sterile pipette tip, and grown for approx. 8 hours in 3 ml of LB containing the appropriate antibiotic at 37°C in an orbital shaker set at 180 rpm. 1 ml of the culture was used to check the plasmid isolated using a QIAprep Spin Miniprep Kit (Qiagen), following the manufacturer's protocol for plasmid purification with a microcentrifuge. Plasmids were screened by restriction digest or sequencing. The remaining positive starter culture was added to 500 ml LB in a 2 L flask and incubated in an orbital shaker overnight at 37°C and 180 rpm. The bacterial cells were harvested by centrifugation at 6700 x g for 15 minutes at 4°C.

The plasmid DNA was extracted from the bacteria using the HiSpeed Plasmid Maxi Kit (QIAGEN). Briefly, the bacterial pellet was re-suspended in 10 ml of the lysis Buffer P1. Buffer P1 contains Tris and EDTA. EDTA chelates divalent metals (primarily magnesium and calcium). Removal of these cations destabilises the cell membrane, producing lysis of the bacterial cells, and also inhibits DNases. 10 ml of Buffer P2 was added, the solution mixed thoroughly by inverting 4-6 times and incubated at room temperature for 5 minutes. Buffer P2 contains sodium hydroxide and SDS. SDS is a detergent which creates holes in the cell membranes and sodium hydroxide loosens the cell walls. This results in release of plasmid DNA and sheared cellular DNA from the cells. Sodium hydroxide also denatures the DNA, producing linearisation of cellular DNA and separation of the strands. 10 ml of Buffer P3 was added (chilled to 4°C), the solution mixed thoroughly by inverting 4-6 times and incubated on ice for 20 minutes. Buffer P3 was a neutralisation buffer containing potassium acetate and allows precipitation of genomic DNA, proteins, cell debris and KDS (combination of acetate and SDS). The solution was then poured into the QIAfilter cartridge and incubated for 10 minutes. During this time, HiSpeed Maxi tip was equilibrated by addition of 10 ml Buffer QBT and emptied by gravity flow.

The supernatant from the QIAfilter was applied to the anion-exchange HiSpeed tip by pressing on the plunger and allowed to enter the resin by gravity flow where the plasmid DNA selectively binds under low salt and pH conditions. The HiSpeed-tip was then washed with 60 ml Buffer QC, which was a medium-salt wash to remove RNA, proteins, metabolites and other low-molecular-weight impurities. The plasmid DNA was then eluted from the HiSpeed tip by addition of 15 ml Buffer QF, a high-salt buffer. As DNA is negatively charged, the addition of salt masks the charges and allows DNA to precipitate. 10.5 ml of isopropanol was added to the plasmid DNA (concentrating the DNA and removing salt). The eluate/ isopropanol mixture was passed through the QIAprecipitator Maxi Module and washed with 2 ml 70% ethanol. The plasmid DNA was then eluted in 1 ml H<sub>2</sub>O before quantification of yield and stored at -20°C.

### **3.3.4 Storage of plasmid DNA**

For long-term plasmid storage, 1 ml of overnight culture was mixed with 500 µl autoclaved glycerol in a sterile cryovial. The glycerol stock was then snap-frozen on dry ice and stored at -80°C.

Glycerol stocks could also be used to inoculate culture media by scraping the frozen stock with a sterile pipette tip and then transferred into 3 ml LB media containing the correct antibiotic.

### **3.3.5 Quantification of nucleic acids**

The concentration of purified DNA was determined by Nanodrop 1000 spectrophotometer (Thermo Scientific). Absorbance wavelength was set at 260 nm and 280 nm. The A<sub>260</sub>:A<sub>280</sub> ratio determines the purity of DNA where a value of 1.8 is indicative of highly purified DNA. The DNA concentration was calculated using the Beer-Lambert law, where an A<sub>260</sub> reading of 1.0 optical density (OD) unit is equivalent to 50 µg/ml double-stranded DNA

### **3.3.6 DNA Sequencing**

DNA sequencing was performed by the University of Dundee Sequencing Service, <http://www.dnaseq.co.uk/>. DNA samples were supplied as per the web instructions, and sequencing carried out using either standard or custom primers. Analysis of DNA sequencing was performed using Genomics Workbench (CLC Bio).

### **3.3.7 Restriction enzymes and Ligation**

All restriction enzymes were purchased by New England Biolabs, for ligation reactions, Rapid DNA Ligation Kit (Roche) was used. Plasmids were quantified by agarose gel electrophoresis.

### **3.3.8 Agarose Gel Electrophoresis**

Agarose gel electrophoresis was utilised to separate DNA molecules by size. This works by moving negatively charged DNA through an agarose matrix via the application of an electrical charge. The Bio-Rad Sub-Cell GT electrophoresis system was used. A 1 % agarose solution was prepared by dissolving agarose in 1x TAE buffer (40 mM Tris-Cl, 20mM glacial acetic acid, 1 mM EDTA) by heating in a microwave oven. The solution was cooled to handling temperature, and 1:10 000 SYBR Safe DNA gel stain (Invitrogen) added. The solution was then poured into a gel mould and allowed to cool and set. DNA samples were prepared for loading using a 1:6 dilution of 6x DNA loading buffer (0.25% bromophenol blue, 0.25 % xylene cyanol FF and 40% sucrose). 1 kb DNA ladder (Promega) was used as a molecular size marker. The gel was run at 100 V for around 45 minutes. The gel was then removed from the tank and visualised on an ultraviolet transilluminator. DNA bands can be cut directly from the gel and purified.

### **3.3.9 PCR and DNA purification**

PCR products and digested DNA were purified using QIAquick PCR Purification Kit and QIAquick Gel Extraction Kit (both from QIAgen) following manufacturer's instructions.

### **3.3.10 Generation of FRET-based constructs**

#### **RI\_epac and RII\_epac**

The Epac1-camps sensor for cAMP (Nikolaev et al. 2004) was kindly provided by M.Lohse (Institute of Pharmacology and Toxicology, University of Wurzburg, Germany). RI\_epac and RII\_epac constructs were generated by fusion of the dimerisation and docking domains (D/D) of RI $\alpha$  (64 aa) or RII $\beta$  (49 aa) to the N-terminus of the Epac1-camps A 27 aa linker A (EAAAK)5A was inserted between the D/D and Epac1-camps to avoid inadequate interactions between the domains, allowing them to work independently (Di Benedetto et al. 2008).

#### **RI-Cygnet-2.1 and RII-Cygnet-2.1**

Cygnet-2.1 was generously supplied by Wolfgang Dostmann, (Departments of Pharmacology and Molecular Physiology and Biophysics, University of Vermont, Burlington). Targeted cygnet-2.1 constructs were created by inserting the D/D of RI $\alpha$  (64 aa) or RII $\beta$  (49 aa) between the NheI and XhoI restriction sites in pcDNA3 cygnet2.1.

### **3.3.11 Generation of Ad5 recombinant vectors**

In order for these FRET-Based constructs to be used in adult ventricular myocytes, they first needed to be produced in an adenovirus. AdV5-PDE2A2wt-mCherry, AdV5-PDE2A2 catalytically dead (D685A-D796A)-mCherry, RI-Cygnet and RII-Cygnet were produced by Vector Biolabs.

For RI\_epac and RII\_epac the AdEasy XL Adenoviral Vector Systems (Agilent Technologies, California) was employed. Briefly, the constructs were inserted into the MCS of pShuttle CMV and confirmed by restriction digest. DNA was purified and linearised by digesting the vector with *Pme I* and gel purifying. BJ5183-AD-1 cells were transformed with the linearised DNA by electroporation then grown overnight at 37°C on LB-kanamycin agar plates. The smaller well isolated colonies were picked and grown in a 3 ml LB-kanamycin broth. Colonies were screened for positive recombinants by digesting 10 µl of miniprep DNA with *PacI* restriction enzyme and running the digestion product on a 0.8 % agarose TAE gel. *PacI* restriction of a recombinant pAdEasy-1 vector should appear as a large band at approximately 30 kb and a smaller band either at 3 kb or 4.5 kb depending on where the recombination took place. Recombinant pAdEasy plasmids were amplified in XL10-Gold ultracompetent cells following the manufacturer's instructions. Purified recombinant adenovirus plasmid was digested with *Pac I* enzyme to confirm desired restriction pattern.

### 3.3.11.1 Adenovirus production in AD-293 Cells

Between 50 µg and 100 µg of viral plasmid DNA was digested overnight with 50 units of *PacI* enzyme. The next day the digested DNA was ethanol precipitated by adding 2 volumes of ethanol and 0.3 volumes of sodium acetate and incubated at -20°C for 1 hour. DNA was centrifuged at 22,000 x g for 30 minutes, supernatant discarded and the pellet washed in 70% ethanol and air dried for 5 minutes. The pellet was resuspended in 20 µl of sterile water.

AD-293 cells were seeded in a 6 well plate to a density of  $7 \times 10^5$  cells per well and grown overnight. Two solutions containing the following were prepared:

**Solution 1:** 450 µl of OptiMEM (Invitrogen) and 3-4 µg DNA per well

**Solution 2:** 450 µl of OptiMEM and 2.5 µl Lipofectamin™ 2000 (Invitrogen) per well.

Solutions were left for 5 minutes at room temperature before mixing and incubating for a further 20 minutes at room temperature. 900 µl of the mixed solution was added drop wise to the wells. Cells were incubated at 37°C and 5% CO<sub>2</sub> for 4 hours before replacing with fresh culture medium (see 3.3.11.4). Plaque formation normally occurred after 3-4 days

(but sometimes could take as long as 10 days). After the first plaques were seen the virus was left for a further 3-4 days to allow it to infect the rest of the cells before it was harvested.

### **3.3.11.2 Harvest virus from AD293 cells**

After 3-4 days the cytopathic effect of the vector caused the cells to detach from the tissue culture dish or flask. In the initial transfection cells may be scraped from the well using a cell scraper. The media containing the cells was collected and the cells were harvested by centrifugation at 750 x g for 10 minutes at room temperature. The supernatant was discarded and the pellet resuspended in 8 ml of PBS. An equal volume of trichlorotrifluoroethane was added and after inversion of the falcon tube and gentle shaking the solution was centrifuged at 1,700 x g for 15 minutes at room temperature. The top aqueous layer was removed and used to infect more AD293 cells to amplify the virus or stored at -80°C until purification by CsCl gradient.

### **3.3.11.3 Amplification of Virus**

AD293 cells were grown until 80-90% confluent in a T150 flask. To this 22 ml of fresh medium and 1 ml of virus was added. Cells took around 3-4 days to fully infect. Cells were harvested as previously mentioned and used to infect 4 T150 flasks. This procedure was repeated until 20-30 flasks were infected. The virus was then harvested and purified by CsCl gradient.

### **3.3.11.4 Medium for AD293 cells**

#### **Culture Medium**

DMEM – High glucose with sodium pyruvate and L-glutamine (Invitrogen)	500 ml
FBS (heat-inactive) (Invitrogen)	10 %

**Freezing Medium**

DMEM – High glucose with sodium pyruvate and L-glutamine (Invitrogen)	50 ml
FBS (heat-inactive) (Invitrogen)	40 %
DMSO	10 %

**3.3.11.5 Adenovirus purification**

Centrifugation on CsCl density gradients was used to purify and concentrate crude adenoviral stocks. Ultra-clear centrifuge tubes 16 mm x 102 mm (Beckman Coulter Ltd, Buckinghamshire) were sterilised with 70% ethanol and then washed with sterile water. A CsCl gradient was produced by sequentially layering 2 ml of CsCl with a density of 1.45 g/cm<sup>3</sup>, 3 ml of CsCl with a density of 1.32 g/cm<sup>3</sup> and 2 ml 40% glycerol. The crude adenoviral supernatant was then added drop wise to the top of the gradient so not to disturb the layers and the remaining space was filled with PBS. The tube was loaded into a rotor and centrifuged at 112,400 x g for 1.5 hours at 4°C with maximum acceleration and zero deceleration. Following centrifugation, a band containing the complete adenovirus can be seen between the two CsCl layers. This was removed by piercing the tube below the virus band using a 21 gauge needle and removing the band in the minimum volume and taking care to prevent disruption of the other bands. Extracted virus was transferred to a Slide-A-Lyzer Dialysis Cassette (molecular weight cut-off of 10000) (Perbio Science UK Ltd) for dialysis after hydration of the cassette for 1 minute in dialysis solution. The virus was dialysed in 5L of 0.01 M Tris pH 8 / 0.001 M EDTA for 6 hours, after which the buffer was changed and supplemented with 10 % glycerol and dialysis repeated overnight. The virus was then removed from the cassette, aliquoted and stored at -80°C.

**3.3.11.6 Titration by end-point dilution**

The Adenovirus titre was determined by performing an end-point dilution assay. Briefly, AD293 cells were plated in 80 wells of a 96-well plate at a 50 % confluence. Serial dilutions of the adenovirus of interest were prepared in a range of  $1 \times 10^{-2}$  to  $1 \times 10^{-11}$  in complete medium and 100 µl of each adenovirus dilution was added to 10 wells each row.

The first row was infected with the highest adenovirus dilution and in the last row 100  $\mu$ l of adenovirus-free medium was added as a control. After 18 hours incubation in a 37°C /5 % CO<sub>2</sub> incubator the medium containing the virus was replaced with 200  $\mu$ l of fresh complete medium. Medium was then changed every 2-3 days. After 8 days of incubation the titre of the adenoviral stock was measured as Plaque Forming Unit/ ml (PFU/ ml) by counting the number of wells containing plaques and using the following formulas:

$$\text{The proportionate distance} = (\% \text{ positive wells above } 50 \% - 50 \%) \div (\% \text{ positive wells above } 50 \% - \% \text{ positive wells below } 50 \%)$$

For example if the titration gives 10/10 positive wells from  $1 \times 10^{-2}$  to  $1 \times 10^{-8}$  dilution, 8/10 positive wells at  $1 \times 10^{-9}$ , 3/10 positive wells at  $1 \times 10^{-10}$  dilution and 0/10 in all the remaining dilution rows, the proportionate distance would be:

$$\text{The proportionate distance} = (80 - 50) \div (80 - 30) = 0.6$$

and

**logID<sub>50</sub>** (*infectivity dose*)

$$= \log \text{ dilution above } 50\% + (\text{proportionate distance } x - 1) \times$$

*dilution factor*

in this case would be:

$$\log \text{ID}_{50} = -9 + (0.6 \times -1) \times 10 = -9.6 \times 10$$

$$\text{ID}_{50} = 10^{-10.6}$$

The tissue culture infectivity dose 50 equals the reciprocal of ID<sub>50</sub>:

$$\text{TCID}_{50} / \text{ml} = 10^{10.6} = 3.98 \times 10^{10}$$

According to the relation  $1 \text{ TCID}_{50} = 0.7 \text{ PFU/ml}$ .

The final titre for this example expressed in PFU/ ml would be:

$$\text{Final Titre} = 2.78 \times 10^{10}$$

The PFU/ ml calculated for the viruses used are:

$$\text{RI}_{\text{epac}}: 2.8 \times 10^{10}$$

$$\text{RII}_{\text{epac}}: 2.8 \times 10^{10}$$

$$\text{Cygnet-2.1}: 5.7 \times 10^{10}$$

$$\text{RI-Cygnet-2.1}: 3.8 \times 10^{10}$$

$$\text{RII-Cygnet-2.1}: 3.5 \times 10^{10}$$

$$\text{AdV5-PDE2A2wt-mcherry}: 1.24 \times 10^{11}$$

$$\text{AdV5-PDE2A2cd (D685A-D796A)-mCherry}: 1.24 \times 10^{11}$$

## 3.4 Protein Analysis

### 3.4.1 Preparation of lysates and protein quantification

Adult rat cardiac myocytes were seeded in a 6 well tissue culture plate, treated as indicated and washed twice with ice cold PBS before adding 200-300  $\mu\text{l}$  lysis buffer (see 3.4.4).

To determine the protein concentration of cell lysates, a Bradford Assay was carried out, using bovine serum albumin (BSA) as the standard curve. In a clear, 96 well plate, known BSA concentrations between 0 and 10  $\mu\text{g}$  were diluted to a final volume of 50  $\mu\text{l}$  with distilled water. The protein samples were diluted in distilled water at a 1:10 ratio, to a final volume of 50  $\mu\text{l}$ . Bradford reagent from Bio-Rad was diluted 1:5 with distilled water and 200  $\mu\text{l}$  added to each well. This reaction causes a colour change from brown to blue, the intensity of which is directly proportionate to the concentration of the protein. The 96 well plate was read at 560 nm using a microplate reader, which provided protein concentrations of each sample.

### 3.4.2 SDS-PAGE

Sodium dodecyl sulphate polyacrylamide gel electrophoresis (SDS-PAGE) was carried out to separate proteins according to their molecular weight. In brief, equal concentration of protein samples were denatured and reduced in 5x SDS-PAGE sample buffer followed by heating at 75°C for 10 minutes. After centrifugation, protein samples were resolved on precast polyacrylamide gels (4-12% NuPAGE Novex Bis-Tris gel, Invitrogen) immersed in MOPS SDS running buffer according to nature of the samples and different protein separation range. Pre-stained protein marker (Bio-Rad) was loaded to the first well of the gel while the protein samples were loaded to the subsequent wells. The gel was run for 30 minutes at 60 V then 1.5 hours at 160 V to allow adequate separation of the proteins.

### 3.4.3 Western immunoblotting

Proteins were electrotransferred onto nitrocellulose membranes (0.45 µm pore, Protran, Whatman GmbH) using X-Cell II blotting modular (Invitrogen) in Nu-PAGE transfer buffer containing 10 % methanol at room temperature for 2 hours at 30 V or overnight at 4°C. Successful transfer was indicated by full transfer of the molecular weight markers onto the nitrocellulose membrane. The membrane was then blocked in TBST with 5 % milk (Marvel) for 1 hour at room temperature with gentle agitation. Membranes were then probed with specific primary antibodies diluted in 1 % milk/TBST solution and incubated overnight at 4°C. The membranes were washed 3 times for 10 minutes each in TBST before adding appropriate horseradish peroxidase (HRP) conjugated anti-immunoglobulin G (IgG) secondary antibody diluted again in 1 % milk/TBST solution. After secondary antibody incubation, membranes were washed and detected by enhanced chemiluminescence (ECL) Western Blotting Substrate (Thermo Scientific) and autoradiography. Chemiluminescent images of immunodetected bands were recorded on blue-light sensitive autoradiography X-ray films (Kodak BioMax MS) which were then developed using the Kodak® X-Omat Model 2000 processor.

Immunoblot intensities were quantitatively analysed using ImageJ, Results, representing the mean of at least three independent experiments, were normalised to the amount of the

GAPDH. This ensures correction for the amount of total protein on the membrane in case of loading errors or incomplete protein transfers.

**Table 3-1. List of primary antibodies and dilutions used for each type of application.**

<b>Antibody</b>	<b>Host</b>	<b>Supplier</b>	<b>Catalogue No.</b>	<b>Dilution</b>	<b>Applications</b>
<b><math>\alpha</math>-actinin (sarcomeric)</b>	Mouse	Sigma	A7811	1:2000	IF
<b>PDE2A</b>	Rabbit	FabGennix	PD2A-101AP	1:500 – 1:2000	WB, IF
<b>PDE3A</b>	Rabbit	FabGennix	PD3-101AP	1:500 – 1:1000	WB, IF
<b>PDE4A</b>	Rabbit	In-house		1:2000	WB,IP
<b>PDE4B</b>	Sheep	In-house		1:1000 – 1:5000	WB, IP, IF
<b>PDE4D</b>	Sheep	In-house		1:1000 – 1:5000	WB, IP, IF
<b>UCRI</b>	Rabbit	In-house			WB
<b>PDE4B1</b>	Rabbit	In-house	12402	1:5000	WB
<b>PDE4B2</b>	Rabbit	In-house	12405	1:5000	WB
<b>PDE4D3</b>	Rabbit	In-house	12407	1:5000	WB
<b>PDE4D5</b>	Rabbit	In-house	12411	1:5000	WB

WB, Western immunoblotting; IP, immunoprecipitation; IF, immunofluorescence

**Table 3-2. List of secondary antibodies and dilutions used for each type of application.**

<b>Antibody</b>	<b>Host</b>	<b>Supplier</b>	<b>Catalogue No</b>	<b>Dilution</b>	<b>Application</b>
<b>Anti-mouse IgG</b>	Goat	Sigma	A5278	1:5000	WB
<b>Anti-mouse IgG</b>	Rabbit	Sigma	A9044	1:5000	WB
<b>Anti-rabbit IgG</b>	Goat	Sigma	A8275	1:5000	WB
<b>Anti-goat IgG</b>	Rabbit	Sigma	A8919	1:5000	WB
<b>Goat anti- mouse AlexaFluor® 568</b>	Goat	Invitrogen	A11004	1:500	IF
<b>Goat anti- rabbit AlexaFluor® 568</b>	Goat	Invitrogen	A11011	1:500	IF
<b>Donkey anti- goat AlexaFluor® 488</b>	Donkey	Invitrogen	A11055	1:500	IF

WB, Western immunoblotting; IP, immunoprecipitation; IF, immunofluorescence

### 3.4.4 Buffers and compounds for SDS-PAGE and Western immunoblotting

#### Cell lysis buffer

Hepes	25 mM
EDTA	2.5 mM
NaCl	50 mM
Sodium pyrophosphate	30 mM
Glycerol	10 %
Triton X-100	1 %

pH 7.5 and store at 4°C

On day of use add one Complete™ EDTA-free protease inhibitor cocktail tablet (Roche) in 50 ml buffer.

#### TBST

Tris-Cl	20 mM
NaCl	150 mM
Tween 20	0.1 %

pH 7.6

#### Basic 5X Laemmli Buffer

SDS	10 %
Tris-Cl	300 mM
pH 6.8	
Bromophenol Blue	0.05 %
Glycerol	50 %
$\beta$ -Mercaptoethanol	10 %

### 3.4.5 Immunoprecipitation (IP) assay

Immunoprecipitation (IP) is a technique that uses antibodies specific to a protein to remove those proteins from solution. The antibody-protein complexes are precipitated out of solution with the addition of an insoluble form of antibody binding proteins. It was decided that this method would be used as there was issues detecting changes in specific PDE4 isoforms as many of these isoforms share similar molecular weights. Therefore immunoprecipitation was used to “pull down” a specific protein of interest which was used for western immunoblotting.

#### **Preparing Beads**

Firstly, a pre-clearing step was performed to reduce non-specific binding to the protein beads (protein A beads were used for rabbit polyclonal antibodies and protein G beads were used for goat or mouse antibodies). The total volume of beads for both the pre-clear and IP steps was calculated (roughly 30  $\mu$ l per pre-clear reaction and 500  $\mu$ l per IP) and washed in cell lysis buffer (3.4.4) containing protease inhibitor before centrifuging for 1 minute at 19,000 x g and removing the supernatant. This was repeated a further two times before resuspending the beads in total volume of lysis buffer required.

#### **IP Protocol**

For endogenous proteins 1 mg of lysate was used. 30  $\mu$ l of prepared beads were added to lysates and rotated at 4°C, end on end, for 30 – 60 minutes. Lysates were then centrifuged at 19,000 x g for 10 minutes at 4°C. The supernatant was collected and 5-10  $\mu$ g of chosen antibody was added (pan PDE4B and pan PDE4D was used at this stage). Beads were retained and washed with lysis buffer to be used as a negative control. Antibody and lysate reaction was rotated end on end at 4°C for 30 minutes before adding 500  $\mu$ l of prepared beads and rotating overnight. The immunocomplexes were then collected by centrifugation at 19,000 x g for 10 minutes and washed three times with lysis buffer. Supernatant was discarded and beads were boiled in Laemmli buffer before centrifuging at 19,000 x g for 5 minutes. The supernatant was collected and proteins separated by SDS-PAGE and Western immunoblotting.

## 3.5 Cell based experiments

### 3.5.1 Manual measurements of cell size

Cardiomyocytes were seeded and maintained as previously described (3.2.2.3).

Cardiomyocytes were either challenged for 24 hours with either 1  $\mu$ M norepinephrine (NE) alone or NE and a specific PDE inhibitor. Control cells were maintained for the same length of time with DMSO added to the medium. Cells were chosen randomly and captured digitally with an ORCA AG (model C4742-80-12AG) camera on the stage of an inverted epifluorescence microscope (Olympus IX81, equipped with an Olympus PlanApoN, 60X, NA 1.42 oil objective) and analysed. Cell size was determined by the sectional area: length of cell x width of cell. Values are expressed as means  $\pm$  S.E.M. A Student's *t*-test was performed to compare the two groups, and the *P* values are indicated.

### 3.5.2 Real-time xCELLigence measurements

The xCELLigence technology (Roche Applied Science) which allows a quantitative measurement of the cell size through real-time cell-electronic sensing (RT-CES) was used according to the manufacturer's instruction. As cardiomyocytes are unable to divide, they tend to increase in cell volume in response to stress. This method allowed us to observe the change in impedance which is automatically converted to cell index and provides a quantitative measurement that reflects the nature of the cells, i.e. cell size.

Cardiomyocytes were counted as before and seeded with 50,000 cardiomyocytes per laminin pre-coated well of the E-Plate 96 (Roche) in triplicates after background measurements were taken. Briefly after 2 hours of culture in supplemented M199 medium, cardiomyocytes were treated with either 1  $\mu$ M NE alone or NE following a 30 minutes or 2 hours pre-treatment with PDE inhibitors. Controls with vehicle (DMSO alone) were also performed. The cultures were continuously monitored for up to 48 hours and the impedance as reflected by cell index (CI) values was set to record every 30 minutes. The xCELLigence data were then analysed using the RTCA software (Roche Applied Science).

The results were expressed by normalised CI, which are derived from the ratio of CIs before and after the addition of compounds.

### 3.5.3 Phosphodiesterase Activity Assay

Measurement of PDE activity was carried out using a radioactive cyclic AMP hydrolysis assay as previously described (Marchmont and Houslay 1980) and is a modification of a historical two-step procedure (Thompson and Appleman 1971). In the first step, samples are incubated with 8- $^3\text{H}$ -labelled cAMP substrate, and PDEs in the sample hydrolyse this to  $^3\text{H}$ -5'-AMP. In the second step, addition of snake venom hydrolyses the 5' AMP to  $^3\text{H}$ - adenosine, and incubation with an anion exchange resin binds any negatively charged, unhydrolysed cAMP, separating it from the adenosine. The amount of  $^3\text{H}$ -adenosine is then calculated by scintillation counting, to determine the rate of cAMP hydrolysis.

#### 3.5.3.1 Protein Sample Preparation

Adult rat ventricular myocytes were plated overnight in a 6 well TC plate and seeded at 100,000 cells per well in their normal growth medium. The cells plus medium were then collected by scrapping the cells from the well and then centrifuged for 1 minute at 19,000 x g to pellet the cells. The medium was removed and the samples were then homogenised in 200  $\mu\text{L}$  of KHEM Buffer (see 3.5.3.4) using a syringe. The samples were again centrifuged at 19,000 x g for a further minute to pellet the debris. The supernatant was transferred to a new 1.5ml Eppendorf tube. Protein sample concentrations were measured by Bradford Assay and stored at  $-20^\circ\text{C}$ .

All steps were performed at  $4^\circ\text{C}$  unless indicated. Samples were measured in triplicate.

### 3.5.3.2 Assay procedure

For this assay 20-25 µg of purified protein was diluted in KHEM buffer to a final volume of 50 µL. If an inhibitor of PDE activity was used the protein was diluted to a final volume of 40 µL of KEM buffer and 10 µL of selected inhibitor. 50 µl of substrate in 50µl of KHEM buffer was used as the blank control. 50µl of cAMP substrate was added to 50µl of the protein sample, mixed, and these were then incubated in a water bath at 30°C for 10 minutes. The samples were then placed in a boiling bath for 2minutes to inactivate the phosphodiesterase and stop the reaction. The tubes were then cooled on ice for 10 minutes. 25 µl of 1 mg/ml snake venom from Ophiophagus Hannah was then added to the reaction tubes, the tubes were mixed thoroughly by flicking, and incubated for a further 10minutes at 30°C. 400 µl of Dowex/ethanol solution was added to each reaction tube, vortexed and then incubated on ice for a further 15 minutes. Following incubation the tubes were then vortexed one final time and centrifuged at 19,000 x g for 2 minutes at 4°C in a refrigerated bench-top centrifuge. 1 ml of Ecoscint scintillation fluid was added to fresh 1.5 ml Eppendorf tubes and 150 µl of supernatant from the reaction tubes was added. 50 µl of cAMP substrate solution was added to two of the tubes to determine total counts per minute for the assay. All tubes containing scintillant were vortexed thoroughly and counted for 1 minute in a beta scintillation counter calibrated for [<sup>3</sup>H].

### 3.5.3.3 Determination of Phosphodiesterase Activity

To determine specific PDE activity contained within any reaction tube the following formula was applied,  $2.61 \times (\text{value} - \text{blank} / \text{average total}) \times 10^{-11} \times 10^{12} \times (1000 / \mu\text{g protein})$  resulting in PDE activity in pmoles/min/mg protein. To assess the effect of PDE inhibition, the activity of samples containing inhibitor was directly compared to an uninhibited control reaction and was expressed as the percentage of the control.

### 3.5.3.4 Buffers and compounds for PDE assay

#### **KHEM Buffer**

KCL	50 mM
Hepes	50 mM
MgCl <sub>2</sub>	1.94 mM
EGTA	10 mM
pH7.4	

Stored at 4°C until required.

Before use, 1 mM DTT and one protease inhibitor cocktail tablet (in 50 ml buffer) was added.

#### **PDE Assay Buffer**

Tris-Cl	20 mM
MgCl <sub>2</sub>	10 mM
pH7.4	

#### **Dowex**

Stock is 1:1 mix of dowex: H<sub>2</sub>O. Prior to use 2 parts of this mix was added to 1 part Ethanol (100 %).

#### **Snake venom**

10 mg/ ml stock in buffer A. Diluted to 1 mg/ ml (in buffer A) prior to use.

### **cAMP Substrate Mix**

2  $\mu$ l of 'cold' + 3  $\mu$ l of 'hot' 8-[<sup>3</sup>H]-labelled cAMP per 1ml of buffer B (i.e. 2  $\mu$ l + 3  $\mu$ l + 995  $\mu$ l buffer).

'cold' unlabelled cAMP stock solution = 1 mM (will be 2  $\mu$ M final)

'hot' 8-[<sup>3</sup>H]- labelled cAMP = 1  $\mu$ Ci/  $\mu$ l (will be 3  $\mu$ Ci/ ml final)

Work out total volume(s) of cAMP mix, Snake venom, Dowex that will be required for whole assay (including pilot) and prepare in advance.

### **Activation of Dowex Exchange Resin**

Dowex 1 x 8-400 was prepared and activated by dissolving 400 g of Dowex resin in 4 L of 1 M NaOH. The solution was stirred for 15 minutes at room temperature and the resin allowed settling. The supernatant was removed and the Dowex resin was washed with distilled water until pH 9.0 (approx 30 times) and allowed to settle after each wash.

The resin was then washed with 4 L of 1 M HCl for 15 minutes at room temperature and allowed to settle. The resin was washed a further 5 times with distilled water and stored at 4°C as 1:1 slurry with distilled water. This procedure generally produced approximately 1 L of Dowex slurry. This Dowex slurry was utilised in the PDE assay as a 2:1 solution of Dowex slurry to 100 % ethanol.

## **3.6 Quantitative Real-Time PCR**

Real-time polymerase chain reaction (PCR) is a technique widely used to determine relative gene expression.

The technique of PCR uses *in vitro* enzyme-catalysed DNA synthesis to create millions of identical copies of DNA from a single or few fragments. PCR amplifies DNA in three steps: (1) Denaturation – separating the individual strands of DNA. (2) Annealing – primers bind to the single stranded DNA. (3) Extension – the thermostable DNA polymerase generates a complimentary DNA product. These steps are repeated for around 40 cycles. The product from the first cycle can be used as a template for the primers in the second cycle and therefore successive cycles will generate and exponentially increasing

quantity of DNA (DNA produced =  $2^n$ , where  $n$  = number of cycles). The PCR product, or final number of DNA copies obtained, is related to the number of initial template copies. However, as the reaction progresses, some of the reagents are consumed as a result of amplification. This depletion will occur at different rates for each replicate. The reactions start to slow down and the PCR product is no longer doubled at each cycle. Theoretically, there is a quantitative relationship between amount of starting target sample and amount of PCR product at any given cycle number. This makes the end point quantification of PCR products unreliable. In order to overcome this limitation, Real-Time PCR was developed (Higuchi et al. 1993). Real-Time PCR detects the emission of a fluorescent indicator during the reaction. The data is then measured at the exponential phase of the PCR reaction and not at the end as in traditional methods.

One of the most common forms of this technique, and the one which was employed in this study, is TaqMan® real-time PCR. This type of probe is labelled with two fluorophores, a fluorescent reporter (i.e. 6-carboxyfluorescein, 6-FAM) at 5' end and with a quencher (i.e. 6-carboxy-tetrametil-rodamine, TAMRA) at 3' end. TaqMan® probes are designed to specifically anneal to a target sequence localised between two PCR primers. When the fluorophores are in close proximity, the quencher absorbs the reported emission. During the final extension step in the PCR cycle the probe is cleaved, so upon excitation (494 nm) the reporter emits a fluorescent signal (518 nm) which can be detected. Therefore, the fluorescent signal detected is proportional to the number of DNA copies generated.

### 3.6.1 RNA extraction

Total RNA was extracted using TRIzol reagent (Invitrogen) which contained phenol and guanidine thiocyanate in a procedure based on the method of Chomczynski and Sacchi (Chomczynski and Sacchi 1987). Cells were seeded in 6 well plates (100,000 cells per well), medium was removed and cells were rinsed with PBS and subsequently lysed with 1 ml of TRIzol® Reagent, directly added into the dish, collected with a scraper and homogenised by passing several times through a 1 ml syringe and a 26 gauge needle. Insoluble material was removed from the homogenate by centrifugation at 16,000 x g in a bench top centrifuge for 10 minutes at 4°C. RNA was separated from DNA and protein by

transferring the supernatant to a new tube and adding 200 µl of chloroform before shaking vigorously and incubating at room temperature for 5 minutes. The aqueous phase was then precipitated with ½ volume of isopropanol and centrifuged at 16,000 x g for 10 minutes at 4°C. The precipitate containing the RNA was then washed with 70% ethanol, centrifuged at 11,000 x g for 5 min, followed by air drying for 10 minutes at room temperature. Finally the RNA was briefly dried under vacuum and re-suspended in RNase-free sterile water. Total RNA was quantified using the Nanodrop 1000 spectrophotometer (Thermo Scientific).

### 3.6.2 Reverse Transcription

Real-time PCR can only amplify DNA, therefore it is crucial to convert RNA to cDNA. Reverse transcription of RNA samples was carried out by using QuantiTect® Reverse Transcription Kit (QIAGEN) according to manufacturer's instructions. This kit provides an optimised mixture of Omniscript Reverse Transcriptase and Sensiscript Reverse Transcriptase, RNase inhibitor, optimised buffer containing dNTPs, and a mix of oligo-dT and random primers.

#### **Genomic DNA elimination:**

A genomic DNA elimination step is performed before starting retro-transcription using the gDNA Wipeout Buffer, 7x provided.

Prepare the mix as follows:

gDNA Wipeout Buffer, 7x	2 µl
RNA template	from 10 pg up to 1 µg
RNase-free water	up to 14 µl

Reaction mix was incubated at 42°C for 2 minutes and then placed on ice to cool before the reverse transcription step.

Quantiscript Reverse Transcriptase	1 $\mu$ l
Quantiscript RT buffer, 5x	4 $\mu$ l
RT primer mix	1 $\mu$ l
RNA template (from previous step)	14 $\mu$ l
Total Volume	20 $\mu$ l

Mix was incubated at 42°C for 15 minutes, then 95°C for 3 minutes to heat-inactivate the reverse transcriptase.

The cDNA can be stored at -20°C or used directly for Real-time PCR.

### 3.6.3 TaqMan real-time PCR

Gene-specific TaqMan probes and PCR primers sets (Eurofins MWG operon) were designed assisted by the Primer 3 software (<http://frodo.wi.mit.edu/primer3/>) If possible; the primers were designed to span an exon-intron-exon boundary to exclude amplification of genomic DNA. 18S rRNA was used as an internal control for normalising relative expression levels in the different samples. Real-time PCR was performed from reverse transcribed cDNA samples using the Platinum Quantitative PCR SuperMix-UDG with ROX (Invitrogen) following the manufacturer's instructions.

Briefly, 25 ng of cDNA were added to a 96-well MicroAmp® Fast Optical Reaction Plate (applied Biosystems) with 7.5  $\mu$ l of Platinum Quantitative PCR SuperMix-UDG with ROX, 2.2  $\mu$ l of nuclease free water (Ambion) and 0.9  $\mu$ l of TaqMan probe mix (containing 0.3  $\mu$ l each of the 10  $\mu$ M primer pairs and 0.3  $\mu$ l of 10  $\mu$ M TaqMan probe. Thermal cycling and fluorescent monitoring were performed using the ABI Prism 7700 Sequence Detection System (Applied Biosystems). For each target gene Real-time PCR was performed in three biological replicates each of which was done in a minimum of three technical replicates:

- Initial denaturation at 95 °C for 2 min
- Then 40 cycles of 15 sec at 95 °C for denaturation, 15 sec at 57 °C for annealing and 1 minute at 60 °C for extension.

- Fluorescence data were collected during the extension step of each cycle. Negative controls using RNA as template were also included in all runs to test for the presence of genomic DNA contamination.

**Table 3-3. Oligonucleotide sequence of primers and probes used for RT-PCR.**

<b>Gene</b>	<b>Oligonucleotide sequence</b>
<b>Atrial natriuretic peptide (ANP)</b>	Forward: 5'-GGATTGGAGCCCAGAGCGGAC-3' Reverse: 5'-CGCAAGGGCTTGGGATCTTTTGC-3' Probe: 5'-AGGCTGCAACAGCTTCCGGT-3'
<b>Brain natriuretic peptide (BNP)</b>	Forward: 5'-AGCCAGTCTCCAGAACAATCCACG-3' Reverse: 5'-AGGGCCTTGGTCCTTTGAGAGC-3' Probe: 5'-GCTGCTGGAGCTGATAAGAGAAAAGT-3'
<b><math>\beta</math>-myosin heavy chain (<math>\beta</math>-MHC)</b>	Forward: 5'-CCAACACCAACCTGTCCAA-3' Reverse: 5'-CAGCTTGTTGACCTGGGACT-3' Probe: 5'-CTGGATGAGGCAGAGGAGAG-3'
<b>Rat PDE2A</b>	Probe: 5'- -3' AGGTGGTGGAGGACAAACAG
<b>Rat PDE3A</b>	Forward: 5'- -3' TCCTCTTTGCCACTCCTACG Reverse: 5'- -3' GTGGTGTTCAGCCTCTTCC Probe: 5'- -3' AGACACTGATGACCCGGAAG
<b>Rat PDE4B</b>	Forward: 5'- ATGTGGCGTATCACAACAGC -3' Reverse: 5'- GTGAAGACAGCATCCAGTGC-3' Probe: 5'- -3' ACGTTCTCCTCTCTACGCCA
<b>Rat 18S rRNA</b>	Forward: 5'-CGCGGTTCTATTTTGTGGT-3' Reverse: 5'-CGGTCCAAGAATTCACCTC-3' Probe: 5'-TGAGGCCATGATTAAGAGGG-3'

Rat PDE4D,  $\alpha$ -actin primers and probes and rat PDE2A primers have been designed and kindly provided by Dr David Henderson (University of Glasgow).

## 3.7 Microscopy

### 3.7.1 Immunostaining and Confocal Imaging

Adult rat ventricular myocytes were prepared as previously described, seeded onto coverslips at 50,000 cells per well of a 6 well TC plate and, depending on experiment, were infected with virus of interest (usually RI\_epac or RII\_epac). In PDE localisation experiments, non-infected myocytes were stained. Cells were fixed with ice cold methanol and incubated for 5 minutes at -20°C, washed 3 times with PBS to remove any methanol residue and permeabilised in PBS containing 0.1 % Triton®X-100 for 5 minutes at room temperature whilst shaking. The slides were then washed with PBS and incubated for 30 minutes with blocking buffer (PBS containing 1 % BSA) at room temperature. One or two primary antibodies were diluted to the desired concentrations (Table 3-1) in blocking buffer, 100 µL of the solution applied to parafilm, and coverslips laid face down onto the antibody for 2 hours at room temperature or left overnight at 4°C. For each coverslip treated with primary antibody, an IgG control was also prepared, using equal amounts of the appropriate normal IgG.

**Coverslips were then washed three times for 10 minutes in PBS, and incubated with the appropriate fluorescently labelled secondary antibody (**

Table 3-2). This step took place for either 1 hour at room temperature, or overnight at 4°C. Coverslips were washed once more in PBS and then mounted on 76 x 26 mm microscopy slides using MOWIOL® 4-88 reagent and left to dry in a 37 °C oven for 1 hour then stored at 4°C in the dark.

Confocal images were acquired using a 63x Zeiss oil immersion objective on a Zeiss Pascal LSM510 laser-scanning confocal microscope (Carl Zeiss). An argon laser was used to excite 488nm fluorescently labelled secondary antibodies. Helium/neon lasers were used to excite 568nm fluorescently labelled secondary antibodies. Zeiss Pascal software was used to gather image files.

## 3.7.2 FRET based imaging

Fluorescence Resonance Energy Transfer (FRET) is a non-radiative process of energy transfer from an excited donor fluorophore to an acceptor fluorophore. This phenomenon can only occur when the two fluorophores are in close proximity to one another. This technique has been exploited to generate genetically-encoded sensors to visualise cyclic adenosine monophosphate (cAMP) dynamics in intact living cells (Zaccolo et al. 2000). A FRET-based indicator of cAMP is usually composed of a cAMP-binding domain and the cyan and yellow variants of the green fluorescent protein, CFP and YFP respectively. Excitation of CFP (430 nm) results in the transfer of the excited state energy to YFP (emitting a signal at 545 nm). Both emissions are collected for analysis. Binding of cAMP to the sensor induces a conformational change which alters the distance between the two fluorophores thereby affecting the energy transfer between them. When this occurs only the CFP emission (480nm) is detected. FRET changes can be expressed as changes in the ratio between CFP emission (480 nm)/ YFP emission (545 nm) upon illumination at a wavelength that excites selectively the donor CFP (430 nm). Changes in FRET can be used in real-time imaging experiments as variations in FRET efficiency correlates with changes in cyclic nucleotide intracellular concentration.

### 3.7.2.1 Imaging set up

The basic FRET imaging setup consists of an epifluorescence microscope, a light source for excitation of the donor fluorophore, a beam splitter to separate acceptor and donor emission signals, a digital camera to collect the signals and a computer to store and analyse the data.

The FRET imaging system used throughout this project is as follows:

**Microscope:** Olympus IX81 inverted microscope.

**Light Source:** Xenon Mercury mixed gas arc burner (MT-ARC/HG LG2076, Ushio).

**Excitation Filters:** CFP: excitation filter ET436/20x, dichroic mirror T455LP, (Chroma Technology). YFP: excitation filter ET500/30x, dichroic mirror T515LP (Chroma Technology).

**Emission Filters:** CFP: emission filter ET480/40m; YFP: emission filter ET535/30m (Chroma Technology).

**Beam Splitter:** Dichroic mirror 505DCLP, YFP emission 545 nm, CFP emission 480 nm (Chroma Technology).

Light emitted by the sample comprises both CFP and YFP emission wavelengths. The dichroic mirror splits the emitted light in two beams. Wavelengths below 505 nm, which include CFP emission at 480 nm, are reflected and directed through a series of mirrors towards to the CFP emission filter. Wavelengths over 505 nm, which include YFP emission at 545 nm, pass through the dichoric and are directed to the YFP filter.

**Objective:** Olympus PlanApoN, 60X, NA 1.42 oil, 0.17/FN 26.5

**Immersion Oil:** Immersion oil "IMMERSOL" 518F , Carl Zeiss

**Camera:** ORCA AG (model C4742-80-12AG, Hamamatsu Photonics K.K., Japan) and HAMAMATSU camera controller.

**Computer:** Dell DE6700, 2.66 GHz Intel Core 2 Duo CPU, 3.50 GB RAM, 400 GB hard drive, Windows XP Professional version 2002

**Image acquisition and analysis:** All devices of this imaging system, such as the shutter, the motorised filter wheel and digital camera are controlled by Cell<sup>^</sup>R software (Olympus BioSystems).

Offline image analysis was performed using ImageJ free software.

### 3.7.2.2 FRET experimental procedure and data analysis

Cardiomyocytes and CHO cells expressing a FRET-based sensor were used to monitor basal intracellular cyclic nucleotide concentration and changes in cyclic nucleotide concentration upon the addition of chosen stimuli.

The day before the experiment, cells are seeded onto a 24 mm laminin coated coverslip as previously described and infected with appropriate FRET-based sensor (for this example a typical experiment using a cAMP FRET-based sensor will be explained). Cells were imaged around 18 hours after infection.

The coverslip was firstly placed into a metal slide holder which, when sealed, creates a bath where stimuli can be directly added. The bath is filled with 900  $\mu$ l of saline solution and maintained at room temperature (for CHO cells D-PBS was used instead).

Before starting the experiment a standard protocol for all experiments was designed (detailed explanation of this protocol can be found in (Gesellchen et al. 2011)). Briefly, the following parameters must be set and remain the same throughout each set of experiments:

**Binning:** Most of the camera detection systems used for FRET have the ability to combine the information in adjacent pixel and make them into one effective superpixel. The benefit of binning is that there is a reduced noise in the signal. A binning of 1x1 means that each individual pixel is used as such; a binning of 2x2 means that an area of 4 adjacent pixels is combined into one larger pixel, and so on. The drawback of binning is the loss of resolution. In the case of 2x2 binning; there is a fourfold increase in signal (the four single pixel contributions), a twofold loss in resolution but a twofold improvement in signal-to-noise.

All experiments in this thesis have been acquired with binning 2x2.

**Exposure Time:** The exposure time determines the period of time cells are illuminated and photons are collected and converted into charges for each channel. Optimal exposure time depends on the expression levels of fluorophores as well as the characteristics of the lamp, the optics and the camera. Generally an exposure time of 50 – 300 ms should be used, depending on the brightness of the sample. Increasing the exposure time allows the photons coming from the sample to accumulate and enhance the intensity of the image. At

the same time this will increase the photobleaching of the fluorophores. There is also the risk of saturation of pixel charges and any further change in the signal cannot be detected. Experiments in this thesis have been acquired at an exposure time of 200 ms.

**Time course and Number of Acquisitions:** The frequency of acquisition defines the interval between each data recording. This time between acquisitions depends on the characteristics of the sensor and the kinetics being investigated, but the normal range is 2 – 60 seconds. A short interval between illuminations may again result in photo-damaging of the cells and photo-bleaching of the signal.

All experiments have been acquired with a frequency of 5 seconds.

After these parameters have been set, the experiment can be started.

A small drop of oil is added to the objective lens before mounting the coverslip. A bright (well infected) cell, which is well attached and not contracting, is selected to perform the experiment.

Cell<sup>^</sup>R software allows for a live display of the ratio between the mean fluorescence intensity of each channel, so it is possible to estimate when the signal has stabilised before adding the stimulus (usually after 25 acquisitions). Further stimuli can be carefully added after each plateau phase. Only once the signal has stabilised after the final stimulus should the experiment be concluded.

The first step in analysing the experiment is to split and align the images taken by the CFP and YFP channels (this and the following steps is conducted offline using ImageJ) resulting in a perfectly superimposed image. A region of interest (ROI) is drawn on the background area and another around the cell of interest. Mean intensities for each acquisition is calculated and both CFP and YFP are subtracted from the background intensities, reducing any artefacts.

cAMP changes are expressed as:

$$\frac{\Delta R}{R_0}\%$$

Where  $\Delta R = R_{t2} - R_{t1}$

$R_{t1}$  is the average of at least 5 ratio ( $I_{CFP}/I_{YFP}$ ) values calculated before the addition of the stimulus;  $R_{t2}$  is the average of at least 5 ratio values at the plateau phase of reached after the addition of the correspondent stimulus.  $R_0$  corresponds to  $I_{CFP}/I_{YFP}$  at basal FRET level.

### 3.7.2.3 Buffers and compounds for FRET

#### Saline Buffer Cell Solution

NaCl	125 mM
Hepes	20 mM
Na <sub>3</sub> PO <sub>4</sub>	1 mM
KCl	5 mM
MgSO <sub>4</sub>	1 mM
Glucose	5.5 mM
CaCl <sub>2</sub>	1 mM

pH7.4, filter sterilised and stored at 4°C.

#### Stimuli:

Isoproterenol, cilostamide, rolipram, IBMX, atrial natriuretic peptide (ANP) and forskolin were all purchased from Sigma-Aldrich. Bay 60-7550 and S-Nitroso-N-acetyl-DL-penicillamine (SNAP) were bought from Cayman Chem.

## 3.8 Statistical analysis

In this thesis, all experiments were performed with an n of 3, unless otherwise specified in the figure legend. Statistical significance was calculated using either an unpaired two tailed t-test in Microsoft Excel or by analysis of variance (ANOVA) using Graph Pad Prism software, as stated in the figure legend. A p value < 0.05 was considered significant.

# 4 Intracellular cAMP signalling dynamics in adult cardiac myocytes.

---

## 4.1 Introduction

3', 5'- cyclic adenosine monophosphate (cAMP) is a ubiquitous second messenger that regulates many cellular functions including excitation contraction coupling (ECC). Stimulation of  $\beta$ -adrenergic receptors ( $\beta$ -ARs) activates adenylyl cyclases (ACs) to generate cAMP, and consequently activates protein kinase A (PKA), its main effector, which in turn phosphorylates several proteins involved in the ECC process. It is now well established that the cAMP/PKA signalling pathway is compartmentalised which results in tight control of the specificity of signalling. One widely reported mechanism relies on PKA binding to A kinase-anchoring proteins (AKAPs). AKAPs are multiscaffolding proteins that anchor PKA to specific intracellular locations in close proximity to specific modulators and targets. PKA must then be selectively activated and this requires that cAMP is produced in discrete compartments. Phosphodiesterase-mediated degradation of cAMP is another well documented mechanism; PDEs represent the only means of degrading cAMP within the cell, and are integral to the compartmentalisation of cAMP. Interestingly, it has also been revealed that PDEs have different intracellular localisations (Mongillo et al. 2004; Mongillo et al. 2006) and displacement of endogenous PDEs from their intracellular anchor sites results in their loss of control over specific cAMP pools (Terrin et al. 2006), thus demonstrating the importance of PDE localisation for maintaining cAMP microdomains and specificity of signalling. There are 5 cAMP PDE families in the heart, and although particular PDE isoforms have been linked with regulating the PKA phosphorylation of certain cardiac proteins involved in ECC, to date most of the details about which PDEs are responsible for the control of cAMP signalling in many subcellular compartments remain to be established.

Our laboratory has previously published that two PKA isoforms, PKA-RI and PKA-RII, define distinct subcellular compartments by binding to specific endogenous AKAPs (Di Benedetto et al. 2008). It was demonstrated that the PKA-RI and PKA-RII compartments have equal access to cAMP, as forskolin treatment resulted in a comparable rise in [cAMP] in the two compartments. In addition, IBMX stimulation revealed comparable levels of PDE activity in both PKA-RI and PKA-RII compartments. Interestingly, selective inhibition of PDE families showed that at basal levels, PDE2 activity is prominent in the PKA-RI compartment but very low in the PKA-RII compartment, whereas PDE4 exerts its activity mainly in the PKA-RII domain. No difference was detected between PKA-RI and PKA-RII upon PDE3 inhibition. At these locations, cAMP is generated selectively by different hormonal stimuli. In neonatal rat cardiomyocytes ISO was found, using FRET and FRAP imaging approaches, to generate a pool of cAMP that selectively activates PKA-RII over PKA-RI and lead to the phosphorylation of TnI, PLB, and  $\beta_2$ -AR. In contrast, prostaglandin 1 (PGE1) selectively activates PKA-RI and does not increase phosphorylation of these targets (Di Benedetto et al. 2008).

More recently our laboratory generated cGMP FRET based sensors targeted to the PKA-RI and PKA-RII compartments in neonatal cardiomyocytes to study the interplay between cAMP and cGMP (Stangherlin et al. 2011). Activation of sGC by S-nitroso-N-acetylpenicillamine (SNAP) generated a comparable rise in cGMP in the PKA-RI and PKA-RII compartments. Interestingly, activation of pGC by ANP resulted in a significantly larger cGMP signal detected in the PKA-RII compartment. Myocytes were then transfected with cAMP biosensors RI\_epac and RII\_epac Stangherlin et al. reported that cGMP can modulate cAMP signalling in these subcellular compartments by regulation of PDE2 and PDE3. Selective pharmacological inhibition of PDE2 and PDE3 found that PDE2 activity is preferentially coupled to the PKA-RII compartment, such that activation of PDE2 by cGMP leads to a selective reduction of cAMP content in this compartment. PDE3 was shown to be mainly coupled to the PKA-RI compartment. The authors showed, using FRET imaging and a catalytically inactive mutant of PDE2A (dnPDE2A), that displacing endogenous PDE2 by overexpressing the mutant PDE is able to reverse the effect of SNAP on the PKA-RII compartment. This data indicates that an active PDE2 associated with the PKA-RII compartment is responsible for the cGMP-dependent reduction of the cAMP response in this locale (Stangherlin et al. 2011).

The above studies, investigating cAMP signalling dynamics in the PKA-RI and PKA-RII subcompartments, have been conducted in neonatal myocytes, but have never before been investigated in adult cardiomyocytes. Adult myocytes are a better model for cardiac function, as neonatal myocytes tend to de-differentiate *in vitro* and lose some of the characteristics that myocytes present in the intact organ *in vivo*. And thus it is important to confirm findings using a model of adult myocytes. In addition, the role of individual PDEs in shaping the cAMP response elicited by the  $\beta$ -adrenergic stimulation in the PKA-RI and PKA-RII compartments is yet to be determined.

In this study, therefore, the role of phosphodiesterases (PDE) families in the control of cAMP levels in the PKA-RI and PKA-RII compartments within primary cultured adult rat ventricular myocytes (ARVM) was investigated.

## Aims

- Measure and compare cAMP dynamics in response to  $\beta$ -adrenergic stimulation in the PKA-RI and PKA-RII compartments.
- Study the role of different PDE families in the modulation of the cAMP response to catecholamines at these locations.

## 4.2 Results

### 4.2.1 Expression of a cAMP FRET-based sensor and its localisation to the PKA-RI and PKA-RII compartments

In order to investigate the *in vitro* cAMP signalling dynamics in specific subcellular compartments in living adult cardiomyocytes, a real-time FRET-based imaging approach was employed. The targeted sensors used in this study (RI\_epac and RII\_epac) are based on the cytosolic FRET-based sensor Epac1-camps, a genetically encoded cAMP sensor consisting of YFP and CFP fluorophores linked to the cAMP binding domain of Epac1

(Nikolaev et al. 2004). RI\_epac and RII\_epac were generated by fusing the dimerisation/docking domain from either PKA-RI $\alpha$  (amino acids 1 to 64) or PKA-RII $\beta$  (amino acids 1 to 49) to the N terminus of the soluble Epac-1 sensor (Di Benedetto et al. 2008) (Figure 4-1). Therefore, these sensors, when expressed in intact cells, will localise where PKA-RI and PKA-RII are normally situated within the cell.

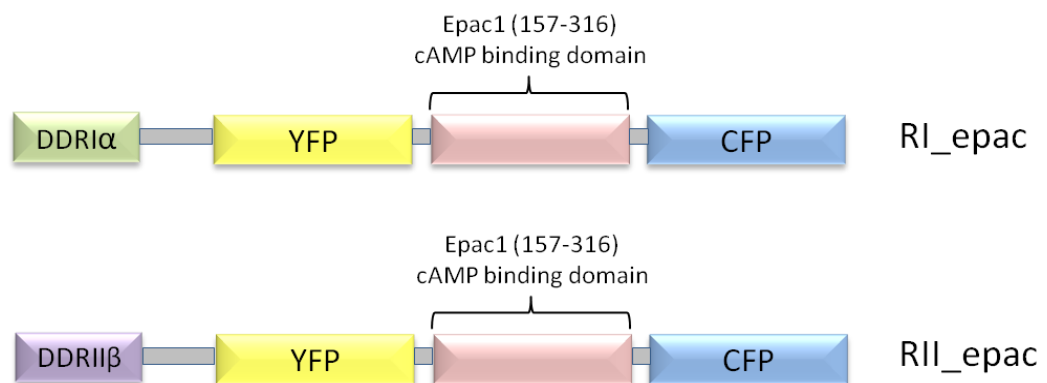


**Figure 4-1. Schematic representation of RI\_epac and RII\_epac FRET-based cAMP sensors.**

To verify if RI\_epac and RII\_epac are targeted to different subcellular compartments in adult cardiomyocytes, co-localisation studies using immunostaining of sarcomeric reference proteins were performed. Adult rat ventricular myocytes (ARVM) transduced with a viral vector carrying the sensors, fixed, and immunostained with antibodies against alpha actinin. Myocytes were then analysed by confocal microscopy. As illustrated in Figure 4-2, both sensors show striated pattern, however RI\_epac appears to have greater co-localisation with alpha actin compared to cells transduced with RII\_epac. These findings are in agreement with previous work in neonatal cardiomyocytes (Di Benedetto et al. 2008), which found that RI\_epac shows a more widespread localisation with overlay on both the Z and M sarcomeric lines whereas RII\_epac was found mainly on the M line in this cell type. This localisation pattern for RII\_epac may seem to make little sense as many targets of PKA-RII are reported to be close to the Z-line, for example t-tubules and junctional SR. One explanation is that there are a number of AKAPs which specifically bind PKA\_RII, as discussed in detail in 1.7.1, which are distributed in other areas of the

myocytes for example AKAP13 and Myospyrn. Co-localisation analysis confirms that although the confocal images show PKA-RII as having M-line distribution, there is co-localisation of this sensor at the Z-line (Figure 4-3). In addition and as previously shown in NRCM, RII\_epac showed a clear localisation to the nuclear membrane. These results confirm that RI\_epac and RII\_epac have the expected localisation in ARVM and that the two reporters localise to different subcellular compartments in this cell type.

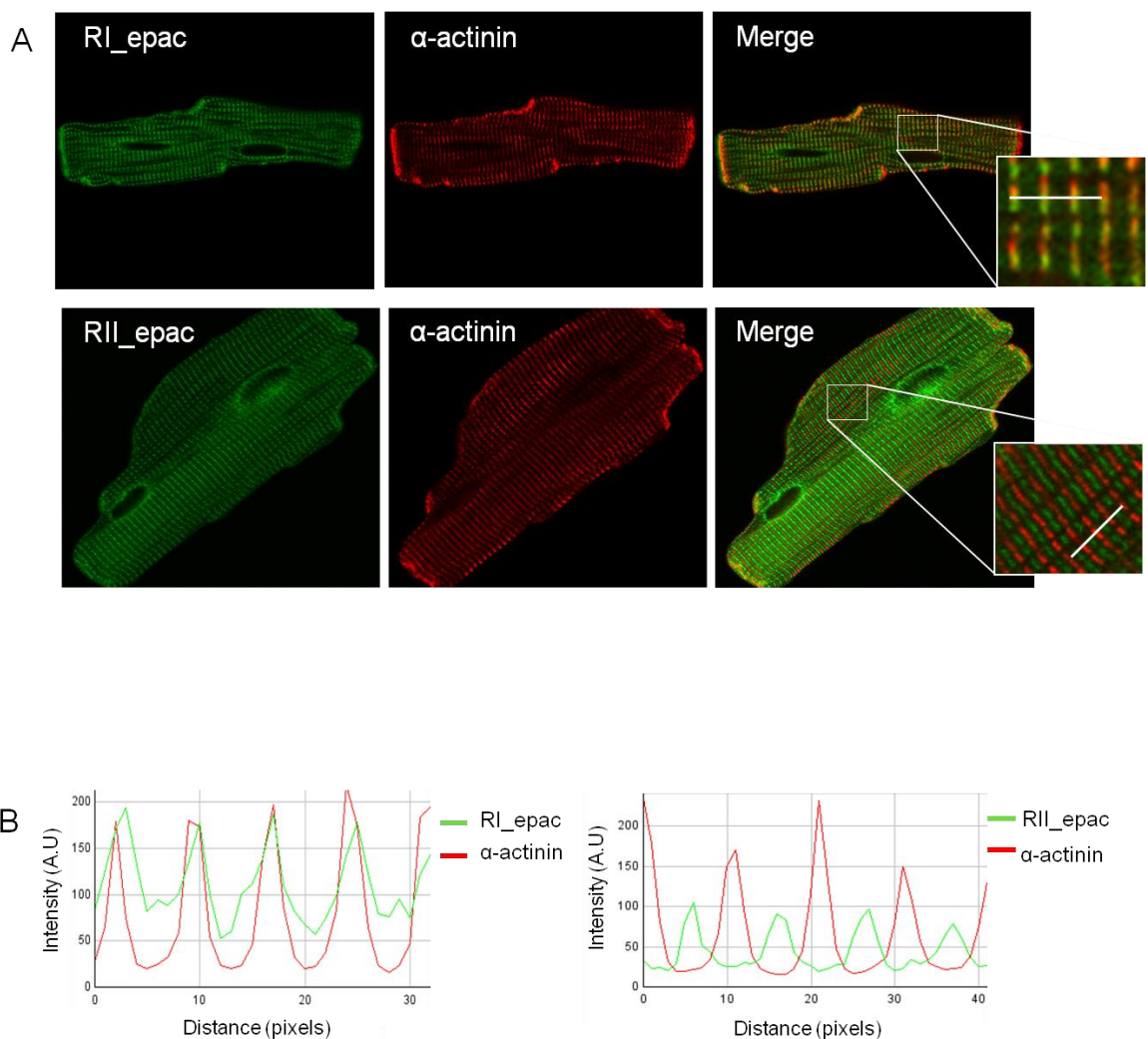


**Figure 4-2. Localisation of RI\_epac and RII\_epac FRET sensors in ARVM.**

**(A)** Cardiomyocytes were transduced with the FRET sensor (green) and then stained for  $\alpha$ -sarcomeric actinin (red), followed by laser scanning confocal microscopic visualisation at 60x magnification. These representative images show the different localisation of the sensors in adult myocytes. **(B)** Representative line intensity profiles (as indicated by a white line on Fig A) of ARVM transduced with RI\_epac or RII\_epac (green) and stained with  $\alpha$ -actinin (red).

To more rigorously assess whether the variation in sensor localisation is significantly different, and therefore confirm that RI\_epac and RII\_epac are targeted to different compartments within the adult cardiomyocyte, the Pearson correlation coefficient (PCC) was calculated (ImageJ with JACoP). The Pearson coefficient ( $r$ ) quantifies the correlation between pixel intensity of the two channels measured.  $r$  values range between -1 and +1. A value of -1 indicates that when one channel signal increases, the other decreases accordingly (perfect negative correlation), and a value of +1 indicates that both channel signals increase in a similar ratio (perfect correlation) (Adler and Parmryd 2010). Figure 4-3, shows the PCC calculated using the fluorescence images acquired at the confocal microscope. The coefficient value was significantly higher in RI\_epac than RII\_epac (RI\_epac:  $0.789 \pm 0.03$ ; RII\_epac:  $0.596 \pm 0.02$ ,  $p < 0.001$ ), confirming a statistical difference in the localisation of these sensors in adult cardiomyocytes. These values also can be expressed as  $\sqrt{\text{PCC}}$  to give the percentage of correlation between sensor and  $\alpha$ -actinin (RI\_epac: ~89%; RII\_epac: ~77%).

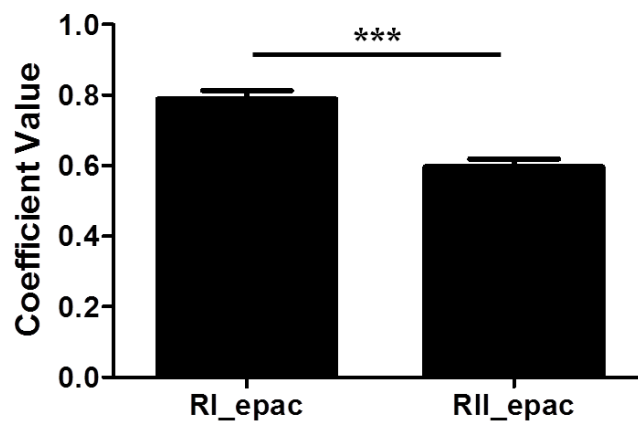


**Figure 4-3. Summary of colocalisation statistics.**

Pearson colocalisation coefficient was calculated using the JACOP plugin and Image J software for both sensors. RI\_epac  $n = 15$ ; RII\_epac  $n = 13$ . Error bars represent SEM. Two tailed; paired t-test, \*\*\*  $p < 0.001$ .

## 4.2.2 Characterisation and properties of RI\_epac and RII\_epac in adult myocytes.

To explore cAMP levels in the subcellular compartments where PKA-RI and PKA-RII normally reside, a FRET-based imaging approach was utilised. FRET allows for high spatial resolution and real-time detection of cAMP signalling dynamics in intact living cells.

ARVM were transduced with an adenovirus vector carrying RI\_epac or RII\_epac and imaged using an epifluorescent microscope the following day (Figure 4-4A). Cells were then challenged with cAMP raising stimuli in order to record the amplitude and kinetics of FRET change in the PKA-RI and PKA-RII subcellular compartments. Changes in intracellular concentrations of cAMP can be determined from changes in FRET. FRET can be expressed as the ratio ( $R$ ) of CFP emission intensity over YFP emission intensity following excitation of the cell at 440 nm ( $R = I_{CFP}/I_{YFP}$ ). Changes in this FRET ratio were expressed as the increase in CFP/YFP ratio over the CFP/YFP ratio at time zero ( $R_0$ ), as described in the Materials and Methods (3.7.2). An example of a typical FRET experiment utilising the RI\_epac and RII\_epac sensors is illustrated below (Figure 4-4B) and shows the differences in the FRET change obtained upon addition of number of stimuli resulting in elevated levels of cAMP in the two compartments.

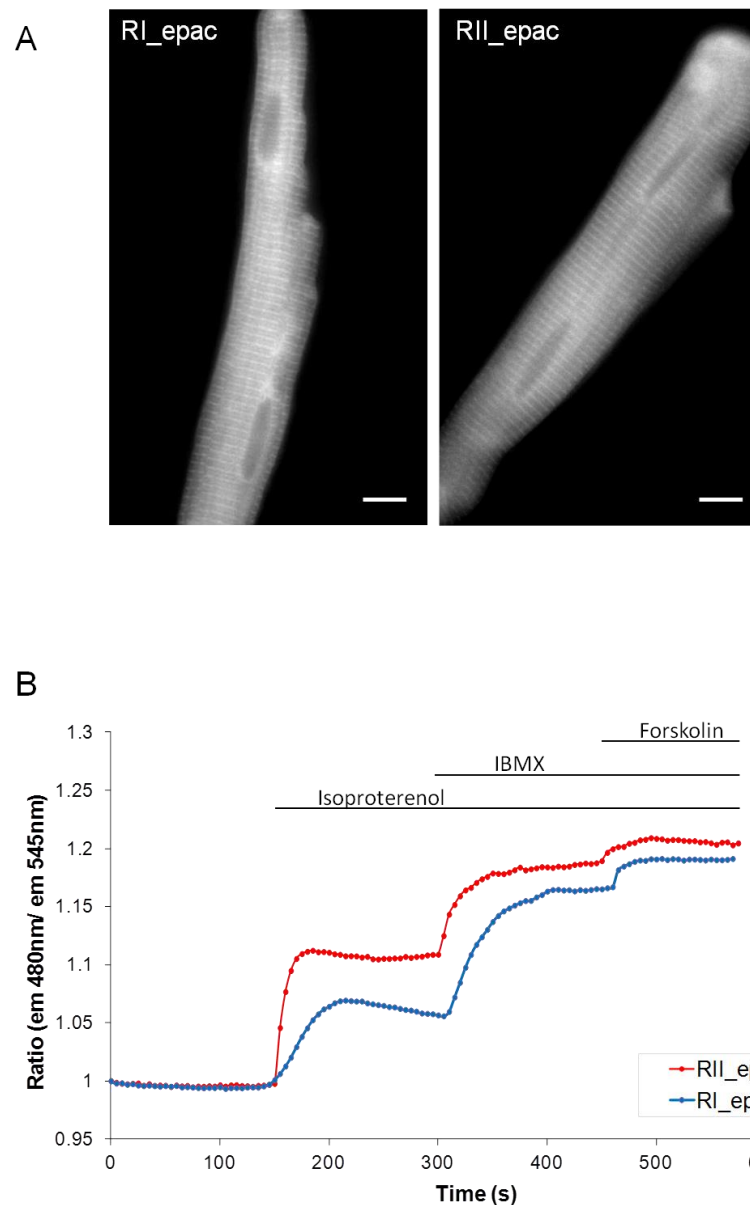


**Figure 4-4. An example of a FRET experiment in cardiomyocytes transduced with the targeted cAMP sensors. RI\_epac and RII\_epac.**

**(A) Image of ARVM expressing RI\_epac (left) or RII\_epac (right). (B) Representative graph of kinetics of FRET change detected in response to 100 nM Isoproterenol, 10  $\mu$ M IBMX and 25  $\mu$ M forskolin recorded in ARVM expressing RI\_epac (blue) or RII\_epac (red).**

In order to assess whether there was a difference in the basal levels of cAMP in the PKA-RI compartment compared to the PKA-RII compartment, a number of FRET images of ARVM expressing each sensor were collected. The basal FRET values were calculated as  $I_{CFP}/I_{YFP}$  upon excitation at 440 nm, where  $I_{CFP}$  is the intensity of CFP emission and  $I_{YFP}$  is the intensity of YFP emission. The results show (Figure 4-5) that the basal level of cAMP

in the PKA-RI and PKA-RII compartments is not statistically different, indicating there is no difference in intracellular cAMP levels in these two subcellular regions in unstimulated myocytes.

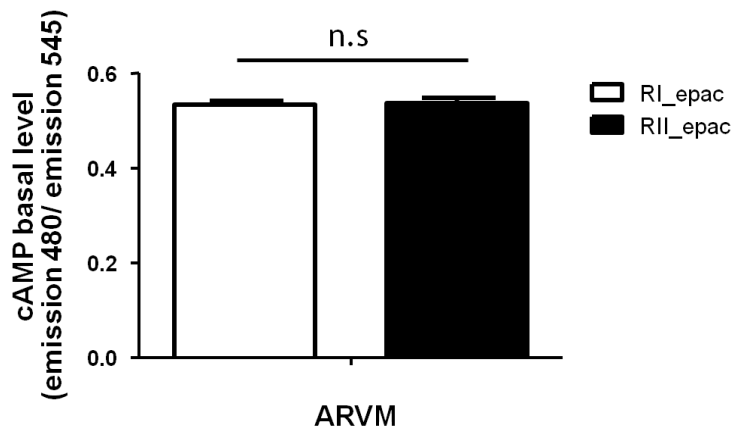


**Figure 4-5. Summary of the basal  $I_{CFP}/I_{YFP}$  ratio values detected in the ARVM transduced with RI\_epac or RII\_epac.**

**RI\_epac:  $R_0 = 0.547 \pm 0.007$ ,  $n = 27$ ; RII\_epac:  $R_0 = 0.566 \pm 0.009$ ,  $n = 25$ . Error bars represent SEM. Two tailed; paired t-test, ns.**

Next, the cAMP response generated in the two compartment by  $\beta$ -adrenergic receptor stimulation was investigated (Figure 4-6). Activation of  $\beta$ -adrenergic signalling was achieved by the addition of the synthetic  $\beta$ -agonist ISO (100 nM) and resulted in an increase in cAMP in both compartments. Interestingly, the rise in cAMP observed in the PKA-RII compartment of the ARVM was significantly higher than that in the PKA-RI compartment. To explore whether there was a difference in phosphodiesterases activity in the two compartments after  $\beta$  receptor stimulation, myocytes were then challenged with 100  $\mu$ M 3-isobutyl-1-methylanxthine (IBMX), a non-selective PDE inhibitor. There was an increase of cAMP in both compartments, which resulted in similar intracellular levels after addition. In order to reach the maximal FRET change ( $\Delta R/R_0$  max) in these sensors, a saturating concentration of 25  $\mu$ M Forskolin (FRSK), an activator of adenylyl cyclase which stimulates cAMP production was administered to the myocytes. The magnitude of response detected was similar for both FRET reporters, indicating that the two probes give the same maximal FRET change at signal saturation. As the sensors have the same

dynamic range, any variations recorded between them can be assumed to reflect a difference in cAMP levels rather than a difference in probe performance.

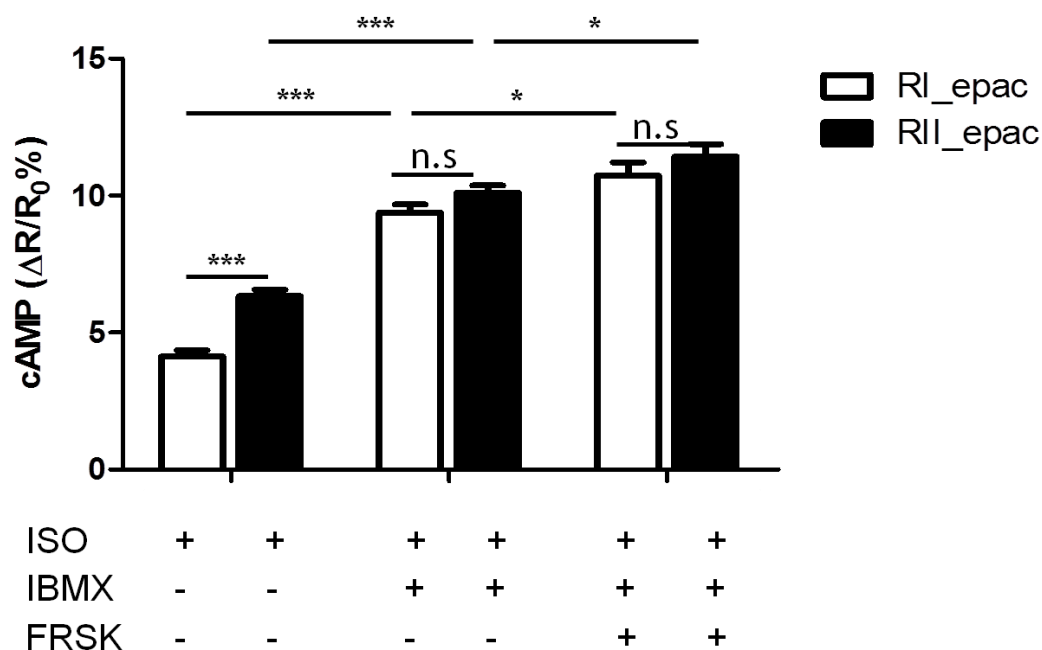


**Figure 4-6. Summary of FRET measurements of cAMP levels in ARVM expressing RI\_epac or RII\_epac.**

All experiments were performed as following; 100 nM Isoproterenol to stimulate  $\beta$ -adrenoceptors to produce cAMP, 100  $\mu$ M IBMX to inhibit PDEs and finally 25  $\mu$ M Forskolin to saturate the sensor. ISO: RI\_epac:  $\Delta R/R_0 = 4.133 \pm 0.221$  %, n = 26; RII\_epac:  $\Delta R/R_0 = 6.204 \pm 0.215$  %, n = 31. IBMX: RI\_epac:  $\Delta R/R_0 = 9.376 \pm 0.311$  %, n = 26; RII\_epac:  $\Delta R/R_0 = 10.112 \pm 0.252$  %, n = 27. FRSK: RI\_epac:  $\Delta R/R_0 = 10.727 \pm 0.480$  %, n = 11; RII\_epac:  $\Delta R/R_0 = 11.17 \pm 0.465$  %, n = 8. Statistical significance calculated by two way ANOVA with Bonferroni's post-test, \* p<0.05, \*\*\* p<0.001.

From the summary of these experiments, there did appear to be some variation in cAMP generation between the PKA-RI and PKA-RII subunits which supported previous work done in the lab using neonatal myocytes (Di Benedetto et al. 2008). The kinetic data for RI\_epac and RII\_epac also indicated there may be dissimilarity in the way cAMP is

generated at these locations. The speed of FRET change after each stimulus was calculated by the formula  $\text{speed} = \Delta\text{FRET}/\Delta t$ , where the FRET ratio detected at the first 5 time-points after the given stimulus was divided by the time in seconds (Figure 4-7). After the addition of ISO into the bath, the RII\_epac sensor reacted significantly more quickly ( $1.3 \pm 0.2$  /second) compared with RI\_epac sensor ( $0.8 \pm 0.1$  /second;  $p < 0.05$ ). However after the addition of IBMX, there was no difference in the speed of FRET change between RI\_epac ( $1 \pm 0.1$  / second) and RII\_epac ( $1 \pm 0.2$  / second). This indicates there is not only a greater level of cAMP production in the PKA-RII compartment after  $\beta$ -adrenergic stimulation, but the rate of cAMP level increase is quicker in this location. In addition, the above results suggest that such difference may at least in part depend on a different contribution of PDEs to the kinetics and amplitude of cAMP change in the two compartments.

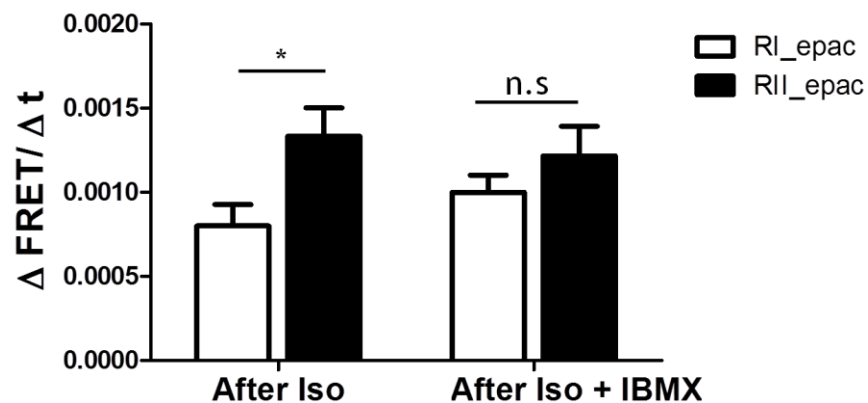


**Figure 4-7. Summary of speed of FRET change ( $\Delta\text{FRET}/\Delta t$ ) after each stimuli.**

ARVM expressing either RI\_epac or RII\_epac were stimulated with Isoproterenol (100 nM) and then IBMX (100  $\mu\text{M}$ ) and the rate of FRET change after each stimuli was calculated. ISO: RI\_epac n = 26; RII\_epac n = 31. ISO + IBMX: RI\_epac n = 26; RII\_epac n = 27. Statistical significance calculated by two way ANOVA with Bonferroni's post-test, \*  $p < 0.05$ .

### **4.2.3 Phosphodiesterase-mediated regulation of cAMP in subcellular compartments in cardiac myocytes.**

Although there was no significant difference in the cAMP levels after non selective PDE inhibition (ISO and IBMX treatment) seen in the summary of FRET experiments conducted (Figure 4-6), it was important to look closer at the contribution that PDEs may play in the control of cAMP level. This was done by taking the final response detected upon addition of ISO + IBMX treatment in these cells and by subtracting the ISO response (Figure 4-8A) to get a clearer idea of the PDEs contribution in determining cAMP levels in the PKA-RI and PKA-RII compartments. In the PKA-RI compartment there was a significantly greater increase in cAMP intensity compared with the PKA-RII compartment, indicating there was a significantly greater contribution of PDEs acting in the PKA-RI compartment compared with the PKA-RII compartment. To explore whether or not this was due to a higher basal level of PDEs activity in the PKA-RI compartment, ARVM transduced with the targeted sensors were challenged with 100  $\mu$ M IBMX alone (Figure 4-8B). This treatment was found to induce a cAMP increase which was comparable in the two locations. These results suggest that it is only after  $\beta$ -adrenoceptor stimulation and cAMP generation that this disparity in the PDE activity in the two compartments can be identified. One possible explanation for this is that a number of PDE, including PDE3 and PDE4, have PKA phosphorylation sites (Omori and Kotera 2007) and therefore activation of PKA by ISO stimulation leads to the modification of PDE activity in a compartment specific manner.

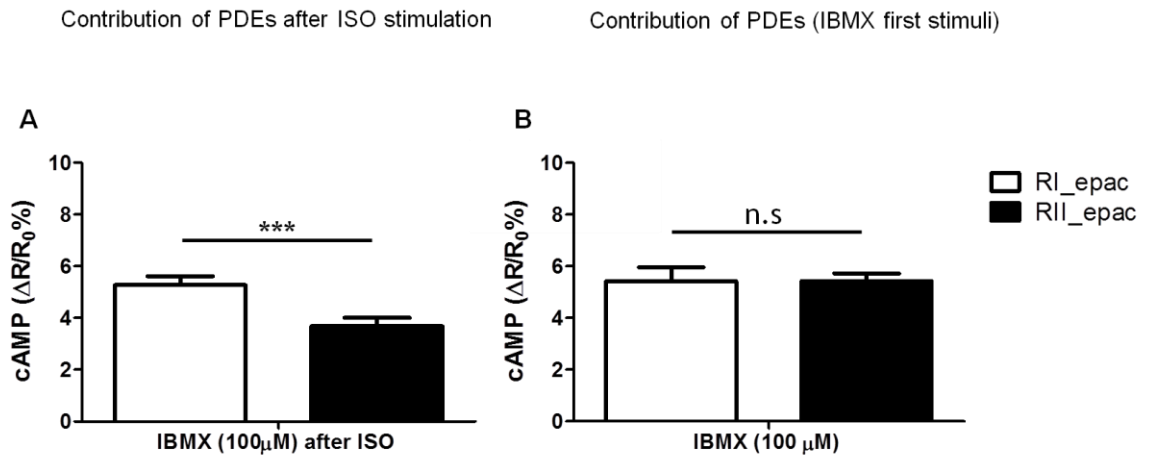


**Figure 4-8. The contribution of phosphodiesterases (PDEs) in ARVM transduced with RI\_epac or RII\_epac.**

**(A)** Myocytes are stimulated first with 100 nM Isoproterenol, then IBMX (100  $\mu$ M). The contribution of the IBMX response alone is shown here. **(B)** Myocytes are treated with IBMX without Isoproterenol. IBMX after ISO: RI\_epac n =26; RII\_epac n = 27. IBMX alone: RI\_epac: n =5; RII\_epac n = 6. Error bars represent SEM. Two tailed; paired t-test, \*\*\* p<0.001.

In order to identify which family of phosphodiesterases may be controlling each subcellular location which could possibly account for the higher PDE activity in the PKA-RI compartment; myocytes were first pre-treated with a selective PDE inhibitor before stimulation of cAMP production with 100 nM ISO. Among the cAMP-hydrolysing PDEs expressed in the heart, selective inhibitors for PDE2, PDE3 and PDE4 but not for PDE1 and PDE8 are commercially available, so the analysis focused on the former. In the experiments investigating the effect of PDE2, ARVM were incubated for 10 minutes with 50 nM of the PDE2 inhibitor Bay 60 7550 at 37°C before imaging. Cells were then challenged as before with ISO, IBMX and then finally with Forskolin to achieve the maximal response. Under basal conditions (Figure 4-9A), there was a comparable level of cAMP in each condition. Upon ISO stimulation (Figure 4-9B), there was a greater cAMP increase in PKA-RII compartment than the PKA-RI compartment in control myocytes. Pre-treatment of the myocytes with Bay 60-7550 resulted in a significantly greater increase in cAMP in both compartments compared to controls. There was a 2 fold increase in the amount of cAMP generated in the PKA-RI compartment and a 1.3 fold increase in the PKA-RII compartment upon PDE2 inhibition. In addition, PDE2 inhibition abolished the difference between the PKA-RI and PKA-RII compartments. Maximal FRET responses

were achieved by saturating the sensors with 100  $\mu\text{M}$  IBMX and 25  $\mu\text{M}$  forskolin (RI\_epac control:  $\Delta\text{R}/\text{R}_0 \text{ max} = 11.042 \pm 0.413$ ,  $n = 9$ ; RII\_epac control:  $\Delta\text{R}/\text{R}_0 \text{ max} = 11.170 \pm 0.465$ ,  $n = 8$ ; RI\_epac + Bay 60-7550:  $\Delta\text{R}/\text{R}_0 \text{ max} = 10.287 \pm 0.285$ ,  $n = 8$ ; RII\_epac + Bay 60-7550:  $\Delta\text{R}/\text{R}_0 \text{ max} = 10.118 \pm 0.433$ ,  $n = 5$ ). These results indicate that although PDE2 is present in both the PKA-RI and PKA-II compartments in the adult myocytes, after  $\beta$ -AR stimulation PDE2 activity appears to be higher in the PKA-RI compartment compared to the PKA-II compartment.

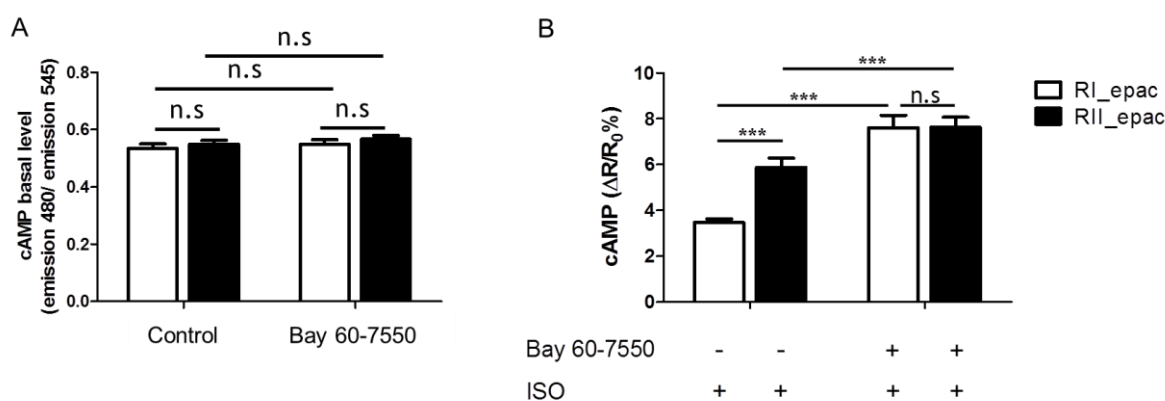


**Figure 4-9. Summary of FRET change upon the selective inhibition of PDE2.**

**(A)** Summary of basal cAMP levels in ARVM in the presence or absence of PDE2 inhibitor Bay 60-7550 (50 nM). RI\_epac control  $n = 9$ ; RII\_epac control  $n = 9$ ; RI\_epac + Bay 60-7550  $n = 18$ ; RII\_epac + Bay 60-7550  $n = 12$ . **(B)** Summary of FRET change induced by 100 nM isoproterenol in the presence or absence of Bay 60-7550. RI\_epac control:  $\Delta\text{R}/\text{R}_0 = 3.47 \pm 0.152$  %,  $n = 8$ ; RII\_epac control:  $\Delta\text{R}/\text{R}_0 = 5.871 \pm 0.405$  %,  $n = 16$ ; RI\_epac + Bay 60-7550:  $\Delta\text{R}/\text{R}_0 = 7.616 \pm 0.528$  %,  $n = 10$ ; RII\_epac + Bay 60-7550:  $\Delta\text{R}/\text{R}_0 = 7.633 \pm 0.427$  %,  $n = 9$ . Statistical significance calculated by two way ANOVA with Bonferroni's post-test, \*\*\*  $p < 0.001$ .

To explore the local contribution on the control of cAMP levels of the PDE3 family of phosphodiesterases, adult myocytes were pre-incubated with 10  $\mu\text{M}$  cilostamide, a selective PDE3 inhibitor. Results similar to PDE2 inhibition at basal levels of cAMP were obtained with cilostamide, and there was no significant differences between the groups measured (Figure 4-10A). As a control again the amount of cAMP generated in the two compartments upon  $\beta$ -adrenergic stimulation was measured, before comparing these

results with ARVM which had been pre treated with cilostamide and stimulated with ISO (Figure 4-10B). It was found that PDE3 inhibition only had an effect on the level of cAMP generated in the PKA-RI compartment, with a 1.4 fold increase in cAMP production. The maximal FRET response was measured again in the presence of this selective inhibitor (figure not shown) and it was found that PDE3 inhibition had no effect on the maximal FRET change at saturation (RI\_epac control:  $\Delta R/R_0 \text{ max} = 10.281 \pm 0.536$ , n =7; RII\_epac control:  $\Delta R/R_0 \text{ max} = 10.264 \pm 0.363$  n = 10; RI\_epac + cilostamide:  $\Delta R/R_0 \text{ max} = 9.051 \pm 0.449$ , n =10; RII\_epac + cilostamide:  $\Delta R/R_0 \text{ max} = 9.198 \pm 0.550$  n = 7). These results indicate that PDE3 controls a pool of cAMP which is functionally coupled to the PKA-RI compartment alone.

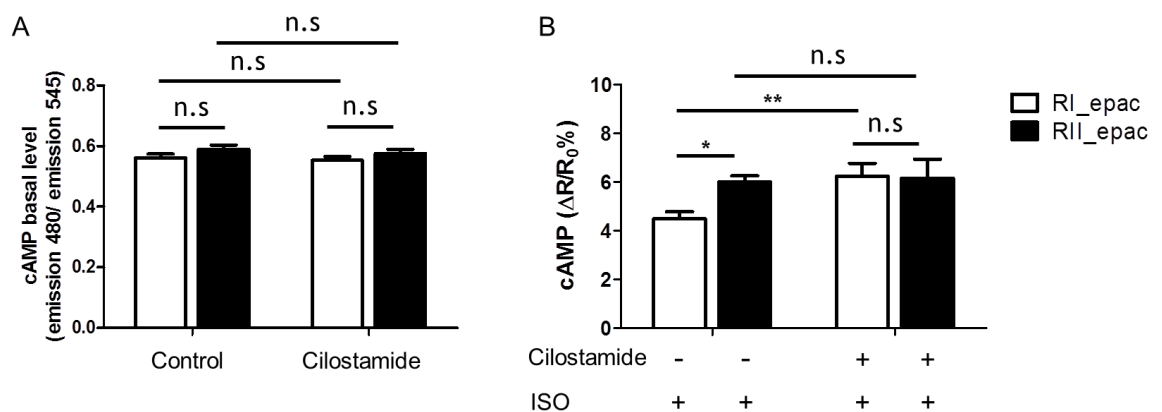


**Figure 4-10. Summary of FRET change upon the selective inhibition of PDE3.**

**(A)** Summary of basal cAMP levels in ARVM in the presence or absence of PDE3 inhibitor cilostamide (10  $\mu\text{M}$ ). RI\_epac control n =7; RII\_epac control n = 10; RI\_epac + cilostamide n =9; RII\_epac + cilostamide n = 7. **(B)** Summary of FRET change induced by 100 nM

isoproterenol in the presence or absence of cilostamide. RI\_epac control:  $\Delta R/R_0 = 4.402 \pm 0.276$  %, n =8; RII\_epac control:  $\Delta R/R_0 = 5.634 \pm 0.276$  %, n = 11; RI\_epac + cilostamide:  $\Delta R/R_0 = 6.23 \pm 0.541$  %, n =11; RII\_epac + cilostamide:  $\Delta R/R_0 = 5.884 \pm 0.834$  %, n = 8.

Statistical significance calculated by two way ANOVA with Bonferroni's post-test, \* $p < 0.05$ , \*\* $p < 0.01$ .

The PDE4 family is expressed at high levels in the heart (Mongillo et al. 2004) and therefore it is important to investigate the role of this family in compartmentalised cAMP

signalling. This was achieved by selectively inhibiting all PDE4 isoforms by pre treating the cells for 10 minutes with 10  $\mu$ M rolipram. As with the other selective inhibitors, rolipram incubation had no effect on basal cAMP levels in adult myocytes (Figure 4-11A). Upon addition of 100 nM ISO in control myocytes (Figure 4-11B) there was a higher generation of cAMP in the PKA-RII compartment compared to the PKA-RI compartment. In myocytes which had been treated with rolipram before imaging there was an increased level of cAMP in both compartments compared with control cells. Results were similar to those found in PDE2 with a larger increase in the PKA-RI compartment (1.8 fold increase) than recorded in the PKA-RII compartment (1.3 fold increase). Again this indicates that although PDE4 isoforms are found in both locations, their effect is predominant in the PKA-RI compartment. The maximal FRET response was measured in the presence of rolipram (figure not shown) and it was found that PDE4 inhibition which had no significant effect on the maximal FRET change at saturation (RI\_epac control:  $\Delta R/R_0 \text{ max} = 10.281 \pm 0.536$ , n = 7; RII\_epac control:  $\Delta R/R_0 \text{ max} = 10.264 \pm 0.363$  n = 10; RI\_epac + rolipram:  $\Delta R/R_0 \text{ max} = 8.697 \pm 0.753$ , n = 7; RII\_epac + rolipram:  $\Delta R/R_0 \text{ max} = 10.522 \pm 0.801$  n = 7).

However, on comparison of the ISO stimulated ARVM pre-treated with rolipram and the saturating response or ARVM pre-treated with rolipram, it was found that there was no significant difference in the PKA-RI compartment. This suggests that the ISO + rolipram response saturated the response in this sensor. No valid conclusions can be drawn for the PDE4 activity in the PKA-RI compartment of ARVM.

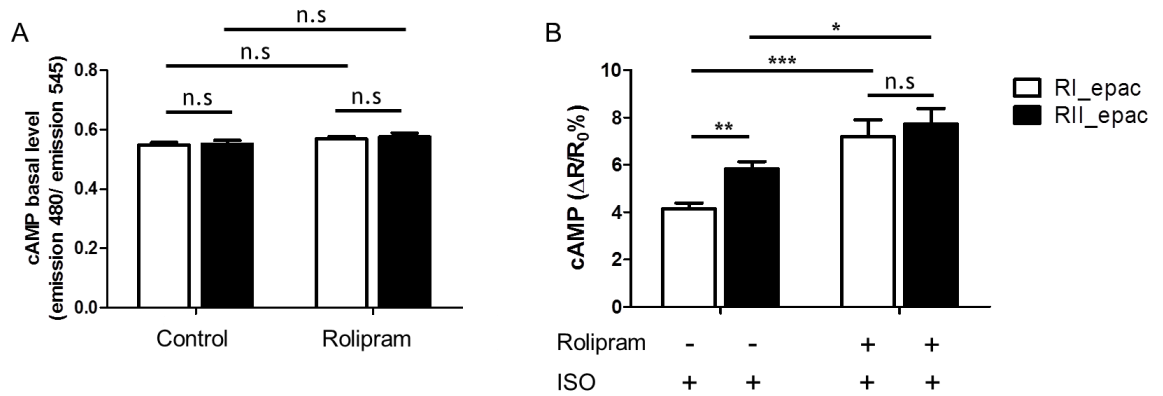


**Figure 4-11. Summary of FRET change upon the selective inhibition of PDE4.**

**(A) Summary of basal cAMP levels in ARVM in the presence or absence of PDE4 inhibitor**

**rolipram (10  $\mu$ M). RI\_epac control n =7; RII\_epac control n = 10; RI\_epac rolipram n =9;**

**RII\_epac rolipram n = 7. (B) Summary of FRET change induced by 100 nM isoproterenol in**

**the presence or absence of rolipram. RI\_epac control:  $\Delta R/R_0 = 4.152 \pm 0.239$  %, n =10;**

**RII\_epac control:  $\Delta R/R_0 = 5.838 \pm 0.299$  %, n = 13; RI\_epac rolipram:  $\Delta R/R_0 = 7.512 \pm 0.68$  %, n**

**=7; RII\_epac rolipram:  $\Delta R/R_0 = 7.733 \pm 0.643$  %, n = 7. Statistical significance calculated by**

**two way ANOVA with Bonferroni's post-test, \*p<0.05, \*\*p<0.01; \*\*\* p<0.001.**

The above figures show that selective inhibition of each family has no effect on basal cAMP, nor does IBMX treatment at basal level. This could be due to compensation by other PDE families controlling the compartment which have not been inhibited (i.e PDE8 which is IBMX insensitive). It is only after  $\beta$ -AR stimulation that any differences in PDE activity are observed. However, Mika and colleagues have shown that in ARVM selective inhibition of PDE2, 3 and 4 under basal conditions does have an effect on cAMP and ECC. The authors show that selective inhibition of PDEs results in an increase in sarcomere shortening and the calcium transient at basal levels as well as after the addition of 1 nM ISO (Mika et al. 2013). Measurements were recorded in isolated myocytes loaded with 5  $\mu$ M Fura-2 AM at stimulated at a frequency of 0.5 Hz before determining changes in sarcomere length and Fura-2 ratio at 512 nm using an IonOptix system. Although this study and Mika et al. investigate the impact of selective PDE inhibition in ARVM and utilise the same inhibitors at similar concentrations, this thesis studies the impact of PDEs in specific compartments deep within the cardiomyocyte whereas Mika and co-workers focus on the functional effects these inhibitors have on ECC and do not record the levels of cAMP. It is possible that there may be an effect on global cAMP which could impact ECC

in the cell, however no changes recorded by FRET in either compartment. It has been shown that more than one PDE family controls the PKA-RI and PKA-RII compartments, therefore it is possible that one family may try to compensate for another when its activity is impaired to maintain the correct level of cAMP required for normal function.

Figure 4-12 provides a summary of the above 3 experiments investigating the PDEs that are responsible for controlling the cAMP signalling in the PKA-RI and PKA-RII subcellular compartments. At the PKA-RI location, PDE2, PDE3 and PDE4 all seem to play a role in the control of cAMP signalling. PDE3 appears to have no effect in the PKA-RII compartment where control of cAMP hydrolysis appears to be mediated solely by PDE2 and PDE4.

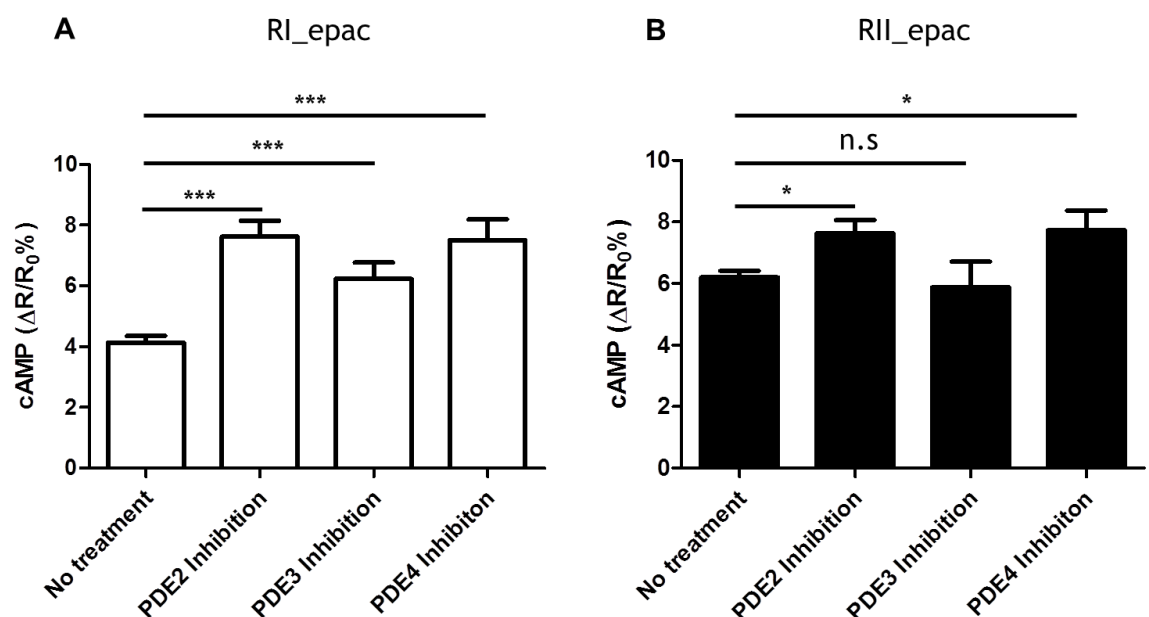


**Figure 4-12. Summary of experiments recording effect of selective PDE inhibition on ISO stimulation.**

ARVM were transduced with adenovirus containing a targeted FRET-based sensor and preincubated for 10 minutes with the selective PDE inhibitor. **A.** Effect of selective PDE inhibition upon ISO stimulation (100 nM) in the PKA-RI compartment. **B.** Effect of selective PDE inhibition upon ISO stimulation (100 nM) in the PKA-RII compartment. Statistical significance calculated by one way ANOVA with Dunnett's post-test, \*  $p < 0.05$ , \*\*\*  $p < 0.001$ .

### 4.3 Conclusions

In this study, the cAMP signalling dynamics within distinct subcellular compartments in adult myocytes was investigated. The involvement of PDEs in regulating the specificity of signalling at these locations was also explored. In order to investigate cAMP signalling in microdomains of the adult myocytes, the genetically encoded FRET-based sensors targeted to the PKA-RI and PKA-RII compartments (RI\_epac and RII\_epac respectively) were cloned into adenoviral vectors allowing them to be expressed in ARVMs.

Immunofluorescence revealed that, as previously shown in neonatal myocytes, when expressed in ARVM RI\_epac and RII\_epac present diverse subcellular localisations. RI\_epac had a broad striated pattern overlaying with both the M and Z sarcomeric lines, whereas RII\_epac shows tighter striated localisation with a very strong signals in correspondence of the M line and a much weaker localization overlaying the Z line, confirming previous findings in NRVMs (Di Benedetto et al. 2008).

A real time FRET based imaging approach with these targeted cAMP sensors was then utilised to study the cAMP signalling dynamics in adult myocytes upon  $\beta$ -AR activation. The results obtained showed that cAMP production upon addition of 100 nM ISO, a  $\beta$ -AR agonist, was significantly higher in the PKA-RII compartment compared with the PKA-RI compartment. No change was detected in the basal cAMP-hydrolytic activity but the contribution of PDEs activity after  $\beta$ -AR stimulation was significantly higher in the PKA-RI compartment. It was hypothesised that the reason for the lower cAMP generation in the PKA-RI compartment may be due to there being a higher activity of endogenous PDEs upon  $\beta$ -AR stimulation.

To explore these findings, selective inhibitors for a number of cardiac PDEs families were employed to try to identify the PDE isoforms responsible for the regulation of cAMP signalling at each subcellular compartment. Interestingly it was found that in the PKA-RI compartment PDE2 and PDE4 families were the main modulators of signalling with a smaller but significant contribution from the PDE3 family, whereas cAMP in the PKA-RII compartment was hydrolysed by PDE2 and PDE4, but not PDE3. This data supports work conducted in rat neonatal myocytes showing that PDE2 and PDE4 play a key role in modulating the cAMP response to  $\beta$ -AR stimulation, whereas PDE3 seems to exert only a marginal effect (Mongillo et al. 2004; Mongillo et al. 2006). Forskolin treatment revealed that PDE3 and PDE4 provide a similar contribution to determining intracellular cAMP

concentration in myocytes (Mongillo et al. 2004). The findings in this thesis further support the hypothesis of a compartmentalisation of cAMP signalling in adult myocytes, as well as the importance of PDE2 and PDE4 in the regulation of cAMP, generated in response to  $\beta$ -AR stimulation, in areas where different subsets of PKA are located. These data illustrate that local pools of cAMP generated in different subcellular compartments of the cardiomyocyte are individually regulated by different PDE isoforms.

# 5 cAMP signalling dynamics in an *in vitro* model of cardiac hypertrophy.

---

## 5.1 Introduction

Cardiac hypertrophy is an adaptive response to an increase in biomechanical stress resulting in an increase in the size of individual myocytes while the number of cells remains unchanged. Hypertrophy is also associated with increased risk of sudden death and progression to heart failure. Cardiomyocyte hypertrophy is defined by a significant increase in myocyte size, enhanced protein synthesis, a higher organisation of the sarcomere and reactivation of the fetal gene programme. These fetal genes include natriuretic peptides (Atrial, Brain and C-type natriuretic peptide),  $\alpha$ -skeletal actin and  $\beta$ -myosin heavy chain ( $\beta$ -MHC), which are commonly used as molecular markers for cardiac hypertrophy (Chien et al. 1991; Yazaki et al. 1993).

One of the most prominent characteristics in hypertrophic hearts is a marked desensitisation and downregulation of  $\beta$ -ARs which can be attributed to sustained catecholamine stimulation which leads to heart failure (Bristow 1998). Under normal conditions catecholamines released from the sympathetic nervous system stimulate the  $\beta$ -adrenergic receptors ( $\beta$ -ARs) which activate adenylyl cyclases (ACs) to generate cAMP. cAMP is a ubiquitous second messenger essential for the regulation of a vast array of intracellular processes including excitation-contraction coupling (ECC) by managing the force, frequency and duration of contraction. In ventricular myocytes cAMP produced in response to catecholamine stimulation of  $\beta$ -ARs consequently activates protein kinase A (PKA), which in turn phosphorylates several proteins involved in the ECC process, thereby increasing contractility (inotropy) and accelerating relaxation (lusitropy) (Bers 2008). However in cardiomyocyte hypertrophy there is impairment of the  $\beta$ -AR/ cAMP/ PKA

signalling resulting in reduced contractile function (Tse et al. 1978; Tse et al. 1979; Engelhardt et al. 1999; Zhang et al. 2005; Osadchii 2007; Abi-Gerges et al. 2009). Cyclic nucleotide phosphodiesterases (PDEs) are the only known enzymes to regulate intracellular concentrations of cAMP by continuously hydrolysing the molecule (Osadchii 2007). Therefore PDEs can regulate contractility in response to different stimuli, for example  $\beta$ -ARs and natriuretic peptide receptors stimulation (Muller et al. 1990; Nishikimi et al. 2006). PDEs have also been reported to participate in cardiac remodelling, where modifications in cardiac and aortic PDE specific activity occur during the onset of heart disease (Lugnier and Stoclet 1979).

For these reasons, PDE inhibitors have been widely used for a number of years as treatment for patients with heart failure. The action of some PDE inhibitors, such as the selective PDE 3 inhibitor milrinone, have been found to be initially beneficial to patients, however long term use of the drug is detrimental to the heart (Jaski et al. 1985; Movsesian and Alharethi 2002). This contradictory effect of cAMP enhancement by PDE inhibition can be explained by the fact that cAMP signalling is compartmentalised. This means that multiple spatiotemporally distinct pools of cAMP can modulate specific cellular functions and it has been reported that each individual pool of cAMP generated is regulated by different PDE families (Movsesian and Bristow 2005). In the context of heart disease, raising cAMP levels in one branch of the signalling pathway may be beneficial, but raising levels throughout the cell and activating a multitude of different pathways may have negative effects.

Until now only a few studies have investigated the role of cAMP signalling and PDE activity in cardiac hypertrophy, and the results have been contradictory. Abi-Gerges and colleagues investigated  $\beta$ -adrenergic regulation of cardiac contractility and cAMP PDE expression in single cardiomyocytes following induction of cardiac hypertrophy (Abi-Gerges et al. 2009). In this study myocytes were isolated from Wistar rats where hypertrophy had been induced by surgical thoracic aortic banding (TAC). Cyclic nucleotide-gated channels (CNG) were over expressed in sham and hypertrophic cardiomyocytes and, using patch clamp recordings of the associated current, a measurement of subsarcolemmal cAMP was produced. The authors reported a loss in total cAMP hydrolytic activity due to a reduction in PDE3 and PDE4 activities in hypertrophied myocytes. Western blot analysis showed a decrease in the expression of PDE3A, PDE4A

and PDE4B whereas PDE4D remained unchanged in hypertrophic cells (Abi-Gerges et al. 2009). More recently, Mokni et al. published their work investigating the activities of different PDE families where hypertrophy had been induced in Wistar rats by chronic infusion of angiotensin II. Utilising a cAMP-PDE activity assay (Thompson and Appleman 1971), Mokni and colleagues described a marked increase in PDE4 hydrolysing activity in hypertrophic myocytes, whereas PDE1, PDE2 and PDE3 activities were unaffected. However another PDE assay investigating cGMP hydrolysing activity found an increase in PDE1, PDE2 and PDE5 activities in the same type of cells. Real time PCR revealed, somewhat in contradiction to the PDE activity assay results, that there was a decrease in mRNA levels of PDE4D and no change in PDE2A, PDE3A, PDE3B, PDE4A, PDE4B or PDE4C. Increases were recorded in PDE1A, PDE1C and PDE5A mRNA levels, supporting the cGMP PDE activity assay results (Mokni et al. 2010).

Although these studies have contrasting results, it should be noted that even though both investigated PDE activity in hypertrophic myocytes, different animal models of hypertrophy were used. Mokni et al. also used cell lysates to conduct the PDE activity assays, whereas Abi-Gerges and co-workers used intact cardiomyocytes; however the experimental set up in the latter case would only allow monitoring of the PDE activity of subsarcolemmal cAMP. As yet there are no studies investigating PDE activity of cAMP compartmentalised signalling in hypertrophic adult cardiomyocytes that investigate subcellular compartments that are deeper than the subsarcolemmal space.

In this study an *in vitro* model of cardiac hypertrophy was set up in a primary culture of isolated adult ventricular myocytes (ARVM) from Wistar rats. cAMP signalling dynamics were studied at defined macromolecular complexes organised by AKAPs within the cardiomyocyte using a real time imaging approach and genetically encoded FRET-based sensors (RI\_epac and RII\_epac) targeted to the locations where PKA-RI and PKA-II normally reside via their interaction with AKAPs.

## Aims

- Establish an *in vitro* model of norepinephrine (NE)-induced cardiac hypertrophy in adult rat ventricular myocytes (ARVM).
- Measure and compare cAMP dynamics in response to  $\beta$ -adrenergic stimulation in the PKA-RI and PKA-RII compartments in hypertrophic myocytes and establish whether there are differences in local cAMP signalling compared to control myocytes.
- Study the role of different PDE families in the modulation of the cAMP response to catecholamines at these locations in hypertrophic ARVM compared to control cells.

## 5.2 Results

### 5.2.1 Norepinephrine induced hypertrophy in an adult myocyte *in vitro* model of cardiac hypertrophy.

It has been previously reported that norepinephrine (NE) plays a key role in the development of some *in vivo* models of cardiac hypertrophy (Gans and Cater 1970; Marino et al. 1991; Tsoporis et al. 1998). Simpson et al. showed that primary cultured neonatal cardiomyocytes maintained in serum-free media and treated with NE undergo hypertrophic growth (Simpson et al. 1982). The development of the hypertrophic phenotype upon NE stimulation was assessed by measuring changes in myocyte size, total cell protein content, myocyte surface area and cell volume. Biochemical studies in spontaneously hypertensive rats (SHR) have revealed increased NE levels in the blood as well as an accelerated NE turnover in the heart (Nagatsu 1974; Nagaoka and Lovenberg 1976). More recently NE stimulation has been shown to induce cardiac hypertrophy in adult rat ventricular myocytes (ARVM) (Ikeda et al. 1991; Amin et al. 2001; Xiao et al. 2001; Kuster et al. 2005; Thandapilly et al. 2011). Ikeda et al. demonstrated that exposure of ARVM to NE caused a significant increase in [<sup>3</sup>H] leucine incorporation and total protein content (Ikeda et al. 1991).

This model of cardiac hypertrophy was chosen as the use of cultured myocytes allows for the analysis of specific variables at a cellular level without interactions from other cell types, as would normally occur in an *in vivo* or *ex vivo* model. NE-treatment of ARVM is also an easy and highly reproducible method to induce cardiac myocyte hypertrophy *in vitro*. Hypertrophic growth is also quick (6-8 hours) using this method which is important as isolated adult myocytes do not undergo division and only survive a few days in culture medium, without the addition of drugs to inhibit contraction. Butanedione monoxime (BDM) is one example of a stimulus which inhibits myosin ATPase and protects the myocardium from damage. BDM has been extensively used in the isolation and culture of mouse myocytes (Kivisto et al. 1995). However, it acts as a non-specific phosphatase in the culture medium and this may lead to significantly altered cellular electrical properties (Verrecchia and Herve 1997; Watanabe et al. 2001).

In the first part of this study a protocol to induce hypertrophic growth of adult cardiomyocytes in culture was developed. Isolated ARVM were treated overnight with 1  $\mu$ M NE in serum free M199 medium.

To assess whether this method induced cardiac hypertrophy in cultured ARVM, several parameters were measured:

**Cell size:** transmitted light images of hypertrophied and control cardiac myocytes from different culture preparations were randomly acquired and the average cell length and longitudinal section area (length x width) of ARVM were calculated using Image J software (Beltrami et al. 2003; Gupta et al. 2005; Banyasz et al. 2008; Miller et al. 2009; Thandapilly et al. 2011). At the imaging set up used for these experiments, one pixel corresponds to 0.07  $\mu$ m when images are acquired using a 40X objective.

**Cell growth (Cell Index):** The xCELLigence technology allows a quantitative measurement of the cell size through real-time cell-electronic sensing (RT-CES) (Vistejnova et al. 2009; Sin et al. 2011). Cardiomyocytes increase in cell volume in response to stress. This method allowed us to observe the change in impedance which is automatically converted to cell index and provides quantitative measurements of cell size.

**Fetal cardiac gene program:** Reactivation of the fetal gene program is a characteristic feature of hypertrophied and failing hearts. Fetal cardiac genes Atrial Natriuretic Peptide (ANP), Brain Natriuretic Peptide (BNP) and skeletal  $\alpha$ -actin mRNA levels were measured

by performing real-time PCR and values were normalised to an invariant endogenous control (in this study 18S rRNA was used as the control) to correct for sample variations in RT-PCR efficiency and errors in sample quantification. Real-time PCR was performed in three biological replicates and an average was taken. n = number of technical replicates (minimum of 3).

As illustrated below (Figure 5-1), myocytes treated overnight with 1  $\mu$ M NE showed a significant increase in cell size. Longitudinal section area was significantly greater (1.54 fold) in NE treated cells. The degree of hypertrophy detected is comparable to values that have previously been reported by a number of authors (Amin et al. 2001; Miller et al. 2009; Thandapilly et al. 2011).

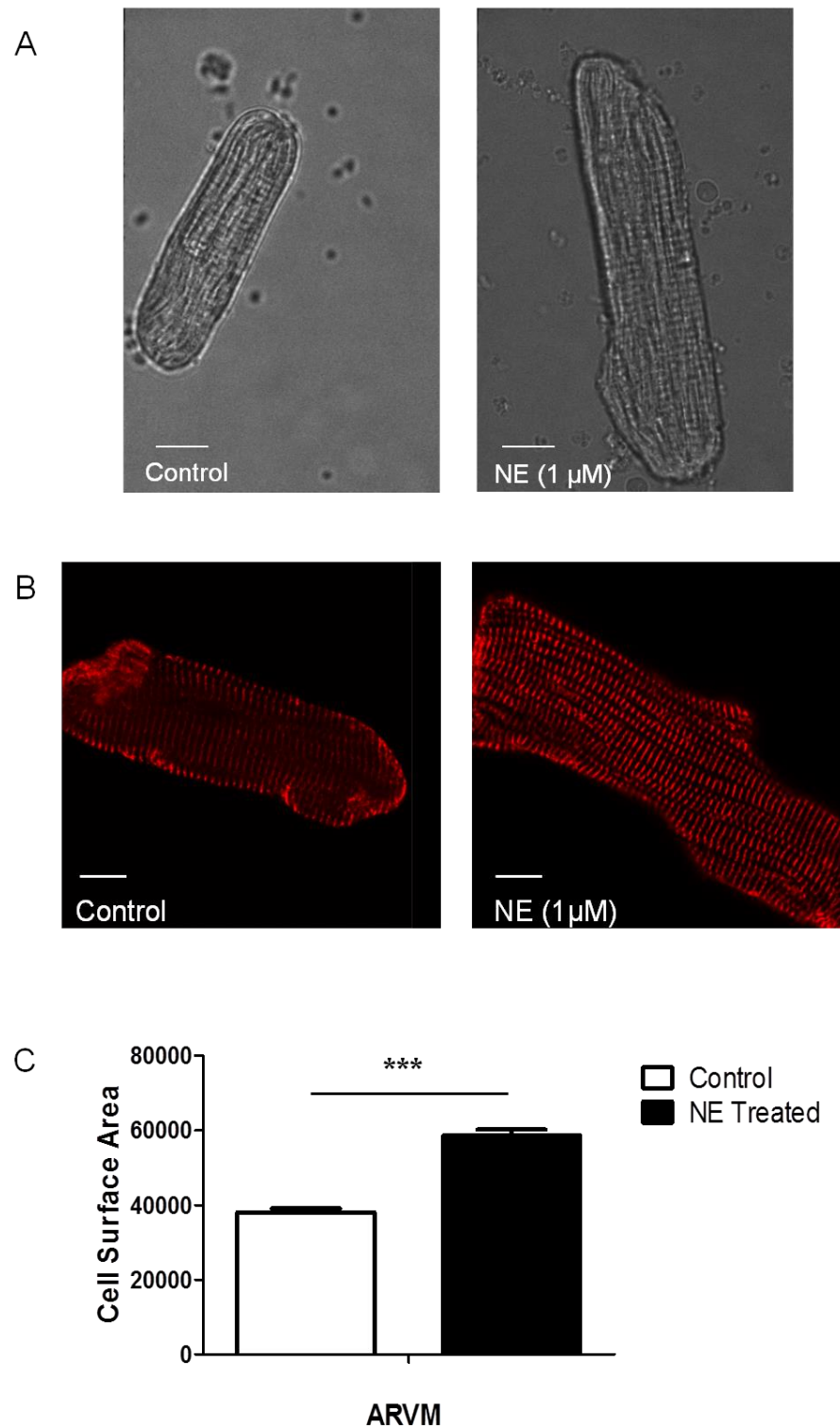


**Figure 5-1. Norepinephrine treatment induces hypertrophic growth in ARVM.**

(A) Representative images of ARVM untreated and treated with 1 $\mu$ M norepinephrine (NE) overnight. (B) Representative images of control and NE treated ARVM stained with  $\alpha$ -actinin. (C) Summary of longitudinal section area calculated for control and NE treated myocytes. Control: 38003.85  $\pm$  997.63 pixels (2660.27  $\pm$  69.83  $\mu$ m<sup>2</sup>), n = 101; NE: 58542.48  $\pm$  1621.56 (4097.97  $\pm$  113.51  $\mu$ m<sup>2</sup>), n = 90. Error bars represent SEM. Two tailed; paired t-test, \*\*\* p<0.001.

Another measurement of the change in cell size after overnight NE treatment was conducted by measuring the increase in cell index. Importantly, the reproducibility of the manual measurement was verified by the results obtained from this RT-CES method. NE treated cells showed a significant 1.58 fold increase in cardiomyocyte size compared to controls after 24 hours of constant monitoring (Figure 5-2).

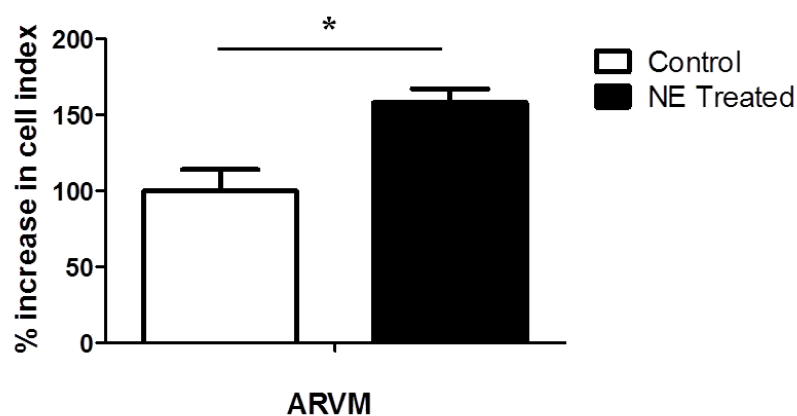


**Figure 5-2. Comparison of growth in control and NE treated ARVM.**

Summary of cell index calculated in control and NE-treated myocytes. Error bars represent SEM. Two tailed; paired t-test,\* p<0.05.

Finally, there was significant increase in ANP and  $\alpha$ -actin mRNA levels tested in NE treated ARVM compared to control (Figure 5-3) and a trend of increased BNP mRNA levels.

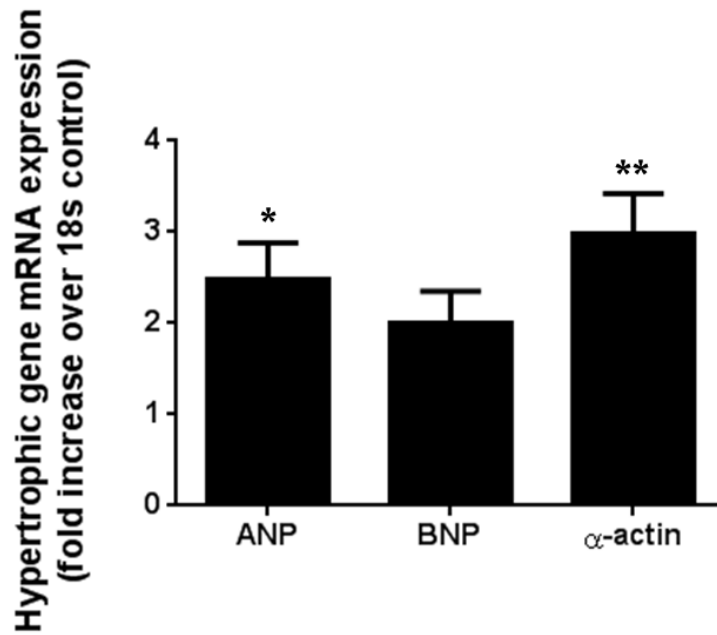


**Figure 5-3. Reactivation of the fetal gene program in NE treated ARVM.**

Summary of RT-PCR results showing increased ANP and α-actin expression level in NE-treated cardiac myocytes. Control =  $1 \pm 0.4$ , n = 29; NE treated ARVM ANP mRNA:  $2.46 \pm 0.41$ , n=29; NE treated ARVM BNP mRNA:  $1.98 \pm 0.36$ , n = 17; NE treated ARVM α-actin mRNA:  $2.96 \pm 0.45$ , n = 19. Error bars represent one way ANOVA with Dunnetts post test, \* p<0.05, \*\* p<0.01.

These data confirm that overnight treatment with 1 μM NE, as previously demonstrated (Ikeda et al. 1991; Xiao et al. 2001; Thandapilly et al. 2011), induces modification of the cellular phenotype that recapitulate a number of changes observed in hypertrophic hearts *in vivo*.

## **5.2.2 Expression and localisation of cAMP FRET-based sensors to the PKA-RI and PKA-RII compartments in hypertrophic myocytes**

In order to investigate whether the targeted cAMP sensor localisation is altered in hypertrophic myocytes, ARVM that had been treated overnight with 1  $\mu$ M NE, were also transduced with adenoviral vector carrying the cAMP FRET sensors RI\_epac and RII\_epac (ie cells were treated with NE and sensor on the same day maintained in culture for the same length of time as control myocytes), fixed and immunostained with antibodies against alpha actinin and imaged at the confocal microscope. As demonstrated in Figure 5-4, the difference in the subcellular localisation of RI\_epac and RII\_epac appears to be attenuated in ARVM. In addition, another main difference in the case of RI\_epac is its increased localisation to the perinuclear region. Thus, it appears that in hypertrophic myocytes the distinction between PKA-RI and PKA-RII compartments is reduced. It should also be noted that hypertrophic myocytes tend to express both sensors at a brighter level than in control cells perhaps due to increased protein synthesis and nuclear transportation.

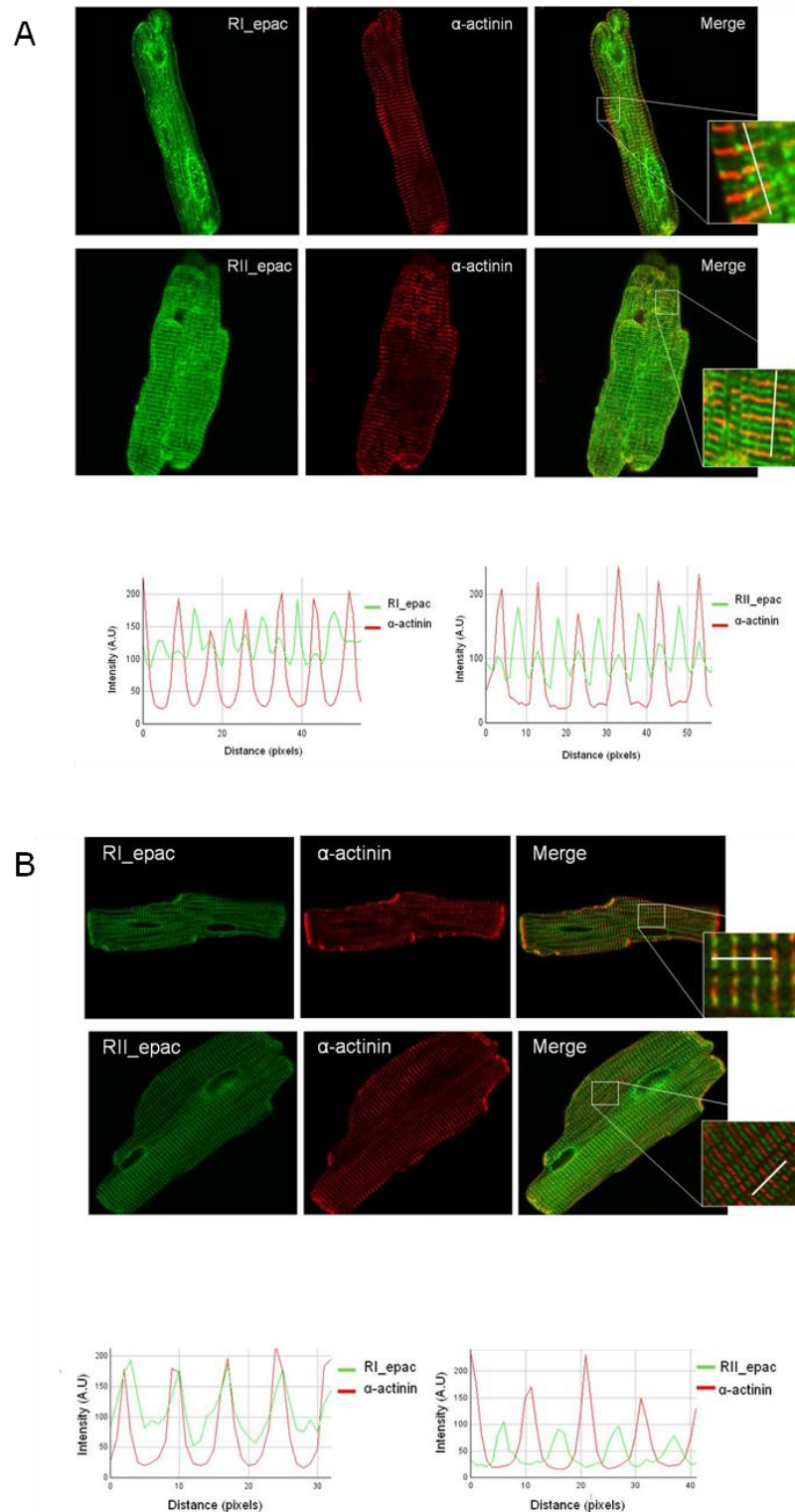


**Figure 5-4. Localisation of RI\_epac and RII\_epac FRET sensors in hypertrophic ARVM.** (A) Hypertrophic cardiomyocytes were transduced with the FRET sensor (green) and then stained for  $\alpha$ -sarcomeric actinin (red), followed by laser scanning confocal microscopic visualisation at 60x magnification. These representative images show the different localisation of the sensors in adult myocytes. Representative line intensity profiles (as indicated by the white line). (B) Representative images of non-hypertrophic myocytes stained for the same markers as previously shown (Figure 4-2).

To verify if the localisation of the two sensors are significantly different in hypertrophic myocytes, as well as to compare the localisation of the sensors to control myocytes, the Pearson correlation coefficient (PCC) value was calculated using ImageJ with JACoP as previously described. Figure 5-5 illustrates the PCC calculated using the fluorescence images acquired at the confocal microscope in control and hypertrophic myocytes. In control myocytes, as shown in Figure 4-3, the coefficient value is significantly higher in RI\_epac than RII\_epac, confirming that there is a difference in the localisation of these sensors in adult cardiomyocytes. However, in hypertrophic myocytes there is no significant difference between the two compartments. When comparing control myocytes with hypertrophic myocytes, there is reduced RI\_epac co-localisation with  $\alpha$ -actinin in the hypertrophic cells and increased RII\_epac co-localisation with  $\alpha$ -actinin in hypertrophic cells compared to control. This data would suggest that there is a redistribution of AKAPs, reflected by the different localisation for RI\_epac and RII\_epac and any further experiments should take into account these changes. Therefore any differences in the response to cAMP raising agents in hypertrophic ARVM, may be the consequence of the fact that the reporters are localised to different subcellular compartments compared to the non-hypertrophic counterparts.

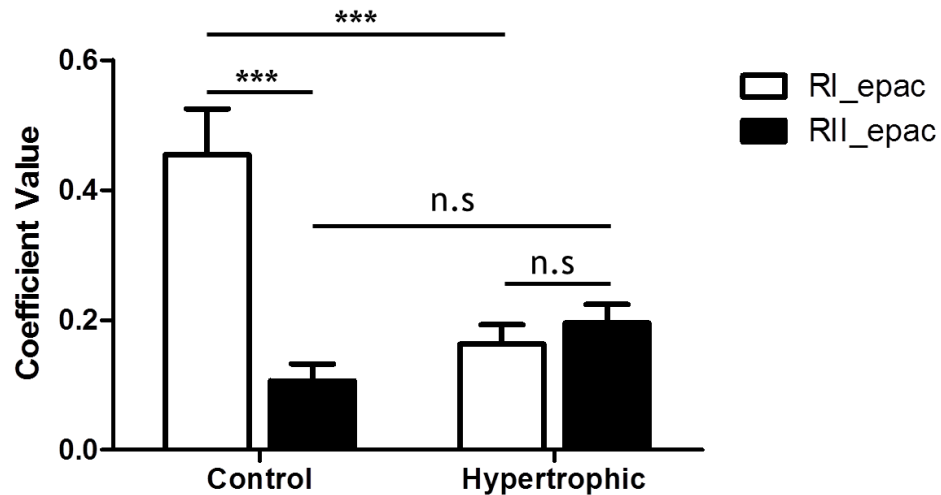


**Figure 5-5. Summary of sensor localisation analysis.**

Pearson colocalisation coefficient calculated using the JACOP plugin for Image J software for both sensors. RI\_epac control:  $0.789 \pm 0.03$ ,  $n = 15$ ; RII\_epac control:  $0.596 \pm 0.02$ ,  $n = 13$ ; RI\_epac hypertrophic:  $0.634 \pm 0.03$ ,  $n = 9$ ; RII\_epac hypertrophic:  $0.685 \pm 0.02$ ,  $n = 7$ . ANOVA with Bonferroni's post test, \*\*\*  $p < 0.001$ .

These values also can be expressed as  $\sqrt{\text{PCC}}$  to give the percentage of correlation between sensor and  $\alpha$ -actinin (RI\_epac hypertrophic: ~80%; RII\_epac hypertrophic: ~83%).

To assess the impact that chronic catecholamine stimulation has on compartmentalised cAMP signalling in ARVM, a FRET-based imaging approach was implemented, as in the previous chapter. ARVM were treated with NE to induce hypertrophy *in vitro* and were subsequently transduced with an adenovirus carrying the targeted FRET-based sensors RI\_epac and RII\_epac (on the same day as NE treatment). Cells were then imaged the following day on an epifluorescent microscope. cAMP production was stimulated by challenging the myocytes with cAMP raising stimuli and the effect of each stimulus was determined in the PKA-RI and PKA-RII subcellular locations. Below (Figure 5-6) is an example of a FRET experiment employing RI\_epac and RII\_epac in hypertrophic ARVM demonstrating the distinct responses obtained in the two compartments upon addition of various stimuli which increase cAMP generation.

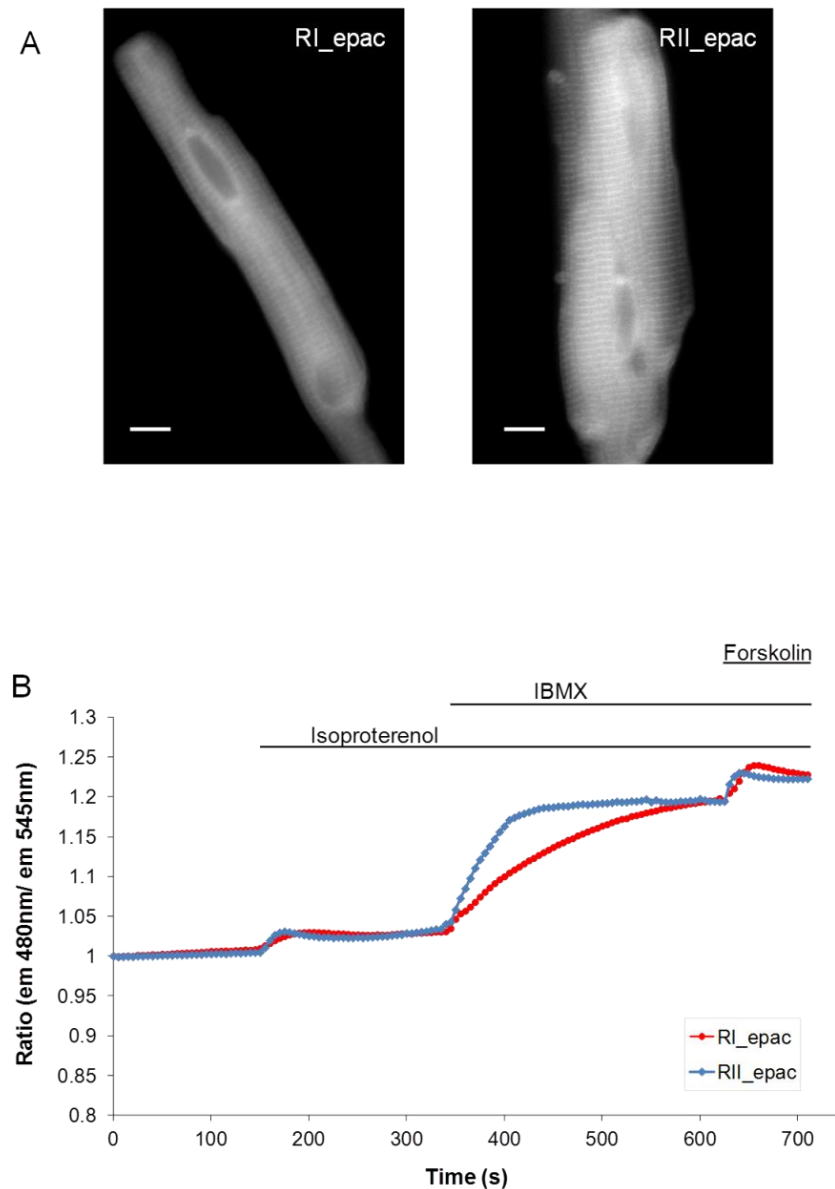


**Figure 5-6. . Representative example of a FRET experiment in hypertrophic cardiomyocytes transduced with the targeted cAMP sensors.**

**(A)** Image of hypertrophic ARVM expressing RI\_epac (left) or RII\_epac (right). **(B)** Representative kinetics of FRET change detected in response to 100 nM Isoproterenol, 10  $\mu$ M IBMX then 25  $\mu$ M forskolin recorded in hypertrophic ARVM expressing RI\_epac (red) or RII\_epac (blue).

To investigate the normal basal cAMP levels in the PKA-RI and PKA-RII compartments in hypertrophic ARVM, FRET images of myocytes expressing either RI\_epac or RII\_epac were acquired in the absence of any stimulus. The basal FRET values were calculated as  $I_{CFP}/I_{YFP}$  upon excitation at 440 nm, where  $I_{CFP}$  is the intensity of CFP emission and  $I_{YFP}$  is

the intensity of YFP emission. These data show (Figure 5-7) that the basal levels of cAMP in the PKA-RI and PKA-RII compartments are not statistically different in hypertrophic myocytes. These results were compared to the same experiment in control cells and it was found there was no difference in the basal cAMP levels in any of the groups, indicating there is no difference in intracellular cAMP levels in these two subcellular regions in hypertrophic myocytes compared with control cells.

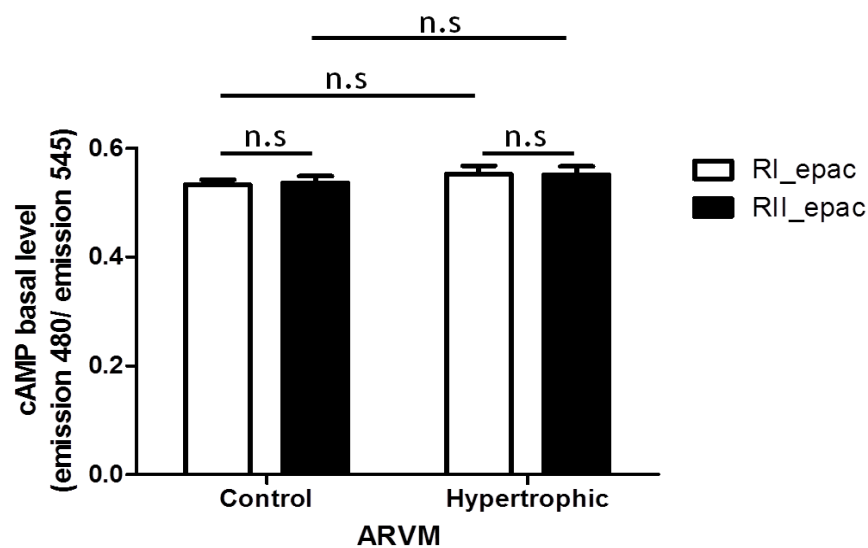


**Figure 5-7. Summary of the analysis of basal  $I_{CFP}/I_{YFP}$  ratio value in control and hypertrophic ARVM expressing RI\_epac or RII\_epac.**

RI\_epac control n = 10; RII\_epac control n = 17; RI\_epac hypertrophic ARVM n = 13; RII\_epac hypertrophic ARVM n = 14. Two way ANOVA with Bonferroni's post test, no significance.

With the aim of assessing the cAMP signalling dynamics in these two subcellular locales, hypertrophic ARVM, which had been previously transduced with adenoviral vector carrying RI\_epac or RII\_epac, were challenged with stimuli to elevate cAMP levels and thus revealing any disparities between the compartments. Cells were stimulated with  $\beta$ -adrenoreceptor agonist ISO (100 nM) which resulted in a similar increase in both the PKA-RI and PKA-RII compartments (Figure 5-8).

The phosphodiesterases activity in the two compartments, after  $\beta$  receptor stimulation, in hypertrophic myocytes was then explored. 100  $\mu$ M 3-isobutyl-1-methylxanthine (IBMX), a non-selective PDE inhibitor was added to the cells, this allowed for the investigation of PDE activity at the two sensor sites. Again there was an increase of cAMP in both compartments (Figure 5-8), which resulted in similar intracellular levels after addition of the stimuli.

In order to achieve the maximum FRET response ( $\Delta R/R_0$  max) of these sensors in this cell type, the myocytes were challenged with a saturating concentration of 25  $\mu$ M Forskolin (FRSK), an activator of adenylyl cyclase which stimulates cAMP production. The degree of FRET change detected was comparable for both the PKA-RI and PKA-RII compartments (Figure 5-8), indicating that the two probes still give the same maximal FRET change at signal saturation in hypertrophic ARVM. This means that these probes have the same dynamic range and therefore any disparities recorded between them can be believed to reflect a variation in cAMP levels rather than a difference in sensor performance.

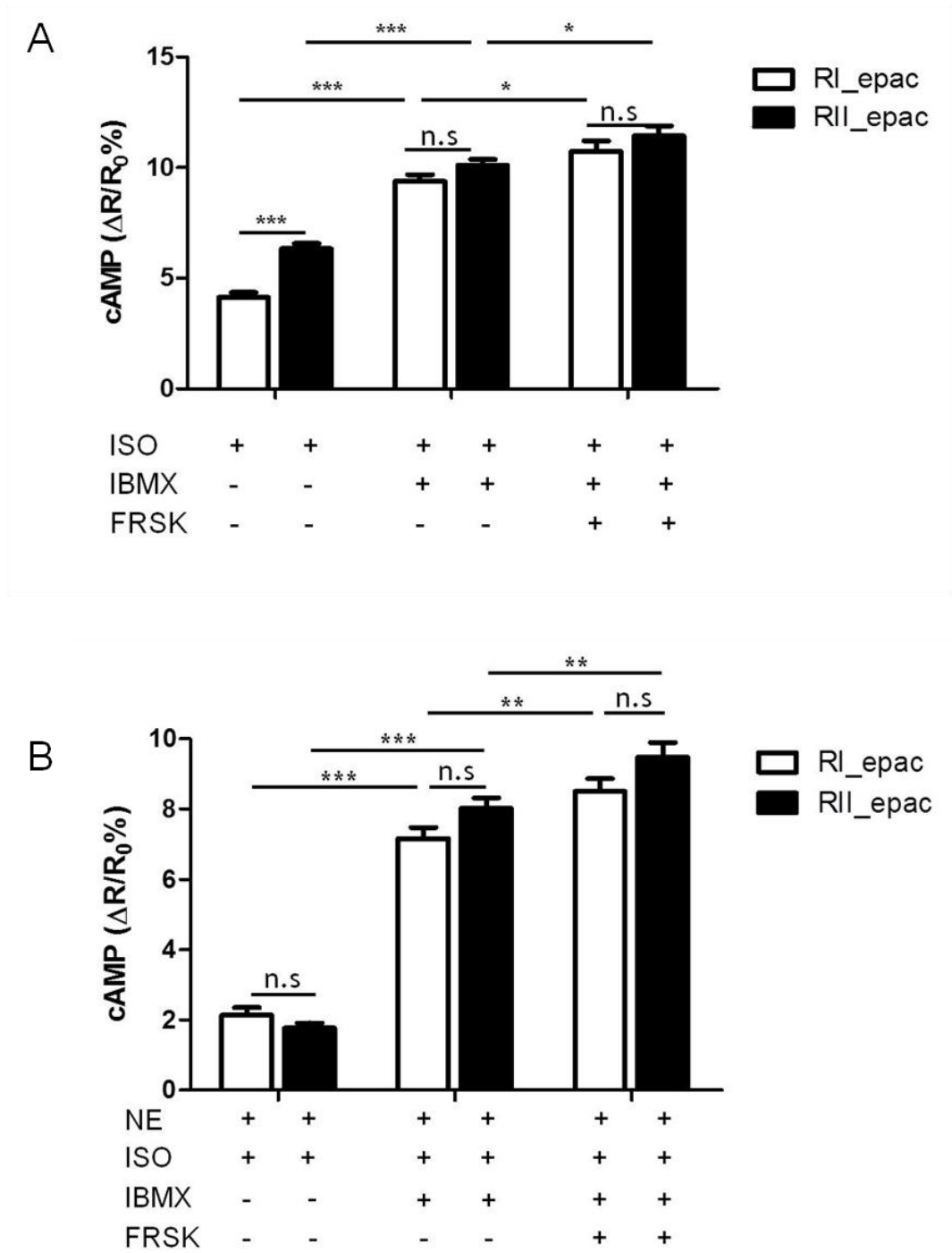


**Figure 5-8. Summary of FRET measurements of cAMP signals in hypertrophic ARVM expressing RI\_epac or RII\_epac.**

(A) Experiment carried out in control ARVM. (B) ARVM were pre-treated overnight with 1  $\mu$ M norepinephrine then 100 nM Isoproterenol, 100  $\mu$ M IBMX and finally 25  $\mu$ M Forskolin. ISO: RI\_epac hypertrophic ARVM:  $\Delta R/R_0 = 2.137 \pm 0.215$  %,  $n = 28$ ; RII\_epac hypertrophic ARVM:  $\Delta R/R_0 = 1.774 \pm 0.146$  %. IBMX: RI\_epac hypertrophic ARVM:  $\Delta R/R_0 = 7.162 \pm 0.316$  %,  $n = 26$ ; RII\_epac hypertrophic ARVM:  $\Delta R/R_0 = 8.023 \pm 0.301$  %,  $n = 15$ . FRSK: RI\_epac hypertrophic ARVM:  $\Delta R/R_0 = 8.505 \pm 0.371$  %,  $n = 16$ ; RII\_epac hypertrophic ARVM:  $\Delta R/R_0 = 9.481 \pm 0.420$  %,  $n = 14$ . Statistical significance calculated by two way ANOVA with Bonferroni's post test, \*  $p < 0.05$ , \*\*  $p < 0.01$ , \*\*\*  $p < 0.001$ .

Although these results do not appear to unveil any differences between RI\_epac and RII\_epac in the hypertrophic ARVM, the kinetic data indicate that there may be disparities in the kinetics of cAMP levels increase in the PKA-RI and PKA-RII compartments. The rate of FRET change after each stimulus was calculated by the formula  $\text{rate} = \Delta\text{FRET}/\Delta t$ , where the FRET ratio detected at the first 5 time points after the addition of the stimulus was divided by the time in seconds. The rate of FRET change detected in hypertrophic myocytes after ISO stimulation was similar for both the RI\_epac and RII\_epac sensors (Figure 5-9) (RI\_epac hypertrophic ARVM:  $0.30 \pm 0.06$  /second; RII\_epac hypertrophic ARVM:  $0.28 \pm 0.06$  /second; ns). However after the addition of IBMX, the FRET response was significantly faster in the PKA-RII compartment compared to the PKA-RI compartment (RI\_epac hypertrophic ARVM:  $0.4 \pm 0.08$  /second; RII\_epac hypertrophic ARVM:  $0.7 \pm 0.1$  /second,  $p < 0.05$ ).

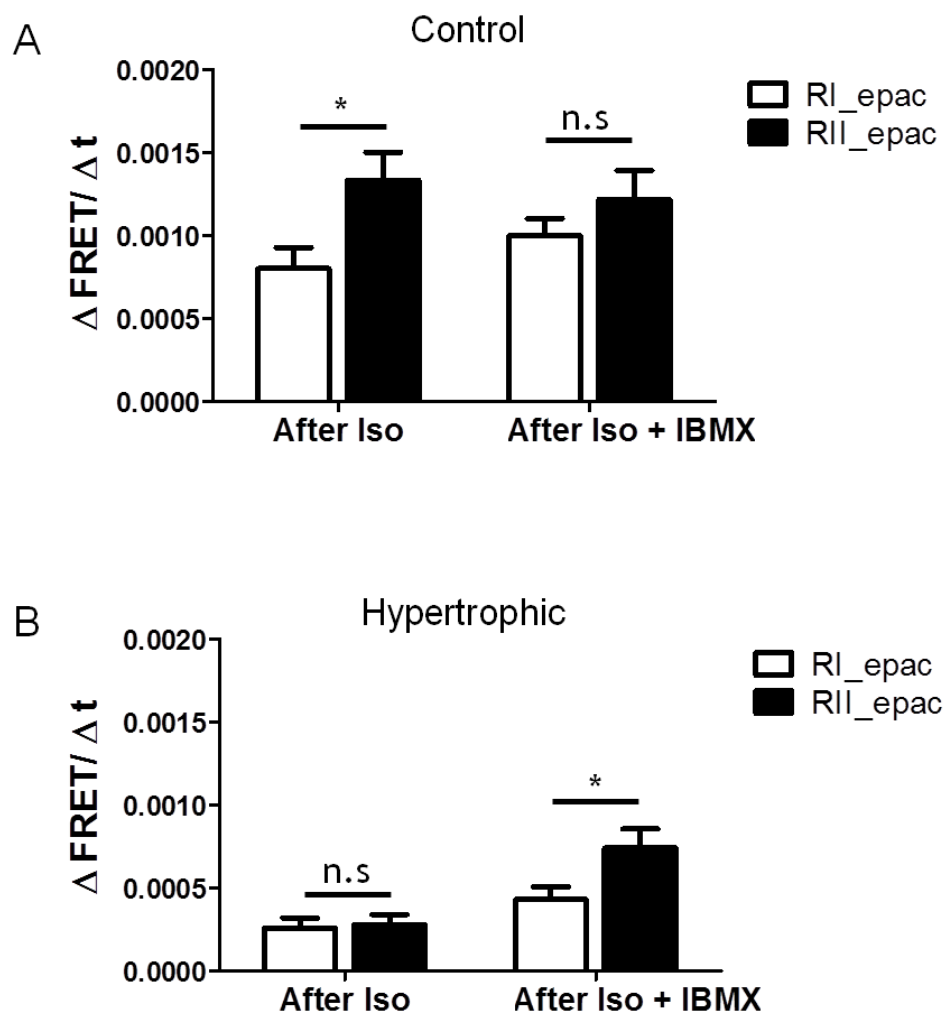


**Figure 5-9. Summary of rate of FRET change ( $\Delta\text{FRET}/\Delta t$ ) after each stimuli.** Rate of FRET change in control (A) or hypertrophic (B) ARVM expressing either RI\_epac or RII\_epac when stimulated with Isoproterenol (100 nM) and then IBMX (100  $\mu\text{M}$ ). Statistical significance calculated by two way ANOVA with Bonferroni's post test, \*  $p < 0.05$ .

On comparison with control ARVM, as shown in the previous chapter (Figure 4-7), when ISO was added to the bath, there was a quicker response in RII\_epac compared to RI\_epac (RI\_epac:  $0.8 \pm 0.1$ / second; RII\_epac:  $1.3 \pm 0.2$ / second) and no difference was documented after IBMX stimulation (RI\_epac:  $1 \pm 0.1$ / second; RII\_epac  $1 \pm 0.2$ / second). From these data, the calculated rate of FRET change is smaller in hypertrophic myocytes in both compartments. After the addition of ISO, control cells respond to the stimulus significantly faster than in hypertrophic myocytes (RI\_epac control vs. RI\_epac hypertrophic:  $p < 0.001$ ; RII\_epac control vs. RII\_epac hypertrophic:  $p < 0.001$ ). The

same can also be said after addition of IBMX (RI\_epac control vs. RI\_epac hypertrophic:  $p < 0.001$ ; RII\_epac control vs. RII\_epac hypertrophic:  $p < 0.05$ ).

### **5.2.3 Comparison of compartmentalised cAMP signalling in control and hypertrophic adult cardiomyocytes.**

The literature shows that cyclic nucleotide signalling is regulated in discrete subcellular compartments to maintain homeostasis and control diverse cellular functions. The compartmentalisation of cAMP was first described in studies conducted in perfused rat hearts stimulated with ISO and prostaglandin (PGE1), where different effects on PKA activation and its downstream targets were reported (Hayes et al. 1979). Further studies have supported this hypothesis that cAMP signalling works in a compartment specific way and that compartmentalisation is regulated by PDEs. Alterations in the cAMP/PKA signalling pathway and changes in PDE activity contributes to the progression of cardiovascular diseases. Thus it was interesting to investigate whether there were any changes in compartmentalised cAMP signalling between control and hypertrophic ARVM.

In control myocytes, activation of  $\beta$ -adrenergic signalling by the addition of the  $\beta$ -agonist ISO (100 nM) induced a larger increase in cAMP in the PKA-RII compartment compared to the PKA-RI compartment. Conversely, ISO stimulation in hypertrophic ARVM resulted in much smaller increase in cAMP in both compartments under investigation with no significant difference between the two locations.

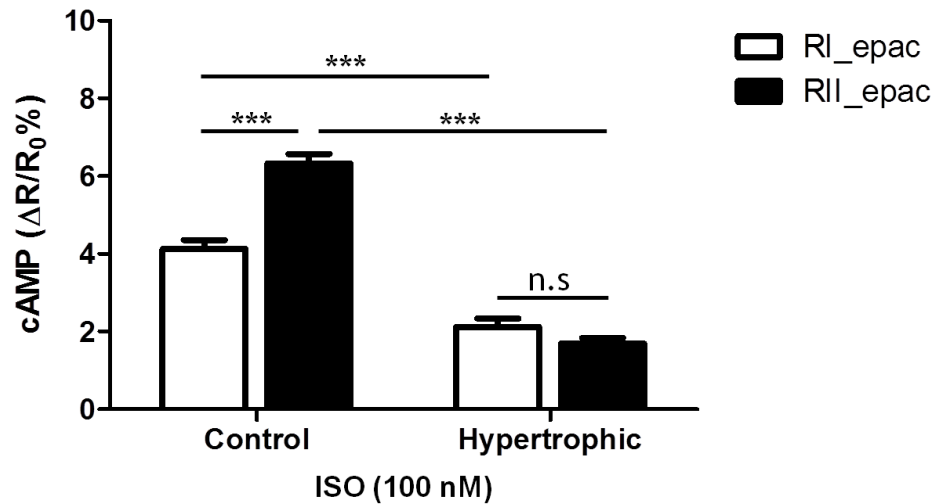


**Figure 5-10. Summary of FRET measurements of cAMP signals in control and hypertrophic ARVM expressing RI\_epac or RII\_epac upon addition of isoproterenol.**

Cardiomyocytes were stimulated with 100 nM isoproterenol – a  $\beta$ -adrenoceptors agonist.

RI\_epac control:  $\Delta R/R_0 = 4.133 \pm 0.221$  %, n = 26; RII\_epac control:  $\Delta R/R_0 = 6.204 \pm 0.215$  %, n = 31; RI\_epac hypertrophic:  $\Delta R/R_0 = 2.137 \pm 0.215$  %, n = 28; RII\_epac hypertrophic:  $\Delta R/R_0 = 1.774 \pm 0.146$  %, n = 34. Statistical significance calculated by two way ANOVA with Bonferroni's post test, \*\*\* p<0.001.

This data illustrates that in hypertrophic ARVM there is a significantly lower cAMP response upon ISO stimulation compared to non-hypertrophic myocytes, which suggests either desensitisation of  $\beta$ -adrenergic receptors upon chronic treatment with NE and/ or increased phosphodiesterase (PDE) activity in hypertrophic myocytes.

After ISO stimulation, cells were then treated with non-selective PDE inhibitor IBMX to assess the PDE activity in the PKA-RI and PKA-RII compartments. Results obtained showed no difference in the two compartments in control myocytes nor was there a difference between the PKA-RI and PKA-RII compartments in hypertrophic myocytes. However when comparing the control and hypertrophic ARVM, control cells generated a significantly greater cAMP rise in both compartments compared to the hypertrophic myocytes.

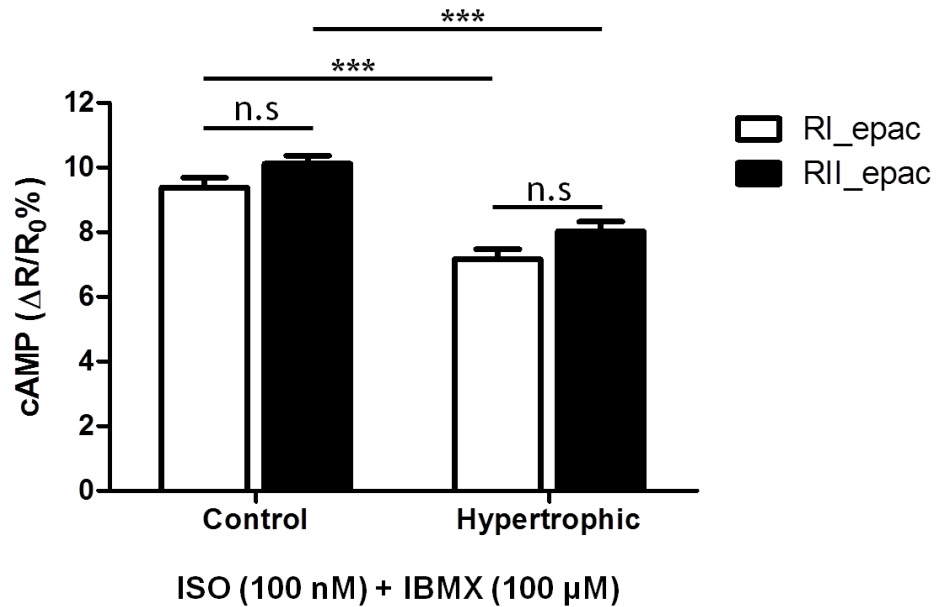


**Figure 5-11. Summary of FRET measurements of cAMP production in control and hypertrophic ARVM expressing RI\_epac or RII\_epac upon addition of isoproterenol and IBMX.**

RI\_epac control:  $\Delta R/R_0 = 9.376 \pm 0.311$  %, n = 26; RII\_epac control:  $\Delta R/R_0 = 10.112 \pm 0.252$  %, n = 27; RI\_epac hypertrophic:  $\Delta R/R_0 = 7.162 \pm 0.316$  %, n = 26; RII\_epac hypertrophic:  $\Delta R/R_0 = 8.023 \pm 0.301$  %, n = 15. Statistical significance calculated by two way ANOVA with Bonferroni's post test, \*\*\* p<0.001.

In order to compare the maximal FRET change ( $\Delta R/R_0$  max) in these control and hypertrophic ARVM, a saturating concentration of 25  $\mu$ M Forskolin (FRSK), an activator of adenylyl cyclase was administered after ISO and IBMX stimulation (Figure 5-12). Again results illustrated no difference in the two compartments in control myocytes nor was there a difference between the PKA-RI and PKA-RII compartments in hypertrophic myocytes. However when comparing the control and hypertrophic ARVM, control cells generated a significantly larger cAMP response in both compartments compared to the hypertrophic myocytes. A number of studies have suggested that adenylyl cyclase function is down-regulated in hypertrophy and heart failure (Chen et al. 1991; Bohm et al. 1992; Bohm 1995; Fung et al. 2002), which could explain why there is a lower cAMP response in hypertrophic myocytes compared to non-hypertrophic ARVM upon forskolin treatment.

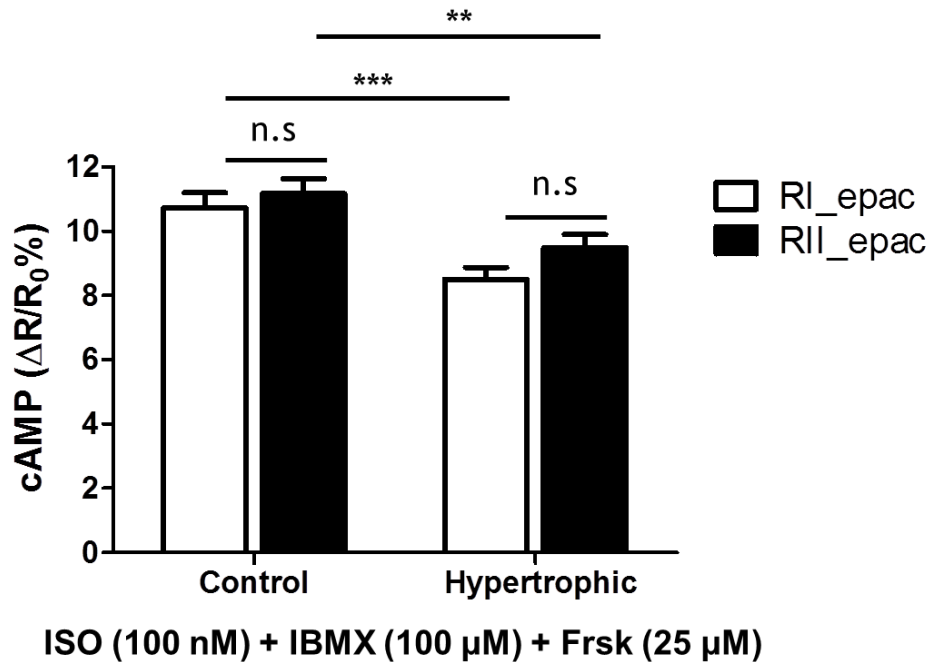


Figure 5-12. Summary of FRET measurements of cAMP production in control and hypertrophic ARVM expressing RI\_epac or RII\_epac upon addition of isoproterenol, IBMX and forskolin.

RI\_epac control:  $\Delta R/R_0 = 10.727 \pm 0.480$  %, n = 11; RII\_epac control:  $\Delta R/R_0 = 11.17 \pm 0.465$  %, n = 8; RI\_epac hypertrophic ARVM:  $\Delta R/R_0 = 8.505 \pm 0.371$  %, n = 16; RII\_epac hypertrophic ARVM:  $\Delta R/R_0 = 9.481 \pm 0.420$  %, n = 14. Statistical significance calculated by two way ANOVA with Bonferroni's post test, \*\* p<0.01.

The data described in Figure 5-11, does not give a clear indication of the PDE activity alone as the response detected is a combination of the responses to ISO and IBMX. To obtain a clearer indication of the PDEs contribution in determining cAMP levels in the PKA-RI and PKA-RII compartments, the PDE contribution in determining the cAMP response was calculated by taking the final response detected upon addition of ISO + IBMX treatment in both control and hypertrophic cells and by subtracting the ISO response for each subcellular compartment (Figure 5-13A). As shown in the previous chapter, in control myocytes a significantly higher cAMP response in the PKA-RI compartment was detected compared to the PKA-RII compartment, indicating there is a greater contribution of PDEs acting in the PKA-RI compartment compared to the PKA-RII compartment. In hypertrophic ARVM the opposite is seen: here the PKA-RII compartment showed a significantly larger FRET change compared to the PKA-RI. To investigate the

impact hypertrophy has on PDE activity; control and hypertrophic ARVM transduced with either RI\_epac or RII\_epac were compared. In the PKA-RI compartment, there was no difference in cAMP response upon IBMX stimulation, however in the PKA-II compartment there was a significantly greater cAMP response in the hypertrophic myocytes compared with the control ARVM. These data indicate that in hypertrophic adult cardiomyocytes, there is an increase in PDE activity selectively associated with the PKA-II compartment.

To investigate whether an increase in the basal activity of PDEs occurs in hypertrophic myocytes, the response stimulation with IBMX (100  $\mu$ M) alone in normal and hypertrophic cardiac myocytes was assessed (Figure 5-13B). In control myocytes, no difference was detected between the PKA-RI and PKA-II compartments upon non-selective PDE inhibition. Nor was there a difference in basal PDE activity in the two compartments in hypertrophic myocytes when IBMX was given as a first stimulus. These results indicate an increased PDE activity selectively in the PKA-II locale of hypertrophic myocytes after catecholamine stimulation compared to non-hypertrophic ARVM.

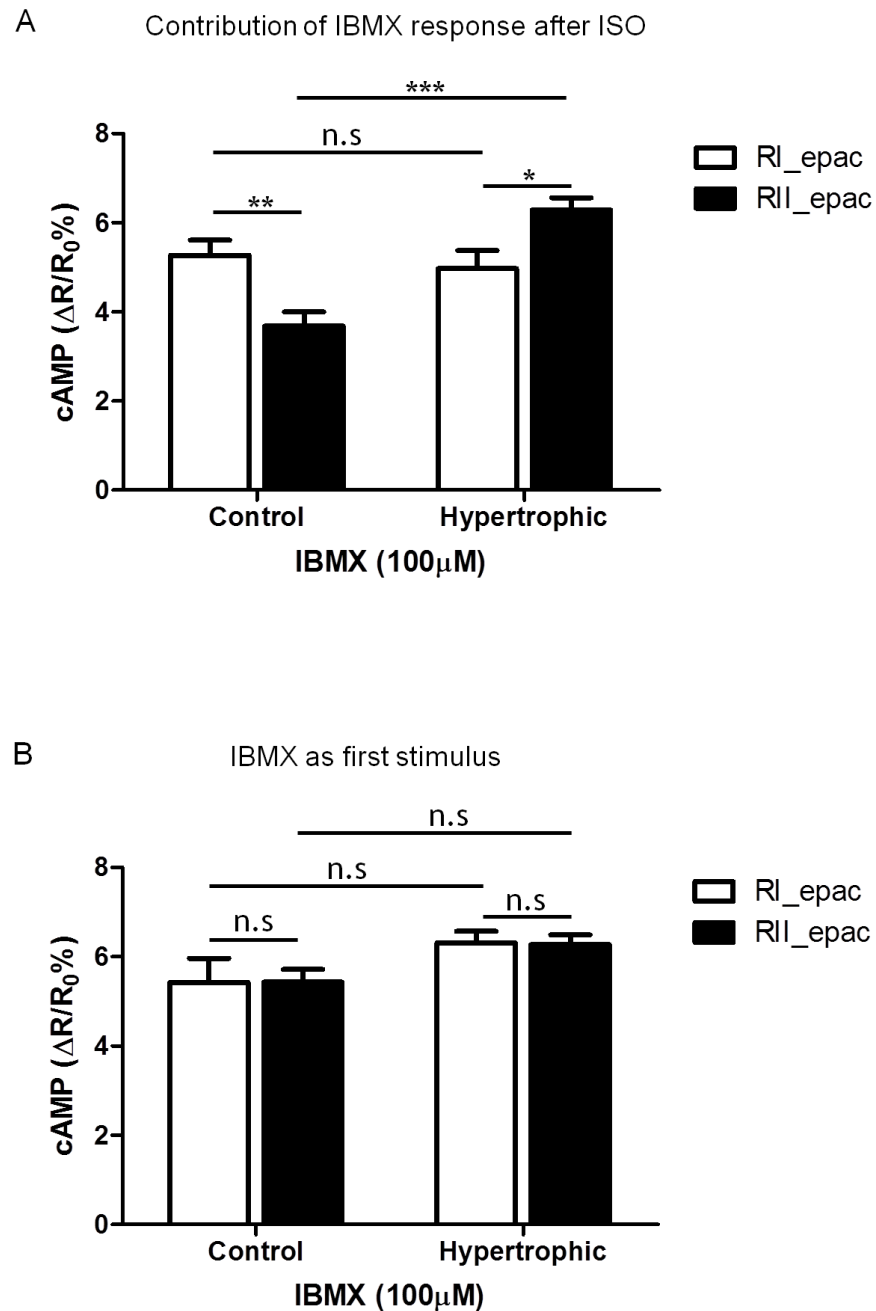


**Figure 5-13.** The contribution of phosphodiesterases (PDEs) in control and hypertrophic ARVM transduced with RI\_epac or RII\_epac.

(A) Myocytes are stimulated first with 100 nM Isoproterenol, then IBMX. The contribution of the IBMX response alone was calculated showing the basal PDE activity. RI\_epac control:  $\Delta R/R_0 = 5.267 \pm 0.344$  %, n = 26; RII\_epac control:  $\Delta R/R_0 = 3.683 \pm 0.318$  %, n = 27; RI\_epac hypertrophic:  $\Delta R/R_0 = 4.968 \pm 0.405$  %, n = 26; RII\_epac hypertrophic:  $\Delta R/R_0 = 6.275 \pm 0.280$  %, n = 15. (B) Myocytes are treated with IBMX without Isoproterenol. RI\_epac control:  $\Delta R/R_0 = 5.425 \pm 0.539$  %, n = 5; RII\_epac control:  $\Delta R/R_0 = 5.432 \pm 0.287$  % n = 6; RI\_epac hypertrophic:  $\Delta R/R_0 = 6.308 \pm 0.262$  %, n = 6; RII\_epac hypertrophic:  $\Delta R/R_0 = 6.272 \pm 0.218$  % n = 6. Statistical significance calculated by two way ANOVA with Bonferroni's post test, \* p < 0.05, \*\* p < 0.01, \*\*\* p < 0.001.

## 5.2.4 Contribution of individual PDEs to the control of the cAMP response to catecholamines in the PKA-RI and type II compartments in hypertrophic myocytes.

In order to explore which of the phosphodiesterase families are responsible for the increased basal cAMP hydrolytic activity in the PKA-RII compartment and for the altered cAMP response to catecholamine stimulation in hypertrophic ARVM, myocytes expressing RI\_epac and RII\_epac were treated with a selective PDE inhibitor before stimulation with 100 nM ISO to induce cAMP synthesis.

For experiments investigating the role of PDE2, both control and hypertrophic myocytes expressing either RI\_epac or RII\_epac were pre-treated with the selective PDE2 inhibitor Bay 60-7550 (50 nM) for 10 minutes at 37°C before imaging. In most cases such treatment did not affect the basal cAMP levels in the myocytes (Figure 5-14) as the level of cAMP detected was comparable in all conditions.

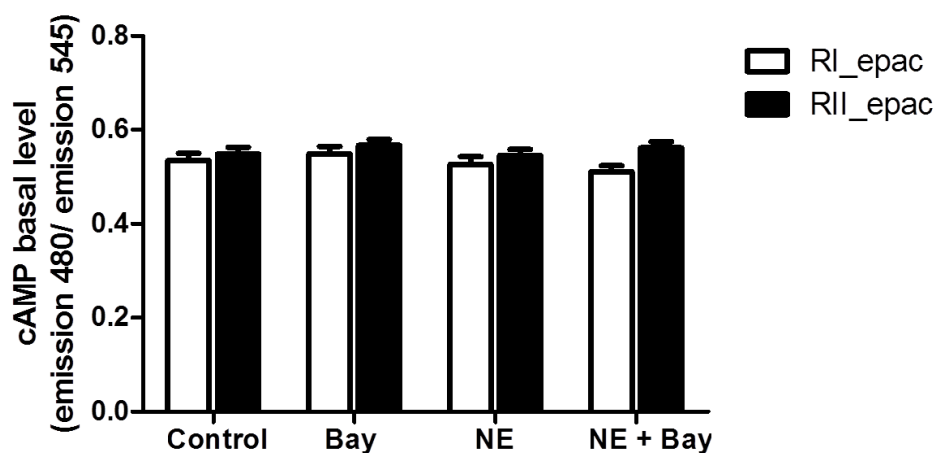
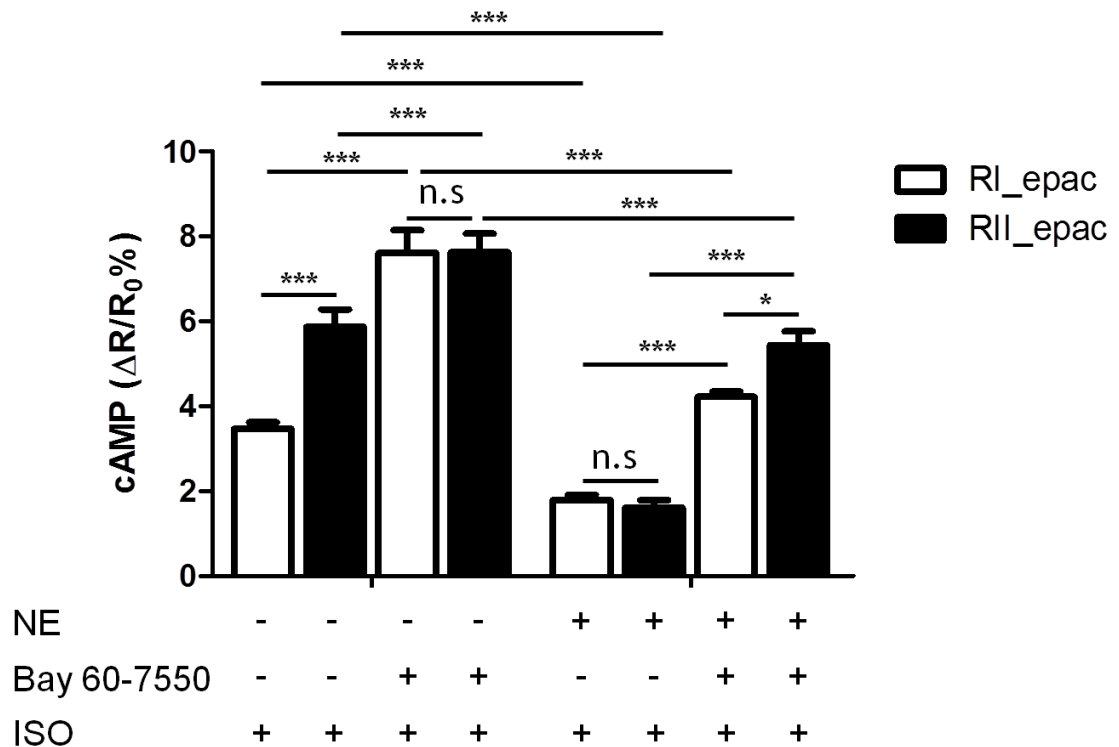


Figure 5-14. Summary of basal cAMP levels in ARVM in the presence or absence of PDE2 inhibitor Bay 60-7550 (Bay) in the control and hypertrophic myocytes (NE).

RI\_epac control: n = 9; RII\_epac control: n = 9; RI\_epac + Bay 60-7550: n = 18; RII\_epac + Bay 60-7550: n = 12; RI\_epac hypertrophic: n = 19; RII\_epac hypertrophic: n = 11; RI\_epac hypertrophic + Bay 60-7550: n = 16; RII\_epac hypertrophic + Bay 60-7550: n = 14. Statistical significance calculated by two way ANOVA with Bonferroni's post test, ns.

As shown in the previous chapter (Figure 4-6), ISO stimulation results in a significantly higher FRET change in the PKA-RII compartment compared to the PKA-RI compartment in control myocyte. Pre-treatment of the myocytes with Bay 60-7550 resulted in a significantly greater increase in the cAMP response to ISO stimulation in both compartments compared to controls (Figure 5-15). As a larger FRET change was detected in the PKA-RI compartment after PDE2 was inhibited with Bay 60-7550 (2 fold increase of cAMP compared to a 1.3 fold increase in the PKA-RII compartment), these results suggest that there is a larger contribution of PDE2 to the control of cAMP levels in the PKA-RI compartment than the in PKA-RII compartment.

In hypertrophic myocytes (Figure 5-15), ISO stimulation caused a similar cAMP rise in both compartments. Pre-treatment of ARVM with PDE2 inhibitor Bay 60-7550 produced a cAMP increase in response to ISO which was significantly higher in the PKA-RII compartment compared to the PKA-RI compartment. Again, there was a 2 fold increase in the amount of cAMP generated in the PKA-RI compartment, the same generated in control myocytes, but a 3.2 fold increase in the PKA-RII compartment when PDE2 inhibitors were present. These results indicate that although PDE2 is present in both the PKA-RI and PKA-RII compartments in hypertrophic ARVM PDE2 appears to contribute more to the control of the cAMP response to ISO in the PKA-RII compartment whereas the contribution of PDE2 in the PKA-RI compartment appears to be unchanged.



**Figure 5-15. Summary of FRET change upon the selective inhibition of PDE2 in control and hypertrophic (NE treated) ARVM.**

Summary of FRET change induced by 100 nM isoproterenol in the presence or absence of PDE2 inhibitor Bay 60-7550. RI\_epac control:  $\Delta R/R_0 = 3.47 \pm 0.152\%$ ,  $n = 8$ ; RII\_epac control:  $\Delta R/R_0 = 5.871 \pm 0.405\%$ ,  $n = 16$ ; RI\_epac + Bay 60-7550:  $\Delta R/R_0 = 7.616 \pm 0.528\%$ ,  $n = 10$ ; RII\_epac + Bay 60-7550:  $\Delta R/R_0 = 7.633 \pm 0.427\%$ ,  $n = 9$ ; RI\_epac hypertrophic:  $\Delta R/R_0 = 1.798 \pm 0.116\%$ ,  $n = 7$ ; RII\_epac hypertrophic:  $\Delta R/R_0 = 1.609 \pm 0.179\%$ ,  $n = 18$ ; RI\_epac hypertrophic + Bay 60-7550:  $\Delta R/R_0 = 4.224 \pm 0.121\%$ ,  $n = 9$ ; RII\_epac hypertrophic + Bay 60-7550:  $\Delta R/R_0 = 5.427 \pm 0.289\%$ ,  $n = 10$ . Statistical significance calculated by two way ANOVA with Bonferroni's post test, \*  $p < 0.05$ , \*\*  $p < 0.01$ , \*\*\*  $p < 0.001$ .

For experiments investigating PDE3, both control and hypertrophic myocytes were transduced overnight with adenovirus carrying the coding sequence for RI\_epac or RII\_epac before pre-treatment with the selective PDE3 inhibitor cilostamide (10  $\mu\text{M}$ ) for 10 minutes at 37°C prior to imaging. Under basal conditions there was a comparable level of cAMP in each condition (Figure 5-16).

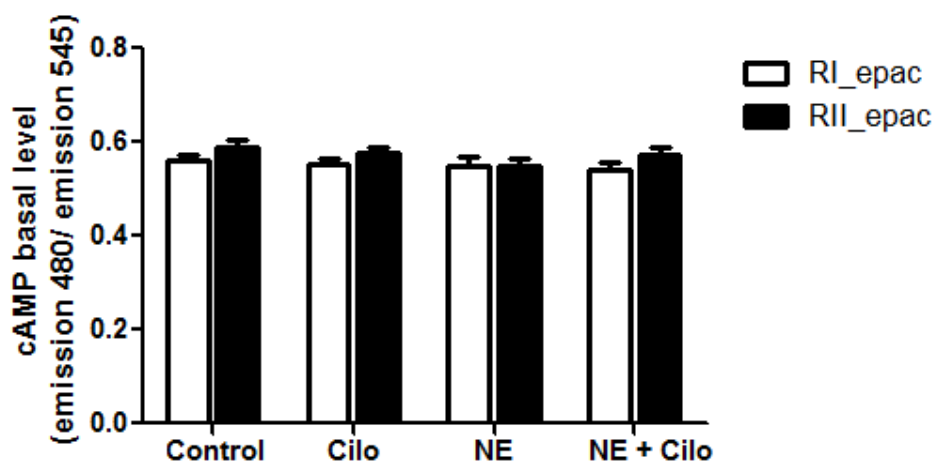


**Figure 5-16.** Summary of basal cAMP levels in ARVM in the presence or absence of PDE3 inhibitor cilostamide (Cilo) in the control and hypertrophic (NE treated) ARVM.

RI\_epac control: n = 8; RII\_epac control: n = 11; RI\_epac + cilostamide: n = 11; RII\_epac + cilostamide: n = 8; RI\_epac hypertrophic: n = 8; RII\_epac hypertrophic: n = 4; RI\_epac hypertrophic + cilostamide: n = 11; RII\_epac hypertrophic + cilostamide: n = 13. Statistical significance calculated by two way ANOVA with Bonferroni's post test.

In control cells stimulated with ISO (Figure 5-17) there was again a higher cAMP response in the PKA-RII compartment in ARVM. Upon pre-treatment with cilostamide, it was found that PDE3 inhibition only had an effect on the cAMP level detected in the PKA-RI compartment, with a 1.4 fold increase in cAMP production.

Hypertrophic myocytes challenged with ISO alone generated a small comparable increase in cAMP in the PKA-RI and PKA-RII compartment (Figure 5-17). When hypertrophic myocytes were preincubated with the PDE3 inhibitor, there was no significant change in either compartment after ISO stimulation. These results indicate that in control myocytes PDE3 appears to be predominantly active in the subcellular location where PKA-RI normally resides, however in hypertrophic myocytes, there appears to be a loss of PDE3 activity in this compartment.

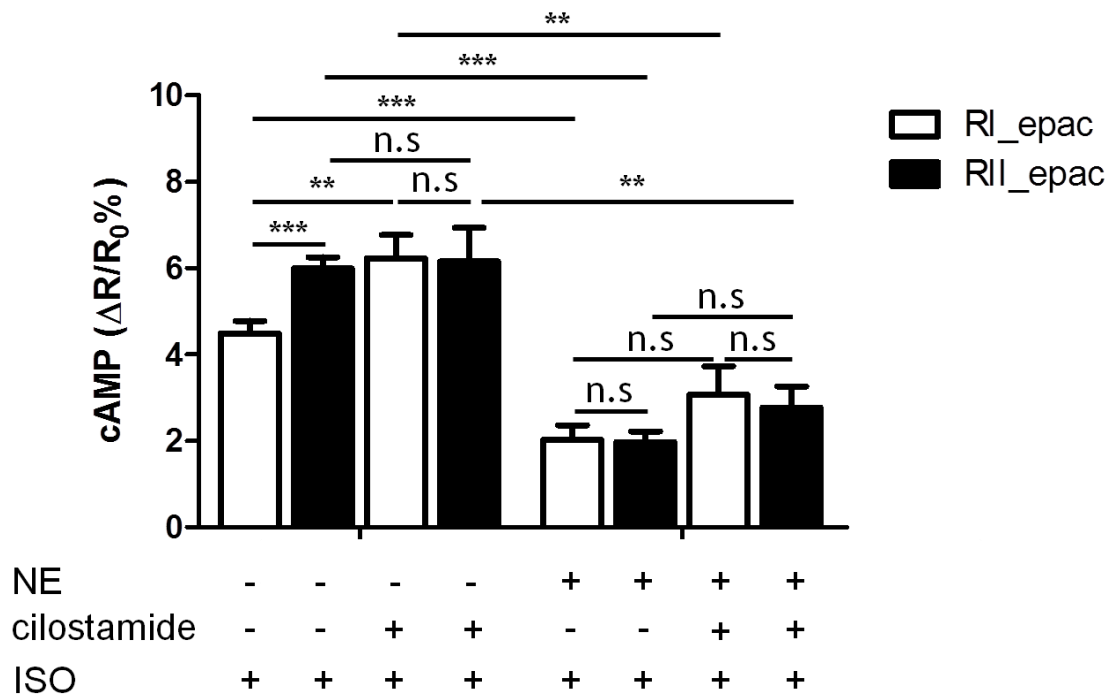
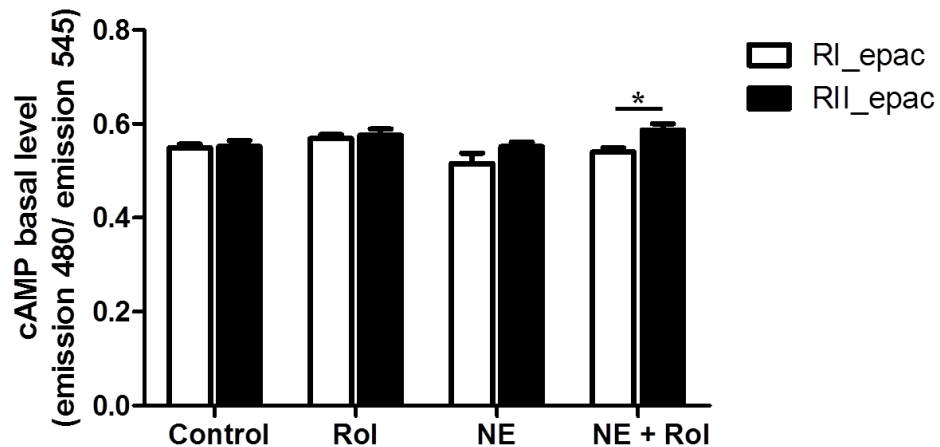


Figure 5-17. Summary of FRET change upon the selective inhibition of PDE3 in control and hypertrophic (NE treated) ARVM.

Summary of FRET change induced by 100 nM isoproterenol (ISO) in the presence or absence of PDE3 inhibitor cilostamide. RI\_epac control:  $\Delta R/R_0 = 4.402 \pm 0.276$  %, n = 8; RII\_epac control:  $\Delta R/R_0 = 5.634 \pm 0.276$  %, n = 11; RI\_epac + cilostamide:  $\Delta R/R_0 = 6.23 \pm 0.541$  %, n = 11; RII\_epac + cilostamide:  $\Delta R/R_0 = 5.884 \pm 0.834$  %, n = 8; RI\_epac hypertrophic:  $\Delta R/R_0 = 2.025 \pm 0.341$  %, n = 16; RII\_epac hypertrophic:  $\Delta R/R_0 = 2.030 \pm 0.239$  %, n = 15; RI\_epac hypertrophic + cilostamide:  $\Delta R/R_0 = 3.075 \pm 0.655$  %, n = 10; RII\_epac hypertrophic + cilostamide:  $\Delta R/R_0 = 2.769 \pm 0.495$  %, n = 11. Statistical significance calculated by two way ANOVA with Bonferroni's post test, \* p<0.05, \*\* p<0.01, \*\*\* p<0.001.

The effect of PDE4 activity on cAMP signalling in hypertrophic myocytes was studied by transducing both control and hypertrophic myocytes with an adenovirus carrying the RI\_epac or RII\_epac reporters overnight before pre-treating the cells for 10 minutes with selective PDE4 inhibitor rolipram (10  $\mu$ M) and incubation at 37°C before experiments began. Under basal conditions there was a comparable level of cAMP in each condition (Figure 5-18). The only exception was the case of hypertrophic myocytes in which PDE4 had been inhibited, where there was a significantly larger basal level of cAMP in the PKA-RII compartment compared to the PKA-RI compartment (p < 0.05).



**Figure 5-18. Summary of basal cAMP levels in ARVM in the presence or absence of PDE4 inhibitor rolipram (Rol) in the control and hypertrophic (NE treated) ARVM.**

**RI\_epac control: n =11; RII\_epac control: n = 6; RI\_epac + rolipram: n =9; RII\_epac + rolipram: n = 9; RI\_epac hypertrophic: n =9; RII\_epac hypertrophic: n = 8; RI\_epac hypertrophic + rolipram: n =12; RII\_epac hypertrophic + rolipram: n = 12. Statistical significance calculated by two way ANOVA with Bonferroni's post test, \*\* p<0.01.**

In control myocytes stimulated with ISO there was a higher generation of cAMP in the PKA-RII compartment (Figure 5-19). Myocytes treated with PDE4 inhibitor rolipram before imaging produced an increased level of cAMP in both compartments compared with control cells. This resulted in a 1.8 fold increase in cAMP in the PKA-RI compartment and a 1.3 fold increase in the PKA-RII compartment.

In hypertrophic myocytes the effect of ISO stimulations was again a similar rise in cAMP in both locations (Figure 5-19). When treated with rolipram before  $\beta$ -AR stimulation, the outcome was a rise in cAMP specifically in the PKA-RII compartment. These findings, when compared to control myocytes, suggest a loss of PDE4 activity in the PKA-RI compartment and a gain of PDE4 activity in the PKA-RII compartment in hypertrophic ARVM.

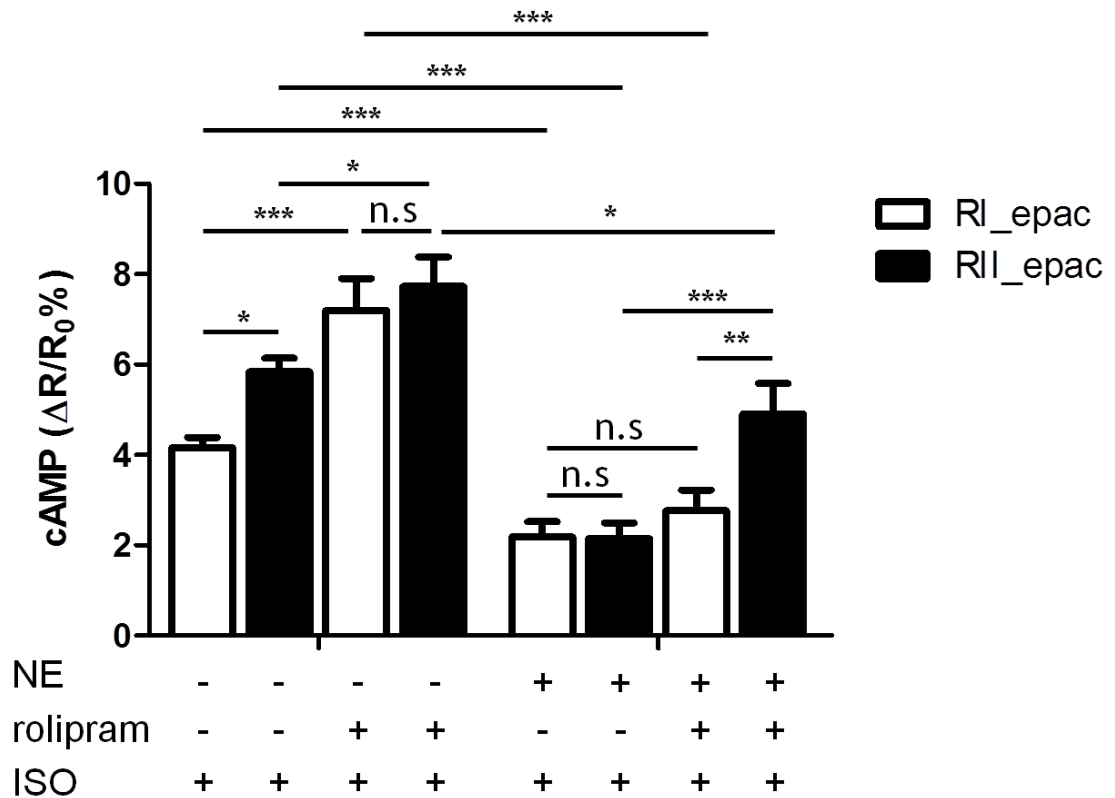


Figure 5-19. Summary of FRET change upon the selective inhibition of PDE4 in control and hypertrophic (NE treated) ARVM.

Summary of FRET change induced by 100 nM isoproterenol (ISO) in the presence or absence of PDE4 inhibitor rolipram. RI\_epac control:  $\Delta R/R_0 = 4.152 \pm 0.239$  %, n =10; RII\_epac control:  $\Delta R/R_0 = 5.838 \pm 0.299$  %, n = 13; RI\_epac + rolipram:  $\Delta R/R_0 = 7.512 \pm 0.68$  %, n =7; RII\_epac + rolipram:  $\Delta R/R_0 = 7.733 \pm 0.643$  %, n = 7; RI\_epac hypertrophic:  $\Delta R/R_0 = 2.181 \pm 0.353$  %, n =12; RII\_epac hypertrophic:  $\Delta R/R_0 = 2.145 \pm 0.354$  %, n = 9; RI\_epac hypertrophic + rolipram:  $\Delta R/R_0 = 2.764 \pm 0.457$  %, n =10; RII\_epac hypertrophic + rolipram:  $\Delta R/R_0 = 4.907 \pm 0.669$  %, n = 10. Statistical significance calculated by two way ANOVA with Bonferroni's post test, \* p<0.05, \*\* p<0.01, \*\*\* p<0.001.

PDE 1, 2, 3, 4, 5, 7, 8 and 9 are known to be expressed in the heart to different extents (Omori and Kotera 2007); however their individual contribution to cAMP hydrolysis in hypertrophic ARVM has not been assessed for all of them. The FRET data above suggests an increase in PDE2 activity in the PKA-RII compartment, a reduction of PDE3 in the PKA-RI and a possibly a partial localisation of PDE4 from the PKA-RI to the PKA-RII compartment. To test this hypothesis PDE activity assays were performed on cell lysates to establish whether total activity of individual PDEs was affected in hypertrophic vs. control

ARVM (Figure 5-20). Lysates were treated with PDE inhibitors and the amount of cAMP hydrolysis was calculated using a phosphodiesterase activity assay (materials and methods 3.5.3 (Marchmont and Houslay 1980)). In this two step procedure, protein from control or hypertrophic ARVM are first incubated with 1  $\mu\text{M}$  8[ $^3\text{H}$ ]-labelled cAMP. In the second step the product of cAMP hydrolysis (5'AMP) is incubated with snake venom which dephosphorylates 5'AMP to adenosine. The non-hydrolysed cAMP (negatively charged) is separated from the neutral charged adenosine with Dowex ion-exchange resin and the amount of adenosine is measured by scintillation counting.

As expected, treatment with the non-selective PDE inhibitor IBMX resulted in a dramatic decrease in cAMP hydrolysing activity. IBMX inhibits all PDE families, with the exception of PDE8 (Wang et al. 2008). No difference was detected between control and hypertrophic myocytes, indicating that there is no difference in the overall PDE activity in the two conditions. Treatment with Rolipram (10  $\mu\text{M}$ ), which inhibits all members of the PDE4 family, revealed the highest hydrolysing activity among all the selective PDE inhibitors, indicating that PDE4 is responsible for the majority of cAMP hydrolysing activity in ARVM. This is in agreement with previous data from Mongillo and co-workers (Mongillo et al. 2004). Again there was no difference recorded in PDE4 activity in control and hypertrophic myocytes. Inhibition of PDE3 with cilostamide (10  $\mu\text{M}$ ) also significantly reduced cAMP hydrolysis in both cell types to a similar level. Inhibition of PDE2 with Bay 60-7550 (50 nM) had the smallest effect of all the PDE inhibitors tested, but still significantly reduced cAMP in both control and hypertrophic adult myocytes to a similar level.

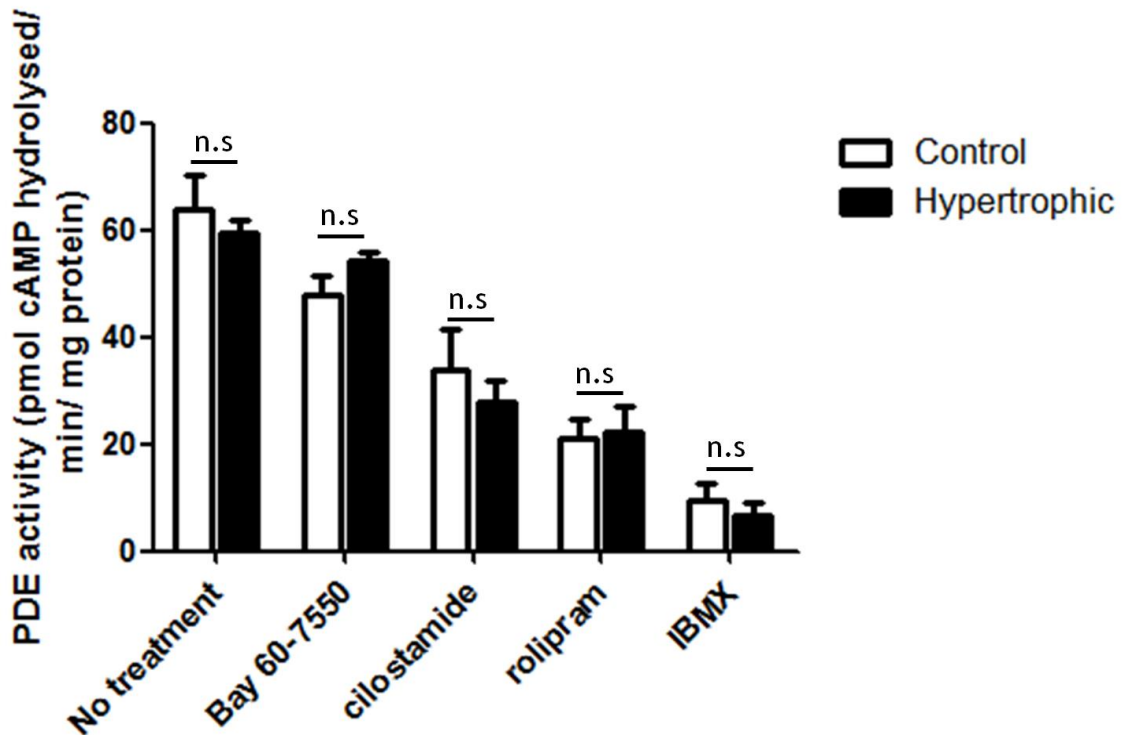


Figure 5-20. cAMP hydrolysing activities of different PDE families in control and hypertrophic ARVM.

ANOVA with Bonferroni's post test, no significance between control and hypertrophic myocytes.

There appears to be no difference in the total activity of individual PDEs in control vs. hypertrophic cells. As the FRET data which showed differences in PDE control over the two subcellular compartments occurred after  $\beta$ -AR stimulation, it would have been interesting to repeat the PDE activity assay in lysates which are pre treated with ISO as well as PDE inhibitors. It is interesting to note that both PDE3 and PDE4 are activated by PKA (Omori and Kotera 2007); therefore ISO treatment could increase the activity of these PDE families in selected compartments of the myocyte. However due to time constraints and difficulty in extracting a sufficient amount of protein from this cell type, these experiments could not be completed.

### **5.2.5 Changes in individual PDE families expression as assessed by protein and mRNA level in hypertrophic ARVM**

To explore whether the observed deranged PDE-mediated control of compartmentalised cAMP signals seen in hypertrophic myocytes is due to altered expression levels of the individual PDEs involved, analysis of both PDE protein levels by Western blot and PDE mRNA levels by real-time PCR were performed using antibodies specific to the known PDE isoforms present in ARVM.

Western blot analysis of the expression level of all PDE were performed in triplicates in control and hypertrophic ARVM; GAPDH was utilised as internal standard to correct for sample to sample variation and loading errors and results were normalised to control ARVM. Similarly, RT-PCR was performed in 3 biological replicates and an average was taken before 18S rRNA was utilised as internal reference and data were then normalised to control myocyte samples. n = number of technical replicates (minimum of 3). At least 3 different animal preparations were used.

For PDE2 (Figure 5-21), the results obtained show that, despite the increase in PDE2 activity detected with FRET imaging in hypertrophic myocytes, no significant difference in PDE2 gene expression or protein levels was found between control and hypertrophic ARVM. These findings suggest that the increased PDE2 activity observed in hypertrophic myocytes selectively in the PKA-RII compartment may be due to activation of PDE2 rather than to a change in the amount of PDE2.

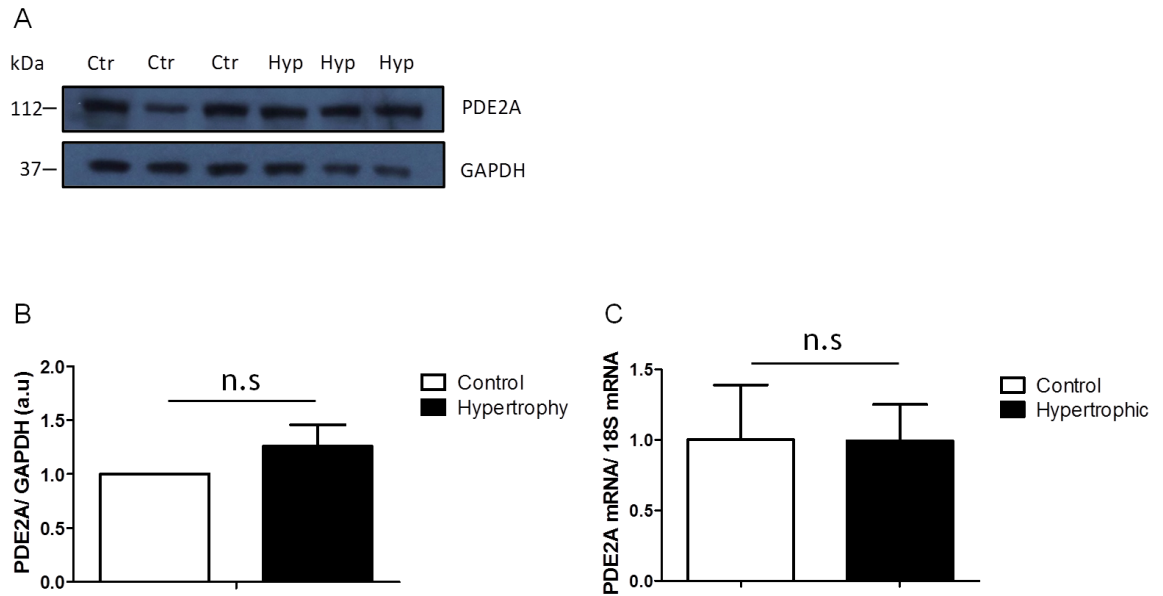


**Figure 5-21. PDE2 mRNA and protein levels in control and hypertrophic ARVM.**

**(A) Western blot of PDE2A and GAPDH in control and hypertrophied ARVM. (B) Western blot quantification: n = 3 (C) Representative RT-PCR showing no significant changes in PDE2A expression level in hypertrophic myocytes as compared to control cells. Control: n = 10; hypertrophic ARVM: n = 10. Error bars represent SEM. Two tailed; paired t-test.**

For PDE3 (Figure 5-22), the results of the expression level analysis show that, despite the apparent decrease in PDE3 activity detected with the FRET imaging approach in hypertrophic myocytes, there was a significant increase in PDE3 gene expression and protein levels in hypertrophic vs. control ARVM.

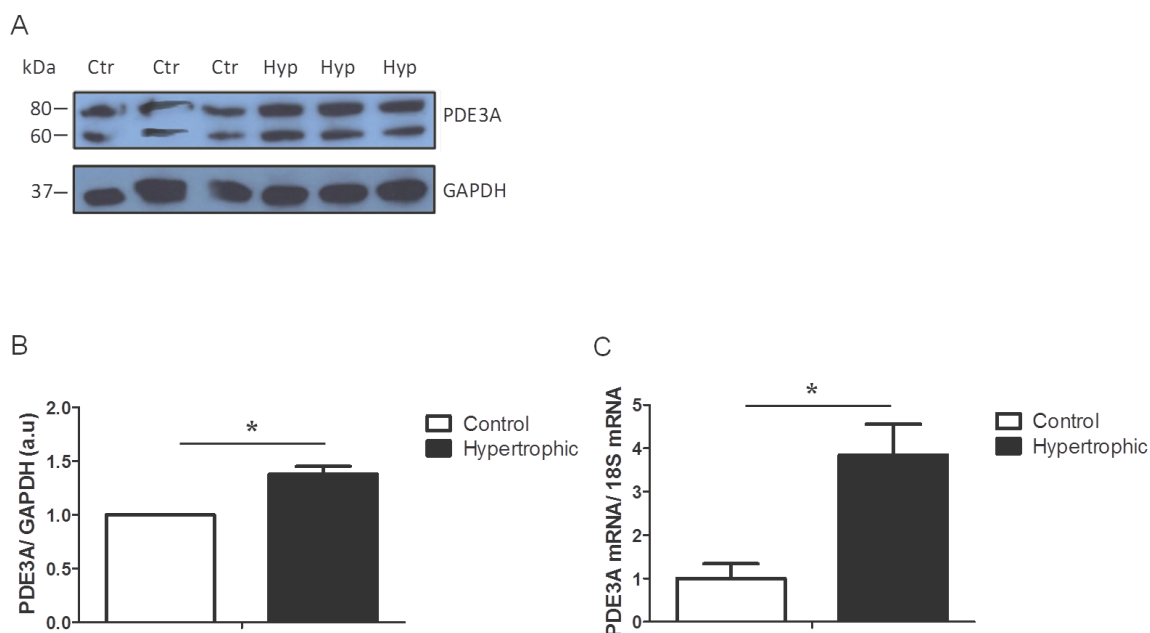


**Figure 5-22. PDE3A mRNA and protein levels in control and hypertrophic ARVM. (A) Western blot of PDE3A and GAPDH in control and hypertrophied ARVM. (B) Western blot quantification: n = 3. (C) Representative RT-PCR showing a small increase in PDE3A expression level in hypertrophic myocytes compared to control cells. Control: n = 15; hypertrophic ARVM: n = 15. Error bars represent SEM. Two tailed; paired t-test, \* p<0.05.**

PDE4 gene expression and protein levels were more challenging to investigate as there is more than one PDE4 gene expressed in the heart. The PDE4 family is highly evolutionarily conserved and it is encoded by four genes, namely PDE4A, PDE4B, PDE4C and PDE4D (Houslay and Adams 2003). These four PDE4 genes further encode 25 different isoforms all with unique N-terminal regions. It has been reported the PDE4C is not present in heart tissue (Kostic et al. 1997) and more recently it was reported that in cardiomyocytes the majority of PDE4 cAMP hydrolytic activity is provided by the PDE4D subfamily, with a small contribution from PDE4B, and virtually no contribution from PDE4A or PDE4C (Mongillo et al. 2004). Based on the above information, this study focused on the analysis of the expression of PDE4B and PDE4D in hypertrophic myocytes.

There are 4 known isoforms of PDE4B (PDE4B1, PDE4B2, PDE4B3 and PDE4B5 which have calculated molecular weights of 83 kDa, 64 kDa, 82 kDa and 57 kDa respectively) and so it was decided that immunoprecipitation (IP), using an antibody that recognises all known PDE4B isoforms, would be the best way to assess PDE4B protein expression. An

IP was performed with an IgG control and probed for an antibody against PDE4B isoforms. After IP only PDE4B1/ PDE4B3 could be detected. No statistical comparison was performed as  $n = 2$ . Neither protein nor mRNA expression levels of PDE4B were significantly altered in hypertrophic myocytes, although the mRNA level showed a small but not significant higher level in hypertrophic myocytes compared to control cells.

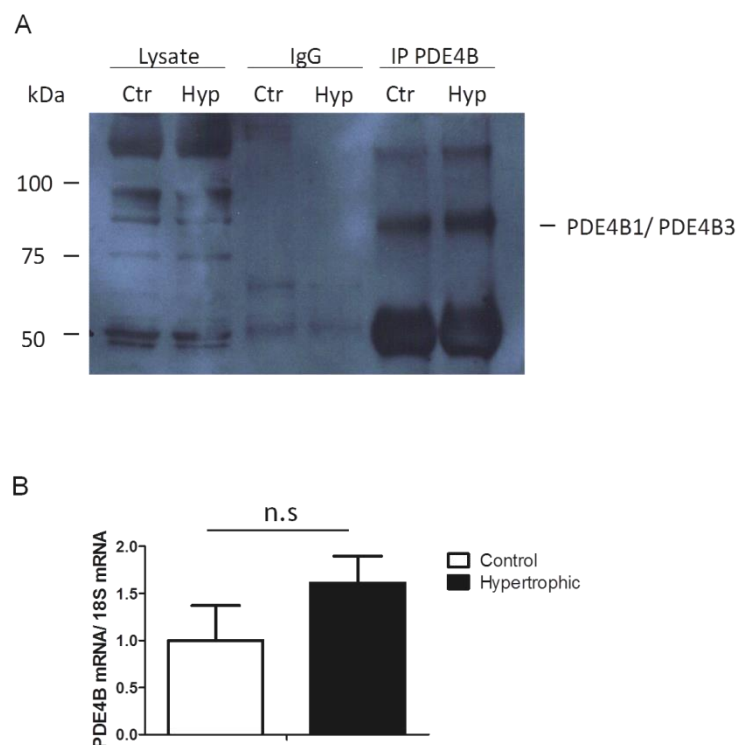


**Figure 5-23. PDE4B mRNA and protein levels in control and hypertrophic ARVM.**

**(A)** Immunoprecipitation (IP) was performed using PDE4B antibody before running Western Blot. Band at ~80 kDa represents PDE4B1 or PDE4B3. **(B)** Representative RT-PCR showing no change in PDE4B expression level in hypertrophic myocytes compared to control cells. Control:  $n = 12$ ; hypertrophic ARVM:  $n = 12$ . Error bars represent SEM. Two tailed; paired t-test.

There are 11 published isoforms of PDE4D with recorded molecular weights ranging between 58 – 91 kDa and therefore it was difficult to detect any clear changes in band intensities when comparing control and hypertrophic myocytes. Immunoprecipitation was performed using IgG as a control, and an immunoblot was then probed with an antibody

raised against all PDE4D isoforms (pan PDE4D). No statistical comparison was performed as  $n = 2$ . No statistically significant changes could be detected in the mRNA or protein expression levels of PDE4D, although the PDE4D mRNA levels showed a small but not significant increase in hypertrophic myocytes.

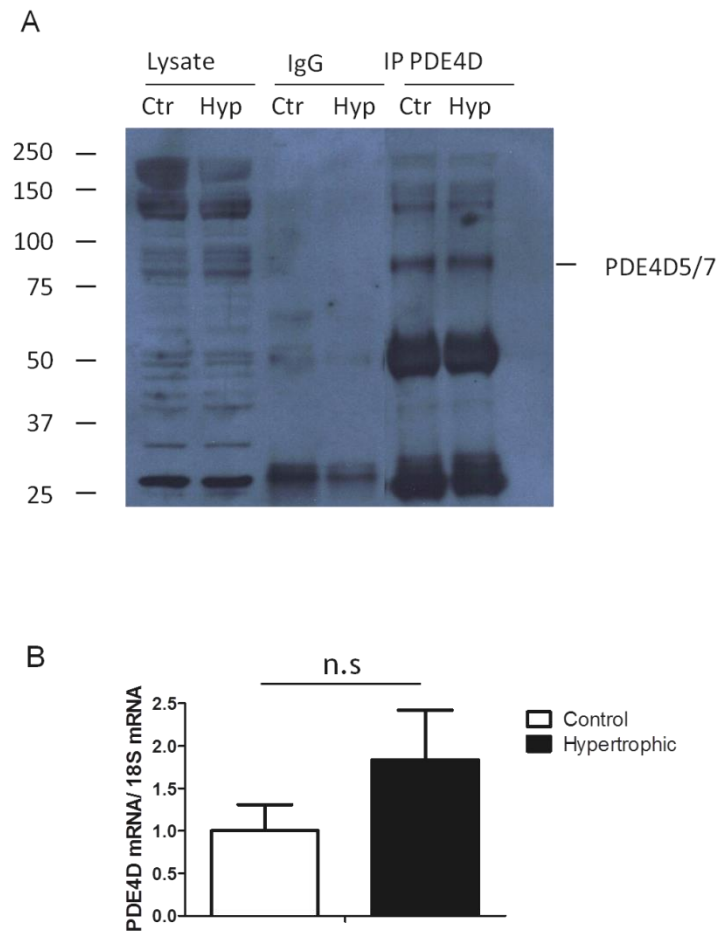


**Figure 5-24. PDE4D mRNA and protein levels in control and hypertrophic ARVM.**

**(A)** Immunoprecipitation (IP) was performed using PDE4D antibody before Western Blotting. Band at ~ 85 kDa represents PDE4D5 or PDE4D7. **(B)** Representative RT-PCR showing no change in PDE4D expression level in hypertrophic myocytes compared to control cells. Control:  $n = 13$ ; hypertrophic ARVM:  $n = 13$ . Error bars represent SEM. Two tailed; paired t-test.

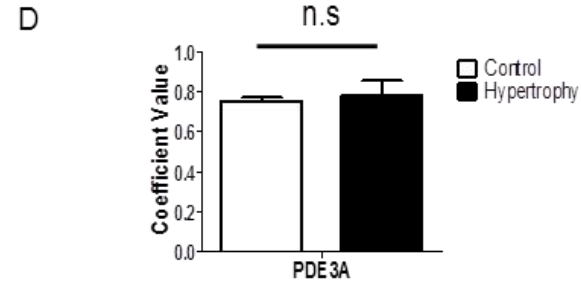
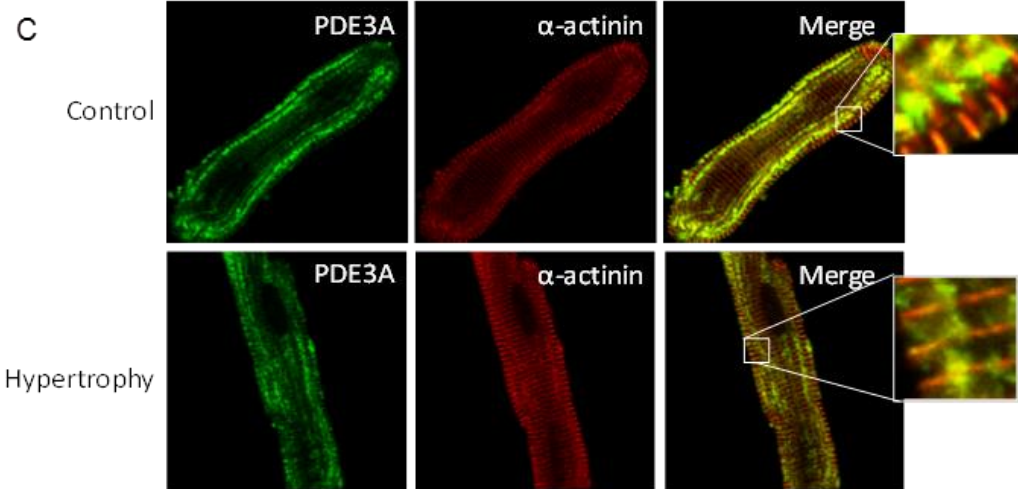
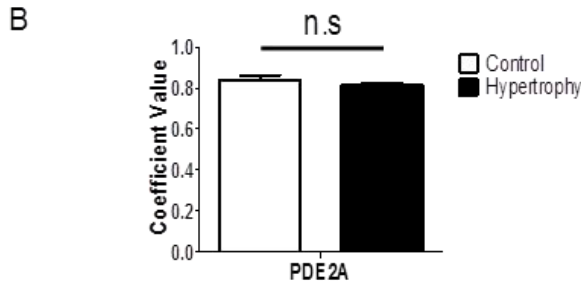
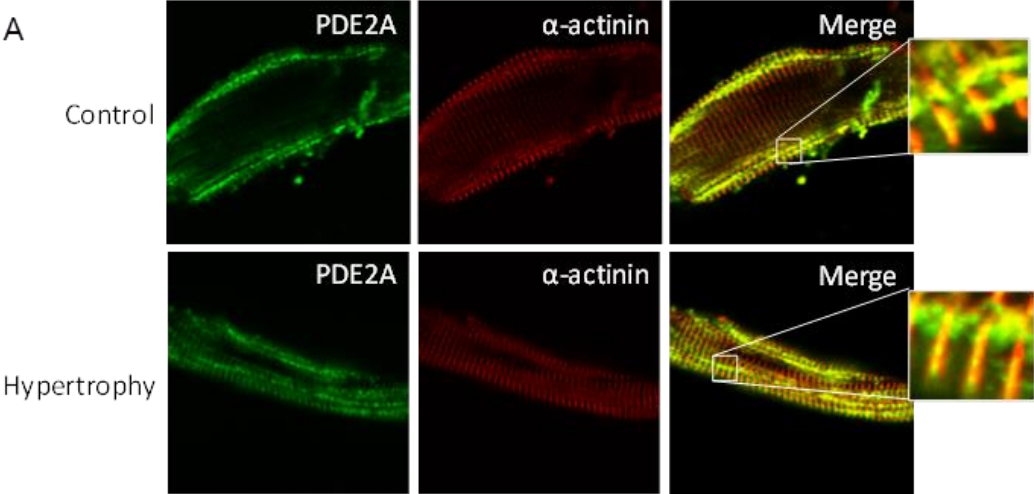
The above results suggest that any alterations in PDE2 and PDE4 activity in hypertrophic myocytes may be due to changes in the activation state of the enzyme rather than protein or mRNA expression levels. The PDE3 FRET results appear to be contradicted by the protein and mRNA levels obtained. This may be explained by a concomitant inhibition of the overexpressed PDE3 in hypertrophic myocytes.

## 5.2.6 Alteration in phosphodiesterase localisation in hypertrophic myocytes

It has been previously published that cardiac phosphodiesterases (PDEs) have distinct subcellular localisations which can be detected by immunostaining and confocal microscopy (Mongillo et al. 2004). Together with this study and the FRET data obtained in this investigation which showed increase PDE2 activity specifically in the PKA-RII compartment and PDE4 shifting from the PKA-RI compartment to the PKA-RII compartment, immunostaining of cardiomyocytes to further explore alterations in PDE localisation was performed.

Control and hypertrophic ARVM were co-stained with anti-PDE (PDE2A, PDE3A, PDE4B or PDE4D) and anti- $\alpha$ -actinin antibodies and cells were imaged using confocal microscopy. The Pearson correlation coefficient (PCC) value was calculated using ImageJ with JACoP plug-in.

Interestingly PDE4B and PDE4D localisation were altered in hypertrophic myocytes where a higher correlation with  $\alpha$ -actinin is detected (expressed as of correlation between PDE isoform and  $\alpha$ -actinin). This data is in line with earlier FRET data in this study (Figure 4-11) suggesting a shift in PDE4 localisation from the PKA-RI to PKA-RII compartment. Immunofluorescence experiments for RI\_epac and RII\_epac with  $\alpha$ -actinin revealed that RII\_epac localises significantly more with  $\alpha$ -actinin in hypertrophic myocytes compared to controls (Figure 5-5). In the heart, PDE4 has been shown to bind to some AKAPs (see 1.7.1). Therefore it is possible to hypothesise that the altered PDE4 localisation may be due to relocalisation of AKAPs which occurs after chronic catecholamine stimulation in ARVM. No change in PDE localisation was detected for either PDE2A or PDE3A.



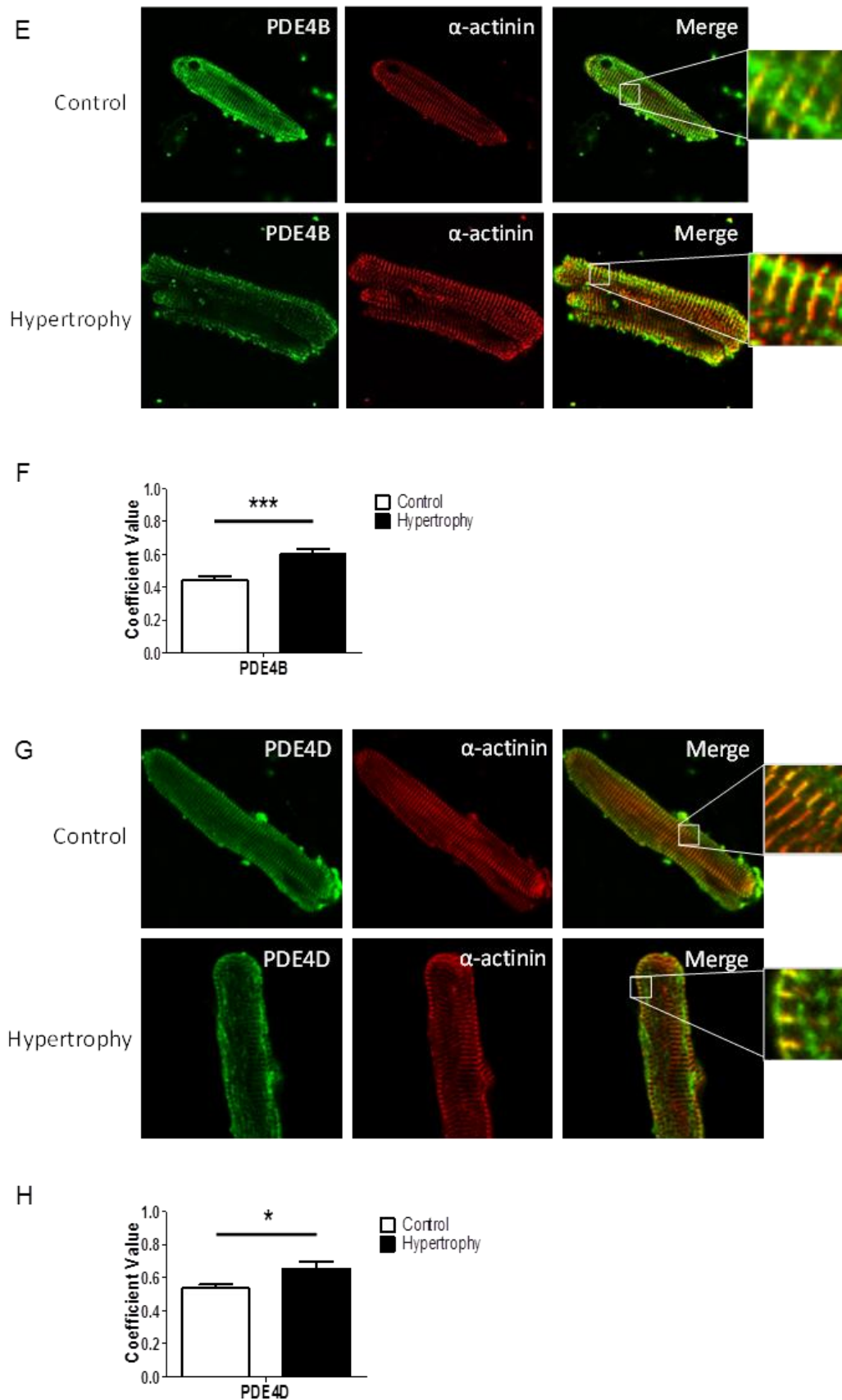


**Figure 5-25. Localisation of PDE families in control and hypertrophic ARVM.** Control and hypertrophic cardiomyocytes stained for PDE of interest (green) and then stained for  $\alpha$ -sarcomeric actinin (red), followed by laser scanning confocal microscopy.

(A) Confocal image of ARVM labelled with anti-PDE2A (green) and anti  $\alpha$ -actinin (red) antibodies. (B) Summary of colocalisation statistics for PDE2A. Control: n = 6; hypertrophy: n = 11. (C) Confocal image of ARVM labelled with anti-PDE3A (green) and anti  $\alpha$ -actinin (red) antibodies. (D) Summary of colocalisation statistics for PDE3A. Control: n = 11; hypertrophy: n = 3. (E) Confocal image of ARVM labelled with anti-PDE4B (green) and anti  $\alpha$ -actinin (red) antibodies. (F) Summary of colocalisation statistics for PDE4B. Control: n = 20; hypertrophy: n = 12. (G) Confocal image of ARVM labelled with anti-PDE4D (green) and anti  $\alpha$ -actinin (red) antibodies. (H) Summary of colocalisation statistics for PDE4D. Control: n = 12; hypertrophy: n = 7. Error bars represent SEM. Two tailed; paired t-test, \* p<0.05, \*\*\* p<0.001.

As earlier FRET data (Figure 4-10) indicated a complete loss of PDE3A activity in the PKA-RI compartment in hypertrophic ARVM, immunostaining was expected to show noticeable alterations in PDE3A localisation. One possible reason that no change in PDE3A localisation was detected is that the cell population tested was low for PDE3A hypertrophic ARVM (n=3) compared to all other groups with large variability between cells. Unfortunately due to time constraints the staining could not be repeated and the population tested could not be increased. Another possible explanation is that PDE3 is inhibited in the PKA-RI compartment of hypertrophic myocytes and therefore a decrease in activity is recorded yet the PDE3 localisation remains unchanged. Further investigation would be required to determine the mechanisms involved. As cGMP can inhibit PDE3 and activate PDE2, it would be interesting to explore whether this mechanism is involved.

## 5.3 Conclusions

In order to assess alterations in cAMP/PKA signalling dynamics and phosphodiesterase regulation in cardiac hypertrophy, an *in vitro* model of hypertrophy was established in adult rat ventricular myocytes (ARVM). Chronic catecholamine stimulation induces cardiac hypertrophy; therefore a model of hypertrophy was set up by treating primary cultured ARVM overnight with norepinephrine (NE). To assess if treatment of ARVM with NE resulted in a hypertrophic phenotype, several markers were considered and

compared between control and NE treated myocytes. These included cell size (both length and longitudinal sectional area), cell index, organisation of sarcomeric units and fetal gene expression. All parameters investigated indicated that overnight treatment of ARVM with NE resulted in the appearance of the expected markers of hypertrophy, indicating that this is an acceptable *in vitro* model of cardiomyocyte hypertrophy.

To study cAMP signalling at different subcellular compartments within the hypertrophic cell, a FRET based imaging approach and cAMP FRET sensors targeted to the PKA-RI and PKA-RII domains were employed. The results showed that after  $\beta$ -AR stimulation with ISO, the level of cAMP produced in both compartments was significantly lower in hypertrophic myocytes compared to control ARVM. Investigation of the contribution of PDE in determining the level of cAMP revealed that there was higher PDE activity in the PKA-RII compartment of hypertrophic ARVM compared to control, whereas the PDE activity in the PKA-RI compartment remained unaltered.

To try to better understand which PDE families are responsible for the increased hydrolytic activity in the PKA-RII compartment of hypertrophic myocytes, selective PDE inhibitors were utilised. The results obtained demonstrate that in hypertrophic myocytes there are variations in all the PDE families studied compared to controls. In control ARVM, PDE2 and PDE4 are mainly associated with the PKA-RI compartment, but some PDE2 activity is also present in the PKA-RII compartment; however in hypertrophic ARVM PDE2 activity was found to be predominantly associated to the PKA-RII compartment and PDE4 activity resulted to be exclusively associated to the PKA-RII compartment, with a complete loss of activity in the PKA-RI compartment. PDE3 activity was found to be coupled only to the PKA-RI compartment in control myocytes, whereas in hypertrophic ARVM, a loss of PDE3 in the PKA-RI locale and no change in the PKA-RII was detected. Immunostaining of PDE localisation in ARVM also showed a change in PDE4B and PDE4D localisation in hypertrophic myocytes supporting the dramatic alterations gathered with the FRET-based imaging technique.

The results of this study show some similarities with data previously published by Abi-Gerges and colleagues, where a decrease in PDE3 activity was found in cardiomyocytes isolated from Wistar rats where hypertrophy had been induced by surgical thoracic aortic banding (TAC) (Abi-Gerges et al. 2009). The same paper also reported a decrease in PDE4

activity, while the results in this thesis show a loss of PDE4 activity selectively in the PKA-RI compartment but an increase in the PKA-RII compartment. Abi-Gerges et al. were also able to show decreasing protein expression of PDE3A, PDE4A and PDE4B which is in contrast to the results obtained here. There are several possible reasons as to why the results in this study differ from the already published data, such as the models of hypertrophy used and the animal models used to investigate hypertrophy. This study explored cAMP dynamics in an *in vitro* model of catecholamine induced hypertrophy in primary cultured adult rat ventricular myocytes, whereas Abi-Gerges et al. used thoracic aortic constriction (TAC) to provoke hypertrophy. Also the techniques used to monitor cAMP signalling could be accountable for the differences reported. Abi-Gerges et al. studied the cAMP signal exclusively in the subsarcolemmal region using whole cell patch clamp and CNG ion channels as a cAMP sensor. This study uses FRET-based imaging and fluorescent Epac sensors targeted to the subcellular compartments where PKA-RI and PKA-RII normally reside. It is plausible that the PDE 3 and PDE 4 activities differ at the cell membrane in hypertrophic ARVM compared with the PKA-RI and PKA-RII compartments as cAMP signalling and PDE localisation is known to be compartmentalised.

One of the key areas of interest for our laboratory is PDE2 control of cAMP signalling in cardiomyocytes. In this study, overall PDE2 activity was shown to increase in hypertrophic myocytes, although PDE2 mRNA and protein expression levels showed no difference from control myocytes. One possible explanation for this result is that PDE2 may undergo activation, resulting in increased activity of this enzyme. Such activation may result from increased cGMP levels and consequent cGMP binding to the GAF domain of PDE2. However, in order to confirm this hypothesis further investigation of cAMP/cGMP interplay in hypertrophic myocytes is required as well as exploring the role of PDEs in the development of cardiac hypertrophy.

# 6 The interplay between cAMP and cGMP and its impact on cardiac hypertrophy.

---

## 6.1 Introduction

The second messenger 3' -5' cyclic guanosine monophosphate (cGMP) is also an important mediator of cardiac function. cGMP reduces cardiac contractility and induces vasorelaxation via protein kinase G (PKG)(Archer et al. 1994). cGMP is synthesised by two isoforms of guanylyl cyclase: the soluble GC (sGC) which is cytosolic and stimulated by nitric oxide (NO) and the particulate GC (pGC), a membrane bound enzyme activated by natriuretic peptides (ANP, BNP and CNP). The two forms of GC have been shown to mediate different functional effects and it has been suggested that, similar to cAMP, cGMP signalling may also be compartmentalised. A study conducted by Gisbert & Fischmeister in 1988 showed that in frog ventricular myocytes, sGC activation causes definite inhibition of the L-type  $\text{Ca}^{2+}$  current ( $I_{\text{CaL}}$ ) induced by isoprenaline, whereas pGC activation has little effect (Gisbert and Fischmeister 1988). Castro et al. demonstrated that in adult rat cardiomyocytes the pGC, but not the sGC activates the cGMP-gated current  $I_{\text{CNG}}$ . The same group also reported that PDE5 controls cGMP generated by the sGC but not by the pGC, whereas PDE2 exclusively controls the cGMP generated by the pGC. (Castro et al. 2006). It should be noted that the technique used in the Castro et al. study relies on the rat olfactory cyclic nucleotide-gated (CNG) channel  $\alpha$ -subunit and the  $\text{Ca}^{2+}$  current  $I_{\text{CNG}}$  as a readout of cGMP levels, which limits the analysis to subsarcolemmal cGMP.

Phosphodiesterases (PDEs), the only cyclic nucleotide degrading enzymes, play a role not only in the spatiotemporal regulation of cGMP signals but also in the cross-regulation of

the cAMP signal by cGMP. In cardiac cells, the potentiation of  $\text{Ca}^{2+}$  currents and the reduction of the responsiveness to  $\beta$ -adrenergic receptor agonists, have been suggested to result from the effects of cGMP on PDE mediated cAMP hydrolysis (Vila-Petroff et al. 1999; Layland et al. 2002). Cardiac myocytes express several PDE isoforms: PDEs 1, 2, 3, 4, 5, 8 and 9. Of these isoforms, there are three families of cGMP-regulated PDEs that hydrolyse cAMP, PDE1, PDE2 and PDE3. These PDE families differ with respect to, affinity and specificity for cAMP and cGMP as well as their subcellular localisation (Martins et al. 1982; Zaccolo and Movsesian 2007). cGMP-mediated inhibition of the cAMP-hydrolyzing activity of PDE1 has been demonstrated only *in vitro*, whereas cGMP regulation of PDE2 and PDE3 has been shown to occur both *in vitro* and *in vivo* (Zaccolo and Movsesian 2007). PDE1 is activated by  $\text{Ca}^{2+}$  and calmodulin, and hydrolyses cAMP and cGMP in a mutually competitive manner. Three PDE1 genes encoding for the proteins PDE1A, PDE1B and PDE1C have been identified to date, all with similar affinity for cGMP ( $K_m=1$  to  $5 \mu\text{mol/L}$ ), but which differ greatly on their affinity for cAMP (Kakkar et al. 1999). PDE1A and PDE1B, show a preference for cGMP, whereas PDE1C hydrolyses the two cyclic nucleotides with equally high affinity (Bender and Beavo 2006). It is still unclear whether PDE1 plays a role in cGMP-mediated cAMP hydrolysis *in vivo*, the major limiting factor for these experiments is a lack of specific PDE1 inhibitors.

cGMP regulation of cAMP hydrolysis occurs by cGMP binding to the GAF-B domain of PDE2, increasing its ability to degrade cAMP by approximately 10 fold (Rosman et al. 1997; Martinez et al. 2002). In the case of PDE3, cGMP acts as a competitive inhibitor of cAMP hydrolysis (Shakur et al. 2001). PDE3 has similar affinities for both cAMP and cGMP, but due to the higher catalytic rate for cAMP, PDE3 is inhibited by cGMP (Degerman et al. 1997). Given the described properties of PDE1, PDE2 and PDE3, modulation of cAMP PDE activity by cGMP can therefore shape intracellular cAMP gradients and the functional effect of cAMP signalling.

More recently the cAMP-cGMP interplay has been explored at a subcellular compartment-specific level within cardiac myocytes. As previously mentioned, Stangherlin et al. performed experiments using FRET based sensors for cAMP and cGMP targeted to the subcellular domains where PKA-RI and PKA-RII normally reside and found that cGMP can strongly modulate cAMP pools in these locations. This study found that in neonatal rat myocytes, PDE2 activity is mainly associated with the PKA-RII subcellular compartment,

whereas PDE3 activity is mainly coupled to the PKA-RI compartment. Stimulation of sGC with S-Nitroso-N-acetyl-D, L-penicillamine (SNAP) increases the cAMP response to ISO selectively in the PKA-RI compartment via inhibition of PDE3, whereas the cAMP response is reduced in PKA-RII compartment via cGMP-mediated activation of PDE2. Stimulation of pGC with atrial natriuretic peptide (ANP) reduced cAMP levels in the PKA-RII compartment via activation of PDE2 but had no effect on the PKA-RI compartment, thus indicating that cGMP signals are also compartmentalised.

These findings are clinically relevant as they may impact on the treatment of pathological conditions such as heart failure. Current treatments of heart failure, depending on the severity and stage of the disease, rely on raising cAMP levels via inotropes and the use of vasodilators and nitrates to increase cGMP levels. Inotropic therapy, via treatment with PDE3 inhibitors, has been shown to significantly improve hemodynamic measurements in patients with heart failure with short term use (Cuffe et al. 2002), yet it is well established that this type of treatment has negative long-term effects on the patient's outcome. For example the Prospective Randomized Milrinone Survival Evaluation (PROMISE) study, which randomised patients with class III/IV heart failure to PDE3 inhibitor milrinone versus placebo, found a 28% increase in risk of death in the treated group and during the Vesnarinone Trial (VEST) found an 11% increase in mortality of treated patients (Packer et al. 1991; Feldman et al. 1993). It has been hypothesised that these negative effects may be due to the fact that cAMP signalling is compartmentalised. GPCRs, ACs, PDEs and cAMP effectors are spatially organised in macromolecular complexes within the cardiomyocyte, to allow selective phosphorylation of targets in response to specific stimuli. The functional outcome of cAMP signalling depends on the location of the subcellular compartment within which cAMP is generated. A global increase of cAMP is not the best approach to treating heart failure as this may result in off target effects.

As cGMP is known to regulate cAMP by modulation of PDE2 and PDE3 in discrete compartments in cardiomyocytes (Stangherlin et al. 2011), this too could have an effect on the use of cAMP PDE inhibitors as a therapeutic treatment in heart disease. Altered levels of cGMP can affect PDE activity and in the case of PDE3 may inhibit the enzymatic hydrolysis of cAMP. It is therefore crucial to have a better understanding of cyclic nucleotide signalling interplay at a subcellular level as this may lead to the development of novel therapeutics for heart disease. In addition to this, numerous studies have indicated

that cGMP and PKG are anti-hypertrophic (1.10.1.1) and thus it is of interest to investigate cGMP signalling in the NE-induced *in vitro* model of cardiac hypertrophy.

## Aims

- Investigate whether unique cAMP/cGMP crosstalk at specific subcellular compartments occurs in adult rat ventricular cardiac myocytes
- Determine how changes in cGMP affect cAMP levels at subcellular sites
- Explore if cGMP and cAMP interplay is altered in an *in vitro* model of cardiac hypertrophy.

## 6.2 Results

### 6.2.1 cGMP-mediated modulation of cAMP levels in the PKA-RI and PKA-RII subcellular compartments.

The question of whether the generation of cGMP could affect the isoproterenol (ISO)-induced cAMP response at a subcellular level in ARVM was first investigated. Previous studies in the laboratory had shown that PKA-RI and PKA-RII isoforms, due to their ability to preferentially anchor to different AKAPs, define distinct subcellular compartments in which cAMP is uniquely regulated. To study cAMP signalling in these two distinct subcellular compartments two FRET reporters for cAMP were designed (RI\_epac and RII\_epac) that are targeted to the intracellular sites where endogenous PKA-RI and PKA-RII normally reside (see 4.2.1).

Cardiomyocytes were transduced with adenovirus carrying either RI\_epac (the cAMP reporter targeted to the PKA-RI compartment) or RII\_epac (targeted to the PKA-RII compartment) and then stimulated with 100 nM ISO. The cAMP response detected at those sites was compared with the response detected in ARVM which had been pre-treated for 10 minutes with either the NO donor S-Nitroso-N-Acetyl-D, L-Penicillamine (SNAP) or

atrial natriuretic peptide (ANP). SNAP, via generation of NO, stimulates the production of cGMP by the cytosolic soluble GC (sGC) whereas ANP activates the particulate GC (pGC) with consequent generation of cGMP by this enzyme localised at the sarcolemma.

The cAMP response to ISO alone was found to be higher in the PKA-RII compartment as compared to the PKA-RI compartment (Figure 6-1) confirming previous results (Di Benedetto et al. 2008). Pre-treatment of cells with the NO donor SNAP (100  $\mu$ M) dramatically affected this response, inducing a significant reduction of the FRET change in the PKA-RII compartment and shows a trend of a higher FRET change in the PKA-RI compartment (Figure 6-1).

In the following set of experiment the effect of ANP treatment was investigated. The cAMP FRET response in control cells treated with ISO alone was again higher in the PKA-RII compartment compared to the PKA-RI compartment (Figure 6-1B), however pre-treatment of the myocytes with ANP exclusively affected the response in the PKA-RI compartment. The FRET change in PKA-RI was greater compared to its control (Figure 6-1B).

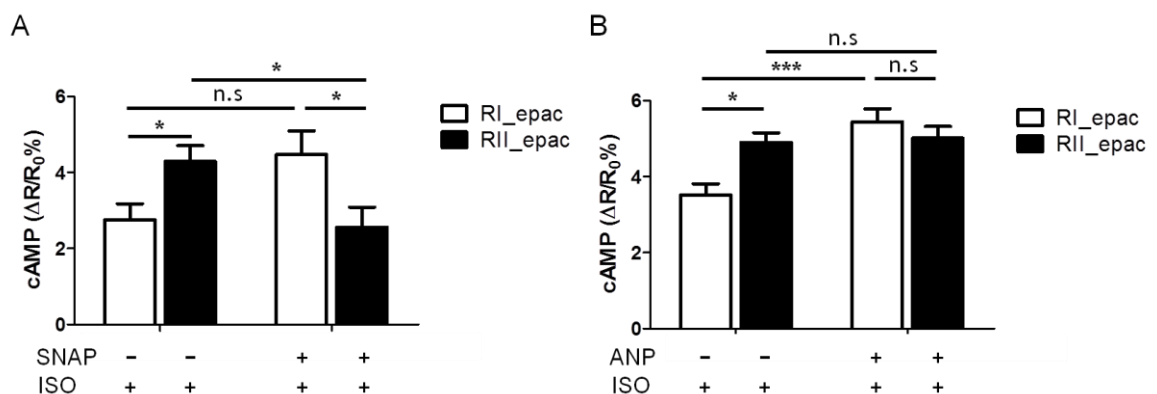


**Figure 6-1. Summary of the effect of cGMP on the cAMP response to isoproterenol in PKA-RI and PKA-RII subcellular compartments.**

Myocytes were preincubated for 10 minutes with (A) SNAP or (B) ANP before stimulating with 100 nM Isoproterenol. (A) RI\_epac:  $\Delta R/R_0 = 2.756 \pm 0.422$  %, n = 7; RII\_epac:  $\Delta R/R_0 = 4.294 \pm 0.418$  %, n = 8; RI\_epac + SNAP:  $\Delta R/R_0 = 4.476 \pm 0.624$  %, n = 7; RII\_epac + SNAP:  $\Delta R/R_0 = 2.561 \pm 0.524$  %, n = 8. (B) RI\_epac:  $\Delta R/R_0 = 3.521 \pm 0.29$  %, n = 15; RII\_epac:  $\Delta R/R_0 = 4.9 \pm 0.25$  %, n = 21; RI\_epac + ANP:  $\Delta R/R_0 = 5.45 \pm 0.341$  %, n = 25; RII\_epac + ANP:  $\Delta R/R_0 = 5.02 \pm 0.30$  %, n = 33. Statistical significance calculated by two way ANOVA with Bonferroni's post test, \*p<0.05, \*\*\* p<0.001.

Together these data indicate that cGMP can affect the response to ISO in a compartment specific manner. Previously it has been shown that SNAP produces a uniform increase in cGMP throughout the cell so that differences observed are unlikely to be ascribed to an uneven generation of cGMP but are instead due the specific localisation of PDEs that are differently modulated by cGMP (Stangherlin et al. 2011). The experiments performed in the presence of SNAP, suggest that PDE3 (which is inhibited by cGMP) is found mainly in the PKA-RI compartment, as increased levels of cGMP lead to the inhibition of PDE3 and therefore an increased concentration of cAMP in the response to ISO. PDE2 (which is activated by cGMP) was found to be mainly associated to the PKA-RII compartment as indicated by the decreased level of cAMP recorded in this compartment (Stangherlin et al. 2011).

The data obtained in ARVM pre-treated with ANP would again suggest that PDE3 is mainly associated with the PKA-RI compartment in the ARVM. However, in the PKA-RII compartment there is no effect suggesting that PDE2 is not activated as seen in the experiments using SNAP. One possible explanation is that cGMP generated by ANP via the pGC does not reach and effectively activate PDE2 (due to a different compartmentalisation of the sGC and pGC and limited diffusion of cGMP). An alternative explanation is that the amount of cGMP generated by pGC is sufficient to inhibit PDE3 ( $K_m$  of cGMP for PDE3 =20 nmol/L) but not sufficient to activate PDE2 ( $K_m$  for cGMP binding to GAF domain of PDE2 =10  $\mu$ mol/L).

To confirm the hypothesis that the effect of SNAP and ANP on the cAMP response to ISO relies on PDE2 and PDE3, additional experiments in which ARVM are stimulated with ISO in the presence of increased cGMP levels plus pharmacological inhibitors of PDE2 and PDE3 were completed.

### **6.2.1.1 The effect of cGMP on the local ISO-induced cAMP response in the presence of selective inhibitors.**

Firstly it was important to assess whether, after cGMP raising agents or the addition of PDE 2 and 3 inhibitors, there was a difference in the cAMP levels in the two compartments that is independent of ISO stimulation, as this may alter the interpretation of the experiments performed in the presence of ISO. Previous work conducted in neonatal

myocytes found that ANP treatment generated a larger pool of cGMP in the PKA-RII compartment and that amount of cGMP produced in the PKA-RI compartment was unable to inhibit PDE3 activity (Stangherlin et al. 2011), therefore SNAP was chosen as the cGMP raising agent. Myocytes infected with RI\_epac or RII\_epac FRET based sensors were either untreated, preincubated with SNAP alone or with the selective inhibitors for 10 minutes before imaging. Basal levels of cAMP were obtained by capturing a number of FRET images of ARVM expressing the cAMP reporter and calculated as previously described (4.2.2). These results confirmed that the basal level of cAMP in the PKA-RI and PKA-RII compartments is not altered upon addition of cGMP raising agents and PDE inhibitors specific for families 2 and 3 as shown in Figure 6-2A.

In control experiments, as previously shown (Figure 4-6), cardiomyocytes treated with ISO (100 nM) alone showed a trend of a higher cAMP response in the PKA-RII compartment than the PKA-RI compartment and ARVM pre-incubated with SNAP (100  $\mu$ M) then stimulated with ISO resulted in a trend of a higher cAMP response in the PKA-RI compartment than the PKA-RII compartment although these results were not always significant due to the increasing number of multiple comparisons made (Figure 6-2B +C). These experiments seemed to confirm previous results (6.2.1) where SNAP treatment created an inversion of the cAMP gradients typically observed in PKA-RI and PKA-RII compartments in response to catecholamine stimulation.

In cardiomyocytes pre-treated with SNAP and the PDE2 inhibitor Bay 60-7550 (50 nM), ISO stimulation generated a comparable FRET change in the PKA-RI and PKA-RII compartments. On comparison with SNAP treatment alone, SNAP treatment in the presence of PDE2 inhibitor results in a significantly greater cAMP response to ISO in the PKA-RII compartment only, whereas there is no further increase in the PKA-RI compartment.

In ARVM pre-treated with SNAP and the PDE3 inhibitor cilostamide (cilo) (10  $\mu$ M), ISO stimulation resulted in a comparable cAMP level generated in both compartments which was not significantly different from ARVM treated with SNAP alone (Figure 6-2C).

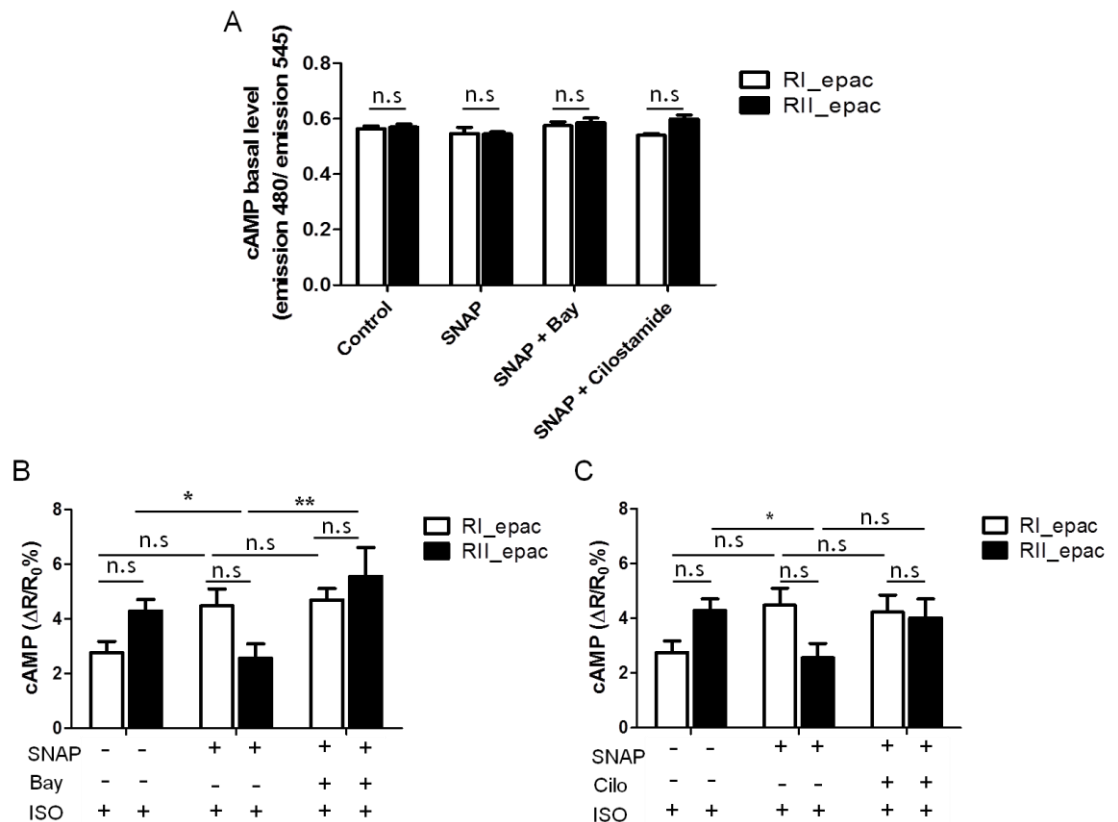


**Figure 6-2. Summary of the effect of cGMP on the cAMP response to ISO in PKA-RI and PKA-RII subcellular compartments after selective PDE inhibition.**

**(A)** Summary of basal cAMP levels in ARVM treated with SNAP and selective PDE inhibitors. RI\_epac control: n = 13; RII\_epac control: n = 12; RI\_epac + SNAP: n = 9; RII\_epac + SNAP: n = 9; RI\_epac + SNAP + Bay 60-7550 n = 5; RII\_epac + SNAP + Bay 60-7550: n = 6; RI\_epac + SNAP + Cilo: n = 6; RII\_epac + SNAP + Cilo: n = 7. **(B)** Myocytes were preincubated for 10 minutes with SNAP (100  $\mu$ M) and PDE2 selective inhibitor Bay 60-7550 (50 nM) before stimulating with 100 nM Isoproterenol. **(C)** Myocytes were preincubated for 10 minutes with SNAP (100  $\mu$ M) and PDE3 selective inhibitor Cilo (10 mM) then 100 nM Isoproterenol. Statistical significance calculated by two way ANOVA with Bonferroni's post test, \*p<0.05, \*\*p<0.01.

In line with previous findings (Figure 5-15), these results indicated that PDE2 activity is mainly associated with the PKA-RII compartment when there is higher than basal cGMP levels, as inhibition of PDE2 with Bay 60-7550 resulted in an increase in cAMP generated in response to ISO stimulation specifically in this compartment. Pre-treated with SNAP

and PDE3 inhibitor Cilostazol had no effect on the ISO response in either compartment of ARVM, as expected if PDE3 is selectively coupled to the PKA-RI compartment and is already inhibited by cGMP induced by SNAP treatment.

### **6.2.2 cGMP-mediated local modulation of cAMP levels in the PKA-RI and PKA-RII compartments in hypertrophic myocytes.**

In the following set of experiments, the observed cGMP-mediated modulation of cAMP signalling at subcellular locations was investigated in hypertrophic myocytes to establish whether this signalling pathway is altered during cardiac hypertrophy. Isolated ARVM were treated overnight in medium containing 1  $\mu$ M NE to induce an *in vitro* model of cardiomyocyte hypertrophy. Experiments were then conducted in the same way as above, by pre-treating the cells with 100  $\mu$ M SNAP for 10 minutes before imaging.

The results showed that the cAMP response to ISO in untreated hypertrophic myocytes was similar in both the PKA-RI compartment and the PKA-RII compartment (Figure 6-3A).

Pre-treatment of the cells with SNAP (100  $\mu$ M) had a no effect on either compartment (Figure 6-3A).

On comparison of SNAP pre-treated control cells with SNAP treated hypertrophic cells; the cAMP generated was significantly less in the PKA-RI compartment only in hypertrophic cells while the PKA-RII compartment remained unchanged (Figure 6-3B).

These data sets are consistent with the information shown in the previous chapter where PDE2 activity is present in both the PKA-RI and PKA-RII compartments of hypertrophic myocytes (Figure 5-15), but importantly that there is a significant loss of PDE3 activity in the PKA-RI compartment in hypertrophic myocytes (Figure 5-17). In hypertrophic cells, SNAP treatment does not reduce cAMP in the PKA-RII compartment as one would expect given the activation of PDE2. This may be due to the fact that in hypertrophic cells PDE2 is already activated.

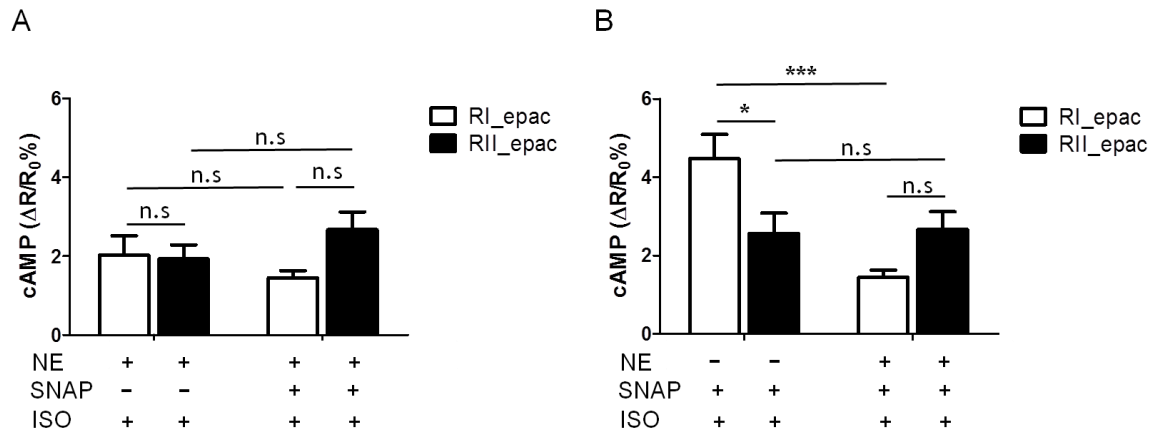


**Figure 6-3. Summary of the effect of cGMP on the cAMP response to ISO in PKA-RI and PKA-RII subcellular compartments in hypertrophic ARVM.**

**(A)** Myocytes were preincubated for 10 minutes with SNAP or before stimulating with 100 nM Isoproterenol. RI\_epac hypertrophic:  $\Delta R/R_0 = 2.026 \pm 0.491$  %,  $n = 8$ ; RII\_epac hypertrophic:  $\Delta R/R_0 = 1.926 \pm 0.364$  %,  $n = 6$ ; RI\_epac hypertrophic + SNAP:  $\Delta R/R_0 = 1.447 \pm 0.184$  %,  $n = 8$ ; RII\_epac hypertrophic + SNAP:  $\Delta R/R_0 = 2.675 \pm 0.449$  %,  $n = 11$ . **(B)** Summary of experiments comparing control and hypertrophic ARVMs after SNAP pre-treatment. RI\_epac + SNAP:  $n = 7$ ; RII\_epac + SNAP:  $n = 8$ . Statistical significance calculated by two way ANOVA with Bonferroni's post test, \* $p < 0.05$ , \*\*\*  $p < 0.001$ .

### 6.2.3 Investigation of cGMP levels at the PKA-type I and PKA-type II locations using targeted cGMP FRET based sensors.

One possible explanation for the observed differences in cAMP signalling and PDE contribution in hypertrophic myocytes in the PKA-RI and PKA-RII subcellular compartments in ARVM is that these may rely on variations in the pools of cGMP. To investigate if this is the mechanism involved, cGMP changes were monitored selectively in the two compartments defined by PKA-RI and PKA-RII using modified versions of the cGMP sensor Cygnet-2.1. This had been previously adapted in our laboratory in the same way as the targeted cAMP sensors, by fusing the dimerisation/docking domain from either RI $\alpha$  (amino acids 1 to 64) or RII $\beta$  (amino acids 1 to 49) to the N-terminus of Cygnet-2.1 (Figure 6-4). In order to achieve expression of these reporters in adult myocytes, these probes had to be cloned into adenoviral vectors. Due to time constraints this stage was

completed by Vector Biolabs. Briefly, Cygnet-2.1 was *XhoI/EcoRI* cut out from pcDNA3.1 and the dimerisation docking domain for RI $\alpha$  and RII $\beta$  were *NheI* cut from another pcDNA3.1 vector “filled in” using Klenow fragment and subcloned *EcoRI* into the multiple cloning site region of pDual-CCM vector. Positive vectors were checked using *PacI/BglIII* digestion. The adenoviral vector was then packaged as previously described (3.3.11).

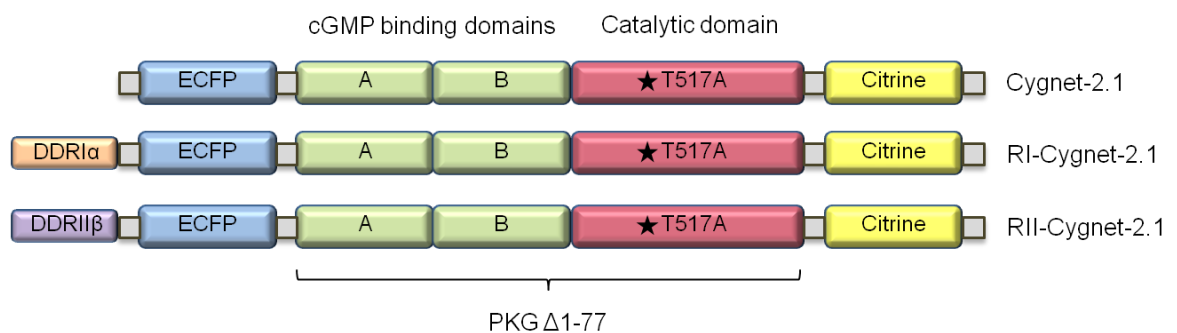


**Figure 6-4. Schematic representation of the FRET-based cGMP sensors used in this study.**

To explore whether changes in PDE activity between control and hypertrophic myocytes are due to different levels of cGMP in the PKA-RI and PKA-RII compartments, the basal level of cGMP was compared at the two locations. For these experiments ARVMs were infected with either RI-Cygnet-2.1 or RII-Cygnet-2.1 and a number of images were taken for each sensor to calculate the basal ratio. Interestingly the basal level of cGMP was found to be higher in the PKA-RI compartment compared to the PKA-RII compartment in cardiac myocytes (Figure 6-5A). As a control to exclude that fusion of the targeting domains to the Cygnet sensor may affect the efficiency of energy transfer and therefore may account for the difference in FRET value detected with the two reporters, the adenovirus containing the two targeted cGMP sensors was used to infect Chinese hamster ovarian (CHO) cells. In this cell type, there was no difference recorded between the two compartments as expected (Figure 6-5B). These data show that in ARVMs the level of cGMP is higher in the PKA-RI compartment under normal conditions.

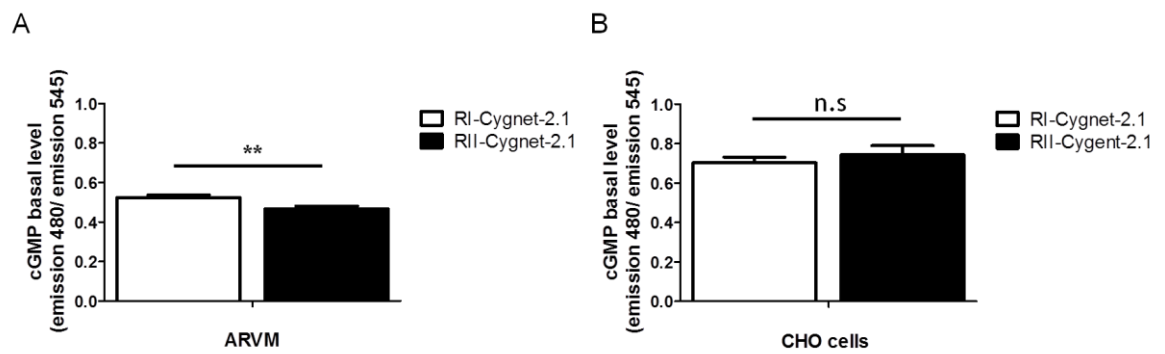


**Figure 6-5. Summary of the basal ICFP/ IYFP ratio values detected with the targeted cGMP sensors RI-Cygnmet-2.1 and RII-Cygnmet-2.1.**

**(A) Summary of basal cGMP levels in ARVM. RI-Cygnmet-2.1: n = 54; RII-Cygnmet-2.1: n = 66.**

**(B) Summary of cGMP levels in CHO cells. RI-Cygnmet-2.1: n = 35; RII-Cygnmet-2.1: n = 26.**

**Error bars represent SEM. Two tailed; paired t-test, \*\*p<0.01.**

In order to investigate whether an increased intracellular cGMP level may be responsible for the increased PDE2 activation detected from the FRET data in hypertrophic myocytes, the global cytosolic cGMP basal levels were calculated and compared to control ARVMs. As illustrated in Figure 6-6A, the basal level of cGMP was significantly higher in the NE treated hypertrophic myocytes compared to control cells. This data suggests that, in hypertrophic myocytes, the increased PDE2 activity is due to higher levels of intracellular cGMP selectively in the PKA-RII compartment. Thus it appears that in hypertrophic myocytes, the basal cGMP levels are increased leading to activation of PDE2 and increased cAMP hydrolysis. As PDE2 is already activated the addition of SNAP would be expected to have little effect on PDE2 activity and cAMP concentration, as observed (Figure 6-3).

To further test this hypothesis, the cGMP levels at the PKA-RI and PKA-RII subcellular locations in hypertrophic myocytes were explored, to observe if there was an alteration which would explain the differences seen in PDE2 and PDE3 activities in this model of disease. In control myocytes (Figure 6-6B), there was a higher basal level of cGMP in the PKA-RI compartment compared to the PKA-RII compartment.

However, in hypertrophic myocytes, there was an increased basal level of cGMP in both compartments compared with control cells, but a greater fold change was detected in the

PKA-RII compartment. The difference in cGMP concentrations between the two compartments in this cell type was abolished.

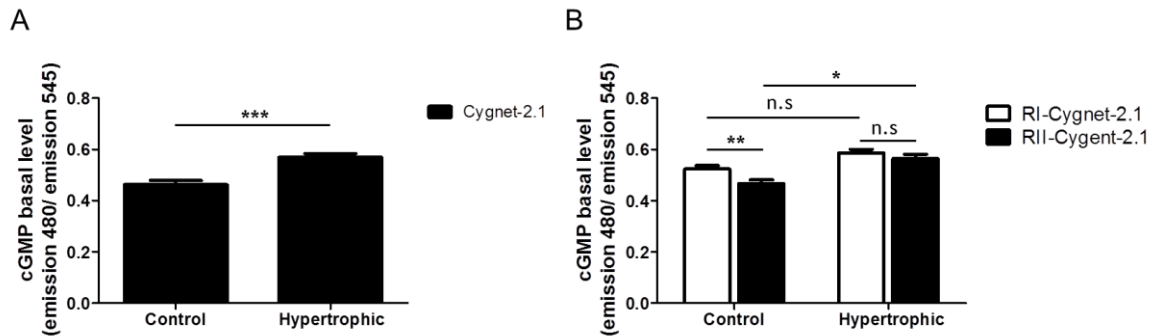


**Figure 6-6. Comparison of cGMP intracellular levels between control and hypertrophic ARVMs.**

**(A) Summary of all the experiments performed in controls and hypertrophic myocytes transduced with Cygnet-2.1. Cygnet-2.1 control: n = 55; Cygnet-2.1 hypertrophic: n = 45. Error bars represent SEM. Two tailed; paired t-test, \*\*\* p<0.001. (B) Summary of all the experiments performed in controls and hypertrophic myocytes transduced with the targeted cGMP sensors. RI-Cygnet-2.1 control: n =54; RI-Cygnet-2.1 control: n = 66; RI-Cygnet-2.1 hypertrophic: n =51; RII-Cygnet-2.1 hypertrophic: n = 53. Statistical significance calculated by two way ANOVA with Bonferroni's post test, \*p<0.05, \*\*p<0.001.**

The higher basal level of cGMP in both compartments of hypertrophic ARVM would mean that in hypertrophic myocytes PDE3 is inhibited more than in control cells while PDE2 activity increases. Although cGMP levels are higher in both PKA-RI and PKA-RII compartments of the hypertrophic ARVM, the greatest increase is in the PKA-RII compartment, and this could explain why the FRET reporters detected a higher PDE2 activation in this compartment (Figure 5-15), but no altered PDE2 protein and mRNA expression was found (Figure 5-21). On the other hand, the increased cGMP level in the PKA-RI compartment of hypertrophic myocytes could explain the observation that PDE3 activity is unchanged in face of an increased level of PDE3 expression (see Figure 5-17 and Figure 5-22).

## 6.2.4 $\beta_3$ -adrenergic receptor signalling in the PKA-R1 and PKA-RII compartments of hypertrophic cardiomyocytes

In the heart, under normal conditions,  $\beta$ -adrenergic stimulation results in increased force and frequency of myocardial contraction and the rate of relaxation. Three types of  $\beta$ -adrenergic receptors ( $\beta$ -ARs) are expressed in cardiac myocytes,  $\beta_1$ ,  $\beta_2$  and  $\beta_3$ -ARs, although the effect of catecholamines in the human heart is generally attributed to  $\beta_1$  and  $\beta_2$ -ARs. These receptors are coupled to Gs proteins and lead to the activation of the cAMP/PKA pathway.

Gauthier and colleagues were the first to demonstrate that  $\beta_3$ -ARs are expressed in the human heart. Stimulation of  $\beta_3$ -ARs with agonist, BRL-37344 (BRL), caused dose-dependent negative inotropic effects. This  $\beta_3$ -AR-mediated negative inotropic effect is not linked to Gs proteins but is coupled to Gi (Gauthier et al. 1996). These inhibitory effects have been more recently found to involve the production of nitric oxide (NO) via activation of endothelial type-3 NO synthase (eNOS), which, in turn, stimulates sGC to produce cGMP (Vaziri and Wang 1999).

Mongillo and colleagues previously reported that NE stimulation of neonatal rat myocytes leads not only to the activation of  $\beta_1$  and  $\beta_2$  adrenoceptors but also to the activation of  $\beta_3$ -adrenergic receptors which are functionally coupled to an endothelial nitric oxide synthase (eNOS). In this study the authors showed that  $\beta_3$ -ARs are involved in NE-induced NO generation, leading to sGC activation, synthesis of cGMP, and activation of PDE2 (Mongillo et al. 2006).

In the failing heart, it is well established that downregulation of  $\beta_1$  and desensitisation of  $\beta_2$ -ARs occurs, however the amount of  $\beta_3$ -AR protein has been shown to increase up to 3 fold in different models of heart failure (Cheng et al. 2001; Moniotte et al. 2001).  $\beta_3$ -ARs are activated at higher catecholamine concentrations than  $\beta_1$ - and  $\beta_2$ -ARs and are relatively resistant to desensitisation (Lafontan 1994). In one study, catecholamine stimulation of a neonatal culture of myocytes from mice with both  $\beta_1$ -AR and  $\beta_2$ -AR knocked out (ADRB1-/-/ADRB2-/-) was found to decrease the frequency of contraction. The  $\beta_3$ -AR agonist CL316243 was able to replicate this effect (Devic et al. 2001). On the other hand,

some investigations have found that  $\beta_3$ -AR produce cardioprotective effects in pressure overload hypertrophy and heart failure via NOS (Niu et al. 2012).

On the basis of the above evidence, it was decided to then investigate the impact of  $\beta_3$  receptor on cAMP levels in the PKA type I and PKA type II subcellular compartments in the ARVM, in order to assess whether the coupling of this receptor to the compartments is altered in hypertrophy. This information may help to explain the altered cGMP concentration in hypertrophic myocytes since  $\beta_3$ -AR stimulation can raise cGMP levels via activated NOS.

In order to explore  $\beta_3$  receptor function, isolated ARVM were transduced overnight with adenovirus containing the targeted cGMP FRET based sensors (RI-Cygnnet-2.1 or RII-Cygnnet-2.1) to record cGMP changes in the PKA-RI and PKA-RII subcellular compartments. Ten minutes prior to imaging, cells were treated with 100 nM  $\beta_3$ -AR antagonist (SR59230A) and basal cGMP levels were measured. In control myocytes, as shown in Figure 6-5, there was a greater concentration of cGMP in the PKA-RI compartment compared to the PKA-RII compartment under normal conditions. In myocytes pre-treated with 100 nM  $\beta_3$ -AR inhibitor (SR59230A), Figure 6-7A, there was a decrease in the basal cGMP in the PKA-RI compartment only, abolishing the difference between the two locales. These data suggest that  $\beta_3$ -ARs are mainly coupled to the PKA-RI compartment in ARVMs as inhibition of  $\beta_3$ -ARs caused a decrease in cGMP levels specifically in this compartment. This data also shows that in the PKA-RI compartment there is constitutive activation of  $\beta_3$ -ARs. This is surprising as the literature indicates that this type of receptor is activated by high levels of catecholamines (Lafontan 1994). Nothing else could be found in the literature to support  $\beta_3$ -AR activation in unstimulated cardiomyocytes without high circulating levels of catecholamines and so further investigation would be necessary to identify the mechanism involved here.

To investigate the  $\beta$ -AR activity in hypertrophic myocytes, the above experiment was conducted in ARVM which had been stimulated overnight with 1  $\mu$ M NE to induce an *in vitro* model of the disease. In hypertrophic myocytes, Figure 6-7B, there was no difference in cGMP basal levels between the two compartments. With the addition of the  $\beta_3$ -AR inhibitor, there was a trend for a decrease in cGMP in the PKA-RII compartment, although this was not significantly different from the untreated myocytes, this resulted in a lower level of cGMP in the PKA-RII compartment compared to the PKA-RI compartment. These

results indicate that in hypertrophic myocytes the  $\beta_3$ -ARs are mainly located in the PKA-RII compartment, as inhibition of  $\beta_3$ -ARs resulted in a smaller cGMP response in this compartment.

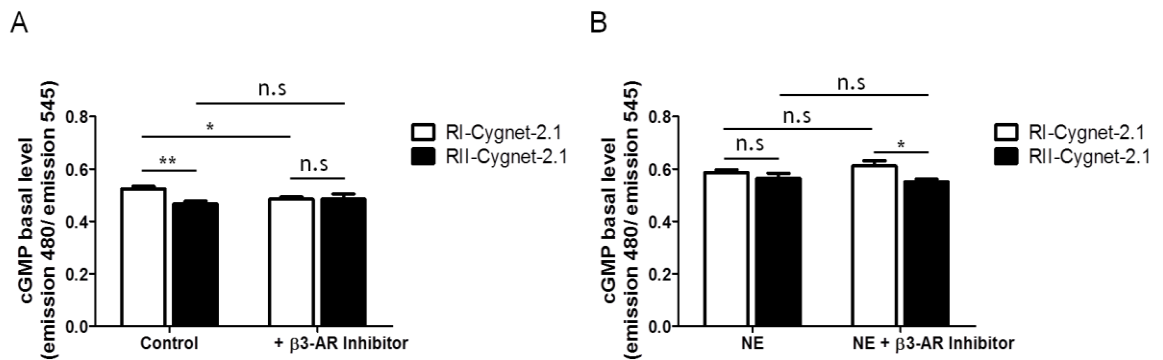


**Figure 6-7. Summary of the investigation of  $\beta_3$ -AR signalling in PKA-RI and PKA-RII compartments in control and hypertrophic ARVM.**

**(A) Summary of FRET experiments in control myocytes transduced with cGMP FRET based sensors RI-Cygnnet-2.1 and RII-Cygnnet-2.1 then treated with 100 nM  $\beta_3$ -AR inhibitor (SR59230A) 10 minutes prior to imaging. RI-Cygnnet-2.1 control: n =54; RII-Cygnnet-2.1 control: n = 66; RI-Cygnnet-2.1 +  $\beta_3$ -AR inhibitor: n =56; RII-Cygnnet-2.1 +  $\beta_3$ -AR inhibitor: n = 55. (B) Summary of FRET experiments in myocytes treated overnight with 1  $\mu$ M NE and transduced with the targeted cGMP sensors. Cells were preincubated for 10 minutes with 100 nM  $\beta_3$ -AR inhibitor (SR59230A). RI-Cygnnet-2.1 hypertrophic: n =51; RII-Cygnnet-2.1 hypertrophic: n = 53; RI-Cygnnet-2.1 hypertrophic+  $\beta_3$ -AR inhibitor: n =59; RII-Cygnnet-2.1 hypertrophic +  $\beta_3$ -AR inhibitor: n = 33. Statistical significance calculated by two way ANOVA with Bonferroni's post test, \* $p$ <0.05, \*\* $p$ <0.001.**

Comparison of control vs. NE-induced hypertrophic myocytes transduced with the targeted cGMP FRET based-biosensors RI-Cygnnet-2.1 and RII-Cygnnet-2.1 in ARVM treated with 100 nM  $\beta_3$ -AR inhibitor (SR59230A) reveals that there is a significantly greater basal level of cGMP in NE treated myocytes.  $\beta_3$ -ARs are inhibited in both conditions, yet there is still a significant increase in both compartments of hypertrophic myocytes, which indicates that cGMP is generated by another route in addition to soluble GC (sGC) activation by  $\beta_3$ -ARs. Perhaps in hypertrophic myocytes there is a higher activation of particulate GC (pGC)

which produces cGMP. This is plausible as there is an increase in ANP expression (fetal gene switch on) in hypertrophic myocytes, which may result in activation of pGC (see 6.1).

## 6.3 Conclusion

cGMP is a ubiquitous second messenger that, along with cAMP, modulates cardiac function. cGMP is generated by both the soluble and the particulate guanylyl cyclases (GCs) in response to nitric oxide and natriuretic peptides, respectively, and activation of the pGC or the sGC produce distinctive downstream effects suggesting that cGMP signalling is also compartmentalised.

It has previously been published that cGMP can alter PDE2 and PDE3 activity and therefore can potentially affect cAMP concentrations. In order to assess if an interplay between cGMP and cAMP signalling occurs in adult rat cardiomyocytes in the PKA-RI and PKA-RII compartments, cells were first treated with GC activators to raise cGMP levels, then the cAMP response to  $\beta$ -AR stimulation was measured and compared to cells with basal levels of cGMP. Myocytes stimulated with 100 nM ISO generated a cAMP response that was significantly higher in the PKA-RII compartment than in the PKA-RI compartment. To measure the effect of cGMP on the cAMP response to ISO in these two compartments, myocytes were pre-treated with the NO donor SNAP, which activates the soluble guanylyl cyclase (sGC) leading to increased intracellular cGMP concentrations. ISO stimulation in these cells resulted in a higher cAMP response in the PKA-RI compartment and a smaller cAMP response in the PKA-RII compartment compared to control cells. Therefore it was hypothesised that PDE2 is mainly associated with the PKA-RII compartment, while PDE3 is mainly coupled to the PKA-RI compartment in ARVM, and upon SNAP treatment the cGMP generated can regulate cAMP signalling in these domains in opposite ways, being PDE2 activated and PDE3 inhibited by cGMP. This was confirmed by pre-treating ARVM with SNAP and a specific PDE inhibitor for PDE2 or PDE3 before ISO stimulation. These findings are in agreement with previously published data in neonatal myocytes (Stangherlin et al. 2011).

When cardiomyocytes expressing either RI\_epac or RII\_epac were treated with ANP to activate the particulate guanylyl cyclase (pGC), addition of ISO did not result in an inversion of the cAMP gradient as was observed in SNAP treated cells. ANP generated a

pool of cGMP which caused an increase in cAMP concentration specifically in the PKA-RI compartment while there was no effect on the PKA-RII compartment. This data again suggests that PDE3 is linked to the PKA-RI compartment in adult cardiomyocytes. Together these findings show that cGMP modulates the cAMP response to ISO in a compartment specific manner in adult myocytes. The functional impact that cGMP has depends upon its source, either pGC or sGC, which have been shown to localise in different compartments throughout the myocyte (Stangherlin et al. 2011). ANP mediated activation of pGC generated a pool of cGMP specifically in the PKA-RI compartment whereas sGC was able to generate cGMP in both the PKA-RI and PKA-RII compartments. cGMP generated by sGC decreases cAMP levels via PDE2 activation and increases cAMP levels via PDE3 inhibition, whereas cGMP generated by pGC selectively increases cAMP levels via inhibition of PDE3.

This data differs from what has been reported in rat neonatal myocytes, where ANP-mediated activation of pGC, generated a pool of cGMP selectively in the PKA-RII compartment which resulted in a reduced cAMP response to ISO via the activation of PDE2 (Stangherlin et al. 2011). It is possible that this is a developmental difference between neonatal and adult cardiomyocytes. It has also previously been reported that cGMP modulation of cAMP signalling is dependent on the intracellular concentrations of cGMP. At low concentrations (< 50 nM) cGMP exclusively inhibits PDE3 activity, whereas at high concentrations (200 – 500 nM), cGMP activates PDE2 (Zaccolo and Movsesian 2007). Therefore it is reasonable to assume that in this case the concentration of cGMP produced by ANP was not high enough to activate PDE2 or that ANP generated a pool of cGMP specifically in the PKA-RI region. PDE3 activity in this compartment could therefore be inhibited at the lower concentrations of cGMP which was produced by pGC. These data further support the hypothesis of a compartmentalisation of cGMP signalling as different stimuli which raise intracellular cGMP levels activate different downstream effectors.

Similar experiments were carried out in hypertrophic ARVM, where SNAP treatment before ISO stimulation resulted in significantly less cAMP detected in the PKA-RI compartment compared to SNAP treated control myocytes. PDE3 is normally active in the PKA-RI compartment of adult myocytes; therefore an increase in cGMP levels (due to SNAP treatment) would normally result in an inhibition of PDE3 activity and a subsequent

increase in cAMP at this region. However this is not the case, but instead there is a reduction in cAMP in the PKA-RI compartment in hypertrophic SNAP treated myocytes compared to SNAP treated control myocytes. This data would suggest a loss of cGMP/PDE3 interaction or alternatively an increase in PDE2 activity in this compartment. PDE2 is found in both the PKA-RI and PKA-RII compartment of the ARVM, but is mainly localised to the PKA-RII compartment in hypertrophic myocytes (see Figure 5-15). It would be expected that SNAP treatment would generate an increase in PDE2 activity via cGMP activation, resulting in a reduced cAMP response in this compartment. However no difference was established between SNAP treated control ARVM and SNAP treated hypertrophic ARVM. This can be explained by the fact that cGMP levels are already raised in hypertrophic myocytes, and therefore PDE2 is already activated in this cell type and SNAP has no further effect on this PDE family.

In this study (Figure 5-15), the FRET experiments indicated there was increased PDE2 activity specifically in the PKA-RII compartment of hypertrophic myocytes but no change in protein or mRNA, and given that PDE2 can be activated by cGMP, it was hypothesised that the increased PDE2 activity may be due to increased levels of cGMP. To test this hypothesis, the FRET based cGMP sensor Cygnet-2.1 was expressed in both control and hypertrophic myocytes in order to gain basal cGMP measurements in these cell types. The outcome was that the basal intracellular cGMP concentrations were higher in hypertrophic ARVM compared to control ARVM. To further investigate whether changes in cGMP levels may be responsible for the altered PDE regulation in the PKA-RI and PKA-RII subcellular locations, the cGMP sensor cygnet-2.1 was genetically modified and targeted to two compartments by fusing the dimerisation/docking domains of RI $\alpha$  and RII $\beta$  of PKA to the N-terminus to generate RI-Cygnet-2.1 and RII-Cygnet-2.1 respectively. Sensors were subcloned in adenoviral vector and myocytes were infected overnight before imaging. The data obtained showed a higher basal level of cGMP in the PKA-RI compartment compared to the PKA-RII compartment in control ARVM. In hypertrophic myocytes, there was a greater cGMP concentration recorded in both the PKA-RI and PKA-RII compartments, but with the greatest fold change in the PKA-RII compartment. These results suggest that increased PDE2 activity detected by FRET imaging in the PKA-RII compartment may be due to the increased cGMP levels recorded in hypertrophic myocytes.

Our laboratory had previously demonstrated that catecholamine stimulation leads to a negative feedback control loop of cAMP signalling in cardiomyocytes, where  $\beta_1$ - and  $\beta_2$ -ARs produce cAMP, and stimulation of the  $\beta_3$  receptor leads to the production of NO, which, sequentially, stimulates sGC to produce cGMP. PDE2 is activated by cGMP and degrades cAMP, therefore acting as a balance for cyclic nucleotide signalling (Mongillo et al. 2006). Under normal conditions, this mechanism would exist to counteract excessive  $\beta$ -adrenergic excitation but would drive cardiac impairment in heart failure by further reducing the already blunted cAMP response. It has been shown that in heart disease,  $\beta_1$ -AR and  $\beta_2$ -AR are downregulated or desensitised respectively, whereas there is an increase in  $\beta_3$ -AR protein (Cheng et al. 2001; Moniotte et al. 2001).

$\beta_3$ -AR signalling was investigated in this model of cardiomyocyte hypertrophy to assess if this mechanism may be responsible for the increased cGMP concentrations measured and the alteration in local PDE2 activity.

Control and hypertrophic myocytes were infected with the targeted cGMP FRET based sensors RI-Cygnat-2.1 and RII-Cygnat-2.1 overnight and pre-treated with 100 nM  $\beta_3$ -AR inhibitor (SR59230A) 10 minutes before imaging. In control cells,  $\beta_3$ -AR inhibition caused a reduction in cGMP in the PKA-RI compartment, which suggests that under normal conditions  $\beta_3$ -ARs are coupled to the PKA-RI compartment. This data may explain the observed higher cGMP level in the PKA-RI compartment compared the PKA-II in control ARVM.

In hypertrophic cells treated with  $\beta_3$ -AR inhibitor, a smaller cGMP concentration was detected in the PKA-II compartment compared to the RI, suggesting that in hypertrophic myocytes there is a greater  $\beta_3$ -AR activity in the PKA-II compartment. This change in the compartment within which  $\beta_3$ -AR inhibition appears to have an effect in terms of cGMP levels could explain why there is higher PDE2 activity in this compartment in hypertrophic ARVM.

These findings indicate that there is interplay between cGMP and cAMP in a compartment specific manner in adult rat cardiomyocytes and that altered PDE2 activity may be due to modified cGMP compartmentalised signalling in hypertrophic myocytes.

# 7 Role of Phosphodiesterase type 2 in the development of cardiac hypertrophy.

---

## 7.1 Introduction

Cardiomyocyte hypertrophy is the cellular response to increased biomechanical stress and is defined by an increase in cardiomyocyte size, enhanced protein synthesis, and a higher organisation of the sarcomere. In hypertrophy, the increased size of the myocytes is initially a compensatory mechanism; however, sustained hypertrophic growth can ultimately lead to a decline in left ventricular function leading to heart failure. Although pathological hypertrophy is in the end a detrimental process, it is nonetheless highly organised by activation of specific intracellular signalling pathways. These signalling pathways are defined as either adaptive, as their activation is crucial for successful remodelling of the heart to compensate for increased stress, or as maladaptive, as activation of these pathways leads ultimately to contractile dysfunction and heart failure. The calcineurin-nuclear factor of activated T-cells (NFAT) signalling pathway, for example, is one of the most studied hypertrophic pathways and is considered to be maladaptive. Phospho-NFAT is cytosolic, but when dephosphorylated by calcineurin, it translocates to the nucleus and promotes transcription of pro-hypertrophic genes in cardiomyocytes (Hogan et al. 2003). The cGMP signalling pathway is considered to be an adaptive response and beneficial as cGMP has been shown to produce anti-hypertrophic effects via PKG mediated phosphorylation of the L-type  $\text{Ca}^{2+}$  channel and reduction of  $\text{Ca}^{2+}$  influx and thereby inhibiting the pro-hypertrophic effects of NFAT/ calcineurin signalling (Fiedler et al. 2002).

A number of studies have reported that production of cGMP can have anti-hypertrophic effects in a range of disease models. Rosenkranz and colleagues reported that increasing cGMP by treatment of atrial natriuretic peptide (ANP) to adult cardiomyocytes could prevent hypertrophy induced by angiotensin II (Ang II) stimulation (Rosenkranz et al. 2003). Another study found that in ventricular cells cultured from the neonatal rat heart, ANP and the NO donor S-nitroso-N-acetyl-D,L-penicillamine (SNAP) cause a decrease in NE induced hypertrophy (Calderone et al. 1998). Furthermore, transgenic mice with deficiencies of neuronal nitric oxide synthase (NOS1) or endothelial nitric oxide synthase (NOS3), causing inhibition of cGMP synthesis, lead to hypertrophic growth of the hearts (Barouch et al. 2003).

This study has so far shown that the contribution of PDE2 to the degradation of cAMP generated in response to ISO is significantly increased in an *in vitro* model of cardiac hypertrophy. PDE2 expression levels were however unchanged in hypertrophic ARVM, thus suggesting that the increased PDE2 activity detected might be due to an increased activation of the enzyme. This increased activation of PDE2 was found to be compartmentalised and to occur specifically in the PKA-RII compartment where PKA-RII normally resides.

Results obtained in chapter 6.2.3 of this study, indicated that cGMP basal levels were significantly increased in hypertrophied ARVM which was mainly associated with an increase of cGMP in the PKA-RII compartment. Thus, it is possible to hypothesise that increased local levels of cGMP might be responsible for the increased PDE2 activity found in hypertrophic cardiac myocytes in the PKA-RII compartment.

It was decided to next investigate whether the increased PDE2 activity, measured in NE treated ARVM, contributes to the development of cardiomyocyte hypertrophy.

## Aims

- Investigate the effect that PDE2 inhibition with Bay 60-7550 has on NE induced cardiomyocytes hypertrophy.
- Measure the effect that increasing PDE2 activity by overexpression of the enzyme has on the hypertrophic growth of adult myocytes *in vitro*.

- Assess what is the signalling pathway downstream of PDE2 that is involved in the regulation of cardiac myocyte size.

## 7.2 Results

### 7.2.1 *In vitro* inhibition of PDE2 with Bay 60-7550 prevents NE induced cardiomyocyte hypertrophy

In order to assess whether increased PDE2 activity (due to increased PDE2 activity specifically in the PKA-RII compartment) promotes the advancement of cardiac hypertrophy, primary cultured ARVM were stimulated simultaneously with 1  $\mu$ M NE and 50 nM Bay 60-7550 overnight before the cells were either imaged to calculate changes in hypertrophic growth by measurement of cell size or collected for mRNA extraction to check for the expression of pro-hypertrophic genes using RT-PCR. As previously mentioned in chapter 3.5.1, cell size was calculated by measuring of longitudinal section area (length x width). One pixel corresponds to 0.07  $\mu$ m when images are collected at 40X objective.

As shown below (Figure 7-1A & B), cell size was significantly increased in myocytes treated overnight with 1  $\mu$ M NE compared to untreated controls. To investigate the role of PDE2 in the development of hypertrophic growth in the adult system, ARVM were simultaneously treated with NE and pharmacological PDE 2 inhibitor Bay 60-7550 (50 nM) overnight before measuring cell size. If the increased PDE2 activity recorded in hypertrophic ARVM is a compensatory mechanism elicited in the attempt to counteract hypertrophy, inhibition of the enzyme should lead to a more pronounced hypertrophic response; on the other hand, if the increased PDE2 activity contributes to the development of the hypertrophic phenotype, inhibition of PDE2 should reduce NE-induced hypertrophy. The longitudinal sectional area was significantly smaller in the myocytes treated with both NE and Bay 60-7550 compared to the ARVM treated with NE alone.

Measurements of ANP mRNA levels further confirmed that inhibition of PDE2 blunts NE-induced hypertrophy in ARVM. As shown in Figure 7-1C, ANP mRNA levels remained at control levels in myocytes treated with both NE and Bay 60-7550, showing almost halved ANP expression compared to cells treated with NE alone. These results indicate that inhibition of PDE2 is able to reduce hypertrophic growth in this model of cardiomyocyte hypertrophy in ARVM. This would suggest that the previously recorded increase in PDE2 activity in NE treated ARVM (Figure 5-15), adds to the development of hypertrophy rather than acting to offset it.

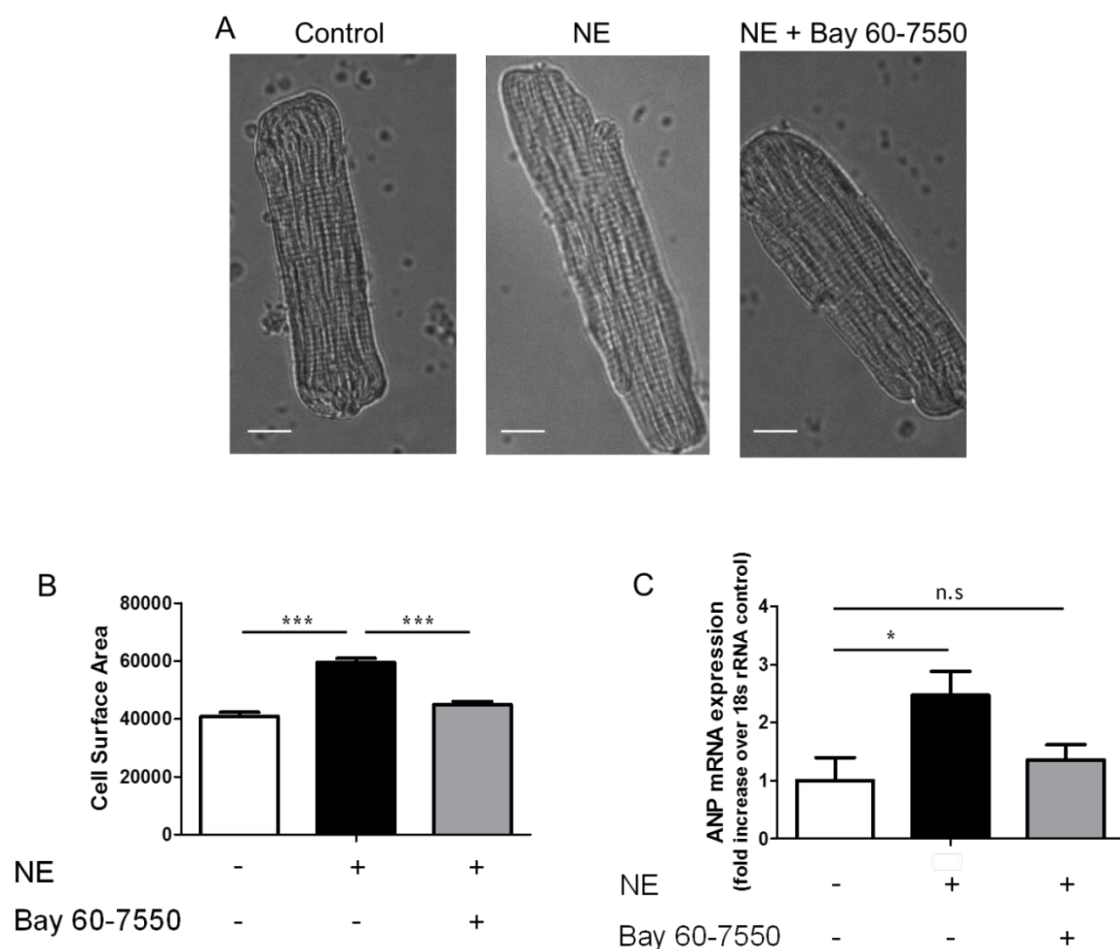


**Figure 7-1. Inhibition of PDE2 prevents hypertrophy induced by norepinephrine treatment in ARVM.**

**(A)** Representative images of untreated, NE (1  $\mu$ M) treated and NE (1  $\mu$ M) + Bay 60-7550 (50 nM) treated isolated ARVM. **(B)** Summary of cell size measurements (longitudinal area = length x width) in ARVM myocytes in the presence of NE or NE + Bay 60-7550. Control: n = 137; NE: n = 142; NE + Bay 60-7550: n = 129. **(C)** Summary of RT-PCR results for ANP expression levels in NE-treated and NE + Bay 60-7550 treated cardiac myocytes. Control: n=29; NE: n=29; NE + Bay 60-7550: n=12. One way ANOVA, \* p<0.05, \*\*\* p<0.001.

## 7.2.2 PDE2 overexpression in ARVM induces hypertrophy

Until now, the results presented in this thesis show that PDE2 activity is significantly higher in hypertrophied myocytes, due to increased PDE2 activity in the PKA-RII compartment, and that pharmacological inhibition of PDE2 can counteract NE induced hypertrophic growth *in vitro*. Therefore, it was decided to investigate whether hypertrophic growth could be induced in primary cultured adult rat cardiomyocytes by increasing PDE2 activity as a result of overexpression of this enzyme.

Myocytes were transduced with an adenovirus carrying PDE2A2 wild type tagged with the red fluorescent protein mCherry (produced by Vector Biolabs). Constructs were tagged with a fluorescent marker as the efficiency of infection is not 100%; therefore the presence of the fluorescent tag allows to easily distinguish between ARVM expressing the recombinant PDE2A2 enzyme from those which do not.

The results summarised in Figure 7-2A&B show that cells overexpressing PDE2A2wt were significantly larger than control ARVM. This data indicates that overexpression of PDE2 is sufficient per se to induce hypertrophic growth of adult cardiac myocytes *in vitro*.

A catalytically dead form of the PDE2A2wt mCherry construct was produced to establish whether the hypertrophic growth is simply due to the overexpression of the PDE2A2 enzyme or if it is due to increased PDE2 activity. This construct was generated by substituting two aspartic acid residues with two alanine residues at positions 685 and 796 in the catalytic site of the enzyme and had previously been demonstrated to abolish the ability of PDE2 to degrade cAMP (Stangherlin et al. 2011). When the catalytically dead PDE2 is overexpressed in cells it is expected to displace the endogenous active PDE2 from any anchoring site within the cell. The construction of Adenovirus containing the mutated PDE2A2 dn mCherry-tagged vectors and the preparation of a high titre virus batch were outsourced from Vector Biolabs.

As illustrated in Figure 7-2C & D, the overexpression of a catalytically dead version of PDE2A2 (PDE2A2 dominant negative, dn) does not induce hypertrophic growth in ARVM.

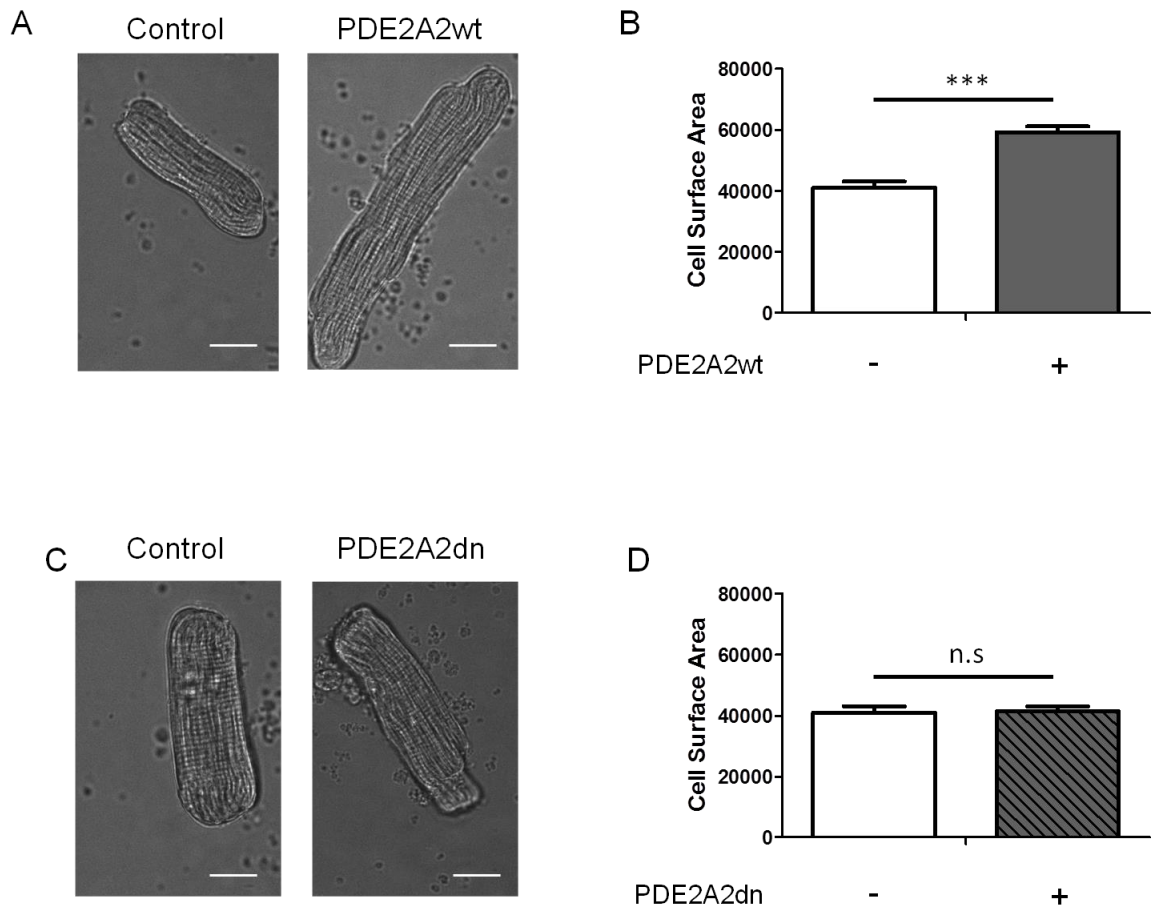


**Figure 7-2. Overexpression of PDE2A2 causes hypertrophic growth in isolated ARVM.** (A) Representative images of ARVMs non-transduced or transduced with PDE2A2wt (wild type). (B) Summary of calculated cell size for ARVM transduced with PDE2A2wt. (C) Representative images of ARVMs non-transduced or transduced with PDE2A2dn (dominant negative). Control: n = 39; PDE2A2wt: n=29. (D) Summary of calculated cell size for ARVM transduced with PDE2A2dn. Control: n = 39; PDE2A2dn: n=25. Error bars represent SEM. Two tailed; paired t-test, \*\*\* p<0.001.

It would be appropriate to have an additional control of ARVM overexpressing a PDE isoform belonging to a different family. However, given the high cost of generating an additional adenovirus and limited funds, it was decided that these experiments would not be performed. Alternatively, parallel experiments were performed in the laboratory where NRVM were transfected with PDE2A2-mCherry, PDE2AdnmCherry or PDE4A4. The results of these experiments showed that as reported in ARVM, overexpression of PDE2A2 induces hypertrophic growth. Cell surface area: control NRVM =  $54933 \pm 2709$  pixels, n = 49; PDE2A2 wild type- transfected NRVM =  $75318 \pm 4421$  pixels, n = 50; p <

0.001), whereas the overexpression of the catalytically dead PDE2A2 had no effect of cell size (control NRVM =  $56597 \pm 3617$  pixels,  $n = 33$ ; PDE2A2-dn NRVM =  $56629 \pm 6227$ ,  $n = 38$ ; ns). The addition control illustrated that neither the overexpression of PDE4A nor the overexpression of its catalytically inactive form had effects on cardiac myocytes cell surface area (control NRVM =  $53960 \pm 4622$ ,  $n = 29$ ; PDE4A4wt NRVM =  $46971 \pm 4911$ ,  $n = 28$ ; ns) (control NRVM =  $50041 \pm 3842$ ,  $n = 28$ ; PDE4Adn NRVM =  $50620 \pm 4238$ ,  $n = 28$ ; ns) (A. Zoccarato, unpublished results).

Together these results would indicate that the catalytic activity of PDE2 is required to induce hypertrophic growth in ARVM and NRVM. As PDE2A2dn displaces endogenous PDE2 from its anchor site, allowing it to freely move throughout the cell, it would appear that the subcellular localisation of PDE2 activity, and therefore the ability of PDE2 to control cAMP levels within a specific subcellular compartment, is also key in the promotion of hypertrophic growth.

### **7.2.3 Exploring the effect that overexpressing the catalytically inactive PDE2A2 has on cAMP signalling dynamic in adult cardiomyocytes**

To investigate the effect displacing endogenously active PDE2 from its anchor sites has on local cAMP pools, using the catalytically dead PDE2 construct in adult myocytes, a FRET-based imaging approach was applied. ARVM were co-transduced with either the targeted FRET-based sensors RI\_epac or RII\_epac and PDE2A2dn mCherry (MOI: 1000) overnight. The cells were then imaged the following day on an epifluorescent microscope. cAMP generation was stimulated by challenging the cardiomyocytes with 100 nM ISO. The results obtained, as illustrated in Figure 7-3A, show that in the PKA-RI compartment ISO stimulation induces a cAMP response which is significantly higher in cells that overexpress PDE2A2dn compared to control myocytes. In the PKA-RII subcellular compartment, there is no difference in cAMP levels upon ISO stimulation in cells transduced with PDE2A2dn compared to control ARVM, however the difference between the PKA-RI and PKA-RII compartment is abolished in myocytes transduced with PDE2A2dn. These data are similar to the earlier findings from chapter 4, where

pharmacological inhibition of PDE2 with Bay 60-7550 (50 nM) before ISO stimulation resulted in a comparable level of cAMP in both the PKA-RI and PKA-RII compartments, but the greatest effect was seen in the PKA-RI compartment (Figure 4-9).

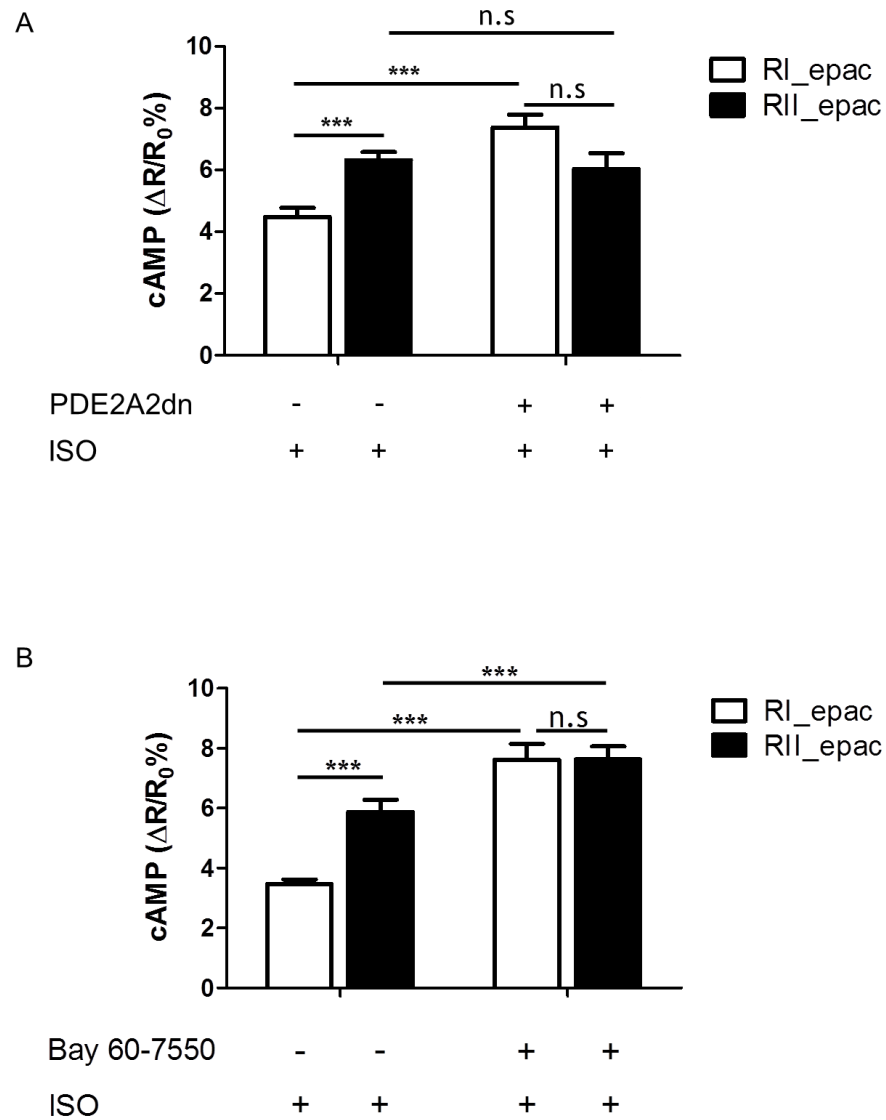


**Figure 7-3. Summary of FRET change in ARVM overexpressing PDE2A2dn.**

Summary of FRET change induced by 100 nM isoproterenol in the presence or absence of (A) PDE2A2dn - RI\_epac control: n = 15; RI\_epac + PDE2A2dn: ΔR n = 6; RII\_epac control: n = 15; RII\_epac + PDE2A2dn: n = 9. (B) PDE2 inhibitor Bay 60-7550 (50 nM) (as previously shown in Figure 4-9). RI\_epac control: n = 8; RII\_epac control: n = 16; RI\_epac + Bay 60-7550: n = 10; RII\_epac + Bay 60-7550: n = 9. Statistical significance calculated by two way ANOVA with Bonferroni's post test, \*\* p<0.01, \*\*\* p<0.001.

n myocytes which had been pre-treated with 1  $\mu$ M NE to induce hypertrophy, before transducing them with the adenovirus containing PDE2A2dn and the targeted FRET reports (Figure 7-4A), ISO stimulation resulted in increased cAMP generation in the PKA-RI compartments compared to control myocytes which did not contain the PDE2A2dn enzyme. There was also elevation of cAMP in the PKA-RII compartment in myocytes transduced with PDE2A2dn after ISO stimulations. Comparison of the two compartments in cells with PDE2A2dn, the cAMP levels were significantly greater in the PKA-RII compartment compared to the PKA-RI compartment ( $p < 0.05$ ). These results were again in agreement with the data obtained using PDE2 inhibitor Bay 60-7550 (50 nM) in NE treated myocytes (Figure 7-4B), where ISO (100 nM) stimulation resulted in increased cAMP production in both the PKA-RI and PKA-RII compartments when myocytes were pre incubated for 10 minutes with Bay 60-7550 compared to ISO treatment alone.

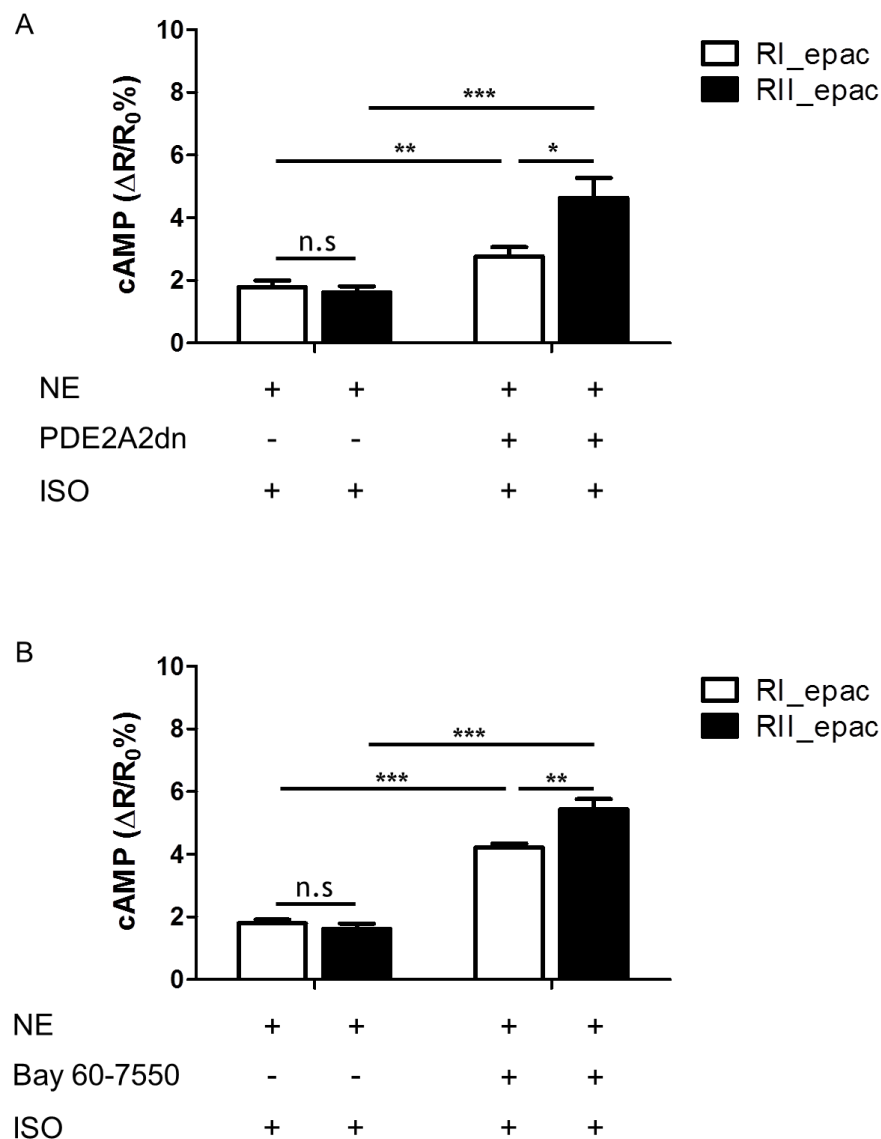


**Figure 7-4. . Summary of FRET change in hypertrophic ARVM overexpressing PDE2A2dn. (A) Summary of FRET change induced by 100 nM isoproterenol in the presence or absence of PDE2A2dn in myocytes pre-treated with norepinephrine to induce hypertrophy. RI\_epac hypertrophic: n = 14; RI\_epac hypertrophic + PDE2A2dn: n = 6; RII\_epac hypertrophic: n = 14; RII\_epac hypertrophic + PDE2A2dn: n = 10. (B) Experiment carried out in the presence of selective PDE2 inhibitor Bay-607550 (as shown in chapter 5.2.4). RI\_epac hypertrophic:  $\Delta R/R_0 = n = 7$ ; RI\_epac hypertrophic + Bay 60-7550: n = 9; RII\_epac hypertrophic: n = 18; RII\_epac hypertrophic + Bay 60-7550: n = 10. Statistical significance calculated by two way ANOVA with Bonferroni's post test, \*  $p < 0.05$ , \*\*  $p < 0.01$ , \*\*\*  $p < 0.001$ .**

Together these data support the hypothesis that cAMP signalling is altered in hypertrophic adult cardiomyocytes due to altered PDE2 activity. In control ARVM, PDE2 is mainly

coupled with the PKA-RI compartment; however with increased catecholamine stimulation, leading to hypertrophic growth, PDE2 activity is increased in the PKA-RII compartment and its activity is found to be more associated with this compartment. Displacement of PDE2 by PDE2A2dn or inhibition of PDE2 with Bay 60-7550 appears to have a similar anti-hypertrophic effect in ARVM, these results strongly indicate that PDE2 is localised in the myocyte and the effect that its inhibition generates on cell growth depends on the modulation of cAMP within a restricted and localised pool of cAMP. Additional investigation is required to further elucidate the signalling pathway involved downstream of PDE2 inhibition and the consequent local rise in cyclic nucleotide levels.

#### **7.2.4 Is the anti- hypertrophic effect of PDE2 inhibition dependent of cAMP/PKA or cGMP/PKG downstream signalling?**

PDE2 is a dual specific PDE, which means it has the ability to degrade both cAMP and cGMP, and therefore the anti-hypertrophic effect of PDE2 inhibition described in this thesis could be mediated by either an increased activation of cAMP and consequent activation of PKA or alternatively by an increase in cGMP levels and activation of PKG. The cGMP/ PKG signalling pathway is widely accepted as a negative regulator in the cardiac remodelling process. The literature reports numerous studies where increased cGMP synthesis by stimulation of natriuretic peptides or NO donors or by the overexpression of guanylyl cyclase reduces cardiac hypertrophy.

Hypertrophy stimulated in isolated ARVM by Ang II treatment was shown to be prevented by the addition of natriuretic peptides (Rosenkranz et al. 2003). Another investigation found mice lacking functional *Npr1* gene, which encodes GC-A (denominated NPRA by the authors) throughout the body showed arterial hypertension with a disproportionate degree of cardiac hypertrophy, and mice with cardiac-specific NPRA deletion develop exaggerated hypertrophy in response to pressure overload (Oliver et al. 1997). Conversely, cardiac overexpression of active GC inhibits pressure-overload hypertrophy and remodelling (Zahabi et al. 2003).

PKG also plays an important role as a negative regulator of cardiac hypertrophy. Zhang and colleagues found that mice with reduced myocyte PKG activity, caused by PDE5 overexpression, develop exacerbated hypertrophy and remodelling in response to pressure overload, and normalizing PKG activity by switching off PDE5 overexpression improves the already established remodelling (Zhang et al. 2010). Another study reported that mice with cardiac-specific deletion of PKGI, revealed more pronounced remodelling to angiotensin II or pressure overload by transverse aortic constriction (Frantz et al. 2011).

However, the role of the PKG pathway in cardiac hypertrophy is still controversial. Lukowski and colleagues showed that in PKG knock-out mice and mice lacking PKG specifically in cardiomyocytes, that there was no difference in degree of cardiac hypertrophy induced by chronic ISO infusion or surgical constriction of the transverse aorta (TAC), when compared to wild type control mice (Lukowski et al. 2010). This study suggests that the development of cardiac hypertrophy is not amplified by the absence of endogenous PKG.

Recently, the involvement of the cGMP selective PDE 5 and of the dual-specific PDE1 in modulating hypertrophic effects both *in vivo* and *in vitro* models of cardiac hypertrophy has been reported (Takimoto et al. 2005; Miller et al. 2009). Takimoto reported that the phosphodiesterase-5A (PDE5A) inhibitor Sildenafil suppresses chamber and myocyte hypertrophy, and improves *in vivo* heart function in mice exposed to chronic pressure overload induced by transverse aortic constriction. PDE5A inhibition was found to deactivate multiple hypertrophy signalling pathways triggered by pressure load (the calcineurin/NFAT, phosphoinositide-3 kinase (PI3K)/Akt, and ERK1/2 signalling pathways) and increase the activation of cGMP-dependent protein kinase (PKG). Miller and colleagues discovered that inhibition of PDE1 activity prevented phenylephrine induced hypertrophy in neonatal and adult rat ventricular myocytes, as well as reducing cardiac hypertrophy induced by chronic ISO infusion *in vivo*. PDE1A was reported as significantly upregulated in both *in vivo* and *in vitro* forms of cardiomyocyte hypertrophy, which plays a critical role a reduction of intracellular cGMP and PKG. In both of these studies the anti-hypertrophic effects of PDE1 and PDE5 inhibition have been suggested to be mediated by activation of cGMP/PKG signalling pathways (Takimoto et al. 2005; Miller et al. 2009) therefore the anti-hypertrophic effects resulting from PDE2 inhibition was investigated to assess whether this process was mediated by cGMP/ PKG signalling.

To establish if cGMP/PKG is involved in the anti-hypertrophic effects of PDE2 inhibition, DT-2, a highly selective inhibitor of PKG (Taylor et al. 2004) was utilised. Hypertrophy was induced in adult rat ventricular myocytes (ARVM) by stimulation with 1  $\mu$ M NE overnight in presence of the selective PKG-inhibitor DT-2, alone or in combination with either Bay 60-7550 or Sildenafil. Sildenafil was used as a control as its anti-hypertrophic effect is known to be mediated by PKG (Takimoto et al. 2005). The hypertrophic growth was judged by calculating the area of the cell (length x width) from the image of a longitudinal section.

First, to ensure the concentration of Sildenafil used was enough to blunt NE effect on ARVM, cells were treated with NE in the presence of 10 nM Sildenafil or 50 nM Bay 60-7550 (Figure 7-5A). The PDE inhibitors had similar effects on cell size and were able to exert anti-hypertrophic effects on the myocytes.

In ARVM incubated with PKG inhibitor DT-2 in the presence of Sildenafil (Figure 7-5B), there was no difference in cell size compared to NE treated cells alone and therefore DT-2 was able to block the anti-hypertrophic effect of the PDE5 inhibitor. However, DT-2 treatment did not affect the anti-hypertrophic action of PDE2 inhibitor Bay 60-7550, as illustrated in Figure 7-5B. These data confirm data published by Takimoto and colleagues, showing that PKG activity is required for the anti-hypertrophic effects of Sildenafil to occur (Takimoto et al. 2005) and indicate that the anti-hypertrophic effect of Bay 60-7550 does not involve PKG signalling.

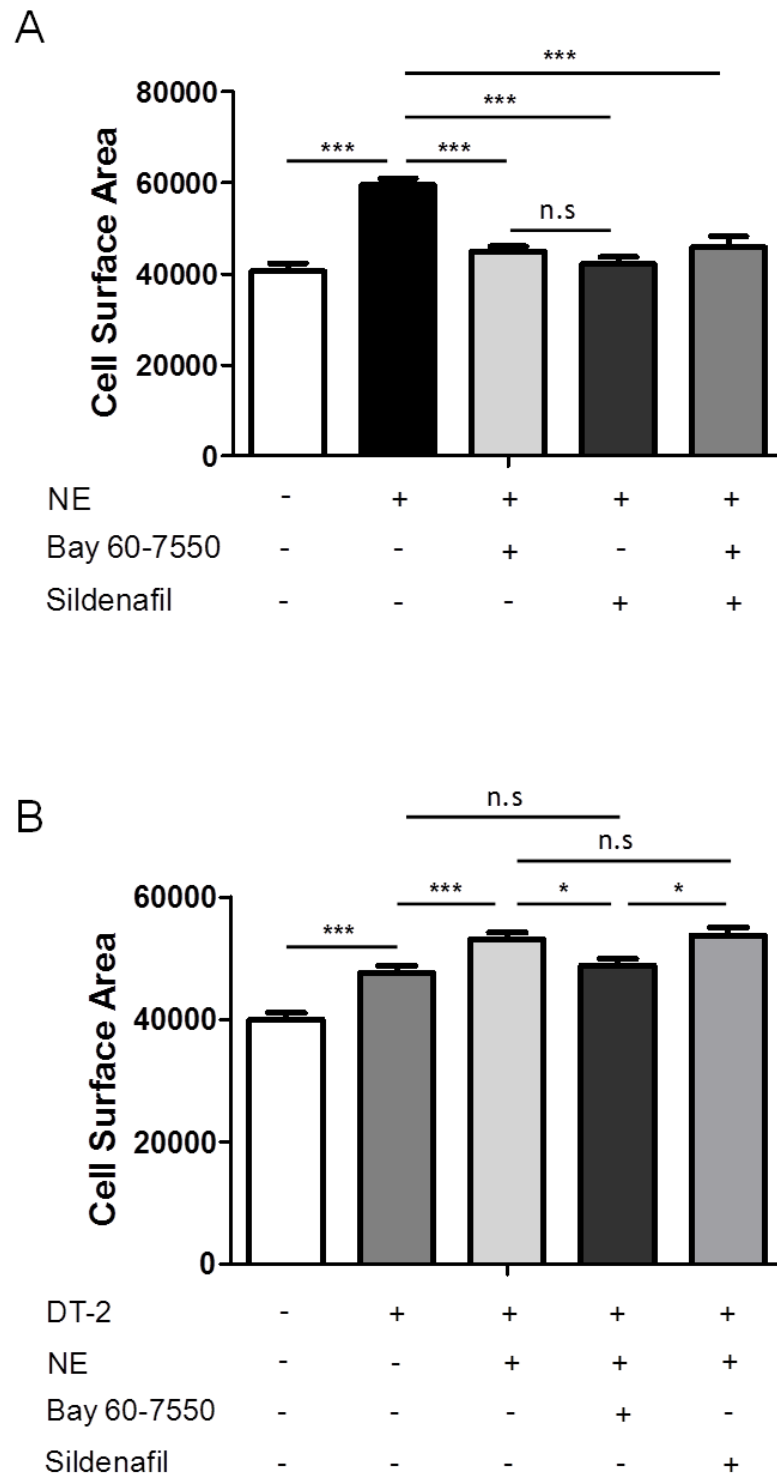


**Figure 7-5. The anti-hypertrophic effects of PDE2 inhibition is PKG independent.**

**(A)** Summary of cell area measurements of ARVM in the presence of NE (1  $\mu$ M) and a combination of Bay 60-7550 (50 nM) and/or Sildenafil (10 nM). Control: n = 106; NE: n = 142; NE + Bay 60-7550: n = 129; NE + Sildenafil: n = 55; NE + Bay 60-7550 + Sildenafil: n = 59. **(B)** Cell size calculated of hypertrophic ARVM in the presence of PKG inhibitor DT-2 and Bay 60-7550 or Sildenafil. Control: n = 97; DT-2: n = 144; DT-2 + NE: n = 158; DT-2 + NE + Bay 60-7550: n = 160; DT-2 + NE + Sildenafil: n = 145. ANOVA with Bonferroni's post-test, \* p < 0.05, \*\* p < 0.01, \*\*\* p < 0.001.

Since the anti-hypertrophic effects of PDE2 inhibition does not seem to require PKG activity, the involvement of the cAMP/PKA signalling pathway was explored next. The above experiment was repeated in the presence of selective PKA inhibitor myrPKI (myristoylated PKA inhibitor) (50  $\mu$ M) (Islam et al. 2008).

The results summarised in Figure 7-6 show that the anti-hypertrophic effects of Bay 60-7550 are completely abolished during the selective inhibition of PKA activity by myrPKI. As anticipated, Sildenafil treatment, even in the presence of 50  $\mu$ M myrPKI, is able to counteract the hypertrophic growth in ARVM induced by NE.

These data are important as they indicate that the anti-hypertrophic effects of PDE2 inhibition are mediated, in part, by cAMP/ PKA and confirm that the anti-hypertrophic effects of PDE5 inhibition are not mediated by PKA signalling but instead by cGMP/PKG.

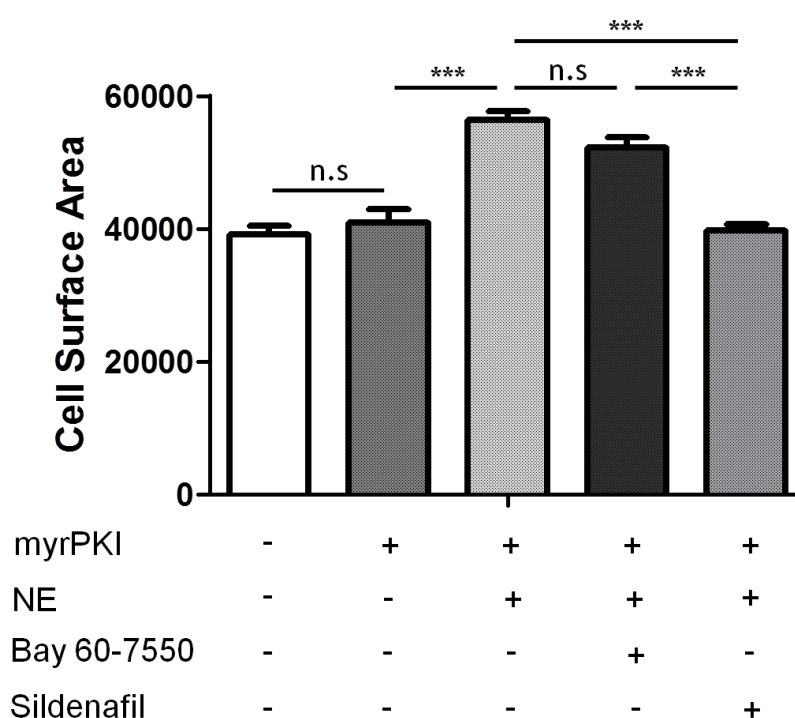


**Figure 7-6. The anti-hypertrophic effects of PDE2 inhibition are PKA-dependent.**

Summary of cell size calculated in hypertrophic ARVM in the presence of PKA inhibitor myrPKI and Bay 60-7550 or Sildenafil. Control: n = 66; myrPKI: n = 93; myrPKI + NE: n = 66; myrPKI + NE + Bay 60-7550: n = 71; myrPKI + NE + Sildenafil: n = 110. Statistical analysis by ANOVA with Bonferonni's post-test, \*\*\* p<0.001.

A classical *in vitro* model of cardiac hypertrophy, reported in numerous investigations, is persistent catecholamine stimulation of  $\beta$ -adrenergic receptors ( $\beta$ -ARs) which are coupled to  $G_{\alpha_s}$ , induces adenylyl cyclase activity leading to increased cAMP/ PKA activity. PKA then phosphorylates several proteins involved in cardiac excitation-contraction coupling and energy metabolism, including activation of L-Type  $Ca^{2+}$  channels and SERCA, resulting in an influx of  $Ca^{2+}$  positively chronotropic, inotropic, and lusitropic effects on the heart. Increased intracellular calcium is also known to activate the calcineurin-NFAT signalling cascade and induce cardiac hypertrophy. In addition to this, increased levels of circulating catecholamines are associated with  $\beta$ -ARs desensitisation. Phosphorylation by PKA can lead to receptor internalisation, uncoupling from G-proteins or downregulation of AR mRNA expression (Lohse et al. 2003). One study showed that transgenic mice overexpressing the catalytic subunit of PKA develop dilated cardiomyopathy with reduced cardiac contractility, arrhythmias, and susceptibility to sudden death due to PKA-mediated hyper-phosphorylation of the cardiac ryanodine receptor and phospholamban (Antos et al. 2001).

PKA is therefore generally considered to be a pro-hypertrophic stimulus. However, in this thesis I have presented data which illustrates that in an *in vitro* model of cardiac hypertrophy, induced by NE stimulation of ARVM, pharmacological inhibition of PDE2 abolishes hypertrophic growth. This anti-hypertrophic effect had been shown to occur via a PKA dependent mechanism.

To study whether enhancement of the cAMP/PKA pathway by inhibition of cAMP-raising agents was pro-hypertrophic in ARVM, isolated adult rat myocytes were treated overnight with inhibitors of PDE2, PDE3 and PDE4 and forskolin, a direct activator of adenylyl cyclase.

Activation of the cAMP signalling pathway by forskolin (1  $\mu$ M) produced a pronounced increase in cell size compared to control cells. Inhibition of PDE3 by cilostamide (10  $\mu$ M) was also able to induce hypertrophic growth in primary cultured ARVM. Treatment with PDE2 inhibitor Bay 60-7550 (50 nM) and PDE4 inhibitor rolipram (10  $\mu$ M) did not alter the size of the cardiomyocytes.

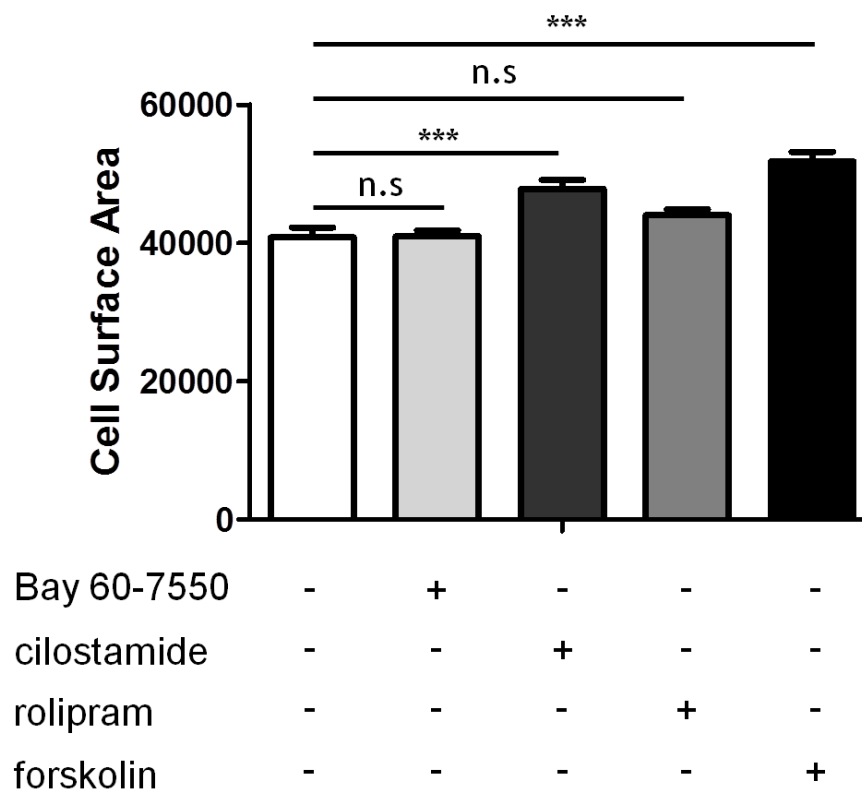


**Figure 7-7. cAMP increase due to forskolin, rolipram or cilostamide, but not Bay 60-7550 stimulation has pro-hypertrophic effects.**

Isolated ARVM were treated overnight with 50 nM PDE2 inhibitor Bay 60-7550, 10  $\mu$ M PDE3 inhibitor cilostamide, 10  $\mu$ M PDE4 inhibitor rolipram or 25  $\mu$ M forskolin before calculating changes in cell size compared with untreated myocytes. Control: n = 137; Bay 60-7550: n = 148; cilostamide: n = 120; rolipram: n = 189; forskolin: n = 112. Statistical analysis by ANOVA with Bonferonni's post-test, \* $p < 0.05$ , \*\*\*  $p < 0.001$ .

Selective inhibition of PDE2 with 50 nM Bay 60-7550 blunts hypertrophic growth of ARVMs caused by chronic NE treatment (Figure 7-1). Selective inhibition of PDE3 and PDE4 was then explored to study whether it had similar anti-hypertrophic effects.

Primary cultured adult cardiomyocytes were treated overnight with NE in the presence of different cAMP-raising agents and imaged the following day in order to calculate cell size. Unlike Bay 60-7550 treatment, inhibition of PDE4 with 10  $\mu$ M rolipram or PDE3 with 10  $\mu$ M cilostamide was unable to prevent the hypertrophic growth induced by NE stimulation, although treatment with these inhibitors did not further increased cell size compared to NE treatment alone.

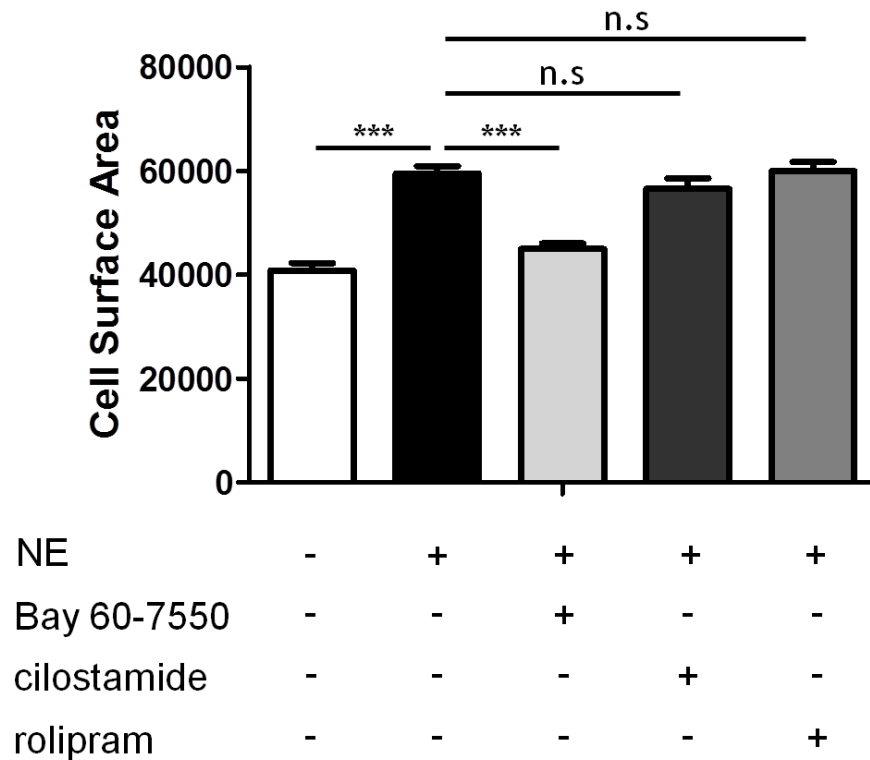


**Figure 7-8. Inhibition of PDE3 or PDE4 did not affect NE-induced cardiomyocytes hypertrophic growth.**

Primary cultured ARVM were treated overnight with 1  $\mu$ M NE in the presence of 50 nM PDE2 inhibitor Bay 60-7550, 10  $\mu$ M PDE3 inhibitor cilostamide or 10  $\mu$ M PDE4 inhibitor rolipram before imaging for cell size measurements. NE: n = 142; NE + Bay 60-7550: n = 129; NE + cilostamide: n = 7; NE + rolipram: n = 66. Statistical analysis by one way ANOVA with Bonferroni's post test, \*\*\* p<0.001.

Together these results show that enhancement of intracellular cAMP via direct activation of adenylyl cyclases, or selective inhibition of PDE3 or of PDE4 promotes hypertrophic growth, whereas enhancement of cAMP via PDE2 inhibition counteracts hypertrophy. It was therefore hypothesised that PDE2 controls a unique pool of cAMP which has an anti-hypertrophic effect in adult cardiomyocytes.

## 7.3 Conclusion

The intracellular signalling pathways controlling cardiac hypertrophy can have either beneficial or deleterious effects. Here, the role that elevated PDE2 activity, as reported in chapter 4, might have on cardiomyocyte hypertrophy was assessed. Cell size measurement and ANP mRNA levels were compared in isolated ARVM treated with both NE and PDE2 inhibitor Bay 60-7550. If PDE2 is involved in the development of cardiomyocyte hypertrophy, then its inhibition should reduce hypertrophic growth. On the contrary, if increased PDE2 activity is an adaptive mechanism to offset hypertrophy, inhibition should lead to a more pronounced hypertrophic phenotype. Results indicated that Bay 60-7550 treatment prevented NE-induced hypertrophic growth and ANP mRNA levels were significantly reduced as compared to ARVM treated with NE alone. These data suggest that PDE2 activity contributes to the development of cardiomyocyte hypertrophy induced by NE treatment *in vitro*. In addition and importantly they show that inhibition of PDE2 with Bay 60-7550 prevents the hypertrophic growth from occurring in primary cultured ARVM.

Overexpression of endogenous PDE2A2 in isolated ARVM resulted in hypertrophic growth of the cells, while overexpression of a catalytically inactive form of PDE2A2 (PDE2A2dn) had no effect on the calculated cell size. These results indicate that an increase in PDE2 activity promotes hypertrophic growth. To study the impact that overexpression of the catalytically inactive PDE2A2, and the consequent displacement of the active endogenous PDE2 from its anchor site, has on compartmentalised cAMP signalling, FRET imaging was applied. The results obtained were similar to earlier results using pharmacological PDE2 inhibitor Bay 60-7550, where in control ARVM PDE2 activity was found mainly associated to the PKA-RI compartment but in hypertrophic myocytes PDE2 activity is predominantly found in the PKA-RII subcellular location. This data suggests that as increased PDE2 activity is a maladaptive response in hypertrophy, selective inhibition of PDE2 in the PKA-RII compartment could produce anti-hypertrophic effects.

It has recently been published that PDE5 and PDE1 regulate cardiac hypertrophy *in vivo* and *in vitro* and the anti-hypertrophic effect upon inhibition of these PDEs is mediated by activation of cGMP/PKG pathways (Takimoto et al. 2005; Miller et al. 2009). As PDE2

has the ability to degrade both cAMP and cGMP, it was decided that the involvement of PKG signalling in the anti-hypertrophic effect produced by PDE2 inhibition would be investigated. Cell size was calculated for hypertrophied ARVM in the presence of selective PKG inhibitor peptide, DT-2, or PKA inhibitor peptide myrPKI and PDE inhibitors Bay 60-7550 and Sildenafil. The results showed that in the presence of DT-2 inhibition of PDE2 with Bay 60-7550 still produced anti-hypertrophic effects, while inhibition of PKA activity prevented the anti-hypertrophic effects of PDE2 inhibition. Therefore PDE2 seems to regulate cardiomyocytes hypertrophy via activation of cAMP/PKA signalling pathway.

Classically, activation of the cAMP/PKA signalling pathway is regarded as being pro-hypertrophic. To investigate if activation of cAMP/PKA signalling promotes hypertrophic growth in adult cardiomyocytes, ARVM were incubated with cAMP raising agents. Adenylyl cyclase activator forskolin (1  $\mu$ M), PDE3 inhibitor cilostamide (10  $\mu$ M) and PDE4 inhibitor rolipram (10  $\mu$ M) all promote cardiomyocytes hypertrophic growth, whereas inhibition of PDE2 with Bay 60-7550 (50 nM) has no hypertrophic effect on ARVM. Only inhibition of PDE2 and not PDE3 or PDE4 was found to reduce hypertrophic growth in ARVM induced by NE overnight treatment. These data are consistent with a model whereby cAMP signalling is compartmentalised and that PDE families are localised in distinct subcellular compartments (Mongillo et al. 2004; Mongillo et al. 2006). Based on this model PDEs can control different pools of cAMP which mediate either hypertrophic or anti-hypertrophic effects via activation of PKA.

## 8 Conclusion and Future Perspectives

---

In this thesis, intracellular signalling and phosphodiesterase regulation of the cAMP/ PKA pathway in cardiac hypertrophy was investigated using real-time FRET-based imaging. cAMP is a ubiquitous second messenger which mediates a huge number of diverse cellular responses. In the heart, cAMP modulates the positive inotropic and lusitropic effects of  $\beta$ -adrenergic receptor ( $\beta$ -AR) stimulation through its main effector PKA, promoting the phosphorylation and activation of key components of the excitation–contraction coupling (ECC) process. It has been demonstrated that cAMP signalling is compartmentalised. Discrete microdomains of cAMP, created by the action of phosphodiesterase enzymes, have been directly visualised in live cells using genetically encoded cAMP sensors and FRET-based imaging (Zaccolo and Pozzan 2002). PKA is anchored to specific subcellular targets by its interaction with A kinase anchoring proteins (AKAPs). Within the cell only particular pools of PKA are exposed to activating concentrations of cAMP at any one time (Colledge and Scott 1999). Thus, signals from one second messenger (in this case cAMP) can result in the activation of distinct signal transduction pathways, and diverse physiological responses (Buxton and Brunton 1983).

Cardiomyocyte hypertrophy is the cellular response to increased hormonal or mechanical stress on the heart. Prolonged hypertrophy is associated with a significant increase in the risk for sudden death or progression to heart failure. A number of signalling pathways have been reported to be altered during cardiac hypertrophy, including the cAMP/ PKA pathway. Chronic catecholamine stimulation results in down-regulation and desensitisation of the  $\beta$ -ARs. This leads to impairment in cAMP signalling and PKA phosphorylation of key components of the ECC process (Frey and Olson 2003; Barry et al. 2008). It has also been shown that, in different models of cardiac hypertrophy, there is altered PDE

expression and activity (Abi-Gerges et al. 2009; Mokni et al. 2010). Therapeutic treatment for dilated cardiomyopathy and heart failure currently involves increasing cAMP generation through  $\beta$ -AR antagonists and PDE inhibitors to try to improve cardiac contractility. PDE3 inhibitors such as milrinone have been shown to have beneficial effects in patients with impaired cardiac function; however long-term use of such drugs resulted in negative side effects such as arrhythmias and increased mortality (Packer et al. 1991; Movsesian 2002; Movsesian and Alharethi 2002). These adverse effects may be explained by the fact that non-selective inhibition of PDE3 would lead to a global increase in intracellular cAMP and activation of PKA, resulting in generalised phosphorylation of all substrates of PKA (Movsesian and Alharethi 2002). It has been suggested that selective modulation of compartmentalised PDEs activity may result in a more effective treatment (Miller and Yan 2010).

In the first part of this thesis, real-time FRET-based imaging approach and the targeted FRET-based sensors for cAMP, RI\_epac and RII\_epac (Di Benedetto et al. 2008), were utilised to study cAMP dynamics in the regions where PKA type I and PKA type II normally reside in adult rat ventricular myocytes (ARVM). It was established that these sensors localise to different compartments in ARVM, where RI\_epac overlays both the M and Z sarcomeric lines, whereas RII\_epac is found mainly on the M line.  $\beta$ -AR stimulation generated a significantly greater level of cAMP in the PKA-RII compartment compared to the PKA-RI compartment in this cell type. These results support the work completed previously in neonatal myocytes (Di Benedetto et al. 2008). The major finding in this chapter was that PDE activity is higher in the PKA-RI compartment compared to the PKA-RII compartment after  $\beta$ -AR stimulation with isoproterenol (ISO). Selective inhibition of different PDE families revealed that PDE2 and PDE4 are mainly coupled with the PKA-RI compartment after ISO stimulation, but also regulate cAMP levels in the PKA-RII compartment. PDE3 was only found to be associated with the PKA-RI compartment.

In the next chapter of this thesis, the same FRET-based sensors were employed to study cAMP dynamics in an *in vitro* model of catecholamine-induced cardiomyocyte hypertrophy.

Primary cultured ARVMs were treated overnight with norepinephrine (NE) to establish an *in vitro* model of cardiomyocyte hypertrophy in adult rat ventricular myocytes (ARVM), replicating chronic catecholamine stimulation of  $\beta$ -ARs that can occur *in vivo* leading to

heart hypertrophy. Myocytes developed a clear hypertrophic phenotype as confirmed by analysis of several parameters, including cell surface area and switch on of the cardiac fetal gene program (ANP and skeletal  $\alpha$ -actin expression levels). Some of these parameters have been then utilised throughout this work as a marker of the hypertrophic phenotype.

FRET-based imaging revealed that in hypertrophic myocytes the difference in cAMP generation between the PKA-RI and PKA-RII compartments upon ISO treatment is abolished. Both compartments also have a significantly reduced response compared to control cells, suggesting down regulation of the  $\beta$ -ARs. The major finding of this part of my work is that global cAMP-hydrolytic activity is significantly increased in hypertrophic ARVM after ISO stimulation and more specifically this increase in PDE activity was found to occur in the PKA-RII compartment. To identify which PDE family may be responsible for the increased enzymatic activity in hypertrophic myocytes, cells were treated with selective PDE inhibitors and compared with control ARVM. Altered activity was found in all the PDE families investigated. There was a significant increase in PDE2 and PDE4 activity in the PKA-RII activity in hypertrophic myocytes. FRET imaging also exposed a loss of PDE3 and PDE4 activity in the PKA-RI compartment.

Interestingly, analysis of both PDE2 mRNA and protein levels indicated that the increased PDE2 activity detected in hypertrophic myocytes does not correlate with an increase in PDE2 expression levels, thus suggesting that PDE2 activity might be post-transcriptionally regulated. Immunostaining of ARVM revealed that PDE4B and PDE4D localisation were altered in hypertrophic myocytes where a higher correlation with  $\alpha$ -actinin is detected. A kinase anchoring proteins (AKAPs) have been shown to form complexes with PDEs in macromolecular complexes, for example mAKAP and Yotiao bind PDE4D3 in close proximity of PKA targets, which results in a tighter regulation of the cAMP signal. Altered PDE4 localisation could signify altered AKAP expression. Relocation of AKAPs was also indicated by immunofluorescence experiments where hypertrophic ARVM were treated with RI\_epac and RII\_epac then stained for  $\alpha$ -actinin and compared to control myocytes. One possibility for future work would be to generate new FRET sensors targeted to specific AKAPs of the heart, which will give a more detailed map of cAMP signalling and PDE control, as well as more information on which AKAPs are relocated in disease models.

In the next part of this thesis, it was demonstrated that, in ARVM, cGMP can alter cAMP levels through the modulation of PDE2 and PDE3 activity. Treatment with the NO donor

SNAP resulted in an inversion of the cAMP gradients in the PKA-RI and PKA-RII regions, upon ISO stimulation. This inversion is dependent on cGMP generation and on the compartment specific modulation of PDE2 and PDE3. In particular my data indicate that there is a functional association between PDE3 and the PKA-RI compartment and PDE2 and the PKA-RII compartment after cGMP production is stimulated. These results confirmed what had previously been published in neonatal myocytes (Stangherlin et al. 2011). FRET microscopy experiments showed that in hypertrophied ARVM, basal cGMP levels are significantly higher than in control cells. It was hypothesised that the increased PDE2 activity recorded in hypertrophic conditions may be due to an increased cGMP-mediated activation of this enzyme, where the largest increase in basal cGMP was recorded in the PKA-RII compartment. Increased cGMP levels in hypertrophic myocytes may be linked to altered  $\beta_3$ -AR signalling, as  $\beta_3$ -AR stimulation can elevate cGMP levels via activated NOS.  $\beta_3$ -ARs were found to be coupled to the PKA-RI compartment in control ARVM, whereas these receptors are mainly associated with the PKA-RII in catecholamine-induced hypertrophic cardiomyocytes.

In the final part of this thesis, it was demonstrated that PDE2 activity is pro-hypertrophic and that inhibition of PDE2 blunts the NE-induced hypertrophic growth. This hypothesis suggests that cGMP mediated activation of PDE2 is pro-hypertrophic. This is in contrast with evidence reported in the literature showing an anti-hypertrophic role of cGMP (Ritchie et al. 1998; Horio et al. 2000; Rosenkranz et al. 2003; Zahabi et al. 2003). One possible explanation for this discrepancy between these results and the literature is that in cardiac myocytes cGMP is also compartmentalised (Castro et al. 2006; Fischmeister et al. 2006; Stangherlin et al. 2011), and thus it is possible that a specific pool of cGMP, by activating PDE2, may play a pro-hypertrophic role, whereas cGMP in a different region may exert anti-hypertrophic effects.

In support of this hypothesis, Yanaka and colleagues published data reporting that PDE2 activity is significantly increased in rats that have undergone surgical thoracic aortic constriction (TAC) to induce cardiac hypertrophy by pressure-overload (Yanaka et al. 2003). This study indicates that cGMP mediated activation of PDE2 plays a role in cardiac hypertrophy. Recently, Aye and co-workers reported a significant increase in PDE2 and PKG in the human failing heart (Aye et al. 2012).

Furthermore, overexpression of PDE2 in ARVM with an adenovirus carrying the wild type enzyme was sufficient enough to induce hypertrophic growth in vitro. These data indicate

that PDE2 is involved in the development of cardiomyocyte hypertrophy. It would be interesting to explore whether PDE2 is increased in other models of cardiac hypertrophy, for example, in models of both adaptive (i.e. exercise induce hypertrophy) or maladaptive (i.e. thoracic aortic constriction (TAC) or isoproterenol infusion) cardiomyocyte hypertrophy, and explore the impact of PDE2 inhibition with Bay 60-7550 in these animals. Another interesting aspect to explore is whether inhibition of PDE2 can reverse the hypertrophic phenotype by investigating the effects of Bay 60-7550 treatments in animal models where cardiac hypertrophy is fully developed.

In cardiac myocytes, activation of the cAMP/ PKA pathway is generally considered to be pro-hypertrophic (Iwase et al. 1996; Engelhardt et al. 1999; Antos et al. 2001). However, in this thesis the anti-hypertrophic effects of Bay 60-7550 were found to be mediated by activation of PKA. To investigate the role of cAMP/PKA signalling in the development of cardiomyocyte hypertrophy, cAMP levels were enhanced using selective PDE inhibitors and forskolin overnight to study whether they promoted hypertrophic growth. Interestingly, there is a noticeable increase in cell surface area of ARVM is when intracellular cAMP content is increased via direct activation of adenylyl cyclases, or via inhibition of PDE3 or PDE4. However, inhibition of PDE2 does not promote hypertrophic growth.

Although this seems to be a contradiction, it is possible that PDE2 controls a distinct pool of cAMP which subsequently activates a subset of PKA that has anti-hypertrophic effects, whereas PDE3 and PDE4 control different pools of cAMP that mediate pro-hypertrophic responses. This idea suggests that in cardiac myocytes PDE2, PDE3 and PDE4 are compartmentalised. Immunostaining of ARVM for these PDEs revealed different localisations of these enzymes. Data previously published by Mongillo et al. in rat neonatal cardiomyocytes also supports this hypothesis (Mongillo et al. 2004; Mongillo et al. 2006). It was recently shown, both *in vitro* and *in vivo*, that PKA phosphorylates NFAT at the level of Ser245, Ser269 and Ser 294 thereby preventing its translocation into the nucleus (Sheridan et al. 2002). The authors showed that mutation of these serines to alanines not only prevents PKA phosphorylation, but also the ability of PKA to oppose calcineurin-mediated dephosphorylation and nuclear accumulation of NFAT. It is possible that PKA mediated phosphorylation of NFAT may be one mechanism through which the pool controlled by PDE2 counteracts catecholamine-induced hypertrophy. However, further experiments are required to confirm this hypothesis, for example western blot analysis of NFAT phosphorylation levels. However, difficulties with antibodies specificity and very

low level of expression of endogenous NFAT may make these experiments difficult to complete. An alternative approach is to overexpress a GFP-tagged version of NFAT in ARVM to increase efficiency of an immunoprecipitation and test the level of NFAT phosphorylation upon treatment with NE, NE and Bay 60-7550 and a combination of NE, Bay 607550 and a PKA inhibitor.

Another way in which PKA may play anti-hypertrophic role was described by Backs and colleagues (Backs et al. 2011). In this work the authors showed that PKA phosphorylates histone deacetylase 4 (HDAC4), thereby promoting the generation of an N-terminal HDAC4 cleavage product (HDAC4-NT) which in turn selectively inhibits the activity of the pro-hypertrophic myocytes enhance factor 2 (MEF2). This is a potentially interesting alternative target and experiments are planned to explore the possibility that this mechanism contributes to the anti-hypertrophic effects of PDE2 inhibition.

The major limitation of this study was that cardiomyocyte hypertrophy was induced *in vitro*. As hypertrophy is a complex multifactorial disease involving a number of different signalling pathways, it would be more relevant to study the role of cAMP in an *in vivo* setting, either by chronic catecholamine exposure *in vivo*, thoracic aortic constriction (TAC) or genetic mouse models of hypertrophy. However, due to time constraints and no experience in this type of *in vivo* experimentation in the lab, it was decided to use a similar *in vitro* model that had already proved successful in neonatal cardiomyocytes. The benefits of *in vitro* investigation of the cAMP signalling pathway in hypertrophy is that this type of treatment is quick, relatively inexpensive, highly reproducible and gives the investigator more control by simplifying the system under investigation, allowing direct study of the single pathway of interest. There are some disadvantages of this type of model, for example, cells are maintained under non-physiological conditions. Cell densities are often less than *in vivo* tissue, which impairs intracellular signalling. Culture conditions are also not homeostatic (sudden exchange of media, continuous depletion of nutrients and accumulation of waste products) could alter results. These factors can sometimes become challenging when trying to extrapolate the results back to the biology of the whole organism and must be taken into consideration. Future work will be carried out in TAC treated rats to see if the same key findings of hypertrophy induced *in vitro* also occur during *in vivo* hypertrophy.

Another drawback of this study is the way in which cell size was calculated. As cardiomyocytes are not flat, a more accurate method to measure myocyte growth would be

to calculate the volume of the cell. This could be done using a confocal microscope and the Z-stack function to take slice by slice images of the cell which can be reconstructed to form a 3D image of the cardiomyocyte, giving the exact dimensions. This method was not applied due to time constraints. Each Z-stack image can take a number of minutes to produce compared to seconds using the bright field option of the epifluorescent microscope. The confocal microscope used was shared between a numbers of different departments and therefore was not always available.

The results in this thesis therefore identify PDE2 as a potential therapeutic target in the treatment of cardiac hypertrophy, however further experiments would be required to gain a better understanding on the role of PDE2 in this disease state. However, as PDE2 is expressed in other tissues, such as the brain, in endothelial cells and in platelets (Bender et al. 2006), global inhibition of this enzyme may result in adverse effects, as previously reported after long-term use of selective PDE3 inhibitors (Packer et al. 1991; Movsesian and Alharethi 2002). In this study, the greatest increase in PDE2 was found to be in the PKA-RII compartment activity in hypertrophic ARVM. Targeted PDE inhibition may be an option to selectively increase cAMP in this compartment without affecting the PDE2 activity in other areas. One possible alternative approach to overcome the potential undesirable effects of global pharmacological PDE inhibition would be the development of disrupting peptides or of small molecules designed to selectively displace the subset of PDE2 which is involved in hypertrophy. Further studies are therefore necessary to expose the specific intracellular localisation of the pro-hypertrophic pool of PDE2, as well as its interaction partners and its potential targets.

The work presented in this thesis advances our understanding of how cAMP/PKA signals are regulated in the PKA-RI and PKA-RII compartments of the heart. Alterations in cAMP signalling and PDE modulation of these compartments have been identified in an *in vitro* model of catecholamine-induced cardiac hypertrophy.

## 9 List of References

---

- Abi-Gerges, A., W. Richter, F. Lefebvre, P. Mateo, A. Varin, C. Heymes, J. L. Samuel, C. Lugnier, M. Conti, R. Fischmeister and G. Vandecasteele (2009). "Decreased expression and activity of cAMP phosphodiesterases in cardiac hypertrophy and its impact on beta-adrenergic cAMP signals." *Circ Res* **105**(8): 784-792.
- Adams, S. R., A. T. Harootunian, Y. J. Buechler, S. S. Taylor and R. Y. Tsien (1991). "Fluorescence ratio imaging of cyclic AMP in single cells." *Nature* **349**(6311): 694-697.
- Adler, J. and I. Parmryd (2010). "Quantifying colocalization by correlation: the Pearson correlation coefficient is superior to the Mander's overlap coefficient." *Cytometry A* **77**(8): 733-742.
- Ahmet, I., M. Krawczyk, P. Heller, C. Moon, E. G. Lakatta and M. I. Talan (2004). "Beneficial effects of chronic pharmacological manipulation of beta-adrenoreceptor subtype signaling in rodent dilated ischemic cardiomyopathy." *Circulation* **110**(9): 1083-1090.
- Ahmet, I., E. G. Lakatta and M. I. Talan (2005). "Pharmacological stimulation of beta2-adrenergic receptors (beta2AR) enhances therapeutic effectiveness of beta1AR blockade in rodent dilated ischemic cardiomyopathy." *Heart Fail Rev* **10**(4): 289-296.
- Akhter, S. A., L. M. Luttrell, H. A. Rockman, G. Iaccarino, R. J. Lefkowitz and W. J. Koch (1998). "Targeting the receptor-Gq interface to inhibit in vivo pressure overload myocardial hypertrophy." *Science* **280**(5363): 574-577.
- Amin, J. K., L. Xiao, D. R. Pimental, P. J. Pagano, K. Singh, D. B. Sawyer and W. S. Colucci (2001). "Reactive oxygen species mediate alpha-adrenergic receptor-stimulated hypertrophy in adult rat ventricular myocytes." *J Mol Cell Cardiol* **33**(1): 131-139.
- Angelo, R. and C. S. Rubin (1998). "Molecular characterization of an anchor protein (AKAPCE) that binds the RI subunit (RCE) of type I protein kinase A from *Caenorhabditis elegans*." *J Biol Chem* **273**(23): 14633-14643.
- Antos, C. L., N. Frey, S. O. Marx, S. Reiken, M. Gaburjakova, J. A. Richardson, A. R. Marks and E. N. Olson (2001). "Dilated cardiomyopathy and sudden death resulting from constitutive activation of protein kinase a." *Circ Res* **89**(11): 997-1004.
- Archer, S. L., J. M. Huang, V. Hampl, D. P. Nelson, P. J. Shultz and E. K. Weir (1994). "Nitric oxide and cGMP cause vasorelaxation by activation of a charybdotoxin-sensitive K channel by cGMP-dependent protein kinase." *Proc Natl Acad Sci U S A* **91**(16): 7583-7587.
- Aye, T. T., S. Soni, T. A. van Veen, M. A. van der Heyden, S. Cappadona, A. Varro, R. A. de Weger, N. de Jonge, M. A. Vos, A. J. Heck and A. Scholten (2012). "Reorganized PKA-AKAP associations in the failing human heart." *J Mol Cell Cardiol* **52**(2): 511-518.

- Backs, J., B. C. Worst, L. H. Lehmann, D. M. Patrick, Z. Jebessa, M. M. Kreusser, Q. Sun, L. Chen, C. Heft, H. A. Katus and E. N. Olson (2011). "Selective repression of MEF2 activity by PKA-dependent proteolysis of HDAC4." *J Cell Biol* **195**(3): 403-415.
- Baillie, G. S., A. Sood, I. McPhee, I. Gall, S. J. Perry, R. J. Lefkowitz and M. D. Houslay (2003). "beta-Arrestin-mediated PDE4 cAMP phosphodiesterase recruitment regulates beta-adrenoceptor switching from Gs to Gi." *Proc Natl Acad Sci U S A* **100**(3): 940-945.
- Banky, P., L. J. Huang and S. S. Taylor (1998). "Dimerization/docking domain of the type Ialpha regulatory subunit of cAMP-dependent protein kinase. Requirements for dimerization and docking are distinct but overlapping." *J Biol Chem* **273**(52): 35048-35055.
- Banky, P., M. G. Newlon, M. Roy, S. Garrod, S. S. Taylor and P. A. Jennings (2000). "Isoform-specific differences between the type Ialpha and IIalpha cyclic AMP-dependent protein kinase anchoring domains revealed by solution NMR." *J Biol Chem* **275**(45): 35146-35152.
- Banner, K. H. and N. J. Press (2009). "Dual PDE3/4 inhibitors as therapeutic agents for chronic obstructive pulmonary disease." *Br J Pharmacol* **157**(6): 892-906.
- Banyasz, T., I. Lozinskiy, C. E. Payne, S. Edelmann, B. Norton, B. Chen, Y. Chen-Izu, L. T. Izu and C. W. Balke (2008). "Transformation of adult rat cardiac myocytes in primary culture." *Exp Physiol* **93**(3): 370-382.
- Barouch, L. A., T. P. Cappola, R. W. Harrison, J. K. Crone, E. R. Rodriguez, A. L. Burnett and J. M. Hare (2003). "Combined loss of neuronal and endothelial nitric oxide synthase causes premature mortality and age-related hypertrophic cardiac remodeling in mice." *J Mol Cell Cardiol* **35**(6): 637-644.
- Barry, S. P., S. M. Davidson and P. A. Townsend (2008). "Molecular regulation of cardiac hypertrophy." *Int J Biochem Cell Biol* **40**(10): 2023-2039.
- Baruscotti, M., A. Barbuti and A. Bucchi (2010). "The cardiac pacemaker current." *J Mol Cell Cardiol* **48**(1): 55-64.
- Bauman, A. L., J. Soughayer, B. T. Nguyen, D. Willoughby, G. K. Carnegie, W. Wong, N. Hoshi, L. K. Langeberg, D. M. Cooper, C. W. Dessauer and J. D. Scott (2006). "Dynamic regulation of cAMP synthesis through anchored PKA-adenylyl cyclase V/VI complexes." *Mol Cell* **23**(6): 925-931.
- Beavo, J. A. (1995). "Cyclic nucleotide phosphodiesterases: functional implications of multiple isoforms." *Physiol Rev* **75**(4): 725-748.
- Beavo, J. A. and L. L. Brunton (2002). "Cyclic nucleotide research -- still expanding after half a century." *Nat Rev Mol Cell Biol* **3**(9): 710-718.
- Beavo, J. A., J. G. Hardman and E. W. Sutherland (1971). "Stimulation of adenosine 3',5'-monophosphate hydrolysis by guanosine 3',5'-monophosphate." *J Biol Chem* **246**(12): 3841-3846.
- Beazely, M. A. and V. J. Watts (2006). "Regulatory properties of adenylyl cyclases type 5 and 6: A progress report." *Eur J Pharmacol* **535**(1-3): 1-12.
- Beltrami, A. P., L. Barlucchi, D. Torella, M. Baker, F. Limana, S. Chimenti, H. Kasahara, M. Rota, E. Musso, K. Urbanek, A. Leri, J. Kajstura, B. Nadal-Ginard and P. Anversa (2003). "Adult cardiac stem cells are multipotent and support myocardial regeneration." *Cell* **114**(6): 763-776.
- Beltrami, A. P., K. Urbanek, J. Kajstura, S. M. Yan, N. Finato, R. Bussani, B. Nadal-Ginard, F. Silvestri, A. Leri, C. A. Beltrami and P. Anversa (2001).

- "Evidence that human cardiac myocytes divide after myocardial infarction." *N Engl J Med* **344**(23): 1750-1757.
- Bender, A. T. and J. A. Beavo (2006). "Cyclic nucleotide phosphodiesterases: molecular regulation to clinical use." *Pharmacol Rev* **58**(3): 488-520.
- Bentley, J. K., D. M. Juilfs and M. D. Uhler (2001). "Nerve growth factor inhibits PC12 cell PDE 2 phosphodiesterase activity and increases PDE 2 binding to phosphoproteins." *J Neurochem* **76**(4): 1252-1263.
- Bers, D. M. (2002). "Cardiac excitation-contraction coupling." *Nature* **415**(6868): 198-205.
- Bers, D. M. (2008). "Calcium cycling and signaling in cardiac myocytes." *Annu Rev Physiol* **70**: 23-49.
- Bers, D. M. and T. Guo (2005). "Calcium signaling in cardiac ventricular myocytes." *Ann N Y Acad Sci* **1047**: 86-98.
- Berthet, J., T. W. Rall and E. W. Sutherland (1957). "The relationship of epinephrine and glucagon to liver phosphorylase. IV. Effect of epinephrine and glucagon on the reactivation of phosphorylase in liver homogenates." *J Biol Chem* **224**(1): 463-475.
- Bessay, E. P., R. Zoraghi, M. A. Blount, K. A. Grimes, A. Beasley, S. H. Francis and J. D. Corbin (2007). "Phosphorylation of phosphodiesterase-5 is promoted by a conformational change induced by sildenafil, vardenafil, or tadalafil." *Front Biosci* **12**: 1899-1910.
- Bogdanov, K. Y., T. M. Vinogradova and E. G. Lakatta (2001). "Sinoatrial nodal cell ryanodine receptor and Na(+)-Ca(2+) exchanger: molecular partners in pacemaker regulation." *Circ Res* **88**(12): 1254-1258.
- Bohm, M. (1995). "Alterations of beta-adrenoceptor-G-protein-regulated adenylyl cyclase in heart failure." *Mol Cell Biochem* **147**(1-2): 147-160.
- Bohm, M., P. Gierschik, A. Knorr, K. Larisch, K. Weismann and E. Erdmann (1992). "Desensitization of adenylyl cyclase and increase of Gi alpha in cardiac hypertrophy due to acquired hypertension." *Hypertension* **20**(1): 103-112.
- Bos, J. L. (2003). "Epac: a new cAMP target and new avenues in cAMP research." *Nat Rev Mol Cell Biol* **4**(9): 733-738.
- Bos, J. L. (2006). "Epac proteins: multi-purpose cAMP targets." *Trends Biochem Sci* **31**(12): 680-686.
- Breckler, M., M. Berthouze, A. C. Laurent, B. Crozatier, E. Morel and F. Lezoualc'h (2011). "Rap-linked cAMP signaling Epac proteins: compartmentation, functioning and disease implications." *Cell Signal* **23**(8): 1257-1266.
- Brenner, B. M., B. J. Ballermann, M. E. Gunning and M. L. Zeidel (1990). "Diverse biological actions of atrial natriuretic peptide." *Physiol Rev* **70**(3): 665-699.
- Bristow, M. R. (1998). "Why does the myocardium fail? Insights from basic science." *Lancet* **352** Suppl 1: S18-14.
- Broillet, M. C. (2000). "A single intracellular cysteine residue is responsible for the activation of the olfactory cyclic nucleotide-gated channel by NO." *J Biol Chem* **275**(20): 15135-15141.
- Brown, H. F., D. DiFrancesco and S. J. Noble (1979). "How does adrenaline accelerate the heart?" *Nature* **280**(5719): 235-236.
- Brunton, L. L., J. S. Hayes and S. E. Mayer (1979). "Hormonally specific phosphorylation of cardiac troponin I and activation of glycogen phosphorylase." *Nature* **280**(5717): 78-80.

- Buechler, J. A. and S. S. Taylor (1990). "Differential labeling of the catalytic subunit of cAMP-dependent protein kinase with a water-soluble carbodiimide: identification of carboxyl groups protected by MgATP and inhibitor peptides." *Biochemistry* **29**(7): 1937-1943.
- Buxton, I. L. and L. L. Brunton (1983). "Compartments of cyclic AMP and protein kinase in mammalian cardiomyocytes." *J Biol Chem* **258**(17): 10233-10239.
- Calaghan, S., L. Kozera and E. White (2008). "Compartmentalisation of cAMP-dependent signalling by caveolae in the adult cardiac myocyte." *J Mol Cell Cardiol* **45**(1): 88-92.
- Calaghan, S. and E. White (2006). "Caveolae modulate excitation-contraction coupling and beta2-adrenergic signalling in adult rat ventricular myocytes." *Cardiovasc Res* **69**(4): 816-824.
- Calderone, A., C. M. Thaik, N. Takahashi, D. L. Chang and W. S. Colucci (1998). "Nitric oxide, atrial natriuretic peptide, and cyclic GMP inhibit the growth-promoting effects of norepinephrine in cardiac myocytes and fibroblasts." *J Clin Invest* **101**(4): 812-818.
- Carlisle Michel, J. J., K. L. Dodge, W. Wong, N. C. Mayer, L. K. Langeberg and J. D. Scott (2004). "PKA-phosphorylation of PDE4D3 facilitates recruitment of the mAKAP signalling complex." *Biochem J* **381**(Pt 3): 587-592.
- Carlson, C. R., B. Lygren, T. Berge, N. Hoshi, W. Wong, K. Tasken and J. D. Scott (2006). "Delineation of type I protein kinase A-selective signaling events using an RI anchoring disruptor." *J Biol Chem* **281**(30): 21535-21545.
- Carr, D. W., Z. E. Hausken, I. D. Fraser, R. E. Stofko-Hahn and J. D. Scott (1992). "Association of the type II cAMP-dependent protein kinase with a human thyroid RII-anchoring protein. Cloning and characterization of the RII-binding domain." *J Biol Chem* **267**(19): 13376-13382.
- Carr, D. W., R. E. Stofko-Hahn, I. D. Fraser, S. M. Bishop, T. S. Acott, R. G. Brennan and J. D. Scott (1991). "Interaction of the regulatory subunit (RII) of cAMP-dependent protein kinase with RII-anchoring proteins occurs through an amphipathic helix binding motif." *J Biol Chem* **266**(22): 14188-14192.
- Castro, L. R., I. Verde, D. M. Cooper and R. Fischmeister (2006). "Cyclic guanosine monophosphate compartmentation in rat cardiac myocytes." *Circulation* **113**(18): 2221-2228.
- Cazorla, O., A. Lucas, F. Poirier, A. Lacampagne and F. Lezoualc'h (2009). "The cAMP binding protein Epac regulates cardiac myofilament function." *Proc Natl Acad Sci U S A* **106**(33): 14144-14149.
- Chen, L., M. L. Marquardt, D. J. Tester, K. J. Sampson, M. J. Ackerman and R. S. Kass (2007). "Mutation of an A-kinase-anchoring protein causes long-QT syndrome." *Proc Natl Acad Sci U S A* **104**(52): 20990-20995.
- Chen, L. A., D. E. Vatner, S. F. Vatner, L. Hittinger and C. J. Homcy (1991). "Decreased Gs alpha mRNA levels accompany the fall in Gs and adenylyl cyclase activities in compensated left ventricular hypertrophy. In heart failure, only the impairment in adenylyl cyclase activation progresses." *J Clin Invest* **87**(1): 293-298.
- Cheng, H. J., Z. S. Zhang, K. Onishi, T. Ukai, D. C. Sane and C. P. Cheng (2001). "Upregulation of functional beta(3)-adrenergic receptor in the failing canine myocardium." *Circ Res* **89**(7): 599-606.
- Chesley, A., M. S. Lundberg, T. Asai, R. P. Xiao, S. Ohtani, E. G. Lakatta and M. T. Crow (2000). "The beta(2)-adrenergic receptor delivers an

- antiapoptotic signal to cardiac myocytes through G(i)-dependent coupling to phosphatidylinositol 3'-kinase." *Circ Res* **87**(12): 1172-1179.
- Cheung, R., M. S. Erclik and J. Mitchell (2005). "1,25-dihydroxyvitamin D(3) stimulated protein kinase C phosphorylation of type VI adenylyl cyclase inhibits parathyroid hormone signal transduction in rat osteoblastic UMR 106-01 cells." *J Cell Biochem* **94**(5): 1017-1027.
- Chien, K. R., K. U. Knowlton, H. Zhu and S. Chien (1991). "Regulation of cardiac gene expression during myocardial growth and hypertrophy: molecular studies of an adaptive physiologic response." *FASEB J* **5**(15): 3037-3046.
- Chomczynski, P. and N. Sacchi (1987). "Single-step method of RNA isolation by acid guanidinium thiocyanate-phenol-chloroform extraction." *Anal Biochem* **162**(1): 156-159.
- Christian, F., M. Szaszak, S. Friedl, S. Drewianka, D. Lorenz, A. Goncalves, J. Furkert, C. Vargas, P. Schmieder, F. Gotz, K. Zuhlke, M. Moutty, H. Gottert, M. Joshi, B. Reif, H. Haase, I. Morano, S. Grossmann, A. Klukovits, J. Verli, R. Gaspar, C. Noack, M. Bergmann, R. Kass, K. Hampel, D. Kashin, H. G. Genieser, F. W. Herberg, D. Willoughby, D. M. Cooper, G. S. Baillie, M. D. Houslay, J. P. von Kries, B. Zimmermann, W. Rosenthal and E. Klussmann (2011). "Small molecule AKAP-protein kinase A (PKA) interaction disruptors that activate PKA interfere with compartmentalized cAMP signaling in cardiac myocytes." *J Biol Chem* **286**(11): 9079-9096.
- Clegg, R. (1996). "Fluorescence Imaging Spectroscopy and Microscopy." *New York: John Wiley & Sons.*: 179-251.
- Colledge, M. and J. D. Scott (1999). "AKAPs: from structure to function." *Trends Cell Biol* **9**(6): 216-221.
- Communal, C., K. Singh, D. B. Sawyer and W. S. Colucci (1999). "Opposing effects of beta(1)- and beta(2)-adrenergic receptors on cardiac myocyte apoptosis : role of a pertussis toxin-sensitive G protein." *Circulation* **100**(22): 2210-2212.
- Conti, M. and J. Beavo (2007). "Biochemistry and physiology of cyclic nucleotide phosphodiesterases: essential components in cyclic nucleotide signaling." *Annu Rev Biochem* **76**: 481-511.
- Cooper, D. M. (2003). "Regulation and organization of adenylyl cyclases and cAMP." *Biochem J* **375**(Pt 3): 517-529.
- Corbin, J. D. and S. L. Keely (1977). "Characterization and regulation of heart adenosine 3':5'-monophosphate-dependent protein kinase isozymes." *J Biol Chem* **252**(3): 910-918.
- Cote, R. H. (2004). "Characteristics of photoreceptor PDE (PDE6): similarities and differences to PDE5." *Int J Impot Res* **16 Suppl 1**: S28-33.
- Crabtree, G. R. (1999). "Generic signals and specific outcomes: signaling through Ca<sup>2+</sup>, calcineurin, and NF-AT." *Cell* **96**(5): 611-614.
- Cuffe, M. S., R. M. Califf, K. F. Adams, Jr., R. Benza, R. Bourge, W. S. Colucci, B. M. Massie, C. M. O'Connor, I. Pina, R. Quigg, M. A. Silver and M. Gheorghide (2002). "Short-term intravenous milrinone for acute exacerbation of chronic heart failure: a randomized controlled trial." *JAMA* **287**(12): 1541-1547.
- Cummings, D. E., E. P. Brandon, J. V. Planas, K. Motamed, R. L. Idzerda and G. S. McKnight (1996). "Genetically lean mice result from targeted disruption of the RII beta subunit of protein kinase A." *Nature* **382**(6592): 622-626.

- Daaka, Y., L. M. Luttrell and R. J. Lefkowitz (1997). "Switching of the coupling of the beta2-adrenergic receptor to different G proteins by protein kinase A." *Nature* **390**(6655): 88-91.
- De Arcangelis, V., S. Liu, D. Zhang, D. Soto and Y. K. Xiang (2010). "Equilibrium between adenylyl cyclase and phosphodiesterase patterns adrenergic agonist dose-dependent spatiotemporal cAMP/protein kinase A activities in cardiomyocytes." *Mol Pharmacol* **78**(3): 340-349.
- De Arcangelis, V., D. Soto and Y. Xiang (2008). "Phosphodiesterase 4 and phosphatase 2A differentially regulate cAMP/protein kinase a signaling for cardiac myocyte contraction under stimulation of beta1 adrenergic receptor." *Mol Pharmacol* **74**(5): 1453-1462.
- de Rooij, J., H. Rehmann, M. van Triest, R. H. Cool, A. Wittinghofer and J. L. Bos (2000). "Mechanism of regulation of the Epac family of cAMP-dependent RapGEFs." *J Biol Chem* **275**(27): 20829-20836.
- de Rooij, J., F. J. Zwartkruis, M. H. Verheijen, R. H. Cool, S. M. Nijman, A. Wittinghofer and J. L. Bos (1998). "Epac is a Rap1 guanine-nucleotide-exchange factor directly activated by cyclic AMP." *Nature* **396**(6710): 474-477.
- Defer, N., M. Best-Belpomme and J. Hanoune (2000). "Tissue specificity and physiological relevance of various isoforms of adenylyl cyclase." *Am J Physiol Renal Physiol* **279**(3): F400-416.
- Degerman, E., P. Belfrange and V. C. Manganiello (1997). "Structure, localization, and regulation of cGMP-inhibited phosphodiesterase (PDE3)." *J Biol Chem* **272**(11): 6823-6826.
- Dessauer, C. W. (2009). "Adenylyl cyclase--A-kinase anchoring protein complexes: the next dimension in cAMP signaling." *Mol Pharmacol* **76**(5): 935-941.
- Devic, E., Y. Xiang, D. Gould and B. Kobilka (2001). "Beta-adrenergic receptor subtype-specific signaling in cardiac myocytes from beta(1) and beta(2) adrenoceptor knockout mice." *Mol Pharmacol* **60**(3): 577-583.
- Di Benedetto, G., A. Zoccarato, V. Lissandron, A. Terrin, X. Li, M. D. Houslay, G. S. Baillie and M. Zaccolo (2008). "Protein kinase A type I and type II define distinct intracellular signaling compartments." *Circ Res* **103**(8): 836-844.
- Dickinson, N. T., E. K. Jang and R. J. Haslam (1997). "Activation of cGMP-stimulated phosphodiesterase by nitroprusside limits cAMP accumulation in human platelets: effects on platelet aggregation." *Biochem J* **323** ( Pt 2): 371-377.
- Diebold, I., T. Djordjevic, A. Petry, A. Hatzelmann, H. Tenor, J. Hess and A. Grolach (2009). "Phosphodiesterase 2 mediates redox-sensitive endothelial cell proliferation and angiogenesis by thrombin via Rac1 and NADPH oxidase 2." *Circ Res* **104**(10): 1169-1177.
- DiFrancesco, D. (1985). "The cardiac hyperpolarizing-activated current, if. Origins and developments." *Prog Biophys Mol Biol* **46**(3): 163-183.
- DiFrancesco, D., A. Ferroni, M. Mazzanti and C. Tromba (1986). "Properties of the hyperpolarizing-activated current (if) in cells isolated from the rabbit sino-atrial node." *J Physiol* **377**: 61-88.
- DiFrancesco, D. and P. Tortora (1991). "Direct activation of cardiac pacemaker channels by intracellular cyclic AMP." *Nature* **351**(6322): 145-147.
- Ding, B., J. Abe, H. Wei, H. Xu, W. Che, T. Aizawa, W. Liu, C. A. Molina, J. Sadoshima, B. C. Blaxall, B. C. Berk and C. Yan (2005). "A positive feedback loop of phosphodiesterase 3 (PDE3) and inducible cAMP early

- repressor (ICER) leads to cardiomyocyte apoptosis." Proc Natl Acad Sci U S A **102**(41): 14771-14776.
- DiPilato, L. M., X. Cheng and J. Zhang (2004). "Fluorescent indicators of cAMP and Epac activation reveal differential dynamics of cAMP signaling within discrete subcellular compartments." Proc Natl Acad Sci U S A **101**(47): 16513-16518.
- Diviani, D., K. L. Dodge-Kafka, J. Li and M. S. Kapiloff (2011). "A-kinase anchoring proteins: scaffolding proteins in the heart." Am J Physiol Heart Circ Physiol **301**(5): H1742-1753.
- Dodge-Kafka, K. L., J. Souhayer, G. C. Pare, J. J. Carlisle Michel, L. K. Langeberg, M. S. Kapiloff and J. D. Scott (2005). "The protein kinase A anchoring protein mAKAP coordinates two integrated cAMP effector pathways." Nature **437**(7058): 574-578.
- Dodge, K. L., S. Khouangsathiene, M. S. Kapiloff, R. Mouton, E. V. Hill, M. D. Houslay, L. K. Langeberg and J. D. Scott (2001). "mAKAP assembles a protein kinase A/PDE4 phosphodiesterase cAMP signaling module." EMBO J **20**(8): 1921-1930.
- Dostmann, W. R., S. S. Taylor, H. G. Genieser, B. Jastorff, S. O. Doskeland and D. OGREID (1990). "Probing the cyclic nucleotide binding sites of cAMP-dependent protein kinases I and II with analogs of adenosine 3',5'-cyclic phosphorothioates." J Biol Chem **265**(18): 10484-10491.
- Douglas, P. S., R. Morrow, A. Ioli and N. Reichek (1989). "Left ventricular shape, afterload and survival in idiopathic dilated cardiomyopathy." J Am Coll Cardiol **13**(2): 311-315.
- Dryer, S. E. and D. Henderson (1991). "A cyclic GMP-activated channel in dissociated cells of the chick pineal gland." Nature **353**(6346): 756-758.
- Engelhardt, S., L. Hein, F. Wiesmann and M. J. Lohse (1999). "Progressive hypertrophy and heart failure in beta1-adrenergic receptor transgenic mice." Proc Natl Acad Sci U S A **96**(12): 7059-7064.
- Erneux, C., D. Couchie, J. E. Dumont, J. Baraniak, W. J. Stec, E. G. Abbad, G. Petridis and B. Jastorff (1981). "Specificity of cyclic GMP activation of a multi-substrate cyclic nucleotide phosphodiesterase from rat liver." Eur J Biochem **115**(3): 503-510.
- Espinasse, I., V. Iourgenko, C. Richer, M. Heimbürger, N. Defer, M. C. Bourin, F. Samson, E. Pussard, J. F. Giudicelli, J. B. Michel, J. Hanoune and J. J. Mercadier (1999). "Decreased type VI adenylyl cyclase mRNA concentration and Mg(2+)-dependent adenylyl cyclase activities and unchanged type V adenylyl cyclase mRNA concentration and Mn(2+)-dependent adenylyl cyclase activities in the left ventricle of rats with myocardial infarction and longstanding heart failure." Cardiovasc Res **42**(1): 87-98.
- Feldman, A. M., M. R. Bristow, W. W. Parmley, P. E. Carson, C. J. Pepine, E. M. Gilbert, J. E. Strobeck, G. H. Hendrix, E. R. Powers, R. P. Bain and et al. (1993). "Effects of vesnarinone on morbidity and mortality in patients with heart failure. Vesnarinone Study Group." N Engl J Med **329**(3): 149-155.
- Fiedler, B., S. M. Lohmann, A. Smolenski, S. Linnemüller, B. Pieske, F. Schröder, J. D. Molkentin, H. Drexler and K. C. Wollert (2002). "Inhibition of calcineurin-NFAT hypertrophy signaling by cGMP-dependent protein kinase type I in cardiac myocytes." Proc Natl Acad Sci U S A **99**(17): 11363-11368.
- Fink, M. A., D. R. Zakhary, J. A. Mackey, R. W. Desnoyer, C. Apperson-Hansen, D. S. Damron and M. Bond (2001). "AKAP-mediated targeting of protein

- kinase a regulates contractility in cardiac myocytes." *Circ Res* **88**(3): 291-297.
- Fischmeister, R., L. Castro, A. Abi-Gerges, F. Rochais and G. Vandecasteele (2005). "Species- and tissue-dependent effects of NO and cyclic GMP on cardiac ion channels." *Comp Biochem Physiol A Mol Integr Physiol* **142**(2): 136-143.
- Fischmeister, R., L. R. Castro, A. Abi-Gerges, F. Rochais, J. Jurevicius, J. Leroy and G. Vandecasteele (2006). "Compartmentation of cyclic nucleotide signaling in the heart: the role of cyclic nucleotide phosphodiesterases." *Circ Res* **99**(8): 816-828.
- Flaherty, M. P., M. Brown, I. L. Grupp, J. E. Schultz, S. S. Murphree and W. K. Jones (2007). "eNOS deficient mice develop progressive cardiac hypertrophy with altered cytokine and calcium handling protein expression." *Cardiovasc Toxicol* **7**(3): 165-177.
- Florio, V. A., W. K. Sonnenburg, R. Johnson, K. S. Kwak, G. S. Jensen, K. A. Walsh and J. A. Beavo (1994). "Phosphorylation of the 61-kDa calmodulin-stimulated cyclic nucleotide phosphodiesterase at serine 120 reduces its affinity for calmodulin." *Biochemistry* **33**(30): 8948-8954.
- Fodstad, H., H. Swan, P. Laitinen, K. Piippo, K. Paavonen, M. Viitasalo, L. Toivonen and K. Kontula (2004). "Four potassium channel mutations account for 73% of the genetic spectrum underlying long-QT syndrome (LQTS) and provide evidence for a strong founder effect in Finland." *Ann Med* **36 Suppl 1**: 53-63.
- Förster, T. (1948). "Zwischenmolekulare Energiewanderung und Fluoreszenz." *Annalen der Physik* **437**: 55-75.
- Fowler, M. B., J. A. Laser, G. L. Hopkins, W. Minobe and M. R. Bristow (1986). "Assessment of the beta-adrenergic receptor pathway in the intact failing human heart: progressive receptor down-regulation and subsensitivity to agonist response." *Circulation* **74**(6): 1290-1302.
- Francis, S. H., M. A. Blount and J. D. Corbin (2011). "Mammalian cyclic nucleotide phosphodiesterases: molecular mechanisms and physiological functions." *Physiol Rev* **91**(2): 651-690.
- Frantz, S., M. Klaiber, H. A. Baba, H. Oberwinkler, K. Volker, B. Gabetaner, B. Bayer, M. Abebetar, K. Schuh, R. Feil, F. Hofmann and M. Kuhn (2011). "Stress-dependent dilated cardiomyopathy in mice with cardiomyocyte-restricted inactivation of cyclic GMP-dependent protein kinase I." *Eur Heart J*.
- Fraser, I. D., S. J. Tavalin, L. B. Lester, L. K. Langeberg, A. M. Westphal, R. A. Dean, N. V. Marrion and J. D. Scott (1998). "A novel lipid-anchored A-kinase Anchoring Protein facilitates cAMP-responsive membrane events." *EMBO J* **17**(8): 2261-2272.
- Frey, N. and E. N. Olson (2003). "Cardiac hypertrophy: the good, the bad, and the ugly." *Annu Rev Physiol* **65**: 45-79.
- Fung, M. L., H. Y. Li and T. M. Wong (2002). "Forskolin fails to activate L-type calcium current in hypertrophied cardiomyocytes of chronically hypoxic rats." *Life Sci* **70**(15): 1801-1809.
- Galie, N., L. J. Rubin and G. Simonneau (2010). "Phosphodiesterase inhibitors for pulmonary hypertension." *N Engl J Med* **362**(6): 559-560; author reply 560.
- Gans, J. H. and M. R. Cater (1970). "Norepinephrine induced cardiac hypertrophy in dogs." *Life Sci* **9**(13): 731-740.

- Gao, M. H., H. Bayat, D. M. Roth, J. Yao Zhou, J. Drumm, J. Burhan and H. K. Hammond (2002). "Controlled expression of cardiac-directed adenylylcyclase type VI provides increased contractile function." Cardiovasc Res **56**(2): 197-204.
- Gao, M. H., T. Tang, T. Guo, S. Q. Sun, J. R. Feramisco and H. K. Hammond (2004). "Adenylyl cyclase type VI gene transfer reduces phospholamban expression in cardiac myocytes via activating transcription factor 3." J Biol Chem **279**(37): 38797-38802.
- Gardner, D. G. (2003). "Natriuretic peptides: markers or modulators of cardiac hypertrophy?" Trends Endocrinol Metab **14**(9): 411-416.
- Gaudin, C., Y. Ishikawa, D. C. Wight, V. Mahdavi, B. Nadal-Ginard, T. E. Wagner, D. E. Vatner and C. J. Homcy (1995). "Overexpression of Gs alpha protein in the hearts of transgenic mice." J Clin Invest **95**(4): 1676-1683.
- Gauthier, C., G. Tavernier, F. Charpentier, D. Langin and H. Le Marec (1996). "Functional beta3-adrenoceptor in the human heart." J Clin Invest **98**(2): 556-562.
- Geoffroy, V., F. Fouque, V. Nivet, J. P. Clot, C. Lugnier, B. Desbuquois and C. Benelli (1999). "Activation of a cGMP-stimulated cAMP phosphodiesterase by protein kinase C in a liver Golgi-endosomal fraction." Eur J Biochem **259**(3): 892-900.
- Gesellchen, F., A. Stangherlin, N. Surdo, A. Terrin, A. Zoccarato and M. Zaccolo (2011). "Measuring spatiotemporal dynamics of cyclic AMP signaling in real-time using FRET-based biosensors." Methods Mol Biol **746**: 297-316.
- Gisbert, M. P. and R. Fischmeister (1988). "Atrial natriuretic factor regulates the calcium current in frog isolated cardiac cells." Circ Res **62**(4): 660-667.
- Goaillard, J. M., P. V. Vincent and R. Fischmeister (2001). "Simultaneous measurements of intracellular cAMP and L-type Ca<sup>2+</sup> current in single frog ventricular myocytes." J Physiol **530**(Pt 1): 79-91.
- Gold, M. G., B. Lygren, P. Dokurno, N. Hoshi, G. McConnachie, K. Tasken, C. R. Carlson, J. D. Scott and D. Barford (2006). "Molecular basis of AKAP specificity for PKA regulatory subunits." Mol Cell **24**(3): 383-395.
- Gray, P. C., J. D. Scott and W. A. Catterall (1998). "Regulation of ion channels by cAMP-dependent protein kinase and A-kinase anchoring proteins." Curr Opin Neurobiol **8**(3): 330-334.
- Gupta, A., N. S. Aberle, 2nd, J. Ren and A. C. Sharma (2005). "Endothelin-converting enzyme-1-mediated signaling in adult rat ventricular myocyte contractility and apoptosis during sepsis." J Mol Cell Cardiol **38**(3): 527-537.
- Gustafsson, A. B. and L. L. Brunton (2002). "Attenuation of cAMP accumulation in adult rat cardiac fibroblasts by IL-1beta and NO: role of cGMP-stimulated PDE2." Am J Physiol Cell Physiol **283**(2): C463-471.
- Hambleton, R., J. Krall, E. Tikishvili, M. Honeggar, F. Ahmad, V. C. Manganiello and M. A. Movsesian (2005). "Isoforms of cyclic nucleotide phosphodiesterase PDE3 and their contribution to cAMP hydrolytic activity in subcellular fractions of human myocardium." J Biol Chem **280**(47): 39168-39174.
- Han, X., Y. Shimoni and W. R. Giles (1995). "A cellular mechanism for nitric oxide-mediated cholinergic control of mammalian heart rate." J Gen Physiol **106**(1): 45-65.
- Harding, V. B., L. R. Jones, R. J. Lefkowitz, W. J. Koch and H. A. Rockman (2001). "Cardiac beta ARK1 inhibition prolongs survival and augments beta

- blocker therapy in a mouse model of severe heart failure." Proc Natl Acad Sci U S A **98**(10): 5809-5814.
- Haunstetter, A. and S. Izumo (2000). "Toward antiapoptosis as a new treatment modality." Circ Res **86**(4): 371-376.
- Hausdorff, W. P., M. G. Caron and R. J. Lefkowitz (1990). "Turning off the signal: desensitization of beta-adrenergic receptor function." FASEB J **4**(11): 2881-2889.
- Hausken, Z. E., V. M. Coghlan, C. A. Hastings, E. M. Reimann and J. D. Scott (1994). "Type II regulatory subunit (RII) of the cAMP-dependent protein kinase interaction with A-kinase anchor proteins requires isoleucines 3 and 5." J Biol Chem **269**(39): 24245-24251.
- Hayes, J. S., L. L. Brunton, J. H. Brown, J. B. Reese and S. E. Mayer (1979). "Hormonally specific expression of cardiac protein kinase activity." Proc Natl Acad Sci U S A **76**(4): 1570-1574.
- Haynes, L. and K. W. Yau (1985). "Cyclic GMP-sensitive conductance in outer segment membrane of catfish cones." Nature **317**(6032): 61-64.
- Heller, W. T., D. Vigil, S. Brown, D. K. Blumenthal, S. S. Taylor and J. Trehwella (2004). "C subunits binding to the protein kinase A RI alpha dimer induce a large conformational change." J Biol Chem **279**(18): 19084-19090.
- Hershberger, R. E., A. M. Feldman and M. R. Bristow (1991). "A1-adenosine receptor inhibition of adenylate cyclase in failing and nonfailing human ventricular myocardium." Circulation **83**(4): 1343-1351.
- Higuchi, R., C. Fockler, G. Dollinger and R. Watson (1993). "Kinetic PCR analysis: real-time monitoring of DNA amplification reactions." Biotechnology (N Y) **11**(9): 1026-1030.
- Hill, J. A. (2003). "Electrical remodeling in cardiac hypertrophy." Trends Cardiovasc Med **13**(8): 316-322.
- Hogan, P. G., L. Chen, J. Nardone and A. Rao (2003). "Transcriptional regulation by calcium, calcineurin, and NFAT." Genes Dev **17**(18): 2205-2232.
- Holtwick, R., M. van Eickels, B. V. Skryabin, H. A. Baba, A. Bubikat, F. Begrow, M. D. Schneider, D. L. Garbers and M. Kuhn (2003). "Pressure-independent cardiac hypertrophy in mice with cardiomyocyte-restricted inactivation of the atrial natriuretic peptide receptor guanylyl cyclase-A." J Clin Invest **111**(9): 1399-1407.
- Horio, T., T. Nishikimi, F. Yoshihara, H. Matsuo, S. Takishita and K. Kangawa (2000). "Inhibitory regulation of hypertrophy by endogenous atrial natriuretic peptide in cultured cardiac myocytes." Hypertension **35**(1 Pt 1): 19-24.
- Houslay, M. D. and D. R. Adams (2003). "PDE4 cAMP phosphodiesterases: modular enzymes that orchestrate signalling cross-talk, desensitization and compartmentalization." Biochem J **370**(Pt 1): 1-18.
- Houslay, M. D., G. S. Baillie and D. H. Maurice (2007). "cAMP-Specific phosphodiesterase-4 enzymes in the cardiovascular system: a molecular toolbox for generating compartmentalized cAMP signaling." Circ Res **100**(7): 950-966.
- Huai, Q., H. Wang, W. Zhang, R. W. Colman, H. Robinson and H. Ke (2004). "Crystal structure of phosphodiesterase 9 shows orientation variation of inhibitor 3-isobutyl-1-methylxanthine binding." Proc Natl Acad Sci U S A **101**(26): 9624-9629.
- Huang, L. J., K. Durick, J. A. Weiner, J. Chun and S. S. Taylor (1997). "Identification of a novel protein kinase A anchoring protein that binds

- both type I and type II regulatory subunits." *J Biol Chem* **272**(12): 8057-8064.
- Ikeda, U., Y. Tsuruya and T. Yaginuma (1991). "Alpha 1-adrenergic stimulation is coupled to cardiac myocyte hypertrophy." *Am J Physiol* **260**(3 Pt 2): H953-956.
- Ishii, T. M., M. Takano, L. H. Xie, A. Noma and H. Ohmori (1999). "Molecular characterization of the hyperpolarization-activated cation channel in rabbit heart sinoatrial node." *J Biol Chem* **274**(18): 12835-12839.
- Islam, A., H. Jones, T. Hiroi, J. Lam, J. Zhang, J. Moss, M. Vaughan and S. J. Levine (2008). "cAMP-dependent protein kinase A (PKA) signaling induces TNFR1 exosome-like vesicle release via anchoring of PKA regulatory subunit RIIbeta to BIG2." *J Biol Chem* **283**(37): 25364-25371.
- Iwase, M., S. P. Bishop, M. Uechi, D. E. Vatner, R. P. Shannon, R. K. Kudej, D. C. Wight, T. E. Wagner, Y. Ishikawa, C. J. Homcy and S. F. Vatner (1996). "Adverse effects of chronic endogenous sympathetic drive induced by cardiac GS alpha overexpression." *Circ Res* **78**(4): 517-524.
- Jarnaess, E., A. Ruppelt, A. J. Stokka, B. Lygren, J. D. Scott and K. Tasken (2008). "Dual specificity A-kinase anchoring proteins (AKAPs) contain an additional binding region that enhances targeting of protein kinase A type I." *J Biol Chem* **283**(48): 33708-33718.
- Jaski, B. E., M. A. Fifer, R. F. Wright, E. Braunwald and W. S. Colucci (1985). "Positive inotropic and vasodilator actions of milrinone in patients with severe congestive heart failure. Dose-response relationships and comparison to nitroprusside." *J Clin Invest* **75**(2): 643-649.
- Jurevicius, J. and R. Fischmeister (1996). "cAMP compartmentation is responsible for a local activation of cardiac Ca<sup>2+</sup> channels by beta-adrenergic agonists." *Proc Natl Acad Sci U S A* **93**(1): 295-299.
- Kakkar, R., R. V. Raju and R. K. Sharma (1999). "Calmodulin-dependent cyclic nucleotide phosphodiesterase (PDE1)." *Cell Mol Life Sci* **55**(8-9): 1164-1186.
- Kasai, H. and O. H. Petersen (1994). "Spatial dynamics of second messengers: IP3 and cAMP as long-range and associative messengers." *Trends Neurosci* **17**(3): 95-101.
- Katz, A. M. (2008). "The "modern" view of heart failure: how did we get here?" *Circ Heart Fail* **1**(1): 63-71.
- Kawabe, J., G. Iwami, T. Ebina, S. Ohno, T. Katada, Y. Ueda, C. J. Homcy and Y. Ishikawa (1994). "Differential activation of adenylyl cyclase by protein kinase C isoenzymes." *J Biol Chem* **269**(24): 16554-16558.
- Kawasaki, H., G. M. Springett, S. Toki, J. J. Canales, P. Harlan, J. P. Blumenstiel, E. J. Chen, I. A. Bany, N. Mochizuki, A. Ashbacher, M. Matsuda, D. E. Housman and A. M. Graybiel (1998). "A Rap guanine nucleotide exchange factor enriched highly in the basal ganglia." *Proc Natl Acad Sci U S A* **95**(22): 13278-13283.
- Keely, S. L. (1977). "Activation of cAMP-dependent protein kinase without a corresponding increase in phosphorylase activity." *Res Commun Chem Pathol Pharmacol* **18**(2): 283-290.
- Kerfant, B. G., D. Zhao, I. Lorenzen-Schmidt, L. S. Wilson, S. Cai, S. R. Chen, D. H. Maurice and P. H. Backx (2007). "PI3Kgamma is required for PDE4, not PDE3, activity in subcellular microdomains containing the sarcoplasmic reticular calcium ATPase in cardiomyocytes." *Circ Res* **101**(4): 400-408.

- Kitamura, T., Y. Kitamura, S. Kuroda, Y. Hino, M. Ando, K. Kotani, H. Konishi, H. Matsuzaki, U. Kikkawa, W. Ogawa and M. Kasuga (1999). "Insulin-induced phosphorylation and activation of cyclic nucleotide phosphodiesterase 3B by the serine-threonine kinase Akt." *Mol Cell Biol* **19**(9): 6286-6296.
- Kivisto, T., M. Makiranta, E. L. Oikarinen, S. Karhu, M. Weckstrom and L. C. Sellin (1995). "2,3-Butanedione monoxime (BDM) increases initial yields and improves long-term survival of isolated cardiac myocytes." *Jpn J Physiol* **45**(1): 203-210.
- Knowles, J. W., G. Esposito, L. Mao, J. R. Hagaman, J. E. Fox, O. Smithies, H. A. Rockman and N. Maeda (2001). "Pressure-independent enhancement of cardiac hypertrophy in natriuretic peptide receptor A-deficient mice." *J Clin Invest* **107**(8): 975-984.
- Komuro, I. and Y. Yazaki (1993). "Control of cardiac gene expression by mechanical stress." *Annu Rev Physiol* **55**: 55-75.
- Kopperud, R., A. E. Christensen, E. Kjarland, K. Viste, H. Kleivdal and S. O. Doskeland (2002). "Formation of inactive cAMP-saturated holoenzyme of cAMP-dependent protein kinase under physiological conditions." *J Biol Chem* **277**(16): 13443-13448.
- Kostic, M. M., S. Erdogan, G. Rena, G. Borchert, B. Hoch, S. Bartel, G. Scotland, E. Huston, M. D. Houslay and E. G. Krause (1997). "Altered expression of PDE1 and PDE4 cyclic nucleotide phosphodiesterase isoforms in 7-oxo-prostacyclin-preconditioned rat heart." *J Mol Cell Cardiol* **29**(11): 3135-3146.
- Krebs, E. G. and J. A. Beavo (1979). "Phosphorylation-dephosphorylation of enzymes." *Annu Rev Biochem* **48**: 923-959.
- Krebs, E. G. and E. H. Fischer (1956). "The phosphorylase b to a converting enzyme of rabbit skeletal muscle." *Biochim Biophys Acta* **20**(1): 150-157.
- Kumar, P., G. S. Francis and W. H. Tang (2009). "Phosphodiesterase 5 inhibition in heart failure: mechanisms and clinical implications." *Nat Rev Cardiol* **6**(5): 349-355.
- Kuster, G. M., D. R. Pimentel, T. Adachi, Y. Ido, D. A. Brenner, R. A. Cohen, R. Liao, D. A. Siwik and W. S. Colucci (2005). "Alpha-adrenergic receptor-stimulated hypertrophy in adult rat ventricular myocytes is mediated via thioredoxin-1-sensitive oxidative modification of thiols on Ras." *Circulation* **111**(9): 1192-1198.
- Lafontan, M. (1994). "Differential recruitment and differential regulation by physiological amines of fat cell beta-1, beta-2 and beta-3 adrenergic receptors expressed in native fat cells and in transfected cell lines." *Cell Signal* **6**(4): 363-392.
- Lakatta, E. G., V. A. Maltsev and T. M. Vinogradova (2010). "A coupled SYSTEM of intracellular Ca<sup>2+</sup> clocks and surface membrane voltage clocks controls the timekeeping mechanism of the heart's pacemaker." *Circ Res* **106**(4): 659-673.
- Layland, J., J. M. Li and A. M. Shah (2002). "Role of cyclic GMP-dependent protein kinase in the contractile response to exogenous nitric oxide in rat cardiac myocytes." *J Physiol* **540**(Pt 2): 457-467.
- Lehnart, S. E., X. H. Wehrens, S. Reiken, S. Warriar, A. E. Belevych, R. D. Harvey, W. Richter, S. L. Jin, M. Conti and A. R. Marks (2005). "Phosphodiesterase 4D deficiency in the ryanodine-receptor complex promotes heart failure and arrhythmias." *Cell* **123**(1): 25-35.

- Leroy, J., W. Richter, D. Mika, L. R. Castro, A. Abi-Gerges, M. Xie, C. Scheitrum, F. Lefebvre, J. Schittl, P. Mateo, R. Westenbroek, W. A. Catterall, F. Charpentier, M. Conti, R. Fischmeister and G. Vandecasteele (2011). "Phosphodiesterase 4B in the cardiac L-type Ca(2)(+) channel complex regulates Ca(2)(+) current and protects against ventricular arrhythmias in mice." *J Clin Invest* **121**(7): 2651-2661.
- Levy, D., R. J. Garrison, D. D. Savage, W. B. Kannel and W. P. Castelli (1990). "Prognostic implications of echocardiographically determined left ventricular mass in the Framingham Heart Study." *N Engl J Med* **322**(22): 1561-1566.
- Li, W., S. Mital, C. Ojaimi, A. Csiszar, G. Kaley and T. H. Hintze (2004). "Premature death and age-related cardiac dysfunction in male eNOS-knockout mice." *J Mol Cell Cardiol* **37**(3): 671-680.
- Lipkin, D., Cook WH, Markham R (1959). "Adenosine-3': 5'-phosphoric Acid: A Proof of Structure 1." *Journal of the American Chemical Society* **81**: 6198-6203.
- Lissandron, V. and M. Zaccolo (2006). "Compartmentalized cAMP/PKA signalling regulates cardiac excitation-contraction coupling." *J Muscle Res Cell Motil* **27**(5-7): 399-403.
- Liu, J., H. Dobrzynski, J. Yanni, M. R. Boyett and M. Lei (2007). "Organisation of the mouse sinoatrial node: structure and expression of HCN channels." *Cardiovasc Res* **73**(4): 729-738.
- Liu, M., T. Y. Chen, B. Ahamed, J. Li and K. W. Yau (1994). "Calcium-calmodulin modulation of the olfactory cyclic nucleotide-gated cation channel." *Science* **266**(5189): 1348-1354.
- Lohmann, S. M., P. DeCamilli, I. Einig and U. Walter (1984). "High-affinity binding of the regulatory subunit (RII) of cAMP-dependent protein kinase to microtubule-associated and other cellular proteins." *Proc Natl Acad Sci U S A* **81**(21): 6723-6727.
- Lohse, M. J., S. Engelhardt and T. Eschenhagen (2003). "What is the role of beta-adrenergic signaling in heart failure?" *Circ Res* **93**(10): 896-906.
- Lopez, M. J., S. K. Wong, I. Kishimoto, S. Dubois, V. Mach, J. Friesen, D. L. Garbers and A. Beuve (1995). "Salt-resistant hypertension in mice lacking the guanylyl cyclase-A receptor for atrial natriuretic peptide." *Nature* **378**(6552): 65-68.
- Lugnier, C. (2006). "Cyclic nucleotide phosphodiesterase (PDE) superfamily: a new target for the development of specific therapeutic agents." *Pharmacol Ther* **109**(3): 366-398.
- Lugnier, C., T. Keravis, A. Le Bec, O. Pauvert, S. Proteau and E. Rousseau (1999). "Characterization of cyclic nucleotide phosphodiesterase isoforms associated to isolated cardiac nuclei." *Biochim Biophys Acta* **1472**(3): 431-446.
- Lugnier, C. and N. Komasa (1993). "Modulation of vascular cyclic nucleotide phosphodiesterases by cyclic GMP: role in vasodilatation." *Eur Heart J* **14 Suppl I**: 141-148.
- Lugnier, C. and J. C. Stoclet (1979). "Age related changes in cardiac and aortic phosphodiesterase activities in normotensive and hypertensive rats." *Biochem Pharmacol* **28**(24): 3581-3587.
- Lukowski, R., S. D. Rybalkin, F. Loga, V. Leiss, J. A. Beavo and F. Hofmann (2010). "Cardiac hypertrophy is not amplified by deletion of cGMP-

- dependent protein kinase I in cardiomyocytes." Proc Natl Acad Sci U S A **107**(12): 5646-5651.
- Lygren, B., C. R. Carlson, K. Santamaria, V. Lissandron, T. McSorley, J. Litzenberg, D. Lorenz, B. Wiesner, W. Rosenthal, M. Zaccolo, K. Tasken and E. Klussmann (2007). "AKAP complex regulates Ca<sup>2+</sup> re-uptake into heart sarcoplasmic reticulum." EMBO Rep **8**(11): 1061-1067.
- Lynch, M. J., G. S. Baillie, A. Mohamed, X. Li, C. Maisonneuve, E. Klussmann, G. van Heeke and M. D. Houslay (2005). "RNA silencing identifies PDE4D5 as the functionally relevant cAMP phosphodiesterase interacting with beta arrestin to control the protein kinase A/AKAP79-mediated switching of the beta2-adrenergic receptor to activation of ERK in HEK293B2 cells." J Biol Chem **280**(39): 33178-33189.
- Macdougall, D. A., S. R. Agarwal, E. A. Stopford, H. Chu, J. A. Collins, A. L. Longster, J. Colyer, R. D. Harvey and S. Calaghan (2012). "Caveolae compartmentalise beta2-adrenoceptor signals by curtailing cAMP production and maintaining phosphatase activity in the sarcoplasmic reticulum of the adult ventricular myocyte." J Mol Cell Cardiol **52**(2): 388-400.
- MacFarland, R. T., B. D. Zelus and J. A. Beavo (1991). "High concentrations of a cGMP-stimulated phosphodiesterase mediate ANP-induced decreases in cAMP and steroidogenesis in adrenal glomerulosa cells." J Biol Chem **266**(1): 136-142.
- Marchmont, R. J. and M. D. Houslay (1980). "Insulin trigger, cyclic AMP-dependent activation and phosphorylation of a plasma membrane cyclic AMP phosphodiesterase." Nature **286**(5776): 904-906.
- Marchmont, R. J. and M. D. Houslay (1980). "A peripheral and an intrinsic enzyme constitute the cyclic AMP phosphodiesterase activity of rat liver plasma membranes." Biochem J **187**(2): 381-392.
- Marino, T. A., M. Cassidy, D. R. Marino, N. L. Carson and S. Houser (1991). "Norepinephrine-induced cardiac hypertrophy of the cat heart." Anat Rec **229**(4): 505-510.
- Martinez, S. E., S. Bruder, A. Schultz, N. Zheng, J. E. Schultz, J. A. Beavo and J. U. Linder (2005). "Crystal structure of the tandem GAF domains from a cyanobacterial adenylyl cyclase: modes of ligand binding and dimerization." Proc Natl Acad Sci U S A **102**(8): 3082-3087.
- Martinez, S. E., A. Y. Wu, N. A. Glavas, X. B. Tang, S. Turley, W. G. Hol and J. A. Beavo (2002). "The two GAF domains in phosphodiesterase 2A have distinct roles in dimerization and in cGMP binding." Proc Natl Acad Sci U S A **99**(20): 13260-13265.
- Martins, T. J., M. C. Mumby and J. A. Beavo (1982). "Purification and characterization of a cyclic GMP-stimulated cyclic nucleotide phosphodiesterase from bovine tissues." J Biol Chem **257**(4): 1973-1979.
- Maruyama, Y., M. Nishida, Y. Sugimoto, S. Tanabe, J. H. Turner, T. Kozasa, T. Wada, T. Nagao and H. Kurose (2002). "Galpha(12/13) mediates alpha(1)-adrenergic receptor-induced cardiac hypertrophy." Circ Res **91**(10): 961-969.
- Marx, S. O., J. Kurokawa, S. Reiken, H. Motoike, J. D'Armiento, A. R. Marks and R. S. Kass (2002). "Requirement of a macromolecular signaling complex for beta adrenergic receptor modulation of the KCNQ1-KCNE1 potassium channel." Science **295**(5554): 496-499.

- Marx, S. O., S. Reiken, Y. Hisamatsu, T. Jayaraman, D. Burkhoff, N. Rosemblyt and A. R. Marks (2000). "PKA phosphorylation dissociates FKBP12.6 from the calcium release channel (ryanodine receptor): defective regulation in failing hearts." *Cell* **101**(4): 365-376.
- Masood, A., Y. Huang, H. Hajjhussein, L. Xiao, H. Li, W. Wang, A. Hamza, C. G. Zhan and J. M. O'Donnell (2009). "Anxiolytic effects of phosphodiesterase-2 inhibitors associated with increased cGMP signaling." *J Pharmacol Exp Ther* **331**(2): 690-699.
- McMurray, J. J. and M. A. Pfeffer (2005). "Heart failure." *Lancet* **365**(9474): 1877-1889.
- Means, C. K., B. Lygren, L. K. Langeberg, A. Jain, R. E. Dixon, A. L. Vega, M. G. Gold, S. Petrosyan, S. S. Taylor, A. N. Murphy, T. Ha, L. F. Santana, K. Tasken and J. D. Scott (2011). "An entirely specific type I A-kinase anchoring protein that can sequester two molecules of protein kinase A at mitochondria." *Proc Natl Acad Sci U S A* **108**(48): E1227-1235.
- Mehats, C., C. B. Andersen, M. Filopanti, S. L. Jin and M. Conti (2002). "Cyclic nucleotide phosphodiesterases and their role in endocrine cell signaling." *Trends Endocrinol Metab* **13**(1): 29-35.
- Mery, P. F., C. Pavoine, F. Pecker and R. Fischmeister (1995). "Erythro-9-(2-hydroxy-3-nonyl)adenine inhibits cyclic GMP-stimulated phosphodiesterase in isolated cardiac myocytes." *Mol Pharmacol* **48**(1): 121-130.
- Metrich, M., A. Lucas, M. Gastineau, J. L. Samuel, C. Heymes, E. Morel and F. Lezoualc'h (2008). "Epac mediates beta-adrenergic receptor-induced cardiomyocyte hypertrophy." *Circ Res* **102**(8): 959-965.
- Mika, D., P. Bobin, M. Pomerance, P. Lechene, R. E. Westenbroek, W. A. Catterall, G. Vandecasteele, J. Leroy and R. Fischmeister (2013). "Differential regulation of cardiac excitation-contraction coupling by cAMP phosphodiesterase subtypes." *Cardiovasc Res* **100**(2): 336-346.
- Milano, C. A., P. C. Dolber, H. A. Rockman, R. A. Bond, M. E. Venable, L. F. Allen and R. J. Lefkowitz (1994). "Myocardial expression of a constitutively active alpha 1B-adrenergic receptor in transgenic mice induces cardiac hypertrophy." *Proc Natl Acad Sci U S A* **91**(21): 10109-10113.
- Miller, C. L., M. Oikawa, Y. Cai, A. P. Wojtovich, D. J. Nagel, X. Xu, H. Xu, V. Florio, S. D. Rybalkin, J. A. Beavo, Y. F. Chen, J. D. Li, B. C. Blaxall, J. Abe and C. Yan (2009). "Role of Ca<sup>2+</sup>/calmodulin-stimulated cyclic nucleotide phosphodiesterase 1 in mediating cardiomyocyte hypertrophy." *Circ Res* **105**(10): 956-964.
- Miller, C. L. and C. Yan (2010). "Targeting cyclic nucleotide phosphodiesterase in the heart: therapeutic implications." *J Cardiovasc Transl Res* **3**(5): 507-515.
- Mokni, W., T. Keravis, N. Etienne-Selloum, A. Walter, M. O. Kane, V. B. Schinikerth and C. Lugnier (2010). "Concerted regulation of cGMP and cAMP phosphodiesterases in early cardiac hypertrophy induced by angiotensin II." *PLoS One* **5**(12): e14227.
- Molkentin, J. D. (2003). "A friend within the heart: natriuretic peptide receptor signaling." *J Clin Invest* **111**(9): 1275-1277.
- Molkentin, J. D. and G. W. Dorn, 2nd (2001). "Cytoplasmic signaling pathways that regulate cardiac hypertrophy." *Annu Rev Physiol* **63**: 391-426.

- Molkentin, J. D., J. R. Lu, C. L. Antos, B. Markham, J. Richardson, J. Robbins, S. R. Grant and E. N. Olson (1998). "A calcineurin-dependent transcriptional pathway for cardiac hypertrophy." *Cell* **93**(2): 215-228.
- Mongillo, M., T. McSorley, S. Evellin, A. Sood, V. Lissandron, A. Terrin, E. Huston, A. Hannawacker, M. J. Lohse, T. Pozzan, M. D. Houslay and M. Zaccolo (2004). "Fluorescence resonance energy transfer-based analysis of cAMP dynamics in live neonatal rat cardiac myocytes reveals distinct functions of compartmentalized phosphodiesterases." *Circ Res* **95**(1): 67-75.
- Mongillo, M., C. G. Tocchetti, A. Terrin, V. Lissandron, Y. F. Cheung, W. R. Dostmann, T. Pozzan, D. A. Kass, N. Paolucci, M. D. Houslay and M. Zaccolo (2006). "Compartmentalized phosphodiesterase-2 activity blunts beta-adrenergic cardiac inotropy via an NO/cGMP-dependent pathway." *Circ Res* **98**(2): 226-234.
- Moniotte, S., L. Kobzik, O. Feron, J. N. Trochu, C. Gauthier and J. L. Balligand (2001). "Upregulation of beta(3)-adrenoceptors and altered contractile response to inotropic amines in human failing myocardium." *Circulation* **103**(12): 1649-1655.
- Movsesian, M. A. (2002). "PDE3 cyclic nucleotide phosphodiesterases and the compartmentation of cyclic nucleotide-mediated signalling in cardiac myocytes." *Basic Res Cardiol* **97 Suppl 1**: 183-90.
- Movsesian, M. A. and R. Alharethi (2002). "Inhibitors of cyclic nucleotide phosphodiesterase PDE3 as adjunct therapy for dilated cardiomyopathy." *Expert Opin Investig Drugs* **11**(11): 1529-1536.
- Movsesian, M. A. and M. R. Bristow (2005). "Alterations in cAMP-mediated signaling and their role in the pathophysiology of dilated cardiomyopathy." *Curr Top Dev Biol* **68**: 25-48.
- Movsesian, M. A. and R. C. Kukreja (2011). "Phosphodiesterase inhibition in heart failure." *Handb Exp Pharmacol*(204): 237-249.
- Muller, B., C. Lugnier and J. C. Stoclet (1990). "Implication of cyclic AMP in the positive inotropic effects of cyclic GMP-inhibited cyclic AMP phosphodiesterase inhibitors on guinea pig isolated left atria." *J Cardiovasc Pharmacol* **15**(3): 444-451.
- Muller, F. U., P. Boknik, J. Knapp, B. Linck, H. Luss, J. Neumann and W. Schmitz (2001). "Activation and inactivation of cAMP-response element-mediated gene transcription in cardiac myocytes." *Cardiovasc Res* **52**(1): 95-102.
- Nagaoka, A. and W. Lovenberg (1976). "Plasma norepinephrine and dopamine-beta-hydroxylase in genetic hypertensive rats." *Life Sci* **19**(1): 29-34.
- Nagatsu, T. (1974). "[Dopamine-beta-hydroxylase in serum--active and inactive forms of a serum enzyme (author's transl)]." *Seikagaku* **46**(2): 53-66.
- Nakamura, T. and G. H. Gold (1987). "A cyclic nucleotide-gated conductance in olfactory receptor cilia." *Nature* **325**(6103): 442-444.
- Neumann, J., W. Schmitz, H. Scholz, L. von Meyerinck, V. Doring and P. Kalmar (1988). "Increase in myocardial Gi-proteins in heart failure." *Lancet* **2**(8617): 936-937.
- Newlon, M. G., M. Roy, D. Morikis, D. W. Carr, R. Westphal, J. D. Scott and P. A. Jennings (2001). "A novel mechanism of PKA anchoring revealed by solution structures of anchoring complexes." *EMBO J* **20**(7): 1651-1662.
- Newlon, M. G., M. Roy, D. Morikis, Z. E. Hausken, V. Coghlan, J. D. Scott and P. A. Jennings (1999). "The molecular basis for protein kinase A anchoring revealed by solution NMR." *Nat Struct Biol* **6**(3): 222-227.

- Nichols, C. B., C. F. Rossow, M. F. Navedo, R. E. Westenbroek, W. A. Catterall, L. F. Santana and G. S. McKnight (2010). "Sympathetic stimulation of adult cardiomyocytes requires association of AKAP5 with a subpopulation of L-type calcium channels." *Circ Res* **107**(6): 747-756.
- Nicol, R. L., N. Frey and E. N. Olson (2000). "From the sarcomere to the nucleus: role of genetics and signaling in structural heart disease." *Annu Rev Genomics Hum Genet* **1**: 179-223.
- Nikolaev, V. O., M. Bunemann, L. Hein, A. Hannawacker and M. J. Lohse (2004). "Novel single chain cAMP sensors for receptor-induced signal propagation." *J Biol Chem* **279**(36): 37215-37218.
- Nikolaev, V. O., A. Moshkov, A. R. Lyon, M. Miragoli, P. Novak, H. Paur, M. J. Lohse, Y. E. Korchev, S. E. Harding and J. Gorelik (2010). "Beta2-adrenergic receptor redistribution in heart failure changes cAMP compartmentation." *Science* **327**(5973): 1653-1657.
- Nishikimi, T., N. Maeda and H. Matsuoka (2006). "The role of natriuretic peptides in cardioprotection." *Cardiovasc Res* **69**(2): 318-328.
- Niu, X., V. L. Watts, O. H. Cingolani, V. Sivakumaran, J. S. Leyton-Mange, C. L. Ellis, K. L. Miller, K. Vandegaer, D. Bedja, K. L. Gabrielson, N. Paolucci, D. A. Kass and L. A. Barouch (2012). "Cardioprotective effect of beta-3 adrenergic receptor agonism: role of neuronal nitric oxide synthase." *J Am Coll Cardiol* **59**(22): 1979-1987.
- Nof, E., D. Luria, D. Brass, D. Marek, H. Lahat, H. Reznik-Wolf, E. Pras, N. Dascal, M. Eldar and M. Glikson (2007). "Point mutation in the HCN4 cardiac ion channel pore affecting synthesis, trafficking, and functional expression is associated with familial asymptomatic sinus bradycardia." *Circulation* **116**(5): 463-470.
- Noyama, K. and S. Maekawa (2003). "Localization of cyclic nucleotide phosphodiesterase 2 in the brain-derived Triton-insoluble low-density fraction (raft)." *Neurosci Res* **45**(2): 141-148.
- Oestreich, E. A., H. Wang, S. Malik, K. A. Kaproth-Joslin, B. C. Blaxall, G. G. Kelley, R. T. Dirksen and A. V. Smrcka (2007). "Epac-mediated activation of phospholipase C(epsilon) plays a critical role in beta-adrenergic receptor-dependent enhancement of Ca<sup>2+</sup> mobilization in cardiac myocytes." *J Biol Chem* **282**(8): 5488-5495.
- Okumura, S., S. Suzuki and Y. Ishikawa (2009). "New aspects for the treatment of cardiac diseases based on the diversity of functional controls on cardiac muscles: effects of targeted disruption of the type 5 adenylyl cyclase gene." *J Pharmacol Sci* **109**(3): 354-359.
- Okumura, S., G. Takagi, J. Kawabe, G. Yang, M. C. Lee, C. Hong, J. Liu, D. E. Vatner, J. Sadoshima, S. F. Vatner and Y. Ishikawa (2003). "Disruption of type 5 adenylyl cyclase gene preserves cardiac function against pressure overload." *Proc Natl Acad Sci U S A* **100**(17): 9986-9990.
- Oliver, P. M., J. E. Fox, R. Kim, H. A. Rockman, H. S. Kim, R. L. Reddick, K. N. Pandey, S. L. Milgram, O. Smithies and N. Maeda (1997). "Hypertension, cardiac hypertrophy, and sudden death in mice lacking natriuretic peptide receptor A." *Proc Natl Acad Sci U S A* **94**(26): 14730-14735.
- Olson, E. N. and R. S. Williams (2000). "Calcineurin signaling and muscle remodeling." *Cell* **101**(7): 689-692.
- Omori, K. and J. Kotera (2007). "Overview of PDEs and their regulation." *Circ Res* **100**(3): 309-327.

- Osadchii, O. E. (2007). "Cardiac hypertrophy induced by sustained beta-adrenoreceptor activation: pathophysiological aspects." Heart Fail Rev **12**(1): 66-86.
- Osadchii, O. E. (2007). "Myocardial phosphodiesterases and regulation of cardiac contractility in health and cardiac disease." Cardiovasc Drugs Ther **21**(3): 171-194.
- Packer, M., J. R. Carver, R. J. Rodeheffer, R. J. Ivanhoe, R. DiBianco, S. M. Zeldis, G. H. Hendrix, W. J. Bommer, U. Elkayam, M. L. Kukin and et al. (1991). "Effect of oral milrinone on mortality in severe chronic heart failure. The PROMISE Study Research Group." N Engl J Med **325**(21): 1468-1475.
- Pandit, J., M. D. Forman, K. F. Fennell, K. S. Dillman and F. S. Menniti (2009). "Mechanism for the allosteric regulation of phosphodiesterase 2A deduced from the X-ray structure of a near full-length construct." Proc Natl Acad Sci U S A **106**(43): 18225-18230.
- Patel, H. H., F. Murray and P. A. Insel (2008). "G-protein-coupled receptor-signaling components in membrane raft and caveolae microdomains." Handb Exp Pharmacol(186): 167-184.
- Patrucco, E., A. Notte, L. Barberis, G. Selvetella, A. Maffei, M. Brancaccio, S. Marengo, G. Russo, O. Azzolino, S. D. Rybalkin, L. Silengo, F. Altruda, R. Wetzker, M. P. Wymann, G. Lembo and E. Hirsch (2004). "PI3Kgamma modulates the cardiac response to chronic pressure overload by distinct kinase-dependent and -independent effects." Cell **118**(3): 375-387.
- Pereira, L., M. Metrich, M. Fernandez-Velasco, A. Lucas, J. Leroy, R. Perrier, E. Morel, R. Fischmeister, S. Richard, J. P. Benitah, F. Lezoualc'h and A. M. Gomez (2007). "The cAMP binding protein Epac modulates Ca<sup>2+</sup> sparks by a Ca<sup>2+</sup>/calmodulin kinase signalling pathway in rat cardiac myocytes." J Physiol **583**(Pt 2): 685-694.
- Pfeifer, A., P. Klatt, S. Massberg, L. Ny, M. Sausbier, C. Hirneiss, G. X. Wang, M. Korth, A. Aszodi, K. E. Andersson, F. Krombach, A. Mayerhofer, P. Ruth, R. Fassler and F. Hofmann (1998). "Defective smooth muscle regulation in cGMP kinase I-deficient mice." EMBO J **17**(11): 3045-3051.
- Pidoux, G. and K. Tasken (2010). "Specificity and spatial dynamics of protein kinase A signaling organized by A-kinase-anchoring proteins." J Mol Endocrinol **44**(5): 271-284.
- Ponsioen, B., J. Zhao, J. Riedl, F. Zwartkruis, G. van der Krogt, M. Zaccolo, W. H. Moolenaar, J. L. Bos and K. Jalink (2004). "Detecting cAMP-induced Epac activation by fluorescence resonance energy transfer: Epac as a novel cAMP indicator." EMBO Rep **5**(12): 1176-1180.
- Qvigstad, E., L. R. Moltzau, J. M. Aronsen, C. H. Nguyen, K. Hougen, I. Sjaastad, F. O. Levy, T. Skomedal and J. B. Osnes (2010). "Natriuretic peptides increase beta1-adrenoceptor signalling in failing hearts through phosphodiesterase 3 inhibition." Cardiovasc Res **85**(4): 763-772.
- Rall, T. W. and E. W. Sutherland (1958). "Formation of a cyclic adenine ribonucleotide by tissue particles." J Biol Chem **232**(2): 1065-1076.
- Redfern, C. H., P. Coward, M. Y. Degtyarev, E. K. Lee, A. T. Kwa, L. Hennighausen, H. Bujard, G. I. Fishman and B. R. Conklin (1999). "Conditional expression and signaling of a specifically designed Gi-coupled receptor in transgenic mice." Nat Biotechnol **17**(2): 165-169.
- Reeves, M. L., B. K. Leigh and P. J. England (1987). "The identification of a new cyclic nucleotide phosphodiesterase activity in human and guinea-pig

- cardiac ventricle. Implications for the mechanism of action of selective phosphodiesterase inhibitors." *Biochem J* **241**(2): 535-541.
- Rehmann, H., J. Das, P. Knipscheer, A. Wittinghofer and J. L. Bos (2006). "Structure of the cyclic-AMP-responsive exchange factor Epac2 in its auto-inhibited state." *Nature* **439**(7076): 625-628.
- Rich, T. C., K. A. Fagan, H. Nakata, J. Schaack, D. M. Cooper and J. W. Karpén (2000). "Cyclic nucleotide-gated channels colocalize with adenylyl cyclase in regions of restricted cAMP diffusion." *J Gen Physiol* **116**(2): 147-161.
- Rich, T. C., K. A. Fagan, T. E. Tse, J. Schaack, D. M. Cooper and J. W. Karpén (2001a). "A uniform extracellular stimulus triggers distinct cAMP signals in different compartments of a simple cell." *Proc Natl Acad Sci U S A* **98**(23): 13049-13054.
- Rich, T. C., T. E. Tse, J. G. Rohan, J. Schaack and J. W. Karpén (2001b). "In vivo assessment of local phosphodiesterase activity using tailored cyclic nucleotide-gated channels as cAMP sensors." *J Gen Physiol* **118**(1): 63-78.
- Richter, W., P. Day, R. Agrawal, M. D. Bruss, S. Granier, Y. L. Wang, S. G. Rasmussen, K. Horner, P. Wang, T. Lei, A. J. Patterson, B. Kobilka and M. Conti (2008). "Signaling from beta1- and beta2-adrenergic receptors is defined by differential interactions with PDE4." *EMBO J* **27**(2): 384-393.
- Richter, W., D. Mika, E. Blanchard, P. Day and M. Conti (2013). "beta1-adrenergic receptor antagonists signal via PDE4 translocation." *EMBO Rep* **14**(3): 276-283.
- Ritchie, R. H., R. J. Schiebinger, M. C. LaPointe and J. D. Marsh (1998). "Angiotensin II-induced hypertrophy of adult rat cardiomyocytes is blocked by nitric oxide." *Am J Physiol* **275**(4 Pt 2): H1370-1374.
- Rivet-Bastide, M., G. Vandecasteele, S. Hatem, I. Verde, A. Benardeau, J. J. Mercadier and R. Fischmeister (1997). "cGMP-stimulated cyclic nucleotide phosphodiesterase regulates the basal calcium current in human atrial myocytes." *J Clin Invest* **99**(11): 2710-2718.
- Rochais, F., A. Abi-Gerges, K. Horner, F. Lefebvre, D. M. Cooper, M. Conti, R. Fischmeister and G. Vandecasteele (2006). "A specific pattern of phosphodiesterases controls the cAMP signals generated by different Gs-coupled receptors in adult rat ventricular myocytes." *Circ Res* **98**(8): 1081-1088.
- Rockman, H. A., K. R. Chien, D. J. Choi, G. Iaccarino, J. J. Hunter, J. Ross, Jr., R. J. Lefkowitz and W. J. Koch (1998). "Expression of a beta-adrenergic receptor kinase 1 inhibitor prevents the development of myocardial failure in gene-targeted mice." *Proc Natl Acad Sci U S A* **95**(12): 7000-7005.
- Roder, I. V., V. Lissandron, J. Martin, Y. Petersen, G. Di Benedetto, M. Zaccolo and R. Rudolf (2009). "PKA microdomain organisation and cAMP handling in healthy and dystrophic muscle in vivo." *Cell Signal* **21**(5): 819-826.
- Rosenkranz, A. C., R. L. Woods, G. J. Dusting and R. H. Ritchie (2003). "Antihypertrophic actions of the natriuretic peptides in adult rat cardiomyocytes: importance of cyclic GMP." *Cardiovasc Res* **57**(2): 515-522.
- Rosman, G. J., T. J. Martins, W. K. Sonnenburg, J. A. Beavo, K. Ferguson and K. Loughney (1997). "Isolation and characterization of human cDNAs encoding a cGMP-stimulated 3',5'-cyclic nucleotide phosphodiesterase." *Gene* **191**(1): 89-95.

- Roth, D. M., H. Bayat, J. D. Drumm, M. H. Gao, J. S. Swaney, A. Ander and H. K. Hammond (2002). "Adenylyl cyclase increases survival in cardiomyopathy." Circulation **105**(16): 1989-1994.
- Ruiz-Hurtado, G., E. Morel, A. Dominguez-Rodriguez, A. Llach, F. Lezoualc'h, J. P. Benitah and A. M. Gomez (2013). "Epac in cardiac calcium signaling." J Mol Cell Cardiol **58**: 162-171.
- Sadhu, K., K. Hensley, V. A. Florio and S. L. Wolda (1999). "Differential expression of the cyclic GMP-stimulated phosphodiesterase PDE2A in human venous and capillary endothelial cells." J Histochem Cytochem **47**(7): 895-906.
- Sadoshima, J., Y. Xu, H. S. Slayter and S. Izumo (1993). "Autocrine release of angiotensin II mediates stretch-induced hypertrophy of cardiac myocytes in vitro." Cell **75**(5): 977-984.
- Sakata, Y., B. D. Hoit, S. B. Liggett, R. A. Walsh and G. W. Dorn, 2nd (1998). "Decompensation of pressure-overload hypertrophy in G alpha q-overexpressing mice." Circulation **97**(15): 1488-1495.
- Saucerman, J. J., J. Zhang, J. C. Martin, L. X. Peng, A. E. Stenbit, R. Y. Tsien and A. D. McCulloch (2006). "Systems analysis of PKA-mediated phosphorylation gradients in live cardiac myocytes." Proc Natl Acad Sci U S A **103**(34): 12923-12928.
- Scapin, G., S. B. Patel, C. Chung, J. P. Varnerin, S. D. Edmondson, A. Mastracchio, E. R. Parmee, S. B. Singh, J. W. Becker, L. H. Van der Ploeg and M. R. Tota (2004). "Crystal structure of human phosphodiesterase 3B: atomic basis for substrate and inhibitor specificity." Biochemistry **43**(20): 6091-6100.
- Selvetella, G., E. Hirsch, A. Notte, G. Tarone and G. Lembo (2004). "Adaptive and maladaptive hypertrophic pathways: points of convergence and divergence." Cardiovasc Res **63**(3): 373-380.
- Sette, C. and M. Conti (1996). "Phosphorylation and activation of a cAMP-specific phosphodiesterase by the cAMP-dependent protein kinase. Involvement of serine 54 in the enzyme activation." J Biol Chem **271**(28): 16526-16534.
- Shakur, Y., L. S. Holst, T. R. Landstrom, M. Movsesian, E. Degerman and V. Manganiello (2001). "Regulation and function of the cyclic nucleotide phosphodiesterase (PDE3) gene family." Prog Nucleic Acid Res Mol Biol **66**: 241-277.
- Sheridan, C. M., E. K. Heist, C. R. Beals, G. R. Crabtree and P. Gardner (2002). "Protein kinase A negatively modulates the nuclear accumulation of NF-ATc1 by priming for subsequent phosphorylation by glycogen synthase kinase-3." J Biol Chem **277**(50): 48664-48676.
- Silberbach, M. and C. T. Roberts, Jr. (2001). "Natriuretic peptide signalling: molecular and cellular pathways to growth regulation." Cell Signal **13**(4): 221-231.
- Simpson, P., A. McGrath and S. Savion (1982). "Myocyte hypertrophy in neonatal rat heart cultures and its regulation by serum and by catecholamines." Circ Res **51**(6): 787-801.
- Sin, Y. Y., H. V. Edwards, X. Li, J. P. Day, F. Christian, A. J. Dunlop, D. R. Adams, M. Zaccolo, M. D. Houslay and G. S. Baillie (2011). "Disruption of the cyclic AMP phosphodiesterase-4 (PDE4)-HSP20 complex attenuates the beta-agonist induced hypertrophic response in cardiac myocytes." J Mol Cell Cardiol **50**(5): 872-883.

- Smith, C. J., R. Huang, D. Sun, S. Ricketts, C. Hoegler, J. Z. Ding, R. A. Moggio and T. H. Hintze (1997). "Development of decompensated dilated cardiomyopathy is associated with decreased gene expression and activity of the milrinone-sensitive cAMP phosphodiesterase PDE3A." Circulation **96**(9): 3116-3123.
- Smith, C. M., E. Radzio-Andzelm, Madhusudan, P. Akamine and S. S. Taylor (1999). "The catalytic subunit of cAMP-dependent protein kinase: prototype for an extended network of communication." Prog Biophys Mol Biol **71**(3-4): 313-341.
- Somekawa, S., S. Fukuhara, Y. Nakaoka, H. Fujita, Y. Saito and N. Mochizuki (2005). "Enhanced functional gap junction neofunction by protein kinase A-dependent and Epac-dependent signals downstream of cAMP in cardiac myocytes." Circ Res **97**(7): 655-662.
- Sonnenburg, W. K., P. J. Mullaney and J. A. Beavo (1991). "Molecular cloning of a cyclic GMP-stimulated cyclic nucleotide phosphodiesterase cDNA. Identification and distribution of isozyme variants." J Biol Chem **266**(26): 17655-17661.
- Stangherlin, A., F. Gesellchen, A. Zoccarato, A. Terrin, L. A. Fields, M. Berrera, N. C. Surdo, M. A. Craig, G. Smith, G. Hamilton and M. Zaccolo (2011). "cGMP Signals Modulate cAMP Levels in a Compartment-Specific Manner to Regulate Catecholamine-Dependent Signaling in Cardiac Myocytes." Circ Res **108**(8): 929-939.
- Sugden, P. H. and A. Clerk (1998). "Cellular mechanisms of cardiac hypertrophy." J Mol Med (Berl) **76**(11): 725-746.
- Sunahara, R. K., C. W. Dessauer and A. G. Gilman (1996). "Complexity and diversity of mammalian adenylyl cyclases." Annu Rev Pharmacol Toxicol **36**: 461-480.
- Sunahara, R. K., C. W. Dessauer, R. E. Whisnant, C. Kleuss and A. G. Gilman (1997). "Interaction of G $\alpha$  with the cytosolic domains of mammalian adenylyl cyclase." J Biol Chem **272**(35): 22265-22271.
- Sutherland, E. W. and C. F. Cori (1951). "Effect of hyperglycemic-glycogenolytic factor and epinephrine on liver phosphorylase." J Biol Chem **188**(2): 531-543.
- Sutherland, E. W. and T. W. Rall (1958). "Fractionation and characterization of a cyclic adenine ribonucleotide formed by tissue particles." J Biol Chem **232**(2): 1077-1091.
- Taigen, T., L. J. De Windt, H. W. Lim and J. D. Molkentin (2000). "Targeted inhibition of calcineurin prevents agonist-induced cardiomyocyte hypertrophy." Proc Natl Acad Sci U S A **97**(3): 1196-1201.
- Takimoto, E., H. C. Champion, M. Li, D. Belardi, S. Ren, E. R. Rodriguez, D. Bedja, K. L. Gabrielson, Y. Wang and D. A. Kass (2005). "Chronic inhibition of cyclic GMP phosphodiesterase 5A prevents and reverses cardiac hypertrophy." Nat Med **11**(2): 214-222.
- Tasken, K. and E. M. Aandahl (2004). "Localized effects of cAMP mediated by distinct routes of protein kinase A." Physiol Rev **84**(1): 137-167.
- Taylor, M. S., C. Okwuchukwuasanya, C. K. Nickl, W. Tegge, J. E. Brayden and W. R. Dostmann (2004). "Inhibition of cGMP-dependent protein kinase by the cell-permeable peptide DT-2 reveals a novel mechanism of vasoregulation." Mol Pharmacol **65**(5): 1111-1119.

- Taylor, S. S., J. A. Buechler and W. Yonemoto (1990). "cAMP-dependent protein kinase: framework for a diverse family of regulatory enzymes." Annu Rev Biochem **59**: 971-1005.
- Taylor, S. S., C. Kim, C. Y. Cheng, S. H. Brown, J. Wu and N. Kannan (2008). "Signaling through cAMP and cAMP-dependent protein kinase: diverse strategies for drug design." Biochim Biophys Acta **1784**(1): 16-26.
- Taylor, S. S., C. Kim, D. Vigil, N. M. Haste, J. Yang, J. Wu and G. S. Anand (2005). "Dynamics of signaling by PKA." Biochim Biophys Acta **1754**(1-2): 25-37.
- Taylor, S. S., E. Radzio-Andzelm, Madhusudan, X. Cheng, L. Ten Eyck and N. Narayana (1999). "Catalytic subunit of cyclic AMP-dependent protein kinase: structure and dynamics of the active site cleft." Pharmacol Ther **82**(2-3): 133-141.
- Tepe, N. M. and S. B. Liggett (1999). "Transgenic replacement of type V adenylyl cyclase identifies a critical mechanism of beta-adrenergic receptor dysfunction in the G alpha q overexpressing mouse." FEBS Lett **458**(2): 236-240.
- Terrenoire, C., M. D. Houslay, G. S. Baillie and R. S. Kass (2009). "The cardiac IKs potassium channel macromolecular complex includes the phosphodiesterase PDE4D3." J Biol Chem **284**(14): 9140-9146.
- Terrin, A., G. Di Benedetto, V. Pertegato, Y. F. Cheung, G. Baillie, M. J. Lynch, N. Elvassore, A. Prinz, F. W. Herberg, M. D. Houslay and M. Zaccolo (2006). "PGE(1) stimulation of HEK293 cells generates multiple contiguous domains with different [cAMP]: role of compartmentalized phosphodiesterases." J Cell Biol **175**(3): 441-451.
- Thandapilly, S. J., X. L. Louis, T. Yang, D. M. Stringer, L. Yu, S. Zhang, J. Wigle, E. Kardami, P. Zahradka, C. Taylor, H. D. Anderson and T. Netticadan (2011). "Resveratrol prevents norepinephrine induced hypertrophy in adult rat cardiomyocytes, by activating NO-AMPK pathway." Eur J Pharmacol **668**(1-2): 217-224.
- Thompson, W. J. and M. M. Appleman (1971). "Characterization of cyclic nucleotide phosphodiesterases of rat tissues." J Biol Chem **246**(10): 3145-3150.
- Thompson, W. J. and M. M. Appleman (1971). "Multiple cyclic nucleotide phosphodiesterase activities from rat brain." Biochemistry **10**(2): 311-316.
- Tremblay, J., R. Desjardins, D. Hum, J. Gutkowska and P. Hamet (2002). "Biochemistry and physiology of the natriuretic peptide receptor guanylyl cyclases." Mol Cell Biochem **230**(1-2): 31-47.
- Tse, J., N. L. Brackett and J. F. Kuo (1978). "Alterations in activities of cyclic nucleotide systems and in beta-adrenergic receptor-mediated activation of cyclic AMP-dependent protein kinase during progression and regression of isoproterenol-induced cardiac hypertrophy." Biochim Biophys Acta **542**(3): 399-411.
- Tse, J., J. R. Powell, C. A. Baste, R. E. Priest and J. F. Kuo (1979). "Isoproterenol-induced cardiac hypertrophy: modifications in characteristics of beta-adrenergic receptor, adenylate cyclase, and ventricular contraction." Endocrinology **105**(1): 246-255.
- Tsoporis, J. N., A. Marks, H. J. Kahn, J. W. Butany, P. P. Liu, D. O'Hanlon and T. G. Parker (1998). "Inhibition of norepinephrine-induced cardiac hypertrophy in s100beta transgenic mice." J Clin Invest **102**(8): 1609-1616.

- Vakili, B. A., P. M. Okin and R. B. Devereux (2001). "Prognostic implications of left ventricular hypertrophy." *Am Heart J* **141**(3): 334-341.
- Vandecasteele, G., F. Rochais, A. Abi-Gerges and R. Fischmeister (2006). "Functional localization of cAMP signalling in cardiac myocytes." *Biochem Soc Trans* **34**(Pt 4): 484-488.
- Vandecasteele, G., I. Verde, C. Rucker-Martin, P. Donzeau-Gouge and R. Fischmeister (2001). "Cyclic GMP regulation of the L-type Ca(2+) channel current in human atrial myocytes." *J Physiol* **533**(Pt 2): 329-340.
- Vaziri, N. D. and X. Q. Wang (1999). "cGMP-mediated negative-feedback regulation of endothelial nitric oxide synthase expression by nitric oxide." *Hypertension* **34**(6): 1237-1241.
- Vecchione, C., L. Fratta, D. Rizzoni, A. Notte, R. Poulet, E. Porteri, G. Frati, D. Guelfi, V. Trimarco, M. J. Mulvany, E. Agabiti-Rosei, B. Trimarco, S. Cotecchia and G. Lembo (2002). "Cardiovascular influences of alpha1b-adrenergic receptor defect in mice." *Circulation* **105**(14): 1700-1707.
- Verboomen, H., F. Wuytack, H. De Smedt, B. Himpens and R. Casteels (1992). "Functional difference between SERCA2a and SERCA2b Ca<sup>2+</sup> pumps and their modulation by phospholamban." *Biochem J* **286** ( Pt 2): 591-595.
- Verrecchia, F. and J. C. Herve (1997). "Reversible blockade of gap junctional communication by 2,3-butanedione monoxime in rat cardiac myocytes." *Am J Physiol* **272**(3 Pt 1): C875-885.
- Vila-Petroff, M. G., A. Younes, J. Egan, E. G. Lakatta and S. J. Sollott (1999). "Activation of distinct cAMP-dependent and cGMP-dependent pathways by nitric oxide in cardiac myocytes." *Circ Res* **84**(9): 1020-1031.
- Vinogradova, T. M., K. Y. Bogdanov and E. G. Lakatta (2002). "beta-Adrenergic stimulation modulates ryanodine receptor Ca(2+) release during diastolic depolarization to accelerate pacemaker activity in rabbit sinoatrial nodal cells." *Circ Res* **90**(1): 73-79.
- Vinogradova, T. M., A. E. Lyashkov, W. Zhu, A. M. Ruknudin, S. Sirenko, D. Yang, S. Deo, M. Barlow, S. Johnson, J. L. Caffrey, Y. Y. Zhou, R. P. Xiao, H. Cheng, M. D. Stern, V. A. Maltsev and E. G. Lakatta (2006). "High basal protein kinase A-dependent phosphorylation drives rhythmic internal Ca<sup>2+</sup> store oscillations and spontaneous beating of cardiac pacemaker cells." *Circ Res* **98**(4): 505-514.
- Vinogradova, T. M., V. A. Maltsev, K. Y. Bogdanov, A. E. Lyashkov and E. G. Lakatta (2005). "Rhythmic Ca<sup>2+</sup> oscillations drive sinoatrial nodal cell pacemaker function to make the heart tick." *Ann N Y Acad Sci* **1047**: 138-156.
- Vistejnova, L., J. Dvorakova, M. Hasova, T. Muthny, V. Velebny, K. Soucek and L. Kubala (2009). "The comparison of impedance-based method of cell proliferation monitoring with commonly used metabolic-based techniques." *Neuro Endocrinol Lett* **30** Suppl 1: 121-127.
- Walsh, D. A., J. P. Perkins and E. G. Krebs (1968). "An adenosine 3',5'-monophosphate-dependant protein kinase from rabbit skeletal muscle." *J Biol Chem* **243**(13): 3763-3765.
- Wang, H., Z. Yan, S. Yang, J. Cai, H. Robinson and H. Ke (2008). "Kinetic and structural studies of phosphodiesterase-8A and implication on the inhibitor selectivity." *Biochemistry* **47**(48): 12760-12768.
- Wang, L., R. K. Sunahara, A. Kruminis, G. Perkins, M. L. Crochiere, M. Mackey, S. Bell, M. H. Ellisman and S. S. Taylor (2001). "Cloning and mitochondrial

- localization of full-length D-AKAP2, a protein kinase A anchoring protein." *Proc Natl Acad Sci U S A* **98**(6): 3220-3225.
- Watanabe, Y., T. Iwamoto, I. Matsuoka, S. Ohkubo, T. Ono, T. Watano, M. Shigekawa and J. Kimura (2001). "Inhibitory effect of 2,3-butanedione monoxime (BDM) on Na(+)/Ca(2+) exchange current in guinea-pig cardiac ventricular myocytes." *Br J Pharmacol* **132**(6): 1317-1325.
- Wettschureck, N., H. Rutten, A. Zywietz, D. Gehring, T. M. Wilkie, J. Chen, K. R. Chien and S. Offermanns (2001). "Absence of pressure overload induced myocardial hypertrophy after conditional inactivation of Galphaq/Galpha11 in cardiomyocytes." *Nat Med* **7**(11): 1236-1240.
- Willoughby, D. and D. M. Cooper (2007). "Organization and Ca<sup>2+</sup> regulation of adenylyl cyclases in cAMP microdomains." *Physiol Rev* **87**(3): 965-1010.
- Winegrad, S. (1999). "Cardiac myosin binding protein C." *Circ Res* **84**(10): 1117-1126.
- Wollert, K. C., B. Fiedler, S. Gambaryan, A. Smolenski, J. Heineke, E. Butt, C. Trautwein, S. M. Lohmann and H. Drexler (2002). "Gene transfer of cGMP-dependent protein kinase I enhances the antihypertrophic effects of nitric oxide in cardiomyocytes." *Hypertension* **39**(1): 87-92.
- Wong, W. and J. D. Scott (2004). "AKAP signalling complexes: focal points in space and time." *Nat Rev Mol Cell Biol* **5**(12): 959-970.
- Wosilait, W. D. and E. W. Sutherland (1956). "The relationship of epinephrine and glucagon to liver phosphorylase. II. Enzymatic inactivation of liver phosphorylase." *J Biol Chem* **218**(1): 469-481.
- Xiang, Y., F. Naro, M. Zoudilova, S. L. Jin, M. Conti and B. Kobilka (2005). "Phosphodiesterase 4D is required for beta2 adrenoceptor subtype-specific signaling in cardiac myocytes." *Proc Natl Acad Sci U S A* **102**(3): 909-914.
- Xiao, L., D. R. Pimental, J. K. Amin, K. Singh, D. B. Sawyer and W. S. Colucci (2001). "MEK1/2-ERK1/2 mediates alpha1-adrenergic receptor-stimulated hypertrophy in adult rat ventricular myocytes." *J Mol Cell Cardiol* **33**(4): 779-787.
- Xiao, R. P. and E. G. Lakatta (1993). "Beta 1-adrenoceptor stimulation and beta 2-adrenoceptor stimulation differ in their effects on contraction, cytosolic Ca<sup>2+</sup>, and Ca<sup>2+</sup> current in single rat ventricular cells." *Circ Res* **73**(2): 286-300.
- Yamamoto, T., S. Yamamoto, J. C. Osborne, Jr., V. C. Manganiello, M. Vaughan and H. Hidaka (1983). "Complex effects of inhibitors on cyclic GMP-stimulated cyclic nucleotide phosphodiesterase." *J Biol Chem* **258**(23): 14173-14177.
- Yanaka, N., Y. Kurosawa, K. Minami, E. Kawai and K. Omori (2003). "cGMP-phosphodiesterase activity is up-regulated in response to pressure overload of rat ventricles." *Biosci Biotechnol Biochem* **67**(5): 973-979.
- Yazaki, Y., I. Komuro, T. Yamazaki, K. Tobe, K. Maemura, T. Kadowaki and R. Nagai (1993). "Role of protein kinase system in the signal transduction of stretch-mediated protooncogene expression and hypertrophy of cardiac myocytes." *Mol Cell Biochem* **119**(1-2): 11-16.
- Yu, F. H., V. Yarov-Yarovoy, G. A. Gutman and W. A. Catterall (2005). "Overview of molecular relationships in the voltage-gated ion channel superfamily." *Pharmacol Rev* **57**(4): 387-395.
- Zaccolo, M. (2009). "cAMP signal transduction in the heart: understanding spatial control for the development of novel therapeutic strategies." *Br J Pharmacol* **158**(1): 50-60.

- Zaccolo, M., F. De Giorgi, C. Y. Cho, L. Feng, T. Knapp, P. A. Negulescu, S. S. Taylor, R. Y. Tsien and T. Pozzan (2000). "A genetically encoded, fluorescent indicator for cyclic AMP in living cells." *Nat Cell Biol* **2**(1): 25-29.
- Zaccolo, M., G. Di Benedetto, V. Lissandron, L. Mancuso, A. Terrin and I. Zamparo (2006). "Restricted diffusion of a freely diffusible second messenger: mechanisms underlying compartmentalized cAMP signalling." *Biochem Soc Trans* **34**(Pt 4): 495-497.
- Zaccolo, M. and M. A. Movsesian (2007). "cAMP and cGMP signaling cross-talk: role of phosphodiesterases and implications for cardiac pathophysiology." *Circ Res* **100**(11): 1569-1578.
- Zaccolo, M. and T. Pozzan (2002). "Discrete microdomains with high concentration of cAMP in stimulated rat neonatal cardiac myocytes." *Science* **295**(5560): 1711-1715.
- Zahabi, A., S. Picard, N. Fortin, T. L. Reudelhuber and C. F. Deschepper (2003). "Expression of constitutively active guanylate cyclase in cardiomyocytes inhibits the hypertrophic effects of isoproterenol and aortic constriction on mouse hearts." *J Biol Chem* **278**(48): 47694-47699.
- Zhang, G., Y. Liu, A. E. Ruoho and J. H. Hurley (1997). "Structure of the adenylyl cyclase catalytic core." *Nature* **386**(6622): 247-253.
- Zhang, K. Y., G. L. Card, Y. Suzuki, D. R. Artis, D. Fong, S. Gillette, D. Hsieh, J. Neiman, B. L. West, C. Zhang, M. V. Milburn, S. H. Kim, J. Schlessinger and G. Bollag (2004). "A glutamine switch mechanism for nucleotide selectivity by phosphodiesterases." *Mol Cell* **15**(2): 279-286.
- Zhang, M., E. Takimoto, S. Hsu, D. I. Lee, T. Nagayama, T. Danner, N. Koitabashi, A. S. Barth, D. Bedja, K. L. Gabrielson, Y. Wang and D. A. Kass (2010). "Myocardial remodeling is controlled by myocyte-targeted gene regulation of phosphodiesterase type 5." *J Am Coll Cardiol* **56**(24): 2021-2030.
- Zhang, Q., M. Lazar, B. Molino, R. Rodriguez, T. Davidov, J. Su, J. Tse, H. R. Weiss and P. M. Scholz (2005). "Reduction in interaction between cGMP and cAMP in dog ventricular myocytes with hypertrophic failure." *Am J Physiol Heart Circ Physiol* **289**(3): H1251-1257.
- Zhang, R., J. Zhao and J. D. Potter (1995). "Phosphorylation of both serine residues in cardiac troponin I is required to decrease the Ca<sup>2+</sup> affinity of cardiac troponin C." *J Biol Chem* **270**(51): 30773-30780.
- Zmuda-Trzebiatowska, E., A. Oknianska, V. Manganiello and E. Degerman (2006). "Role of PDE3B in insulin-induced glucose uptake, GLUT-4 translocation and lipogenesis in primary rat adipocytes." *Cell Signal* **18**(3): 382-390.